Evaluating the peripheral airways in asthma: further development of novel non-invasive assessment tools.

Thesis submitted to the degree of

Doctor of Philosophy at the University of Leicester

By

Márcia Soares

Department of Infection, Immunity and Inflammation

2019

Evaluating the peripheral airways in asthma: further development of novel non-invasive assessment tools.

Márcia Soares

Abstract

Asthma is characterised by inflammation, damage, ventilation inhomogeneity and dysfunction of the small airways (arbitrary defined < 2mm diameter) but no standardised non-invasive biomarkers are available, leading to a lack of well-established clinical evaluation and treatment pathways. In this thesis, novel approaches and candidate biomarkers to probe the periphery are further developed, using forced oscillation techniques (FOT), particles in exhaled air (PExA) and oxygen enhanced MR imaging (OE-MRI).

FOT techniques are explored using clinical population, comparative device studies and a 3-D printed model. These studies provide further evidence to support resistance at 5 Hz minus resistance at 20 Hz (R5-R20) parameter as small airways dysfunction detection tool. Furthermore, clinical and printed airway models show that two different FOT devices generate dissimilar measurements of airways impedance with evidence of proportional systematic bias. These results highlight the need for further standardisation across FOT measurement devices.

Feasibility and repeatability of the PExA technique is explored further in adult asthma. Additionally, candidate biomarkers surfactant protein A (SPA) and albumin are evaluated in independent adult asthma cohorts. Proteins demonstrate good repeatability within and between-visits and strongly relate with spirometry but not decline over time. A clinically important phenotype of asthmatic patients with multiple markers of peripheral airway dysfunction is identified and demonstrates significantly lower levels of SPA and albumin. PExA is feasible across the spectrum of asthma severity and could be used to identify small airway disease phenotype in clinical trial settings.

Preliminary results from imaging with OE-MRI and physiological parameters show that OE-MRI biomarkers are associated with exacerbations and eosinophilic airway inflammation. High fine particle fraction bronchodilator led to improvement of OE-MRI markers of ventilation inhomogeneity which appeared to track with improvements in the multiple breath washout measure of small airway conductive ventilation heterogeneity (Scond).

The biomarkers developed further in this thesis are potentially suitable for exploration as endpoints in small airway targeted therapy trials.

Acknowledgements

Firstly, I'd like to thank all the patients that helped me with my studies and made it worthwhile. Without them none of this research would have been possible. I met interesting and amazing people through the years and I will be forever grateful.

I want to thank my supervisor Professor Siddiqui. Without his valuable help, guidance, challenges, support, I wouldn't have been able to get where I am and finish this arduous piece of work. A really massive thank you Salman.

Valuable guidance was given by Dr Haldar, Professor Brightling, Professor Wardlaw and Dr Gonem- thank you all for your suggestions and critique.

I'd like to thank my BRC family: Bev, Michelle B, Karen, Milly, Amisha, Sarah P, Sarah C, Sarah G, Sarah T, Selina, Amanda, Nicola, Tracy, Su, Pam, Nicole, Kate, Maria, Sheena, Deb, Adelina, Latifa, Richard, Chris W, Rashid, Ruth, Leena, Jo, Sushila, Lea, Vicky, Michelle C, Claire, Anne, Paula, Alex, Michael, Amanda, Adam, Dimos, Rob, Bo, Safina, Jeanette, Fiona. Thank you all for keeping me sane during these years, for your help, but mostly for your friendship- you are the best team and will always be in my heart.

A big thanks to DD Vara and everyone from the physiology department and sputum lab, I will always remember your support and welcoming attitude towards me.

A special appreciation goes to Professor Anna-Carin, Per, Hatice, Katia, Emilia and Marianne from Gothenburg, and also John Owers-Bradly, James, members of Bioxydyn, Dan, Jo W, Matt and Brody for all your help over the years making all these projects possible. And while in the subject, a big thanks to the MK5- the Leicester PExA 1.0 instrument. We had our moments, but I will miss you!

I'd like to thank my project funders: AirPROM, Chiesi and NAPP pharmaceuticals and Ayasdi (Menlo Park, California) and Dr Devi Ramanan for access to the Ayasdi CORE and Python SDK platforms for TDA analysis.

Mum, Susana, Carlos, Francisco and all my closest family and friends- you all helped me to keep my chin up, stay strong and look forward to the future, even if you didn't know you were. I Love you all.

Lastly, I'd like to dedicate this work to the two most important men in my life. Alex, this thesis is as mine as it is yours. Thank you for standing by me during these years, for always helping me look at the bright side, for showing me the way, in every situation, good or bad. How lucky am I to be spending the rest of my life with you, facing other challenges, achieving many goals, together always. To finalise- dad, I know, no matter where you are, that you are proud of me. You made this possible, by teaching me to always work hard and always face life with a smile on my face.

Statement of work personally performed

All work described in this thesis was performed under supervision of Professor Salman Siddiqui and Dr Pranab Haldar.

I have been involved intellectually in all the studies reported in this thesis, as well as assisting in protocol design, ethics and amendments applications.

I took a major role in: recruiting all patients for every study, clinical characterisation of all the patients, performing all the physiological tests, peripheral blood samples, sputum samples and PExA samples.

I travelled to Gothenburg-Sweden in two occasions to analyse PExA samples with Prof Anna-Carin Olin's group, performing 25% of protein analysis.

I performed all the validation experiments with the printed airways physical model, in FOT and IOS devices with valuable help from James Thorpe and John Owers-Bradly, data collection and statistical analysis.

I collected all the data, performed data quality control and collation, made the majority of the statistical analysis and interpretation of the data with precious input from Professor Siddiqui and Dr Matthew Richardson.

Invaluable help was given by Bioxydyn Ltd and Radiology department at Glenfield Hospital, who provided access to the OE-MRI platform and MRI scan analysis.

Abstracts and publications arising from this thesis

Abstracts

Soares M, Migrodskaya E, Olin AC, Siddiqui S. Small airways obstruction and exhaled particles in asthma. European Respiratory Journal. 2014 Sep 1;44(Suppl 58):3407. *(Oral presentation, ERS 2014)*

Soares M, Gonem S, Singapuri A, Hargadon B, Brightling C, Siddiqui S. Small airways obstruction and asthma exacerbations. European Respiratory Journal. 2014 Sep 1;44(Suppl 58):P3004. *(Poster presentation, ERS 2014)*

Soares M, Migrodskaya E, Olin AC, Siddiqui S. Relationship between small airways bio-markers and airways closure. European Respiratory Journal. 2015 Sep 1;46(suppl 59):PA1027. *(Thematic poster, ERS 2015)*

Soares M, Bordas R, Thorpe J, TimmermanB, Brightling C, Kay D, Burrowes K, Owers-Bradley J, Siddiqui S. Validation of impulse oscillometry R5-R20 as a small airways dysfunction detection tool in adult asthma. (2016): OA4968. *(Oral presentation, ERS 2016)*

Soares M, Foy B, Kay D, Owers-Bradley J, Siddiqui S, The Evaluation of Frequency Dependence of Resistance using a Patient-Specific 3D Printed Airway Model and Computational Simulation. *(Thematic poster, ERS 2017)*

Soares M, Ulloa J, Wormleighton J, Barnes D, Parker G, Siddiqui S, The Impact of a High Fine Particle Fraction Inhaled Long Acting β2 Agonist (Formoterol) on Airway

Function in Asthma: Evaluation with Oxygen Enhanced MRI and Multiple Breath Washout. *(Thematic poster, ERS 2017)*

Soares M, Koca H, Olin AC, Siddiqui S, Repeatabillity of PExA SPA and albumin as small airways dysfunction candidate biomarkers in Asthma. *(Thematic poster, ERS 2018)*

Soares M, Richardson M, Thorpe J, Owers-Bradley J, Siddiqui S, Comparison of Forced and Impulse Oscillometry Measurements: A Clinical Population and Printed Airway Model Study. (*Poster Discussion, ERS 2018*)

Publications

Foy B^, **Soares M^**, Bordas R, Richardson M, Bell A, Singapuri A , Hargadon B, Brightling C, Burrowes K, Kay D, Owers-Bradley J, Siddiqui S. Lung Computational Models Provide Unique Insights into the Clinical Role of the Small Airways in Asthma. *(Manuscript submitted to American Journal of respiratory and critical care medicine, December 2018, ^shared first-authorship)*

Soares M, Mirgorodskaya E, Koca H, Viklund E, Richardson M, Gustafsson P, Olin AC, Siddiqui S. Particles in exhaled air (PExA): non-invasive phenotyping of small airways disease in adult asthma. Journal of breath research. 2018 Sep 14;12(4):046012.

Soares M, Richardson M, Thorpe J, Owers-Bradley J, Siddiqui S, Comparison of Forced and Impulse Oscillometry Measurements: A Clinical Population and Printed Airway Model Study. (*Manuscript accepted by Nature Scientific Reports November 2018*)

Soares M, Mirgorodskaya E, Koca H, Richardson M, Olin AC, Siddiqui S. Short-term Repeatabillity and Longitudinal Change of Particle in Exhalaed air Derived SPA and Albumin in Adult Asthma. *(Manuscript in preparation for Plos One)*

Soares M, Ulloa J, Tibletti M, Wormleighton J, Hargadon B, Parker G, Barnes D, Siddiqui S. Evaluation of bronchodilator responses to inhaled Fluticasone/Formoterol in Moderate to Severe Asthma using Dynamic Oxygen Enhanced MRI . *(Manuscript in preparation for Thorax)*

List of contents

List of tables

List of figures

Abbreviations

ACQ	Asthma Control Questionnaire
ADCs	Apparent diffusion coefficients
AHR	Airway hyperresponsiveness
Albumin	Human serum albumin
AQLQ	Asthma Quality of Life Questionnaire
ATS	American Thoracic Society
AX	Reactance area
BAL	Bronchioalveolar lavage
BALF	Bronchioalveolar lavage fluid
BDP	Beclomethasone dipropionate
BMI	Body mass index
BSA	Bovine serum albumin
BTPS	Body temperature and pressure, saturated
BUD	Budesonide
C	Capacitance
CC	Closing capacity
CDI	Convection-dependent inhomogeneity
Cet	End-expiratory inert gas concentration
CEV	Cumulative expired volume
CF	Cystic fibrosis
COPD	Chronic obstructive pulmonary disease
CoV	Coefficient of variation
CRD	calcium-dependent carbohydrate recognition domain
CT	Computed tomography
CV	Closing volume
DCDI	Diffusion-convection-dependent inhomogeneity
DDT	Dithiothrietol
DLCO	Diffusing capacity of the lung for carbon monoxide
DPI	Dry powder inhalers
DPPC	Dipalmitoyl-phosphatidylcholine
DSeq	Equipment dead space
EBC	Exhaled breath condensate

ELISA	Enzyme-Linked Immunosorbent Assay
EnF	Enhancing fraction of the lung
eNose	electronic nose
EoxFB	Regional extraction of gas from the lung by blood
EPAP	Expiratory positive airway pressure
ERS	European Respiratory Society
FAO	Fixed airflow obstruction
FEF 25-75	Forced expiratory flow at 25-75% of vital capacity
FEF 50	Forced expiratory flow at 50% of vital capacity
$FeNO_{50}$	Fractional exhaled nitric oxide at 50ml/s
$FeNO_{200}$	Fractional exhaled nitric oxide at 200mls/s
FEV_1	Forced expiratory volume in 1 second
FEV_3	Forced expiratory volume in 3 seconds
FM	Formoterol
FOT	Forced oscillation technique
FP	Fluticasone
FRC	Functional residual capacity
FRCcalc	Functional residual capacity calculated from dimensions of lung model
FRCmbw	Functional residual capacity calculated using multiple breath inert gas washout
FRCpleth	Functional residual capacity measured with body plethysmography
Fres	Resonant Frequency
fSAD	Functional small airway disease
FVC	Forced vital capacity
GINA	Global Initiative for Asthma
3-He (^{3}He)	3-Helium
HEPA	High-Efficiency Particulate Arrestance
HRCT	High resolution computated tomography
HU	Hounsfield Units
IAF	Image acquisition form
IC	Inspiratory capacity
ICC	Intraclass correlation coefficient
ICS	Inhaled corticosteroid
IEP	Internet exchange protocol

IgE	immunoglobulines
IOS	Impulse oscillometry
IPF	Idiopatic pulmonary fibrosis
IPAP	Inspiratory positive airway pressure
KCO	Carbon monoxide transfer coefficient
KORA	Cooperative Health Research in the Region Augsburg
Kox	Rate of transfer of gas via the diffusing airways and membranes into the lung tissue water and blood plasma
KoxFb	effective rate of blood flow in the capillaries
LABA	Long-acting β-agonist
LCI	Lung clearance index
LCIds	Dead space component of lung clearance index
LCIideal	Ideal lung clearance index
LCIvent	Specific ventilation inequality component of lung clearance index
LLN	Lower limit of normal
LoD	Limit of detection
LoQ	Limit of quantification
LTRs	Lung transplant recipients
MCID	Minimal clinically important difference
MEFV	Mid portion of the maximal expiratory flow-volume curve
MBW	Multiple breath inert gas washout
MDI	Metered dose inhaler
MLD	Mean lung density
$MLD_{E/I}$	MLD expiratory/inspiratory ratio
MMEF	Maximal mid-expiratory flow
MRI	Magnetic resonance imaging
MR	Moment ratio
MS	Mass spectrometry
MTT	Mean transit time
NICE	National Institute for clinical excellence
N_2	Nitrogen
NO	Nitric Oxide
O_2	Oxygen

ΔPO_2	Maximum change in partial pressure of oxygen in lung tissue when switching from air to 100% oxygen
OB/BOS	Obliterative bronchiolitis (syndrome)
OE-MRI	Oxygen enhanced Magnetic resonance
OPC	Optical particle counter
P	Pressure
PBS	Phosphate-Buffered Saline
PC20	20% fall in FEV1 during methacholine challenge test
PEF	Peak expiratory flow
PET	Positron emission tomography
PEx	Particles in exhaled air
PExA	Particles in exhaled air method
PRM	Parametric response map
Q	flow
R (Rrs)	Resistance
ΔRrs	Inspiratory minus expiratory resistance
R20	Resistance at 20Hz
R5	Resistance at 5Hz
R10	Resistance at 10 Hz
R5-R20	Frequency dependence of resistance
Raw	Airway resistance measured by body plethysmography
Rc	Central airway resistance
RF	Radiofrequency
RL	Total lung resistance
ROC	Receiver operating characteristic
Rp	Peripheral airway resistance
rpm	rotations per minute
RSD	Residual standard deviation
RV	Residual volume
RTLF	Respiratory tract lining fluid
SABA	Shot-acting β-agonist
Sacin	Acinar ventilation heterogeneity
SAO	Small airway obstruction
Scond	Conductive ventilation heterogeneity

SD	Standard deviation
SE	Spin echo
SF6	Sulphur Hexafluoride
SIII	Phase III slope
SnIII	Concentration-normalised phase III slope
SO	Strahler Order
SR	Standardised residual
SPA	Surfactant protein A
SPB	Surfactant protein B
SPC	Surfactant protein C
SPD	Surfactant protein D
SPECT	Single photon emission computed tomography
SVC	Slow vital capacity
T1	Longitudinal relaxation time
T2	Transverse relaxation time
TDA	Topological Data Analysis
Tdown	Exponential washout dynamics of ΔPO_2
TH2	T-helper 2
TLC	Total lung capacity
TO	Turnover (multiples of FRC)
Tvent	Effective mixing time of oxygen from the mouth, via the conducting airways and into the bronchioles
Tup	Exponential wash-in dynamics of ΔPO_2
VA	Alveolar volume
VC	Vital capacity
VDanat	Anatomical dead space
VDresp	Effective respiratory dead space
VH	Ventilation heterogeneity
VOC	Volatile organic compound
VT	Tidal volume
WHO	World Health Organisation
X (Xrs)	Reactance
X5	Reactance at 5Hz
ΔXrs	Inspiratory minus expiratory reactance

129-Xe (^{129}Xe) Xenon

Z Impedance

1. Introduction

1.1 Overview

The small airways compartment of the lungs has been a hot topic in the respiratory sciences for the last few decades. However, due to the difficulty in accessing the periphery non-invasively, sampling and visualisation with imaging approaches, progress in the field of phenotyping the small airways with a view to understand their clinical importance has been limited. Perez has very elegantly summarised the outstanding issues related with the small airways involvement in disease in two important points. Firstly, should we assess the periphery in routine practice in poorly controlled patients and what widely available method should be used? Secondly, what is the benefit of using small particle inhaler therapy (and other therapies) on specific small airways physiological and clinically relevant parameters (1).

Asthma is a serious inflammatory condition, causing 3 deaths a day in the UK alone and currently affecting about 235 million people worldwide (2). This complex disease is characterised by intermittent typical symptoms, such as wheeze, cough, shortness of breath and sporadic worsening of symptoms (exacerbations) (3–6).

Despite the evidence of small airways involvement and importance in several lung conditions, there isn't an universally accepted physiological method to characterise the periphery and the primary tools to serially evaluate small airways dysfunction in a clinical environment are gold standard lung function methods, such as spirometry and lung volumes (7–9).

The forced oscillation technique (FOT), and its variant impulse oscillometry (IOS), are non-invasive, simple physiological methods that use externally applied pressure signals and resultant measured pressure, flow response and phase relationships to determine lung mechanical parameters (10). Few indices of resistance and reactance can be derived and due to the multiple oscillation frequencies used, a dissection of large and small airway behaviour appears to be possible. Increased resistance at 5 minus 20 Hz (R5-R20) has been associated with peripheral dysfunction of the airways, and studies have shown some interesting relationships between R5-R20 and small airways inflammation, exacerbations and response to small particle formulation inhaled steroids in adult asthma (11–13).

Recently a novel non-invasive technique to sample liquid particles from the small airways- particles in exhaled air method (PExA) has been reported (14). PExA has been applied to a variety of assays (e.g. proteomics and mass spectroscopy) to evaluate biomarkers from the exhaled particles (PEx), including proteins and phospholipids and these particles appear to be associated with the degree of small airways dysfunction in asthma and chronic obstructive pulmonary disease (COPD) (15–17).

As a novel imaging approach in asthma, dynamic oxygen-enhanced magnetic resonance imaging of the lungs (OE-MRI) represents a unique method for obtaining regional ventilation and perfusion-related information by monitoring the delivery of 100% inspired oxygen to the exchange tissues and blood compartment of the lung. Its application to the asthmatic population is potentially of value to assess small airways disease, without contrast agent, radiation or expensive noble gases (18–20).

The first part of this introductory section is dedicated to the physiology and pathophysiological processes involved in small airways disease. Secondly, the focus will be on the definition of asthma and links between asthma and small airways disease, considering the current literature available. Thirdly, physiological, inflammatory and imaging methods to assess the small airways and its dysfunction non-invasively will be described, with focus on forced oscillation techniques, particles in exhaled air and oxygen-enhanced magnetic resonance imaging.

1.2 Small airways physiology

Leonardo da Vinci's drawings and descriptions of the airway tree during the 15th century prove that the curiosity and interest about the human lung and the physiology of breathing was present many centuries ago (21). The lungs are divided into lobes, three on the right and two on the left, and the tree-like airway network in humans is a complex and asymmetrical architectural structure, containing twenty-three generations of millions of dichotomous branches and over three hundred million alveoli. The trachea, bronchi, bronchioles and terminal bronchioles represent the first fourteen generations, the so-called conducting airways, followed by the more distal nine generations where gas exchange occurs including transitional bronchioles, respiratory

bronchioles, alveolar ducts, alveolar sacs and the alveoli (22,23). **Figure 1.1** shows a representation of the branching structure and different generations of the airways.

Figure 1.1 Branching structure of the airway tree

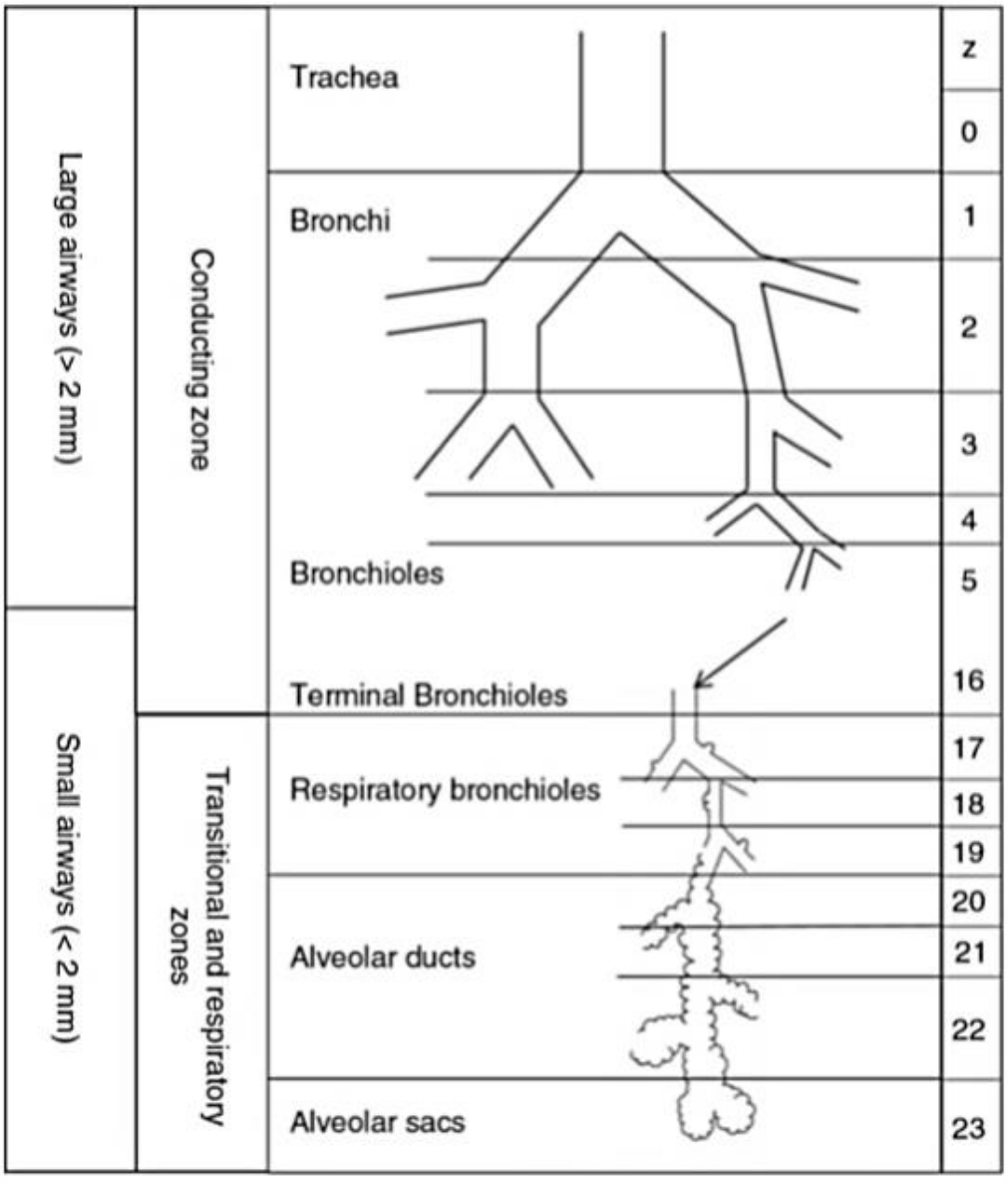

[Adapted from (24)]

Work conducted by Weibel and Gomez in the sixties generated a model of the morphometry of the conducting airways, utilising five human lungs (25). Similarly, Horsfield and Cumming had developed a method for numbering the bronchial tree generations, based on the airways greater than 0.07cm of diameter, utilizing a single pair of human lungs (26). These studies have concluded that the proximal airway branching is variable and asymmetrical. Bordas *et al* have recently described another method to annotate virtual airway models called Strahler Order (SO), based on the Horsfield order. The SO of a branch is the number of branches between the given location, and the nearest terminal bronchiole, a convenient and standardised method for describing branching hierarchical networks, more reliable than airway generation as the path length to the terminal bronchioles varies widely across different parent airways (27).

The study of the anatomy and physiology of the small airway compartment, also known as the 'silent zone' of the lungs, has involved many complex techniques [e.g. physiological tools (24), imaging (28), inhaled aerosols (29), immunohistochemistry (30) and micro CT of resection tissue (31)] over the years.

Starting around generation 8^{th} of the airway tree (21), small airways have an internal diameter of less than 2mm, lack cartilage and include small conducting airways and intra-acinar airways (32). The main structural difference between large and small airways resides in their cross-sectional area. Thus, given the fact that the same flow is divided through many more branches in the peripheral compartment, its velocity decreases dramatically and consequentially laminar flow takes place, and this type of flow is independent of gas density (33). Unlike the larger airways, airway surface liquid lining the small airways has low surface tension, protecting the small airways from closing al low lung volumes (34).

Airway resistance is triggered by force of friction in the airways, causing opposition to the flow, and is defined as the ratio of driving pressure to the rate of airflow. The peripheral airways in healthy individuals contribute very little to the overall resistance, because of the increased cross-sectional area, where small airways are arranged in parallel (35). The overall contribution of the small airways to the total resistance in normal subjects is about 10%. The advent of airway resistance investigation dates 1967, with the work conducted by Macklem and Mead on open-chest living canines using a

retrograde catheter (36). The results showed evidence that obstruction of the peripheral airways affects gas distribution and exchange in the periphery, but no noticeable changes were detected in the overall resistance. The catheter used by the pair had a tip of 2mm in diameter and they used it to arbitrary define central airways as those above 2mm and smaller airways those below 2mm in diameter. This distinction between large and small airways was accepted and remains unchanged since then, despite its random origin. Regardless of where exactly in the airway tree in commences, patients with disease and dysfunction within the small airways (such as in asthma and COPD) have important clinical characteristics, such as greater severity and worst long-term outcomes, which render the importance of better accessibility through new methods (37). A couple of years later, Brown *et al* used small beads to occlude the large and small airways in excised lung lobes from dogs and pigs (38). The main differences encountered between the two species was the presence or absence of collateral ventilation channels: pigs showed a reduction in the vital capacity by about 50% after small airway obstruction, whereas in dogs, there was no effect on the vital capacity, attributed to the presence of collateral ventilation, however, there was an increase in pulmonary resistance of about 10% in both species. Likewise, humans have collateral ventilation, and therefore, increased peripheral resistance may not be detected until later with simple tests of flow limitation such as spirometry. Although scarcely explored in small airways dysfunction context, other techniques might give better insights of this phenomena. For example, the different frequencies applied during forced oscillation techniques might lead to a better detection of early increased resistance, even in the presence of collateral channels, but it is yet to be explored. In patients with COPD due to have lung volume reduction surgery, this is achieved by endobronchial in vivo measurements or anatomical analysis from CT scans (39). Kaminsky *et al* also explored the collateral channels in their investigations of peripheral airway mechanics. They utilised a stop-flow method with a wedged bronchoscope to measure the decline of segment pressure, in both asthmatics and healthy controls. They concluded that the predominant site of resistance were the collateral channels and that asthmatic individuals had more collateral airways narrowing and lower compliance, highlighting the differences in peripheral lung mechanics present in asthmatic individuals (40). Another study utilised a wedged bronchoscope technique to evaluate the functional significance of parenchymal inflammation in patients with nocturnal asthma, concluding that the distal collateral channels are altered at night in these patients,

exhibiting diurnal variation and high peripheral resistance values at night (41). Other invasive techniques to study the small airways compartment have been explored over the years. Yanai *et al* wedged a catheter-tipped micromanometer of 3mm diameter into the right lower lobe, to divide the central and peripheral airway resistance in different groups of patients. The results demonstrated that patients with bronchial asthma and airflow obstruction, emphysema and chronic bronchitis had an increase predominantly in peripheral resistance and that the airway periphery is the main site of increase airway resistance in patients with established obstructive lung disease (42).

The conducting and respiratory compartments of the lungs differ not only in their structure but also in their cellular composition. Conducting airways from the larynx to the terminal bronchioles have structural components such as cilia, goblet cells and cartilage that surround the cylindrical muscular airway lumen. In contrast, respiratory bronchioles do not contain goblet cells or cartilage. The alveoli epithelium is composed mainly by type I and type II alveolar cells (pneumocytes) (43). The respiratory tract lining fluid (RTLF) is a thin heterogeneous layer that covers the respiratory epithelium and varies along the airway tree. In the distal airways, the RTLF is arranged in a two-phase layer with an aqueous phase containing lamellar bodies and tubular myelin and a superficial layer- the pulmonary surfactant (44). Pulmonary surfactant is a complex lipo-protein substance lining the alveolar surface of the lungs, produced in the alveolar type II cells, and is vital for the normal breathing, alveolar stability and host defence (45,46). During the last few years, the involvement of surfactant and its composition in the pathophysiology of respiratory diseases and its role in immunomodulation has been a particular point of interest.

It is well recognised that airway inflammation and remodelling spreads across the central and small airways and overall lung parenchyma (47). Methods such as post-mortem tissue histological analysis, induced sputum, transbronchial biopsies and imaging methods have shown multiple levels of evidence that the small airways play an important role in the inflammatory process, not only in asthma, but also in COPD, idiopathic pulmonary fibrosis (IPF), sarcoidosis and obliterative bronchiolitis (OB) (48). McDonough *et al* used multidetector CT scans to show a relationship between narrowing and obstruction of the small airway prior to the alveoli destruction caused by emphysema in COPD, which caused increased airway resistance (49). A study conducted by Hogg and colleagues on resected small airways from COPD patients have

provided evidence that inflammatory mucus accumulates in the periphery, leading to airway thickening and remodelling (50). In asthma, a multicellular inflammatory process takes place, involving mast cells, eosinophils, neutrophils, T cells and mediators, cytokines and chemokines, amongst others (51). The inflammatory process in COPD is associated with lymphocyte and plasma cell infiltration. Interestingly, the term "small airways disease" was introduced by Hogg *et al* in an effort to describe all the pathological pathways present in the peripheral compartment in COPD patients, not only inflammatory (52). In interstitial lung disease, the alveoli and peripheral airways are the main site of disease, characterised by parenchymal inflammation, termed alveolitis, fibroblastic proliferation and interstitial fibrosis (53). The involvement of peripheral airways in sarcoidosis is possibly linked to the formation of granulomas with secondary peri-bronchial fibrosis (54).

Despite its scientific and clinical importance in the field, the techniques mentioned in the previous section are only applicable in small scale studies, due to their invasive nature, complexity, cost, time required and potential complications. The need to develop non-invasive methods to assess the small airways in clinical physiology facilities is eminent, not only due to their mechanical involvement but also the biological trait associated. In this thesis, a few novel and non-invasive physiological methods to assess the small airways compartment will be described in detail and further developed.

1.3 Small airways disease and dysfunction

1.3.1 Overview

Exploring the small airway disease is an arduous and complex task in its own right, with different connotations and implications according to different areas of expertise: pathology, pulmonology and radiology (55). As mentioned previously, central and peripheral airways were firstly partitioned by Macklem and Mead in the early sixties. The small airways disease notion was then described by Hogg and colleagues, back in 1968, based on chronic airflow obstruction, loss of bronchioles, presence of mucus plugs, inflammation and fibrosis (52). In fact, Hogg underpinned small airway research largely with immunopathological studies in COPD and recently combined with micro CT studies (56). Other developments have emerged since, based on histological, clinical

and radiological correlations (57). The conditions associated to the small airways according to these classifications identified several types of bronchiolitis, mineral dust-associated airway disease, emphysema, asthma, uncommon conditions such as diffuse idiopathic neuroendocrine cell hyperplasia and non-primarily pulmonary, such as, collagen vascular disease, bone marrow transplantation and inflammatory bowel disease.

Small airway research in asthma will be described further in this section.

1.3.2 Small airway disease and dysfunction in adult Asthma

Definition of asthma

Asthma is a complex, heterogeneous and chronic inflammatory disease of the airways, affecting 1-18% of the population around the globe and 5.4 million people in the UK alone (2,58). The term "asthma" has ancient origins from the Greek word "azein" meaning to breathe hard, but it wasn't until the beginning of the 20th century that the condition was recognised as an inflammatory disease. Although recent statistics show a decrease in the number of deaths due to asthma attacks, and the majority of patients have mild to moderate asthma controlled by inhaled corticosteroids and bronchodilators, this disease is still a significant health and economic burden, more so the fraction of patients with severe asthma requiring high numbers of hospitalisations, rounding about 5 to 10% of the total number of cases (59).

Due to its complex nature, asthma and severe asthma definition has been a challenge and numerous classifications can be found in the literature. The most up-to-date definition by The Global Initiative for Asthma (GINA) report (2017 update) states: "Asthma is a heterogeneous disease, usually characterised by chronic airway inflammation. It is defined by the history of respiratory symptoms such as wheeze, shortness of breath, chest tightness and cough that vary over time and in intensity, together with variable expiratory airflow limitation." (2)

This GINA definition highlights the variable nature of symptoms, inflammation and airway hyperresponsiveness in asthma, which can develop at any age and in association

with many different factors such as genetics, environment and occupational exposure, and can manifest in several distinct phenotypes(60).

In 2009, the World Health Organisation (WHO) gathered experts and resources from all over the world to propose an uniform definition of severe asthma and the outcome states "uncontrolled asthma which can result in risk of frequent severe exacerbations (or death) and/or adverse reactions to medications and/or chronic morbidity, including impaired lung function or reduced lung growth in children" (61).

The heterogeneous and multidimensional nature of this global health problem is unquestionable, and its complex pathophysiological characteristics are still to be fully elucidated.

The understanding about asthma phenotypes and endotypes (underlying biological mechanisms) is of great value (62–64). A disease phenotype is defined as an observable characteristic that must be related to either the underlying genetics, environmental influences or a mixture of both, with no necessarily direct relationship with intrinsic disease mechanisms (64). Several strategies have been used to identify asthma phenotypes, from those related to aetiology, clinical presentation, trigger factors, and pathophysiological characteristics culminating in four well-established clinical phenotypes: early-onset atopic, late-onset eosinophilic, aspirin-intolerant and obesity-related (62), however, others such as exercise-induced and nocturnal asthma are also described. The value of subgrouping asthma in different phenotypes is undisputable, which can lead to better determined and targeted therapies according to one's individualised biology.

Small airways disease and dysfunction in asthma

The clinical relevance of small airways dysfunction in obstructive diseases such as asthma, is still a mix of unclearness and lack of consensus, despite the increase in evidence of its involvement in both early and severe disease (65). In fact, there is evidence of small airways dysfunction in several asthma phenotypes such as nocturnal asthma, exercise-induced asthma and allergic asthma (66–70). However, a specific "small airway phenotype" has been suggested but is yet to be established (71). Moreover, small airways dysfunction might be driven by a pathological disease in the peripheral airway, as for example asthma. On the other hand, dysfunction might be

present due to abnormal lung development and prematurity, without a pathological disease (72).

Several studies have linked small airways dysfunction to asthma symptoms, asthma control, exacerbations and asthma treatment (51), which will be discussed further in this chapter. The idea that asthma is solely a larger airway disease has long been discarded. A recent review article by Postma *et al* refer to 19 studies where small airways impairment was assessed by surgical and transbronchial autopsy samples (73). Post-mortem samples from patient who have died from fatal asthma and control subjects were examined by Carroll *et al*, which revealed the presence of airway eosinophilic inflammation not only in the larger airways, but also in the small airway compartment, accompanied by airway remodelling (74,75). It was concluded that structural changes were predominantly present in the small airways compartment in non-fatal asthma. One might speculate what triggering factors could be associated with this remodelling, such as lack of therapy in the peripheral compartment.

The impact of the peripheral airway compartment in asthma has a close link to airway resistance. As mentioned previously, the small airways account for only about 10% of the total lung resistance, therefore, disease may be spreading and accumulating in the "silent zone" of the lung for a long time before it can be detected by traditional lung function. A study conducted by Perez and colleagues in a large asthmatic population presenting normal forced expiratory volume in 1 second (FEV_1) and FEV_1/forced vital capacity (FVC), showed that more than half of the patients presented small airways dysfunction, measured by forced expiratory flow at 25-75% of vital capacity (FEF_{25-75}), forced expiratory flow at 50% of vital capacity (FEF_{50}), difference between FVC and slow vital capacity (SVC) and residual volume over total lung capacity (RV/TLC) (76).

Asthma treatment is a very important factor for disease progression and control and the small airways may be of great interest, as an area to be targeted with small-particles drug. Most of the currently available asthma therapy inhalers, both dry powder inhalers (DPI) and metered-dose inhalers (MDI) emit large drug particles and achieve poor levels of total lung deposition (around 10-20%) (77). A review article published recently by Usmani shows that some efforts are being made to study the use of smaller inhaler particles of both inhaled corticosteroids (ICS) monotherapy and combination ICS/ Long-acting β-agonist (LABA), citing that over twenty clinical trials were

conducted in the past few years on this subject (78). The take home messages so far are that smaller particles have comparable and in some cases better efficacy, leading to a reduction in the daily ICS dose and greater asthma control and quality of life. But further research and evidence is needed to reach a therapeutic strategy for an effective treatment, with further large clinical trials, comparison between extra fine and non-extra fine therapy and use of advanced physiological and imaging tools available.

Persistent or difficult to treat asthma is not uncommon and represents a serious burden (79,80). These patients lack control optimisation accompanied by high levels of airway inflammation, worsening of symptoms, despite topical therapy, which can then lead to accelerated decline in lung function and early development of fixed airflow obstruction (FAO), largely associated with morbidity. The factors associated with difficult asthma are not fully understood but some evidence points to poor patient adherence (81), inadequate inhaler technique (82) and corticosteroid resistance (83). However, the small airways may be a key factor for this lack of control, particularly patients with airflow limitation not being adequately treated by conventional therapy.

The symptomatology in asthma has been linked to the peripheral airways in various studies and with several tools. Reports from Schiphof-Godart have shown that patients with small airways dysfunction had worst symptoms like wheeze, difficulty in breathing deeply, greater airway hyperresponsiveness and exercise-induced symptoms, when compared to the control asthmatic group (84). Similar results were found earlier by the Kaminsky group, reporting that peripheral airway resistance at baseline correlated with the exacerbated symptoms of exercise-induced bronchoconstriction (69). Cold, dry air can be a trigger for peripheral airway constriction thus worsening of symptoms in asthma, and it has been shown that asthmatic patients have an increase in peripheral resistance after hyperventilation test with cold, dry air (85). Small airways dysfunction induced by cold and dry air could potentially be in the origin of exercise-induced asthma in winter sports athletes, due to repeated peripheral airway hyperpnoea exposure in those weather conditions (86), but further research is needed in the topic.

It appears that disease within the small airways increases the risk of exacerbation frequency in asthma (87,88). However, the mechanism is not entirely understood and the well-established risk factors for increased number of exacerbations are: history of severe exacerbation (especially in the previous 6 months), uncontrolled asthma

symptoms, low FEV_1, poor inhaler technique/adherence, smoking, obesity, pregnancy and blood eosinophils (2). Evidence suggests that peripheral airways resistance is increased in asthmatic patients undergoing an exacerbation and elevated closing volume (CV), closing capacity (CC) and ventilation inhomogeneity demonstrated by nitrogen washout (89,90).

Despite the increasing evidence of the small airways involvement in asthma progression, symptoms and control, there is still a lack in the asthma recommendations specifically dedicated for this burden (91), not only in targeted therapies but also in specific tools and methods to assess small airways dysfunction, which will be explored in the next section of this chapter.

1.4 Physiological methods to assess small airways

1.4.1 Gold standard methods

Spirometry

Ideally, an optimal test able to explore small airways dysfunction in clinical settings would be readily available, non-invasive, easy to perform by the patient and analyse by the operator/ clinician, requiring only passive cooperation from the patient (i.e., tidal breathing) , with strong reference values in order to compare results across different sites. To date, the most readily accessible methods to study small airways non-invasively are still the spirometric measurements, requiring forced expiratory manoeuvres (92). Its wide availability, basic equipment requirements and easy usage makes it an attractive method. However, the main indices derived from spirometry: FEV_1, peak expiratory flow (PEF) and FEV_1/FVC ratio reflect mostly variability or reversibility of airway obstruction and there has been an extensive search for a spirometric parameter that reflects the small airways compartment specifically (93). Mathematical models described in the recent years, have shown that the first 1.5 seconds of the forced expiratory curve reflect primarily the contribution of the wave

speed limitation, attributed to the first 4 generations of the airways tree. The second portion of the flow limitation occurs after 1 second and moves distally in the airway, due to the frictional and turbulent dissipation of gas energy (94). It is then irrefutable that FEV_1 reflects mainly the calibre of the central airways, though, there may be other alternative spirometric indices that could give some information about the periphery.

Undoubtedly, the index derived from spirometry that has been linked to the periphery more often is the mid portion of the maximal expiratory flow-volume curve (MEFV), also known as FEF_{25-75}. Indeed, this value has formerly been considered a marker of small airway obstruction (95) but it has also been a target of extensive debate and critique. In theory, a forced expiration in a partially obstructed airway would trigger partial and premature collapse at a point closer to the alveolus, which could then be assessed with lung volumes below 50% of the vital capacity, affecting primarily the FEF_{25-75}. While the theoretical grounds are certainly correct, FEF_{25-75} usefulness has been target of various critiques due to its wide normal range and poor discriminatory ability (96). Moreover, Gelb *et al* have shown that in the presence of normal FEV_1/FVC, FEF_{25-75} is also within normal range, discarding its ability to detect early disease (97). FEF_{25-75} is usually considered abnormal when below 75 to 80% and in some cases lower, which can potentially lead to lack of diagnosis, and the recommendation is to use the 95% confidence limits to find the lower limit of normal (LLN). Having said that, the number of false-negative results is still high using 95% confidence of FEF_{25-75}, especially in older adults (>60year old) (96). Thus, FEF_{25-75} is far from being the gold standard index to evaluate small airways dysfunction and therefore, it will not be used as a comparison or reference in the work developed in this thesis. On the other hand, direct link between biomarkers and indices explored with different clinical outcomes will be utilised.

Another spirometric index that has recently been acquiring some interest is FEV_3/FVC, the fraction of the FVC that had been expired during the first 3 seconds of the FVC. In the early 80's, two groups (Crapo *et al* and Miller *et al*) have made efforts to publish reference equations to include FEV_3 and FEV_3/FVC, in order to overcome the high variability and usage of <75 to 80% of the FEF_{25-75} predictive values (98,99). To confirm that in a population of smokers [from the National Health and Nutrition Examination Survey (NHANES III)] FEF_{25-75} would misidentify normality and true peripheral expiratory limitation, Hansen *et al* utilised FEV_3/FVC to characterise

expiratory obstruction. However, one of the limitations was that this study was far from covering the heterogeneity of the overall population (96). Morris *et al* have recently suggested that FEV_3/FVC might represent a marker of early lung injury (100). A small group of subjects with isolated reduction in FEV_3/FVC (preserved FEV_1/FVC) presented hyperinflation, air trapping and loss of diffusing capacity of the lung for carbon monoxide (DLCO), which shows its potential value on identifying patients with very mild and early airway obstruction. Over a thousand patients were included in a study recently conducted in Turkey by Börekçi and colleagues, looking at the diagnostic added values of 1minus-forced expiratory volume expired in 3 seconds/FVC (1-FEV_3/FVC) in small airways dysfunction and air trapping (101). The results were extremely interesting, with mean 1-FEV_3/FVC of 4.9% in patients without fixed airflow obstruction and 24.1% in the group with fixed airflow obstruction, reflecting its potential value on peripheral airway investigations.

The ratio of FVC to SVC might hold some valuable information about the periphery and expiratory air trapping, and investigation have taken place to validate its utility (102). The authors chose a population with OB after lung transplantation (disorder that affects predominantly the small airways), where FVC/SVC was measured cross-sectionally and longitudinally. Decreases in FVC/SVC were found significantly higher in patients with OB, however the median percentage change was only -4.4 compared to -39.0 for FEV_1 and -72.4 for FEF_{25-75}, which undermines the overall results and overall usefulness of the index. Another variant of this parameter is the FEV_1/SVC. Barros *et al* studied the presence of airway obstruction in over 1000 patients, assessed by FEV_1/FVC and FEV_1/SVC (103). Results showed that the latter identified a larger number of individuals with airflow obstruction, which could lead to a better and early diagnosis in obstructive lung diseases, such as asthma.

Other investigations have taken place along the years with few indices derived from the moments of the spirogram, such as mean transit time (MTT) and moment ratio (MR). These indices have the advantages of their broad description of the spirogram, not being limited by the size of the lungs (volumes) and focus on prolongation of expiratory time, where variability is greater, and more information can be derived (104,105). However, these parameters are yet to be linked to the small airways.

FVC might be currently the favourite candidate to assess the gas trapping due to peripheral airways dysfunction by simple spirometry. Its relationship to airway obstruction and air trapping has been studied over the years. Sorkness *et al* evaluated spirometry in a group of severe and non-severe asthmatics, reporting a pattern of air trapping (significantly higher RV/TLC) in those with compromised FVC, when compared to the non-severe group (106). Moreover, fall in FVC during methacholine challenge test has also been suggested to better characterise airway narrowing in the periphery, rather than the typical 20% fall in FEV_1 (PC20), which varies greatly between asthmatic subjects (107–109). Papi *et al* conducted a double-blind, randomised study in over 220 patients with mild to moderate asthma, to compare two combination therapies: beclomethasone dipropionate (BDP)/ formoterol or fluticasone (FP)/ salmeterol. They identified a greater FVC improvement in the patients receiving extra-fine combination (BDP/formoterol), indicating that these drug particles potentially reached peripheral airways, accounting for improved efficacy (110). Increased airway closure and airway hyperresponsiveness have been linked to small airways disease, which in asthma is associated with recurrent exacerbations (111). In summary, FVC changes can be utilised as a marker of airway closure, which are more sensitive and periphery-specific than FEV_1.

Lung volumes

As mentioned in the previous section, one of the small airway disease manifestations is the accumulation of air trapping in the periphery, which can be detected not only by a compromised FVC but also with sensitive parameters provided by lung volume measurements such as body plethysmography or helium dilution: RV and its proportion to the total lung capacity (RV/TLC) (24,112). For instance, Jain *et al* demonstrated that, in an asthmatic population, RV correlated significantly better with FEF_{25-75} than FEV_1 and presence of abnormal RV/TLC ratio, in the presence of normal FEV_1/FVC and no significant bronchodilator response (113). Similarly, Perez *et al* conducted a study to look at the prevalence of small airways obstruction in a group with asthma, defined by the presence of either: functional Residual Volume (FRC)> 120% predicted, RV> + 1.64 residual standard deviation (RSD), RV/TLC> + 1.64 RSD, FEF_{25-75}< – 1.64 RSD, FEF 50<– 1.64 RSD, SVC-FVC> 10%, as previously stated (76). Their results pointed

again for the importance of the use of lung volume parameters, which were abnormal before the onset of abnormal spirometric indices, and present in over half of the patients with preserved FEV_1 and FEV_1/FVC. Two studies conducted by Kaft *et al* showed that RV correlates with peripheral airway resistance in asthma (measured by wedge bronchoscope) and that treating a group of patients with asthma with montelukast improves air trapping (reduces RV) without any change in spirometric values (67,114).

The ratio of single breath lung volume (measured by helium dilution) over total lung capacity (measured by an alternative method such as plethysmography) [alveolar volume (VA)/TLC] represents an index of ventilation distribution, the proportion of the lung volume that is poorly ventilated, reflecting the patch of ventilation effects (115). Huang and Que have recently demonstrated in an abstract that abnormalities in VA/TLC, either raised (air trapping) or decreased (ventilation maldistribution), were identified in the absence of changes in FEF_{25-75} or RV/TLC (116). That said, it is likely that this parameter once again represents the airways overall, not only the periphery.

Airway resistance measured by body plethysmography (R*a*w) may also play an important role in detecting increased obstruction and response to bronchodilator, with higher sensitivity than spirometry (117). Then again, this parameter represents the entire airway tree resistance, which limits its applicability in the study of isolated small airway dysfunction (9).

1.4.2 Forced oscillation methods

FOT, firstly described by DuBois and colleagues during the fifties (118), is a technique that uses externally applied pressure signals and resultant flows to determine lung mechanical parameters, delivered by a computer-driven loudspeaker or piston, to the respiratory system during normal tidal breathing (10). This technique assesses the impedance (Z) of the airways to air flow by measuring pressure (P) and flow (Q) at the mouth, which are then used to calculate the ratio of pressure and flow at each frequency. Z, the sum of all the forces opposing the pressure impulses, comprises of a resistive component (R), which describes the in-phase (real) component of P/Q, and reactance (X), which describes the out-of-phase (imaginary) component of P/Q. FOT can be used

to assess Z over a wide range of frequencies, typically from 5 to 35Hz. Resistance defines the dissipative mechanical properties of the respiratory system and reactance is related to the energy storage capacity (elastic properties and inertive forces) (119).

This technique is linked to various advantages in clinical practice: it is simple, quick, non-invasive and only requires passive co-operation from the patients, which represents a step forward when it comes to access lung function in adults with physical and cognitive limitations in clinical environments (120). Moreover, a large percentage of elderly adults cannot perform spirometry within the acceptable and repeatable ATS/ERS criteria and can be time consuming (121).

IOS is a type of FOT, with small differences regarding the impulses applied (rectangular waveform impulses rather than a pseudorandom noise signal) and the data output (122), developed later in the seventies by Michaleson *et al* (123). In this variant, the waveform delivered is an impulse that is mathematically decomposed to a continuous spectrum of frequencies, rather than a sine wave at a single frequency or a combination of sine waves at multiple discrete frequencies (124). IOS has emerged and has been used as a measurement of pulmonary function in paediatric populations, however, its value as a measurement of airway obstruction in adult population is still debated (125). A number of indices of resistance are derived from forced oscillation techniques, representing a combination of oropharynx, larynx, trachea, large and small airways as well as lung parenchyma and chest wall: for instance, resistance at 5Hz (R5) representing the total airway resistance; resistance at 20 Hz (R20) representing mainly the larger airways (126). Resistance is always positive and nearly independent of oscillation frequency in health (between 5 and 35 Hz). However, in the presence of airway obstruction, central or peripheral, R becomes disproportionally increased. Peripheral obstruction will lead to increased resistance at low frequencies, the so-called frequency-dependence of resistance (119,124). Thus, subtracting R20 from R5 (R5-R20) constitutes another valuable parameter, which has been associated with the small airways compartment. Studies have shown a link between R5-R20 and small airways inflammation (11), exacerbations (12) and response to small particle formulation inhaled steroids in adult asthma (13), which will be discussed in greater detail in this section. Theoretical models have been developed in order to explain this phenomenon, attributing heterogeneous ventilation time constants between parallel lung units and non-linear viscoelastic properties of the airways, and neighbouring tissues, as trigger

factors (127–129). Hantos *et al* conducted pioneering research in the field using a oesophageal balloon technique in 5 healthy volunteers during apnoea, in order to divide low-frequency resistance (0.25 to 5 Hz) into pulmonary and chest wall compartments (130). Their results showed that frequency dependence of resistance was associated with mechanical properties of the chest wall, therefore, another triggering factor to be considered. On the other hand, increased resistance in the central airways leads to an increase in both R5 and R20 simultaneously, with no visible frequency dependence of resistance.

Reactance (X or Xrs) includes the mass-inertive forces of moving air column (inertance) and the elastic properties, known as compliance of the lung periphery, expressed as capacitance (C), closely associated with the capacity of the respiratory system to store energy (131). X, defined as inertance minus 1/capacitance, depends on frequency and therefore increases from being negative (elastive) al low frequencies to positive (inertive) at high frequencies, where large airways play a dominant influence. Therefore, Xrs sign can be positive or negative depending on the phase relationship between the pressure and flow signals. Reactance at 5 Hz (X5) is an important index associated with capacitance, which has a close link to peripheral airways and becomes more negative in the presence of small airway disease. The resonant frequency (Fres) is the oscillation frequency at which reactance is zero, when flow and pressure are perfectly in phase and forces transition from capacitive to inertive dominance at higher frequencies. Frequency dependence of resistance leads to increased Fres, which in normal subjects is approximately 8-12Hz (119). The integrated low-frequency reactance between 5Hz and the resonant frequency is known as area of reactance (AX). This index is closely correlated with R5-R20 which will become increased with changes in the small airway patency and compliance (124).

Despite the potential clinical value of forced oscillation techniques as small airway dysfunction detection tools, to date there has been no definite validation. Research in the area strongly suggests that the variation in resistance is heterogeneous, continuous and dependent upon changes in the airway diameter and smooth muscle, however, is not clear how alterations in the airway diameter in a multi -branching tree can trigger these changes (132). The multiplicity nature of factors involved in the forced oscillation outcomes contributes to the challenge of technique establishment. The ‘constant phase model’ is the most widely-used inverse model to understand the factors contributing to

impedance (133). However, this model has limitations, such as taking into account only the viscoelastic properties of the airway, disregarding heterogeneous airway constriction (127). Models based on computational algorithms are promising, only limited by the computational power. Image-functional modelling links FOT with an imaging platform, such as helium MRI (^{3}He-MRI) and high resolution computed tomography (HRCT) scans to understand ventilatory defects and interactions between serial and parallel airways, and small airways involvement (134,135).

Research utilizing forced oscillation techniques in asthma is ongoing and growing. Recently, Galant *et al* have published a comprehensive review on impulse oscillometry as part of asthma management in adults and children (136). In the younger populations, IOS shows superiority in relation to spirometric indices at predicting loss of asthma control. In adults, IOS is seen as a complementary tool to FEV_1 in assessing peripheral airway obstruction, but further work is needed to reach a consensus on IOS reference values, applicable to the broad population.

Manoharan *et al* compared IOS and spirometry in terms of valuable diagnostic information and their indices' relationship to oral steroids and inhaled shot-acting β-agonist (SABA), in over four hundred patients. Once more, both techniques were complementary in their usefulness as markers of asthma control in persistent asthmatic patients, on oral steroids and SABA (137). Likewise, Jung-Won Park *et al* found that IOS parameters [R5, Resistance at 10 Hz (R10) and R5-R20] distinguished between individuals with asthma and controls (138). Moreover, resistance decreased after bronchodilator in asthma and had similar diagnosis of bronchodilation to FEV_1. Other studies have shown that resistance derived from forced oscillation techniques is sensitive to various degrees of bronchodilation, in both asthma (139) and COPD (117). Hozawa *et al* compared two groups of asthmatic patients, one undergoing treatment with budesonide/ formoterol (BUD/FM) and the other fluticasone/formoterol (FP/FM), for four weeks (13). Patients on BUD/FM presented significantly improved small airways outcomes measured by IOS, as well as improvements in fractional exhaled nitric oxide at 50ml/s ($FeNO_{50}$) and asthma control questionnaire (ACQ). This may suggest that BUD/FM particles reach the small airway compartment better. Gonem and colleagues have however reported dissimilar results (140). R5-R20 and AX were not significantly different between patients with mild and severe asthma and didn't correlate with asthma outcomes, which could have been due to the fact that measurements were

performed after bronchodilator, eliminating the proximal airway tone impact on small airways.

The issue of effort-dependency often faced when assessing respiratory mechanics with spirometry is without a doubt a limitation. Research has shown a significant increase in airway resistance parameter in severe asthma, compared with moderate status and control subjects, which supports the use of FOT methods to assess changes in respiratory mechanics, especially when spirometry isn't a valid option (141). However, detailed inspection of the test output is mandatory, as glottis closure during the forced oscillation measurements has been shown to increase R5 and affect measurement results (142).

Anderson and colleagues analysed a population with mild to moderate asthma, who underwent Spirometry (FEV_1, FEF_{25-75}) and IOS (R5, R5-R20, Fres), in order to assess the degree of small airways dysfunction. Results showed higher R5-R20 in GINA step four patients, when compared to patients in lower GINA step treatments. What was more interesting were the significantly lower values of R5 in patients receiving extra-fine ICS inhaler when compared to standard ICS therapy, superior to FEV_1, which showed no differences, enhancing the potential role of oscillometric parameters in early peripheral dysfunction detection (143).

Forced and impulse oscillation techniques are potentially a valuable tool to detect early disease not only in asthma, but other conditions such as COPD. Saadeh *et al* have recently demonstrated in a COPD population that IOS parameters, especially AX and R5 decreased significantly after bronchodilator and follow-up, with unaffected FEV_1 (144). Lung function follow-up on patients after lung transplant is often difficult with normal spirometry. Hamakawa *et al* have shown that FOT is useful in assessing lung periphery in those patients, giving insights on acute rejection and response to therapy (145). Inspiratory minus expiratory resistance and reactance has been a parameter of interest in recent years. Paredi and colleagues have shown that ΔX5 (inspiratory-expiratory) differentiated patients with asthma and COPD, which might indicate greater peripheral airway narrowing in the latter group, but further research is needed (146).

Gonem and colleagues found that impedance measured by IOS was associated with asthma exacerbations, and its predictive value, by means of entropy algorithm

measurements (12). Moreover, the group found that sample entropy of R5-R20 was the parameter better associated with the group with frequent exacerbations phenotype.

Even though FOT and IOS techniques have similar outcomes and have been used in an alike manner, it is unclear whether the use of different oscillation techniques leads to different impedance outcomes and to date, very few studies have compared FOT and IOS. Tanimura and colleagues have compared IOS with MostGraph (MG) FOT technique, using phantom models, and concluded that the two devices did not generate identical results (147). Similarly, Hellinckx *et al* analysed impedance across 3 different devices: IOS, classical FOT and body plethysmography in a small population, concluding that the values provided by both oscillation techniques were similar but not identical and different from plethysmografic resistance (148). However, larger-scale studies and in disease are lacking.

Ideally, different FOT and IOS apparatus would be capable of generating matching results, which would be comparable across different sites and clinical settings, with a unique set of reference values that could be used unanimously. However, this is yet to be achieved.

1.4.3 Multiple breath inert gas washout

Ventilation heterogeneity (VH) is the inhomogeneity and unevenness pattern of ventilation distribution in the airways and is a fundamental characteristic of lung function in asthmatic and COPD patients, where gas mixing is reduced. The pathophysiology process behind VH in asthma is associated with increase in labile airway tone, regional air trapping, end-expiratory airway closure and shift in distribution of ventilation to apex, which leads to the formation of lung filling defects and independent airway responses (149). VH can be measured non-invasively using the single or multiple breath gas inert washout (MBGW or MBW), described in the fifties by Robertson *et al* (150) and a comprehensive standardisation document for the multiple breath inert gas washout test has been recently published (151). Three main indices can be derived from MBW. Lung clearance index (LCI), representing the overall ventilation heterogeneity, that can suggest generalised or regional variations in ventilation. LCI is defined as “the number of turnovers [(TO) (multiples of FRC)]

required to clear the lung of the inert gas marker to 1/40th of the initial concentration" (151). Scond and Sacin represent the conductive (flow-dependent) and acinar (diffusion-dependent) components of ventilation, respectively, terms adopted by Verbanck *et al* (152). These terms were first described as convection dependent inhomogeneity (CDI) and diffusion convection dependent inhomogeneity (DCDI), correspondingly (153). Scond and Sacin are derived from the analysis of the phase III inert gas washout slopes, believed to represent the alveolar phase, which is influenced by the two mechanisms CDI and DCDI. A rapid rise in the slope in the initial five breaths is characteristic of disease at the periphery.

Different inert gases with different properties have been used for the MBW test, including sulphur hexafluoride (SF_6), helium (He) and nitrogen (N_2) (only required for the washout, and oxygen during wash-in phase). These gases are not absorbed by the alveoli, but their concentration during the test is used to calculate the indices mentioned previously, usually with mass spectrometer. Diffusion with He is more proximal than SF_6, hence the latter is better suited to study peripheral airway abnormalities.

Gonem *et al* have recently validated a SF_6 photoacoustic gas analyser for the measurement of MBW, as an accurate and repeatable method for the measurement of FRC (154) and further developed LCI ventilation measurement with two novel parameters LCIds (respiratory dead space) and LCIvent (ventilation inequality) (155). These studies were conducted using an Innocor^{TM} device that uses photoacoustic spectroscopy to evaluate SF_6 washout curves. Horsley *et al* used the same technique in control and cystic fibrosis (CF) subjects (children and adults), showing a superior signal:noise ratio and reduced greenhouse gas when compared to a mass spectrometer device (156).

MBW techniques have been mainly used in CF populations. That said, several studies in adult asthma have emerged in the last few decades using MBW, which was mainly utilised in children in the early days (157,158). Evidence of VH was found in a study conducted by Verbanck *et al*, where patients with asthma demonstrated only partial reversible acinar impairment (even with normal diffusing capacity), as opposed to no reversibility observed in COPD patients, after inhalation of salbutamol (159). Likewise, a group studied if MBW indices of ventilation heterogeneity were more sensitive than FEV_1 in detecting peripheral airway disease in children, before and after salbutamol or placebo (160). LCI remained high after bronchodilator, despite a positive change in

FEV_1, therefore, LCI was a more sensible detector of residual VH and early (peripheral) disease. Gustafsson and colleagues assessed VH in a paediatric population pre and post salbutamol; their findings revealed that only Scond remained abnormal post BD, suggestive of peripheral conducting airways inflammation (161). Another study by Verbanck and colleagues have shown that in mild adult asthma, reversibility was observed with the Scond index, revealing early markers of VH in the small conductive airways (162).

Clinical significance of VH was assessed by Farah *et al* in an adult asthma population (163). Patients demonstrated an improvement in VH markers (Sacin, Scond) three months after high-dose ICS treatment, which matched improvement in symptoms and ACQ and revealed its usefulness in monitoring small airway function as a response to therapy. Another study by the same group showed that VH predicts clinical response to ICS therapy (improved symptomatology), and that small airways dysfunction predicts symptomatic improvement to increased ICS dose (164). Similarly, Thompson *et al* have shown in asthmatic individuals undergoing exacerbation, that abnormalities in the acinar area were significantly increased (when compared to stable subjects) and directly correlated with airflow obstruction (FEV_1), with marked improvements after therapy (165). Moreover, a study found significant correlations between raised Sacin and raised alveolar nitric oxide levels, in asthmatic patients on high doses of ICS, which supports strategically targeted therapy to the respiratory bronchioles and distally (166).

VH abnormalities in MBW tests have been described in other disease modalities such as COPD , airway-hyper-responsiveness (167) and lung transplant studies (168). Research has shown evidence that therapy with LABA doesn't affect MBW markers in COPD patients, even with spirometric and inspiratory capacity (IC) improvements (169). However, other studies revealed that MBW distinguishes healthy controls and COPD patients, as well as separation amongst COPD subjects based on smoking pack year history (170), emphasising the importance of early detection to empower smoking cessation.

In sum, MBW modalities have great potential to assess small airways dysfunction and VH in asthma. Yet, these techniques are still limited to specialist centres and test analysis is time consuming and a globally accepted analysis tool is lacking. Moreover, studies have used different inert gases, which could account for the differences

encountered in some studies, as well as the fact that measurements are performed both before and after bronchodilator in different investigations.

1.4.5 Imaging

Modern imaging methods have contributed greatly to reach a better understanding of the structural attributes of ventilation heterogeneity and assessment of severe asthma (171,172). Understanding the small acinar airways branching pattern is of great value, and numerous studies have used different techniques to do so. Binocular dissecting microscope was used by Horsfield and Cumming in the sixties, showing that the branching pattern within lobules was more symmetrical than in more proximal airways and that the branching pattern from proximal to distal airways was a symmetrical dichotomy, where number of branches in each generation increase by a factor of 2 with each division (26,173). Stereology was a different technique used by Weibel *et al*, showing that the calibre of small acinar airways reduce to a much lesser extend with each generation, when compared to the larger airways (174). Novel advances in non-invasive imaging have strengthened the study of morphological changes and structure and anatomical function relationships in the periphery. In the recent years Micro Computed Tomography (Micro-CT) scan has gained popularity with studies in resected lung specimens, and interesting results have been originated, regarding branching length and diameter across different generations (175).

HRCT technology has been used to assess function, air trapping and airway geometry in patients with asthma, COPD and other airway diseases (176,177). Currently, only the first six generations are reached with HRCT, thus the small airways compartment cannot be visualised directly with a HRCT. However, airways with a diameter of 2-2.5mm and above can (178), even though problems related with artefacts and cardiogenic oscillations may be encountered. Each voxel displayed in a HRCT image corresponds to its specific attenuation, which are then changed to voxels in a three-dimensional space. Attenuation is measured in Hounsfield Units (HU), from -1024 (low attenuation) to +3071 (high attenuation). In normally ventilated lungs, attenuation will increase during expiration, with decreased air volume. However, small airways disease will generate areas with air trapping, which will show lower attenuation (<-850 HU) on expiratory CT (179). Another index that measures air trapping is the mean lung density

(MLD) [Expiratory to Inspiratory (E/I) ratio], enabling the analysis of the volume expired from the total volume inspired and extent of air trapping (180).

Several studies have explored correlations between HRCT and physiological measurements (181,182). Ueda *et al* have evaluated lung density, clinical and physiological outcomes in a population with asthma, finding a strong correlation between $MLD_{E/I}$, spirometric values and RV/TLC, suggestive of small airways disease (180). Another group found that decreased lung density during asthma exacerbations is reversible and related with spirometry (183). Bussacker *et al* conducted one of the larger studies on air trapping, showing that quantitative HRCT and air trapping markers are valuable tools to identify a phenotype of patients with high risk of severe disease, associated with several risk factors such as: pneumonia, neutrophilic inflammation and atopy (176). Research has shown a positive change in air trapping after ICS therapy in mild and moderate asthma (184,185). Hartley and colleagues have found significant correlation between $MLD_{E/I}$, spirometric parameters and RV in a population with COPD, concluding that emphysema and small airways status contribute independently to disease severity (186). Galbán *et al* have recently developed a technological platform based on HRCT to identify different disease phenotypes, the parametric response map (PRM) (187). PRM represents an attractive tool to identify disease extent, providing singular resolution and differentiation between individuals with emphysema and functional small airways disease (fSAD).

Modern HRCT methods have contributed greatly to reach a better understanding of the structural attributes of ventilation heterogeneity in asthma, however, these techniques are associated with a number of limitations: use and exposure to ionising radiation and lack of functional data. Gas trapping is not a specific diagnostic tool for small airways disease and other diseases such as pulmonary vascular disease presents mosaic attenuation patterns (188).

Other imaging approaches such as positron emission tomography (PET) or ^{3}He-MRI have been utilised and multi-scale mathematical models have been derived to investigate the relationship between imaging measurements and disease severity (189). Gonem *et al* have recently shown that in asthmatic patients, Sacin is strongly associated with increases in long-timescale apparent diffusion coefficients (ADCs) obtained from hyperpolarised He diffusion. This finding suggests that SF6 derived Sacin is a potential

measure of structural asymmetry within the acinar airways. Moreover, patients with high Sacin in this study were more likely to have severe asthma and fixed airflow obstruction, but further research and longitudinal studies are needed (190). Another key crucial obstacle to remember with hyperpolarised MR imaging is the requirement of costly polarisation equipment and specific apparatus (191).

Oxygen-Enhanced MRI

Oxygen-enhanced magnetic resonance (OE-MR) imaging was originally proposed in 1996 as a technique to evaluate regional ventilation using molecular oxygen as the contrast agent (192). Molecular oxygen contains two unpaired electrons and is weakly paramagnetic. When oxygen is exchanged between air in the alveoli and parenchymal tissue water and blood in the capillary beds, the oxygen does not only couple to haemoglobin but also dissolves as molecular oxygen in the blood plasma and tissue water (18). Since oxygen is paramagnetic, the dissolved molecular oxygen then shortens the T1 (longitudinal relaxation time) leading to a detectable signal change.

OE-MR imaging of the lungs represents a unique method for obtaining regional ventilation-related information by monitoring the delivery of elevated levels of inspired oxygen to the exchange tissues of the lung.

OE-MRI offers the possibility to assess lung function in three different forms. Ventilation is essential for oxygen-induced reduction of T1 relaxation. Signal enhancement is reached with diffusion of oxygen between the alveoli and blood capillaries, in an intermediate phase. Finally, pulmonary vascular perfusion leads to reduced T1 values as oxygen can shorten T1 relaxation in the blood phase (192,193). Therefore, T1 signal during OE-MRI represents MRI signal in voxels averaged from the lung parenchyma and blood phase (194,195).

Parameters derived from dynamic OE-MRI include changes in O_2 partial pressure (ΔPO_2), wash-in and washout time constants of ΔPO_2 (Tup and Tdown, respectively), and enhancing fraction of the lung (EnF) (191). Studies have shown that ΔPO_2 correlates with arterial PO_2, with T1 shortening values correlating with arterial blood oxygen pressure (196).

Despite being a recent technique, some investigators have asserted the potential for clinical application of dynamic oxygen-enhanced MR imaging for evaluation of

regional ventilation and oxygen, applying this technique in normal ventilation (193,196,197) and several lung conditions with ventilation abnormalities (194,198,199), cancer (200), cystic fibrosis (201) and interstitial pneumonia (198).

A study conducted by Kershaw *et al* investigated ΔPO_2 in a group of healthy controls and asymptomatic smokers (202). Regardless of the limited number of patients included, their results showed important differences in the ΔPO_2 curve shape and height between groups, potentially due to worst lung function in the latter group.

The functional diagnostic value and the additional regional ventilation patterns offered with OE-MRI have started to be explored in patients with obstructive small airway diseases such as asthma and COPD (203,204). Ohno *et al* investigated the efficacy of OE-MRI and HRCT to assess function and disease classification in asthma, concluding that both are promising and effective in a similar manner. FEV_1% predicted showed correlation with all enhancement parameters from MR imaging and mean lung density and body surface area derived from CT scans, in different asthma clinical stages. However, these observations were derived from static O_2 signal enhancement, rather than dynamic and quantitative measurements, which reflect better lung function status (203). Zhang and colleagues have recently conducted a preliminary study involving four mild asthmatic patients and six severe asthmatics, utilizing dynamic OE-MRI. Their results demonstrated feasibility and sensitivity to severity in these patients across a wide range of OE-MRI derived parameters, as well as good intra-observer agreement in data analysis (191). Results showed significantly smaller enhancing fraction, and maximal ΔPO_2 change in the severe asthmatic group, as well as larger interquartile range for Tup. Moreover, imaging readouts had good correlation with lung function.

Morgan *et al* utilised dynamic OE-MRI in a group of COPD patients, randomised to two different groups (placebo and single-dose inhaled formoterol 9 mcg), and a further scan 8 week after treatment with either budesonide /formoterol or formoterol alone (20). Both single dose and 8 weeks treatment led to changes on the OE-MRI parameters, such as increased oxygen extraction (EoxFb), increased lung oxygenation time and lung washout time (Tdown).

In the last decade, McGrath *et al* have developed a novel physiological two-compartmental model of gas mixing and ventilation heterogeneity derived from dynamic OE-MRI data. The model describes a number of parameters associated with

gas delivery and transport in the airways, and associated diffusion and gas transfer across the alveolar capillary membrane in the small airways (205). The novel parameters include Kox, relative to the diffusing capacity of the alveolar membrane; EoxFb, the effective rate of blood flow in the capillaries and Tvent, the effective mixing time of oxygen from the mouth, via the conducting airways and into the bronchioles. This model has been applied to a group of healthy controls and smokers, detecting important changes in the new derived parameters in the latter group, that weren't present in parameters utilised so far or spirometry, suggesting airway inflammation, oedema at the alveoli and reduced perfusion.

Comparatively to hyperpolarised gas imaging, either with ^{3}He or 129-Xenon (Xe), OE-MRI offers numerous advantages: oxygen is easily reached and found in MR facilities; oxygen ventilation technique provides ways to directly study oxygen uptake from the air space to the pulmonary blood system and is extremely cost-effective, without expensive equipment and gas requirements, such as specialised radiofrequency transmitter/receiver coils (206). Yet, the number of studies using OE-MRI in asthma and COPD are very limited and more research and validation is required.

1.5 Breath inflammatory markers of small airway disease

1.5.1 Overview

The multicellular process involved in asthma inflammation has been a target of extensive research and debate over the years and several inflammatory markers originated from various invasive or semi-invasive techniques have been selected. As previously mentioned in this introductory section, biopsies have been utilised in the past to study this process, being one of the few methods where it is possible to analyse parenchyma from the peripheral airway tissue. However, the information obtained from a lung biopsy is not a black and white clear answer, especially in patchy heterogeneous disease, where the sample may miss the area with inflammation. Moreover, the eminent risks associated with the procedure leads to an individual decision, therefore, far from being an ideal small airway dysfunction biomarker (207). Blood and sputum specimens are often collected from asthmatic individuals to assess inflammation. Increased blood

eosinophils are associated with severe and late onset asthma (208), and other inflammatory processes related with increased airway vascular leakage have been studied with serum (209,210), but not fully comprehended. Sputum inflammatory cells may provide some information on the periphery status and several protocols have been proposed over the years (211,212). Yet, several issues have been associated with this techniques, despite its use in asthma management (213), such as reproducibility, standardisation, unknown dilution, lack of specificity regarding the small airway compartment, time consuming and expertise-demanding techniques and potential patient discomfort during the procedure (214). Likewise, bronchioalveolar lavage (BAL) methods have been associated with standardisation problems (215); the fluid recovered from BAL contains both cells and acellular components mainly from the respiratory section, however, the instilled solution recovered and dilution factor varies, may be contaminated with blood and its origin is uncertain. Additionally, even though it is a safer procedure than a transbronchial biopsy, complications may arise, and anaesthetic may be required.

The history of modern breath analysis started during the 18th century, with the first efforts coming from Lavoisier and his interest in oxygen and carbon dioxide (216). Certainly, the air we exhale every minute contains thousands of different compounds and more than five hundred volatile organic compounds (VOCs) have been detected in exhaled breath, endogenous and exogenous. The most widely used and validated molecule in asthma is the nitric oxide (NO), which is an established valuable tool for asthma diagnosis and management (217). Furthermore, the study of non-volatile compounds is unequivocally vital as well. Whenever we breathe, cough, speak or sneeze, aerosol particles are formed in the airways and leave the body by exhalation (218). To date, exhaled breath condensate (EBC) has been the preferred and most explored method to collect non-volatile particles, however, there are a number of limitations associated with this condensation method.

1.5.2 Breath analysis in asthma

Asthma is a multifaceted inflammatory disease presenting multiple and variable features. The development of a platform with readily available data from multiple analytical methods and biomarkers in a clinical environment represents the ultimate goal in asthma diagnosis, management and treatment optimisation. While the achievement of this type of approach is still far from being reached, research towards it is most certainly taking shape. A biomarker is "almost any measurement reflecting an interaction between a biological system and a potential hazard, which may be chemical, physical or biological. The measured response may be functional and physiological, biochemical at the cellular level, or a molecular interaction" (219). Moreover, a biomarker needs to be reliable, repeatable and stable. Several technologies are being explored for the biomarker discovery in asthma, in diverse 'omics areas: genomics, transcriptomics, proteomics, lipidomics, metabolomics and breathomics (220). These methods aim to acquire large-scale datasets from a single sample.

The study of breath has the advantage of being non-invasive and potentially a simple and a rapid diagnostic method. Breathomics (or breath metabolomics) is the term utilised to describe the measurement of VOCs in breath samples. Lawal *et al* have recently publish a review article on exhaled breath analysis across different VOCs collection techniques (221). They found over a hundred original articles, presenting a miscellaneous of different breath sampling portions, containers used for collection and pre-concentration methods. Thus, the main setback in the establishment of standardised methods for VOCs sampling and analysis is its variety across different sites. The end-tidal breath air collection is more popular than late-expiratory breath or mixed expiratory breath, mainly due to its close link to the alveolar air and high concentration of endogenous VOCs. The electronic nose (eNose) is a method gaining increased popularity, which is a cheaper and easier alternative than the gold standard gas-chromatography coupled to mass spectrometry. Research utilising these methods suggests that asthma and healthy controls can be distinguished with accuracies of 80-100% (222), and differences have been shown between asthma and COPD (223). Yet, a further validation between different eNose devices is crucial for correct mapping, with identical sensors and same responses. Other VOCs profiling studies in asthma have shown great potential and promising outcomes. Smolinska *et al* have used the gas chromatography time of flight mass spectrometry method in a group of highly

symptomatic children to assess inflammation (224). Results showed that VOCs profile was associated with oxidative stress caused by inflammation, therefore, useful in asthma screening. Ibrahim and colleagues have sampled VOCs in a small group of asthmatics and healthy controls, finding important differences in the VOCs profile between health and asthma and more importantly, between different asthma phenotypes (225).

Nitric oxide, generally released from the epithelial cells, is by far the most widely used breath test in respiratory medicine and has been approved by the FDA and endorsed by the UK National Institute for Clinical Excellence (NICE) as a diagnostic tool in asthma (226). Increased FeNO is an unquestionable marker of inflammation and has been of great use in asthma management and steroid treatment adherence and optimisation (227,228). FeNO is typically measured at a constant flow rate of 50mls.s^{-1}, however, studies have utilised FeNO measurements at different flow rates to probe the distal airways (alveolar NO). Van Veen *et al* demonstrated that alveolar NO was closely correlated with other markers of the peripheral airways [RV/TLC, FRC, closing capacity (CC)] in severe asthma (229), but more validation in this area is required.

EBC is the most widely used method to sample non-volatile exhaled particles, however, the EBC sample contains volatile and semi-volatile particles as well. It is a simple, non-invasive technique that uses tidal breathing and cooling method, with several devices commercially available. Several inflammatory markers have been detected in EBC samples, such as mediators, oxidants, ions and pulmonary surfactant (230). Moreover, pH, adenosine and other substances detected with this technique have been used in the study of asthma and COPD (231). One of the most recent advances with this technique was brought by Robroeks *et al*, utilising a multiplex platform to analyse samples from EBC in asthmatic patients and controls (232). They found increased levels of some inflammatory cytokines and chemokines selected between the two populations. However, despite the large number of studies with biomarkers derived from EBC, this technique presents a number of issues and therefore, not a suitable method to sample non-volatile endogenous particles efficiently. The use of cooling to condensate water vapour leads to loss of droplets; particles collected cannot be monitored and consequently the fraction of particles sampled is difficult to predict. Moreover, adjustment of the measured aqueous concentrations according to the amount of sampled material is impractical and EBC is collected during tidal breathing, leading to very low

number of droplets of interest and unknown sample origin, potentially missing the small airway compartment (233).

1.5.3 Particles in exhaled air- the PExA method

Non-volatile particles acquired from exhalations are liquid droplets, aerosols, such as proteins and lipids, which have a two-phase system of gas and condensed particles. Any method to sample these kind of particles have to take into account their natural formation and deposition process (234).

Particles in exhaled air method (PExA) is a novel, simple and non-invasive method to collect non-volatile droplets from the airways, first reported by Almstrand and colleagues in Sweden (14). The advent of PExA was prompt by Professor Anna-Carin Olin's group at the department of Occupational and Environmental Medicine and expertise of Evert Ljungstrom, Professor of Atmospheric Chemistry, in the early 2000's. Their research was triggered by the need of an optimised non-volatile particles sampling method, in order to examine work-related respiratory conditions and inflammatory lung diseases. Nine prototypes of the PExA instrument (PExA 1.0) were developed at the Sahlgrenska Academy and distributed mainly at a few Swedish research sites, and one at the Leicester Respiratory Research Centre, in 2012 (**figure 1.2**). In 2015, an updated, optimised and miniaturised PExA instrument (PExA 2.0) was tested and designed and is now CE marked (more details can be found on http://pexa.se/en/). Their first step in the PExA development was to study the particles sizes, distribution and number, achieved by means of an optical particle counter (235). In the PExA method, particles are sampled by impaction, which directs the aerosol through a nozzle and the output stream to an impaction plate (236). Particles size and velocity influence their inertia and impaction and adjusting the velocity of the air stream will influence the size of the particles sampled.

Different breathing manoeuvres generate different particle amounts and sizes. Tidal breathing generates the least number of particles, with a diameter of <0.3μm (237). On the other hand, cough and exercise produce the higher amounts of particles. Cough is generated due to an increased pleural pressure, which increases the flow more than in a

forced exhalation. During forced exhalation, forces from the RTLF and airway wall create a two-phase concurrent flow and choke point, where highest air velocity and dynamic air compression occurs (238).

PExA is believed to allow the collection of endogenous particles deriving from the respiratory tract lining fluid (RTLF), which arise from the lung periphery. There is no certainty regarding the mechanism in which these particles are formed, but the most plausible theory about the formation and behaviour of particles in the lung sits in the reopening of closed airways. According to this model, in an early phase while exhalation till residual volume takes place, the peripheral airways, at the level of the terminal bronchioles, form a blocking liquid menisci of surfactant particles, due to instabilities of the liquid lining fluid and its tendency to strive for minimal surface energy, and the airway wall elasticity. During the next inhalation, this liquid bridge is ruptured, allowing a shower of particles to be released during the subsequent exhalation (239). **Figure 1.3** shows a representation of this model. Coupled with these views, recent studies have shown that the optimal breathing manoeuvre for PEx (material collected) sampling is to instruct the patients to exhale till RV, followed by a five seconds breath hold and a full inspiration and exhalation, when the particles are collected (240). Likewise, Almstrand *et al* showed that emission of particles did not differ significantly with changes in the exhalation flow, but changes in airway closure manoeuvres triggered changes in particle numbers, especially in the smaller particle sizes (<1μm), believed to represent the peripheral airways (241). During airway closure manoeuvres, particle deposition needs to be taken into account, which can happen through gravitational sedimentation, impaction, diffusion, interception, electrostatic attraction or even coagulation with other particles, due to interactions between airway morphology, ventilation and aerosol properties (236). In the peripheral airways, the main mechanism responsible for particle deposition is gravitational settling. The size distribution of particles following airway closure manoeuvre and tidal breathing, described by Holmgren *et al* showed that for both mechanisms, most particles sit around 0.7μm, but smaller particles are also found with airway closure (0.2 to 0.5μm) (242). Particles over 7μm are not sampled with the PExA method and are unlikely to come from the peripheral airways (243).

Despite the early nature of results, the PExA technique has been successfully used to quantify different exogenous components from the peripheral airways and surfactant

components in different preliminary research projects, being able to identify and quantify different proteins and phospholipids from the RTLF in different population groups (15–17,244,245).

Figure 1.2: PExA 1.0 instrument

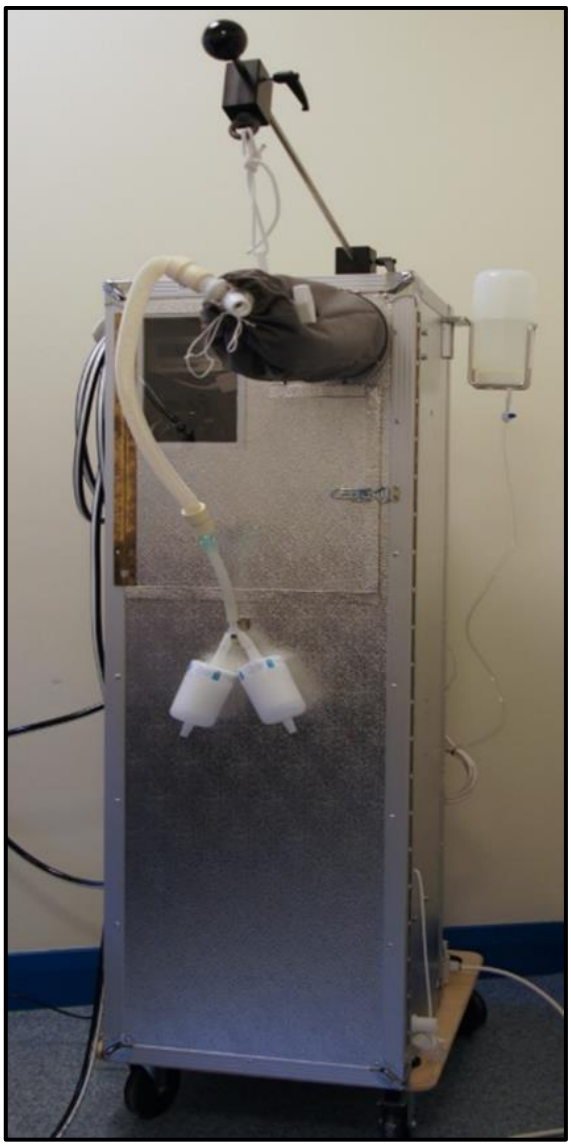

Figure 1.3: Particle formation model

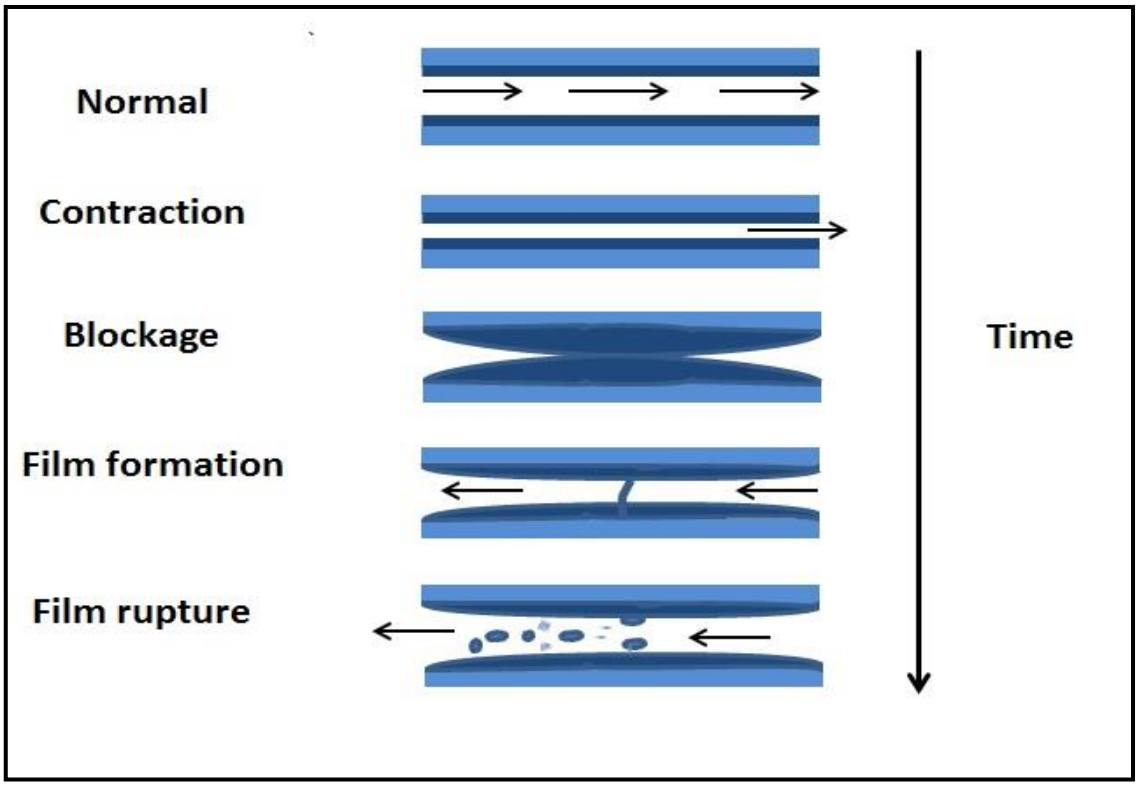

From the functional residual volume point (**normal**), a full exhalation takes place till residual volume, which leads to a **contraction** of the peripheral airways. The airway lining fluid tends to form a **blockage**, which then leads to a **film formation**. This film is then **ruptured** in the next full inhalation, bringing a shower of surfactant particles, collected in the following exhalation. *(figure adapted with permission from Per Larsson).*

1.5.4 PExA and potential small airways biomarkers

SPA and Albumin

During the last few years, the involvement of surfactant in the pathophysiology of respiratory diseases and its role in immunomodulation has been a particular point of interest. For instance, Liu and colleagues have shown that abnormally increased resistance in asthma can be due to dysfunction in the surfactant (246).

Proteins constitute about 10% of the surfactant area and four have been identified: surfactant protein A (SPA), surfactant protein B (SPB), surfactant protein C (SPC) and surfactant protein D (SPD). SPA and SPD are hydrophilic, with an important role in the host defence (247). On the other hand, SPB and SPC are intensely hydrophobic and interact with surfactant phospholipids to optimise the surface tension lowering function (248). SPA, secreted by type II and club cells, is the most abundant protein in the surfactant and one of the most abundant in PEx (244). SPA has a molecular weight of about 32kDa and has three distinct domains: collagenous, linking region and a globular region, culminating in a bouquet-like appearance. The globular region contains a calcium-dependent carbohydrate recognition domain (CRD) that binds to phospholipids, type II cells and micro-organisms (249). Consequently, it is believed to interact with cell surfaces of microorganisms, with important functions such as modulating immune cells responses and enhances the phagocytosis of bacteria and viruses by neutrophils (250). SPA is encoded by two genes (SP-A1 and SP-A2), with both structural and functional differences (251).

The majority of SPA in humans is found in the alveoli, and very little in the epithelium of proximal airways. Thus, in the search for small airways dysfunction and its inflammatory pathway, especially in asthma, SPA might constitute a key factor and a potential biomarker. SPA is likely to participate and modulate the allergic cascade in asthma, through the binding between antigen and immunoglobulins (IgE). Studies have demonstrated that SPA plays a role on regulating the expression of BALF proteins involved in host defence and redox regulation (252). Interestingly, in a study conducted by Graaf and collaborators, reduced levels of SPA in BALF from asthmatic subjects were found, when compared to healthy subjects (253). Similarly, Wang and colleagues have shown recently that SPA from BALF of asthmatic subject is defective in abrogating inflammation, triggered by mycoplasma pneumoniae (254). Likewise, Pastva

et al have shown in mice models that SPA influences and modulates the Th2-associated inflammation, where models with SPA -/- had greater eosinophilia, Th-2 associated cytokine and IgE levels (255).

Albumin is the second most abundant protein in PEx (244). It is a major plasma protein, mainly produced in the liver and constitutes around 50% of the plasma proteins in health. Its major role is to transport substances in the blood, act as an anti-oxidant and regulate fluid balance in the tissues (256). Albumin is a disease marker for many inflammatory conditions and can be used clinically to treat several diseases. Albumin crosses the capillary wall into the interstitial fluid and back to blood through the lymphatic system. The concentration of albumin in the RTLF is still uncertain but its presence in the airways might reflect the breakdown of the alveolar basement membrane or increased airway vascular permeability (210,257). Indeed, the link between plasma protein leakage and higher levels of inflammation in asthma have been explored in many studies (256,258). Interestingly, both hypotheses that albumin in the RTLF could be increased or decreased due to airway inflammation should be considered, due to different behaviours towards hydrostatic pressure.

To date, promising yet exploratory studies have been conducted using the PExA technique applying proteomics. Larsson *et al* demonstrated that SPA can be detected in healthy subjects, more than in serum or EBC. Moreover, PEx SPA showed good intra-individual repeatability, from 2 separate sampling sessions in healthy subjects (16). The same author conducted a study in a small asthma population looking at the effect of birch pollen in PEx SPA and albumin levels. Preliminary results showed no significant differences in the concentration of these proteins, however, the number of particles decreased significantly, which can indicate small airway compromise and airway closure (259). In COPD, SPA levels seem to be reduced, weakening host defence function and leading to higher number of exacerbations, as Larstad and colleagues showed in a small pilot study (17). Recently, Ericson *et al* applied the PExA method to a population of stable lung transplant recipients (LTRs) and a small population of patients developing OB. They found lower levels of SPA and albumin in the OB group, as well as lower amounts of particles (260).

There is a need to further understand the role of SPA and albumin in the inflammatory process in asthma, especially in the small airways compartment. While in early stages,

PExA seems to represent a valuable non-invasive tool to do so, and more studies, validation and answers are required.

Exhaled particles number

The number of particles exhaled in each breath and size distribution from PEx could constitute a potential biomarker on its own. RTLF has been shown to influence particle formation process, which could be altered due to inflammation and increased airway closure (258,261). As presented by Larsson *et al* in a pilot study, particle mass and exhaled number have high variability between subjects, in both health and disease, however, intra-subject variability seems to be much lower and could be used to monitor inflammatory status (16). Bake and collaborators have recently reported a study on 126 healthy subjects, attending a single PExA session following the standard breathing manoeuvre. They found that PExA particles concentration did not differ between genders, however, older individuals exhaled higher number of particles and reference equations were generated according to age, weight and spirometry (262). Yet, no solid data is available in disease.

Phospholipids

Surfactant is a very rich matrix, majorly composed by phospholipids (about 80%), more specifically, dipalmitoyl-phosphatidylcholine (DPPC). A study on altered airway surfactant phospholipid composition and reduced lung function in asthma with BAL and sputum, conducted by Wright and colleagues, showed that DPPC was decreased in sputum and this dysfunction might induce asthmatics to further surfactant inhibition by proteins in acute asthma, contributing to airway closure (263). Phospholipids are abundant in PEx and few preliminary studies have shown some interesting findings. Almstrand *et al* demonstrated that PEx phospholipids saturated to unsaturated ratios were different between heathy controls and asthmatic individuals (15). Likewise, Bredberg and colleagues found significant differences in the phospholipid matrix between healthy controls and smokers, thus, the latter group might have had lung function compromised due to RTLF changes (245). More recently, Larsson *et al* reported a study on 11 healthy controls, to evaluate the influence of different breathing

manoeuvres on PEx phospholipid composition, concluding that the breathing techniques do have an influence in lipid concentration and can be potentially selective in terms of airway compartment being sampled (264).

1.6 Recognising the gaps in small airway disease investigation

Table 1 summarises the methods described, highlighting their invasive/non-invasive nature, measurements and outcomes derived, advantages and limitations of each method to assess the small airways compartment, as a reflection based on this introductory section. Invasive or semi-invasive techniques are far from ideal in clinical settings, presenting potential risks, side-effects and unclear usefulness in small airway disease examination. Spirometry and lung volumes lack sensitivity, despite its wide use in clinical settings, especially in asthma diagnosis and management. Furthermore, approximately 20% of patients between the age of 55 and 80ys cannot perform high quality spirometry and the procedure is time consuming (125). It is clear that the lack of repeatability, standardisation and validation in heterogeneous and large populations of non-invasive methods, rapid and easily applied (i.e. across all age ranges) such as oscillometry techniques and breath analysis, is a major limiting factor. These factorshave delayed our understanding of the importance (or not) and standardisation of definitions of small airways dysfunction and disease in asthma and other respiratory diseases where the small airways is a causal factor in disease progression, e.g. COPD and ILD.

The right-hand side column shows the work developed in this thesis, underlined for each method used. **Figure 1.4** shows a diagram highlighting the main domains of work conducted in this thesis, in broad terms, which will be explored in more details in the aims and objectives section following introduction. In summary, small airways disease and dysfunction will be explored non-invasively with the PExA method, in a search for inflammatory and biological potential biomarkers. Forced and impulse oscillation techniques will be used to assess and validate physiological makers of small airway dysfunction. These methods will be implemented in patients with asthma, asymptomatic smokers and healthy controls. In addition, OE-MRI will be explored further as a novel imaging technique applied in severe asthma.

Table 1: Summary of small airways biomarkers assessment tools and their characteristics

	Methods	Measurements	Outcomes	Advantages	Limitations	Work developed in this thesis
Invasive/ Semi-invasive	BAL	Inflammatory cells and mediators	Inflammation	Access to tissues adjacent to airspaces, cells from RTLF	Blood contamination, standardisation problems, unknown dilution Possible complications	___
	Lung biopsy	Lung tissue	Inflammation	Access of peripheral lung parenchyma	Invasiveness Sedation Blood contamination Possible complications,	___
	Sputum Induction	Inflammatory cells and mediators, Late phase sputum	Inflammation in the central airways	Inflammatory cells profile, high reproducibility	Time-consuming, need staff training, lack of small airway specificity	___
Standard Physiology	Spirometry	FEV_1, FEF_{25-75}, FEV_1/FVC, FEV_3/FVC, FEV/SVC	Expiratory flow limitation primarily in central airways	Simple, reproducible, widely available, standardised	Effort-dependent, lack of small airway specificity	FVC link to small airway inflammation and lung function change
	Plethysmography	RV, RV/TLC, Raw	Air trapping, specific total airway resistance	Simple, reproducible, widely available, standardised	lack of small airway specificity	___

Non-invasive research methods	FOT/IOS	R5-R20, AX, X5, Fres	Airway resistance and airway elastance as well as the heterogeneity of both	Simple and quick, sensitive to early changes, possible to discriminate between large and small airways	Lack of validation and reference values, limited to specialist centres	R5-R20 validation Link with small airway inflammation and decline Inter-device comparison
	MBW	LCI, Sacin, Scond, LCIds, LCIvent, CC, CV	Ventilation heterogeneity	High reproducibility, sensitive to early changes, possible to discriminate between large and small airways	limited to specialist centres, time-consuming	Link with small airway inflammation Link with imaging biomarkers
Exhaled Breath	FeNO	$FeNO_{50}$, $FeNO_{200}$	Inflammation	Quick, easy, hand-held, sensitive to treatment in asthma	lack of small airway specificity, equipment costs, affected by smoking, upper airways disease, dietary factors and iNOS mutations	___
	VOCs	Breath volatile organic compounds	Inflammation	Rapid, non-invasive, possible disease detection and status evaluation	Lack of standardisation and specificity to small airways	___
	PExA	Proteomics, lipidomics, RNA/DNA, exhaled particles (non-volatile airway surface liquid)	Inflammation Airway closure	Non-invasive, simple, potential information about peripheral inflammation;	Lack of validation and limited to few specialist centres	Feasibility, repeatability and reproducibility of assessments; link to small airway

				miscellaneous of possible biomarkers in asthma		dysfunction measurements in asthma and longitudinal lung function change
Imaging	HRCT chest	$MLD_{E/I}$, airway wall thickness and geometric measurements, image registration methods applied to scans acquired at 2 or more lung volumes e.g. PRM-fSAD	Air trapping	Quick to perform, quantitative and qualitative analysis; widely available	Expensive, time-consuming analysis, unable to visualise small airways directly, radiation dose	___
	Hyperpolarised MRI	ADC	Regional ventilation defects, diffusion	No radiation; high resolution structure and function information	Expensive equipment, limited to specialist centres, lack of validation	___
	OE-MRI	ΔPO_2, Tup, Tdown, Tvent, Kox, EoxFb	Regional and temporal ventilation defects, diffusion	No radiation, no need to use expensive gases, good spatial and temporal information	Time-consuming, expensive, limited to few specialist centres, lack of validation	Feasibility assessment in moderate to severe asthma Tool to assess inhaled pharmacological response to high particle fraction drug
	Nuclear medicine (scintigraphy, SPECT, PET)	Receptor or drugs distribution		Information about disease heterogeneity; can help with drug site targeting	Radiation dose, limited to specialist centres; not specific to small airways	___

Definition of abbreviations: BAL (F): Bronchioalveolar lavage (fluid); RTLF: Respiratory tract lining fluid; FEV_1: Forced expiratory volume in 1 second ; FEF 25-75: forced expiratory flow at 25-75% of vital capacity; FEV_3: Forced expiratory volume in 3 seconds ; FVC: Forced vital capacity; SVC: Slow vital capacity; RV: Residual volume; TLC: Total lung capacity; Raw: Resistance measured by body plethysmography ; FOT: Forced oscillation technique; IOS: Impulse oscillations; R5-R20: Resistance at 5Hz minus Resistance at 20Hz; AX: Area of reactance; X5: Reactance at 5Hz; Fres: Resonant frequency; LCI: Lung clearance index; Sacin: Acinar ventilation heterogeneity ; Scond: conductive ventilation heterogeneity; LCIds: LCI dead space; LCIvent: Ventilation inequality LCI ; CC: Closing capacity; CV: Closing volume; $FeNO_{50}$: Fractional exhaled nitric oxide at 50mls/s; $FeNO_{200}$: FeNO at 200mls/s; VOCs: Volatile organic compounds; PExA: Particles in exhaled air method ; $MLD_{E/I}$: expiratory to inspiratory mean lung density; fSAD: Functional small airway disease; MRI: Magnetic resonance imaging; ADC: Apparent diffusion coefficient; ΔPO_2: ; Tup: wash-in time; Tdown: washout time; Tvent: O_2 mixing time; Kox: O_2 transfer rate; EoxFB: O_2 extraction rate; SPECT: single photon emission computed tomography; PET: Positron emission tomography.

Figure 1.4: Syntheses of methods and domains explored in this thesis

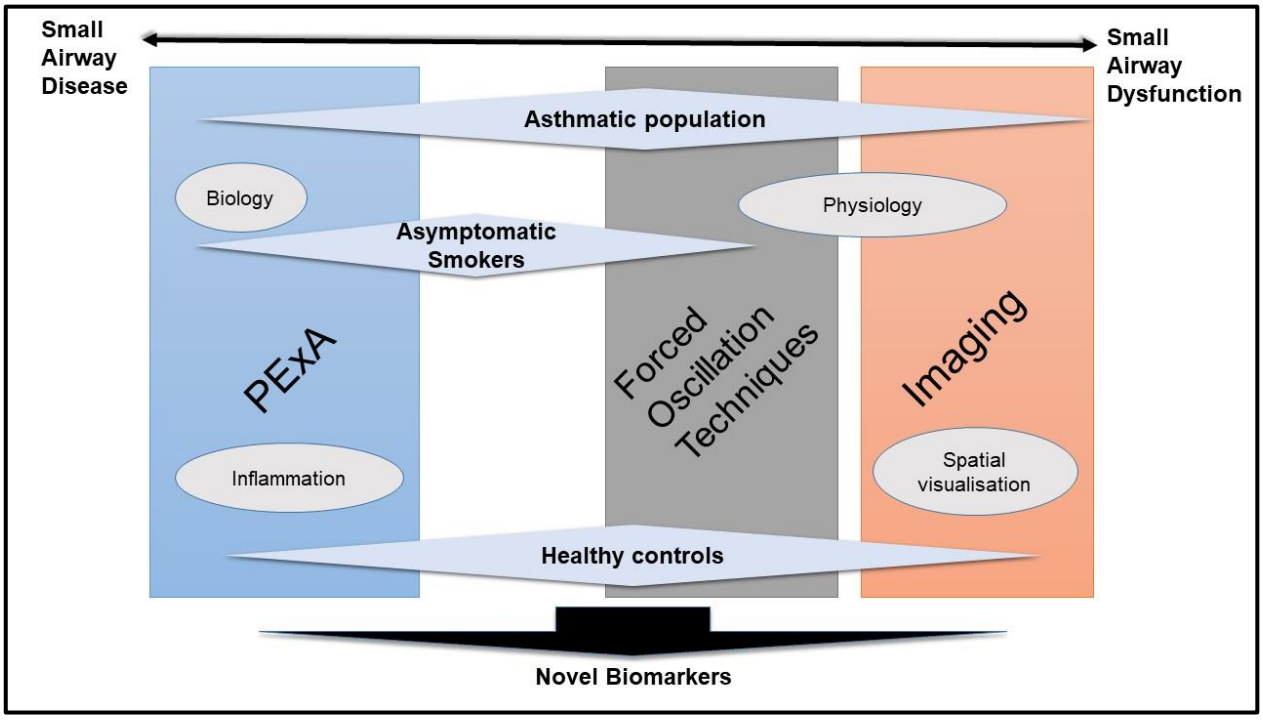

Summary of the methods used to explore potential candidate small airways disease and dysfunction biomarkers in our studies, in patients with asthma, asymptomatic smokers and healthy controls.

1.7 Aims and hypothesis

The overall aim of this project was to further validate and explore candidate non-invasive biomarkers of small airways dysfunction, utilising novel approaches: forced oscillation techniques, particles in exhaled air and oxygen-enhanced MR imaging. I hypothesise that all techniques have potential added value to address the clinical need for a better and detailed characterisation of the peripheral airways in asthma. An ideal approach would be to explore all the different biomarkers and outcomes in a single population. However, due to the nature of this study and the different strands of work conducted, different populations were utilised. Figure 1.5 shows a schematic representation on how the different populations relate and overlap amongst studies.

Detailed hypothesis and aims are presented below.

1.7.1 **To validate impulse oscillometry derived R5-R20 as a small airway dysfunction detection tool in adult asthma.**

R5-R20 may be a measure of small airways dysfunction, however, it has yet to be validated from an anatomical and clinical perspective (136). I therefore aimed to validate this tool in a clinical population and using the pooled results from two phase-2 clinical asthma trials.

I hypothesised that:

a) Population with small airways dysfunction would present poorer asthma control, quality of life and increased asthma exacerbations (in both the presence and absence of abnormal spirometry).

b) R5-R20 is a forward predictor of spirometric (FEV_1, FVC) decline, in adult asthma.

c) R5-R20 would be a sensible marker to detect small airways disease and clinical patient related outcomes change in anti-inflammatory intervention trials.

1.7.2 **To compare forced (FOT) and impulse oscillometry (IOS) measurements in a clinical population and physical model.**

The use of commercialised forced oscillation techniques to assess airway physiology in obstructive diseases such as asthma has become more broadly used in the past decade. However, it is yet to be established how comparable the resistance and reactance measurements are across different commercial devices.

I therefore sought to compare the two most widely available and utilised FOT devices: Impulse Oscillometry System (IOS) and Tremoflo FOT (Thorasys) in a clinical adult population and using a 3D printed CT scan-based airway model of the large airways and a reactance volume standard.

I hypothesised that the resistance and reactance measured in both devices would be comparable and not subject to proportionate systematic bias.

1.7.3 **To clinically validate surfactant protein A (SPA) and albumin derived from particles in exhaled air (PExA) as non-invasive biomarkers of small airways disease in asthma.**

The application of the PExA method in asthma has been scarce and involving limited number of individuals (15,259), despite method optimisation in the last few years. Moreover, little is known about the role of SPA and albumin in the small airways disease pathophysiological process. I therefore aimed to:

a) Assess the feasibility of acquiring PExA measurements in a large population of individuals with asthma including severe asthma.
b) Link PExA SPA and albumin biomarker concentrations to physiological measures of small airways dysfunction: IOS, MBW, spirometry.
c) Evaluate whether a combination of measures capturing small airways dysfunction and PExA biology may identify a phenotype of asthmatic patients with small airways disease.

1.7.4 **To assess the short and long term repeatabillity within visit, 2 week, 3 month and 2-3 years of PEx SPA and albumin as small airways dysfunction biomarkers.**

Larson *et al* has reported the repeatability of PExA outcomes on two different occasions, in a healthy population, with a standardised manoeuvre (16). Moreover, studies have shown great variability amongst healthy individuals (262), but no data is available in asthmatic populations, therefore, the short term and long term stability of PExA biomarkers has not been reported. I therefore aimed to:

a) Evaluate the repeatability of PExA biomarkers % SPA and % albumin within visit, at 2 weeks and three months in asthmatics and healthy volunteers.

b) Understand if baseline % SPA and % albumin levels are associated with increased lung function decline in asthmatic individuals.

1.7.5 **To evaluate the role of dynamic OE-MRI in moderate to severe asthmatics.**

Very few studies have utilised OE-MRI in adults with moderate to severe asthma (191). Moreover, it has been suggested that ventilation heterogeneity, a marker of small airways impairment, can improve with treatment (164), more specifically fine particle fraction ICS/LABA formulations (265).

My aim was to assess the effect of two single inhalations of flutiform (fluticasone/formoterol 250/10mcg) an inhaled drug with a high fine particle fraction on OE-MRI and standard MBW derived ventilation heterogeneity parameters in a population with moderate to severe asthma. I hypothesised that OE-MRI measurement would be associated with patient related outcome measures in asthma and that OE-MRI measures of ventilation heterogeneity would be responsive indices to high fine particle fraction inhaled formoterol.

Figure 1.5 Diagram of the different study cohorts

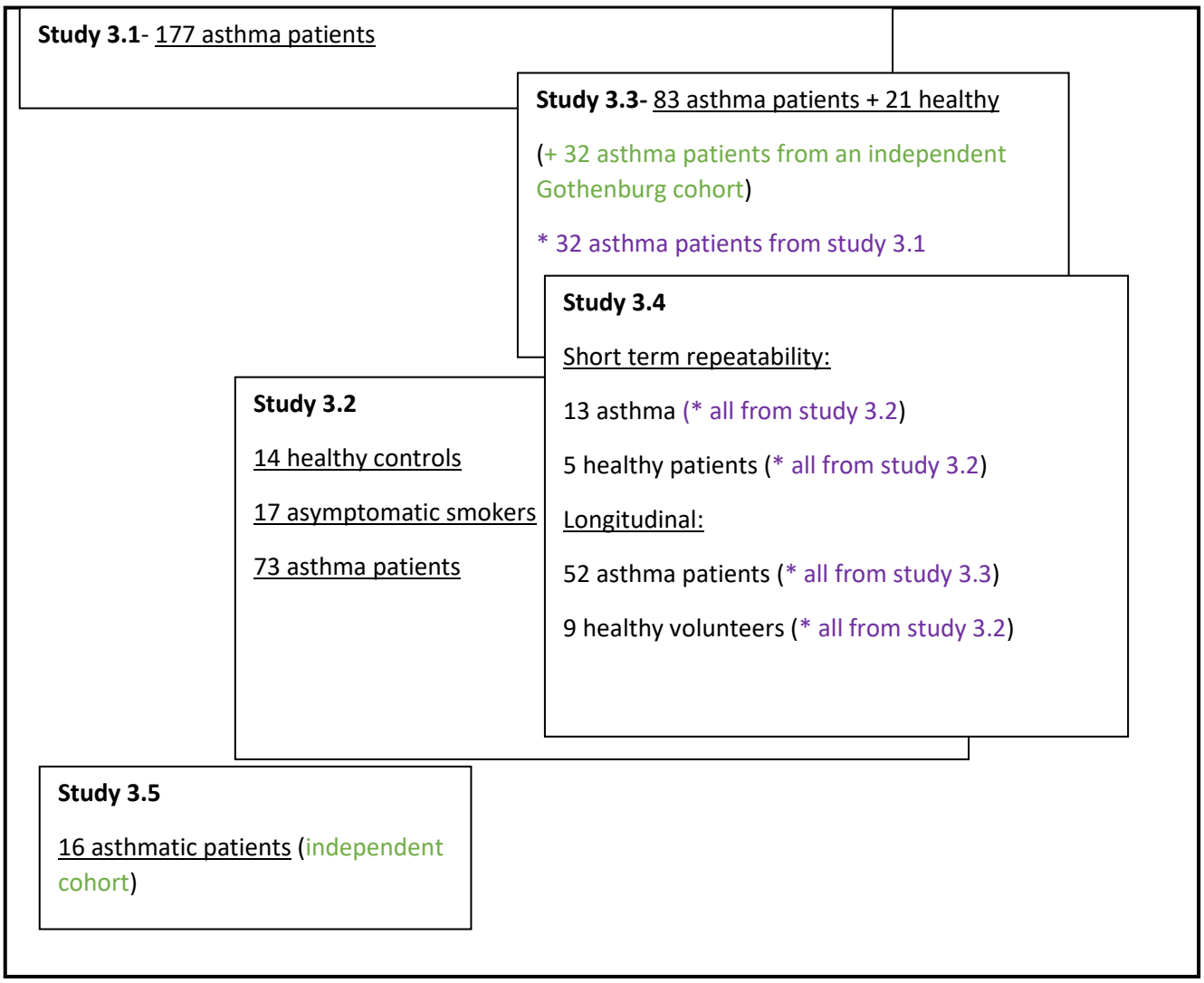

2. Methods

2.1 Clinical methods

2.1.1 Baseline demographics and history

Current asthma medication was recorded, as well as current medical problems, smoking history and pack years of exposure, exacerbation frequency [exacerbations were defined according to the ATS/ERS criterion (266)], age of asthma onset and previous history of hospital and ITU admissions. When required, a physical examination was performed.

2.1.2 Peripheral blood

Peripheral blood was collected for full blood count, eosinophil and neutrophil counts and processed by the pathology laboratory in Glenfield Hospital.

2.1.3 Allergen skin testing

Subjects were instructed to withhold anti-histaminic therapy for at least 72h prior to testing. Allergen skin test was performed using a panel of common allergens (cat fur, dog dander, grass pollen, *Dermatophagoides petronyssinus*, tree, *Cladosporium*, *Penicillum notatum* and *Aspergillus fumigatus*), with normal saline and histamine as controls. A wheal response ≥ 2mm larger than negative control for one or more allergens constituted atopy, accessed 15 minutes after skin prick.

2.1.4 Fractional exhaled nitric oxide

Fractional exhaled nitric oxide (FeNO) was measured using an electrochemical analyser, Niox Vero (NIOX; Aerocrine, Stockholm, Sweden), at a 50ml/sec flow rate, prior to any other measurements and before administration of any inhaler medications on the day, in accordance to the ATS/ERS recommendations for FeNO measurements (217).

2.1.5 Juniper asthma control questionnaire (ACQ) score

JACQ or ACQ is a well-known and validated questionnaire, consisting of 7 elements: 6 questions about various aspects of symptoms control and inhaler usage and the 7th field measures airflow obstruction, expressed as pre-bronchodilator % predicted FEV_1 (267). For each question, asthmatics describe their symptoms control for the preceding week, on a severity scale from 0 to 6 and pre- bronchodilator % predicted FEV_1 also scored on a scale of 0-6. A modified and validated form of the ACQ was used (268), where point 7 of the questionnaire was excluded. The total score of the 6 symptoms and inhaler usage questions was divided by 6, to give the overall score. The minimum clinical significant difference between visits for the modified ACQ score was 0.5.

2.1.6 Juniper asthma quality of life questionnaire (AQLQ)

The Juniper asthma quality of life is a well validated questionnaire to access asthma related quality of life (269). AQLQ comprises 32 questions, representing 4 domains: symptoms (12 questions), activities (11 questions), emotion (5 questions) and environment (4 questions). Each item is score between 1 and 7 and higher scores indicate better outcomes. A score is calculated for each of the 4 domains and the arithmetic average of all the domains scores is the overall score. A shorter version of AQLQ, the MiniAQLQ, has been developed and tested with good outcomes (270), however, the standardised version of the questionnaire was used.

2.2 Lung function

2.2.1 Spirometry

All participants performed spirometry in accordance with the ATS/ERS guidelines (271) using a Vitalograph spirometer (Vitalograph, Maids Moreton, Buckingham, MK18 1SW). Patients were seated comfortably with their feet firmly on the floor. After appropriate explanation, and exclusion of contra-indications by the operator, patients were asked to perform a full inspiration to TLC followed by a forced exhalation in the mouthpiece, as fast as possible for as long as possible until RV, with continuous

encouragement from the technician. The manoeuvre was repeated between three to eight times, with at least one-minute rest in between each attempt, until the acceptability and repeatability criteria was reached, with the best two values of FEV_1 and FVC differing no more than 5% (or 100mls) (271). The best value of FEV_1 and FVC were recorded, from any of the acceptable manoeuvres. The reference values and lower limit of normality (LLN) for each patient were calculated in accordance with the Global Lung Initiative 2012 equations (272).

2.2.2 Airway responsiveness: methacholine challenge test

Bronchial hyper-responsiveness was expressed as the concentration of methacholine required to cause a 20% fall in FEV_1 (PC20), using the standard tidal breathing protocol previously described (273). The test was performed if subjects fulfilled the test safety criterion, including an FEV_1 greater than 1L and stable asthma. Subjects inhaled saline followed by doubling doses of methacholine 0.03-16mg/ ml, for 2 minutes each, breathing tidally and wearing a nose clip, via a Wright's nebuliser with an output of 0.13 ml/min. FEV_1 was measured at 30 and 60 seconds after each dose, including saline; an extra FEV_1 assessment was performed at 90 seconds if the second value was inferior to the first one. The lowest FEV_1 result on each session was used to calculate the % drop from baseline. A fall greater than 20% of the baseline FEV_1 value led to termination of the procedure, or after the highest dose of methacholine. PC20 was calculated by linear interpolation of the log-dose response plot.

2.2.3 Sputum induction

A sputum induction protocol previously described has been used (267,274). Fifteen minutes after administration of 400mcg of salbutamol via spacer, patients performed spirometry, and the best FEV_1 value was recorded. This value was then used to calculate 10 and 20 % FEV_1 fall during induction. Subjects inhaled increasing concentrations of 5ml of saline, for 5 minutes, via an ultrasonic hand-held nebuliser (EasyNEb II by FLAEM), starting with 3%, followed by 4% and 5%. Patients were instructed to breathe tidally and wear a nose clip. After each session of 5 minutes, patient rinsed their mouth, blew their nose (to avoid contamination) and encouraged to

expectorate into the sterile sputum sample pot, followed by a FEV_1 manoeuvre. If FEV_1 fall was less than 10%, the following concentration was given. With a fall greater than 10% but less than 20%, the same concentration was given but if FEV_1 fall was greater than 20%, no further inhalations were performed and 400mcg of salbutamol was administered, with spirometric assessments after 15minutes.

Sputum was processed by adding 4x volume/ weight of 0.1% dithiothrietol (DDT) for cell count and supernatant extraction and storage at -80°C for future mediator assay.

2.2.4 Measurement of lung volumes by body plethysmography

Body Plethysmography was performed with a constant volume plethysmograph, according to the ATS/ERS recommendation (275). Participants were seated in a sealed box, in an upright position, connected to a rubber mouthpiece and single use filter, wearing a nose peg and keeping both hands on their cheeks for support. After the initial tidal breathing, patients were asked to pant gently against a closed shutter, which automatically closed at the end of a normal tidal breath (FRC) and open after an acceptable pressure measurement during the panting manoeuvre. The process was repeated 3 to 4 times in each test, terminating with a slow VC manoeuvre, in order to calculate TLC and RV. Thoracic gas volume and plethysmographic FRC (FRC_{pleth}) were calculated automatically by the software, according to Boyle's law, from pressure changes in the box and at the mouth. A minimum of three acceptable tests were performed and the test ended when the repeatability criteria was achieved (FRC within 10% between highest and lowest value).

2.3 Additional small airway physiology

2.3.1 Multiple breath washout

Patient testing procedure

MBW was performed using a modified Innocor photoacoustic gas analyser (Innovision A/S, Odense, Denmark), with 0.2% SF6 inert tracer gas, as described previously (151). Tests were performed following the standard guidelines: participants were encouraged

to maintain a tidal breathing pattern through the test of around 1L, with a good seal around the mouthpiece and nose clip on at all times. The first stage of the test was the wash-in phase, where patients breathed an air mixture containing 0.2% SF6 via an open-circuit flow system, until the expired SF6 concentration was within 0.004% of the inspired concentration for at least three breaths and rounding 0.2% SF6. On the second stage, participants were switched to room air, and asked to continue breathing at the same rate and pattern. The test was terminated when the end-tidal concentration of SF6 fell below $1/40^{th}$ of the original concentration (≈0.005%) for at least three consecutive breaths. According to the recommendations (190), the test was repeated two to five times to ensure at least two FRC results within 10%. If two consistent tests could not be obtained, the results for that participant were not used.

Multiple breath washout data analysis

Prior to data analysis, an initial inspection of each test was performed to both wash-in and washout phases, using a second custom MATLAB software [MATLAB 2015a, Natick, Massachusetts: The MathWorks Inc., 2015] looking at essential quality criteria such as at least three consecutive breaths with end tidal gas concentration values below $1/40^{th}$ of starting inert gas concentration and at least 6 turnovers (TO). Other desirable parameters included: absence of irregular breaths, no sudden drop in the inert gas concentration, sufficient breath size for phase three slope analysis and equilibration of SF6 gas during the wash-in cycle. These tolerances were introduced and customized through specific formulas in the MATLAB program.

A number of parameters were derived from the raw MBW data, including lung clearance index (LCI) and phase three slope derived measures of conductive (Scond) and acinar (Sacin) ventilation heterogeneity as previously described (276).

2.3.2 Particles in exhaled air- PExA

PExA instrument

A schematic representation of the PExA instrument is illustrated in **figure 2.1**. In essence, the subject breathes filtered air (HEPA filter) through a two-way mouthpiece non- rebreathing valve, into a box kept at 36 degrees. Inside the box, there is a Grimm 1.108 optical particle counter [OPC (Grimm Aerosol Technik GmbH & Co, Ainring, Germany)], which monitors the particles concentrations and sizes distributions with 1 s resolution. There is an impactor (modified 3-stage/ 2-stage PM 10 Impactor, Dekati Ltd., Tampere, Finland) with a hydrophilic polytetrafluoroethylene membrane impaction substrate (PTFE, diameter 25 mm; Merck Millipore Ltd., Cork, Ireland). The particles are drawn through the impactor by vacuum pump and collected by impaction on the membrane according to their size. An ultrasonic flow sensor (OEM flow sensor, Spiroson-AS, Medical Technologies, Zürich, Switzerland) measures flow-rates during the breathing manoeuvres, with a graphical display. Excess flow goes into a reservoir containing a vent to buffer the exhaled air and supplied with particle-free and humidified air (Respiratory Humidifier Fisher&Paykel MR 700), also kept at 36 degrees and flow rate of 280 $mL.s^{-1}$.

Impactor

Figure 2.2 A and B shows both cascade impactors used in the studies conducted, from Dekati. Impactor A presents three stages and impactor B two. Impactor A was only used in part of the population in study 3.3, when it was switched to impactor B and used for most of the measurements. The principles are the same, particles are directed through a nozzle and towards a membrane placed on the sampling plate. Both impactors were modified so the plate used collected particles on the size range 0.5-7.0μm in diameter, by adjusting the nozzles directly above the impaction plate and increasing the flow rate through the impactor. This sampling method has an efficiency of around 100%. The hydrophilic PTFE membrane from Milipore (FHLC02500) had a diameter of 25mm and compatible with the impactor lock ring system. After sampling, the membrane was cut around the section where particles were deposited, using a clean scalpel and placed in a polypropylene tube.

Particle counter

The OPC instrument and output can be seen in **figure 2.3 A** and **B**. The instrument uses light scattering, resulting from particle illumination by a laser beam. The concentration data was shown in 8 different size ranges, with 1 second resolution, recalculated by Holmgren *et al*: 0.41-0.55; 0.55-0.70; 0.70-0.92; 0.92-1.14; 1.14-1.44; 1.44-2.36; 2.36-2.98; 2.98-4.55 (242).

Assuming the exhales aerosols have similar properties to water (density of 1.0g.mL^{-1}), the mass of PEx was calculated as:

M (kg) = E. F (L.s^{-1}) . V (m^3) . D (kg.m^{-3}) . T(s) . C (n.L^{-1})

(M= sampled mass by the impactor; E= impactor sampling efficiency; F= volumetric flow rate through the impactor; V= particle volume; D= particle density; T=time; C= particle number per litre of exhaled volume).

Particle formation and sampling

According to the particle formation model described in section 1 of this thesis, in an early phase while exhalation till residual volume takes place, the peripheral airways form a blocking liquid menisci of surfactant particles; during the next inhalation, this liquid bridge is ruptured, allowing a shower of particles to be released during the subsequent exhalation.

During the sampling session, participants were coached to perform the PExA breathing manoeuvre (**figure 2.4 A**) which consisted of participants first exhaling to RV and then holding their breath for 5 seconds. Participants then inhaled rapidly to TLC and exhale steadily (maximum peak flow of 2000L/s). In between breathing manoeuvres, participants respired tidally. Subjects performed breathing manoeuvres wearing a nose clip, via a mouthpiece and a two-way, non-rebreathing valve into the PExA box.

Participants were asked to breathe tidally for one to two minutes prior to PExA sampling in order to prevent contamination from exogenous particles in ambient air. During this time, they inhaled particle-free filtered air via a HEPA filter. The two-way

valve was closed at this time so all exhaled air during tidal breathing was directed into the room, and no particles from exhaled breath were collected in the impactor.

Subsequently, the vacuum pump was turned on, commencing the particle sampling. Air was drawn through the impactor at 16L/min from the vacuum pump to provide the gas stream through which particles were collected onto the impactor. Clean, particle-free air was added to the reservoir at 18.5 L/min to act as a buffer and ensure there was always positive air pressure in the system, so no room air entered the instrument.

Participants were instructed to perform the specified breathing manoeuvre repeatedly until a sufficient mass of PEx (mainly 50-100 ng) had been collected.

Expiratory flow content was split between the OPC to monitor and estimate the number of particles collected in each breath, and the impactor. The instrument was modified so the exhaled flow could be controlled. Particle and flow output can be seen on **Figure 2.5**.

Figure 2.1 Schematic representation of the PExA instrument

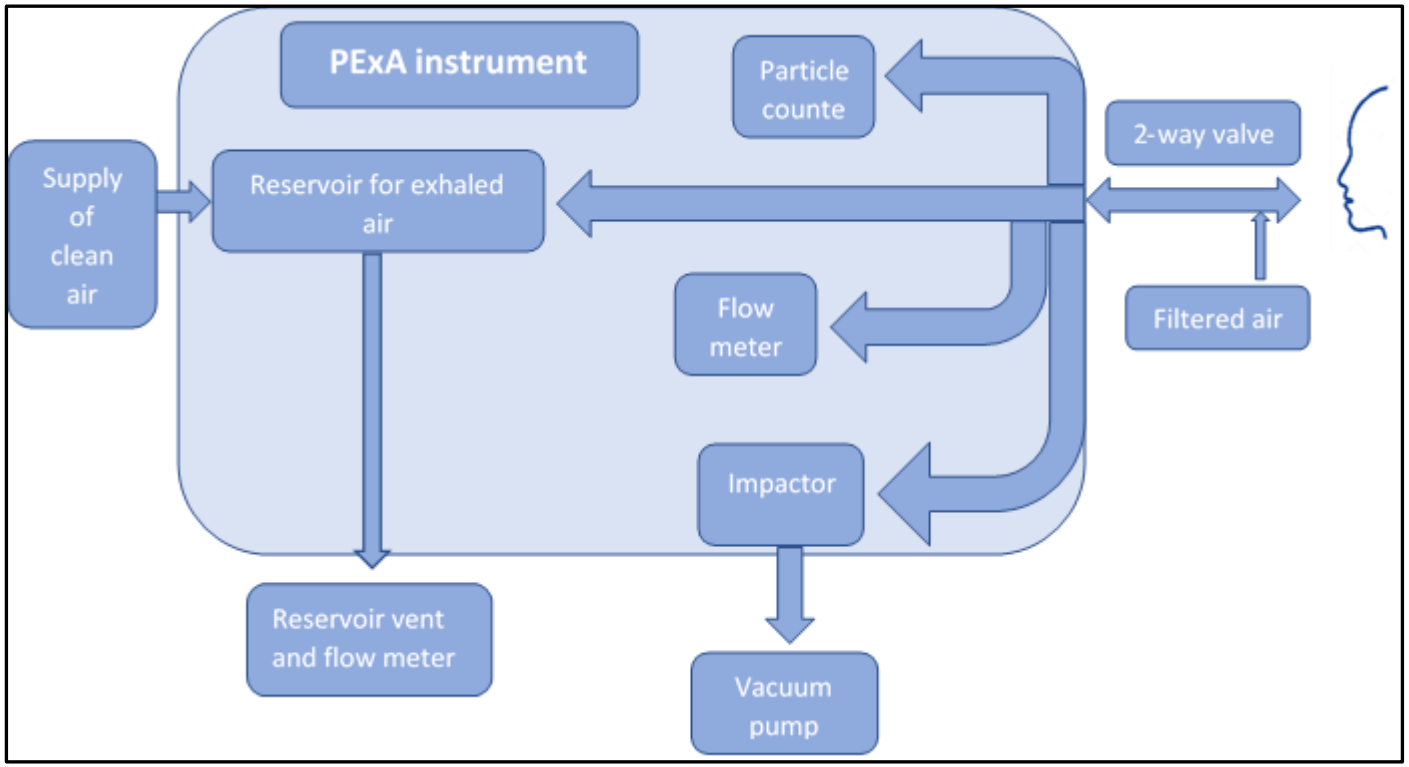

Schematic representation of the PExA system housed in the thermally insulated box showed in picture 1.1.

Figure 2.2 Cascade Impactors

A- 3-stage cascade Impactor impactor

B- 2 stage modified cascade impactor

Impactor housing and plates showing the location of the sampling filter.

Figure 2.3 Optical particle counter instrument (A) and output (B)

A: Optical particle counter instrument

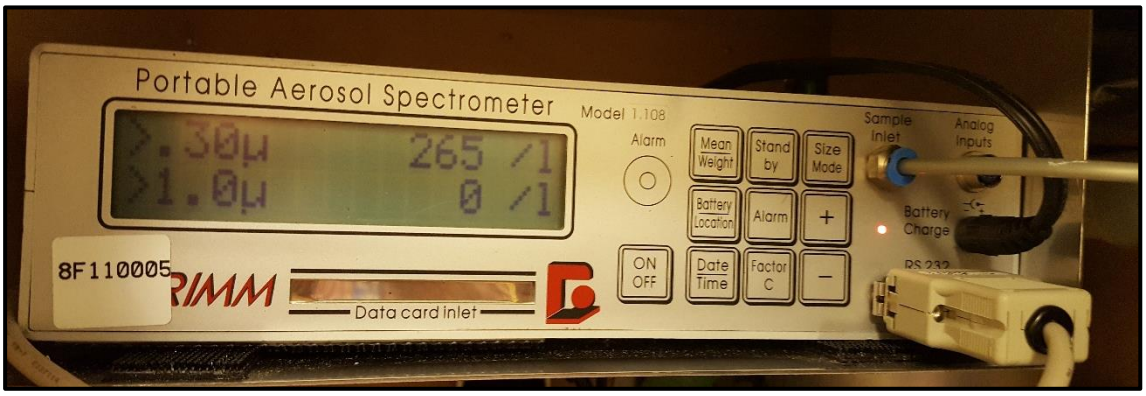

B: Optical particle counter output

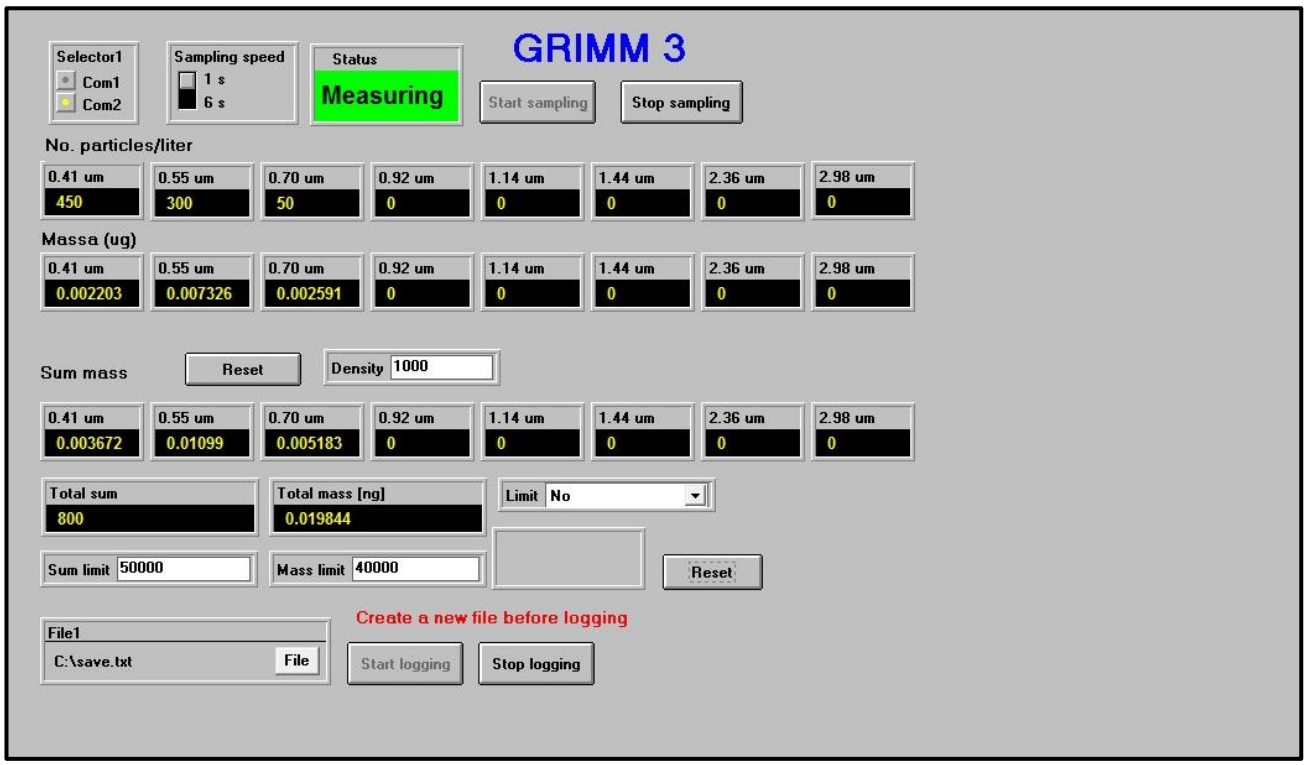

(A) Real-time counting of particles by the GRIMM instrument; (B) Screenshot of software showing real-time counting and sorting of particles in each bin (0.41µm to 2.98µm), from the optical particle counter.

Figure 2.4 Breathing manoeuvre required for PEx sampling

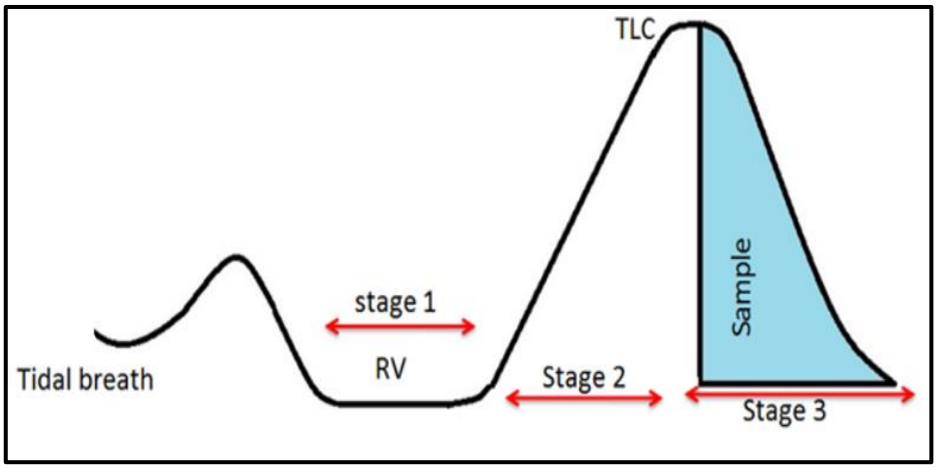

Definition of abbreviations: RV: Residual volume; TLC: Total Lung capacity.

Figure 2.5 Particle and flow output in a typical patient

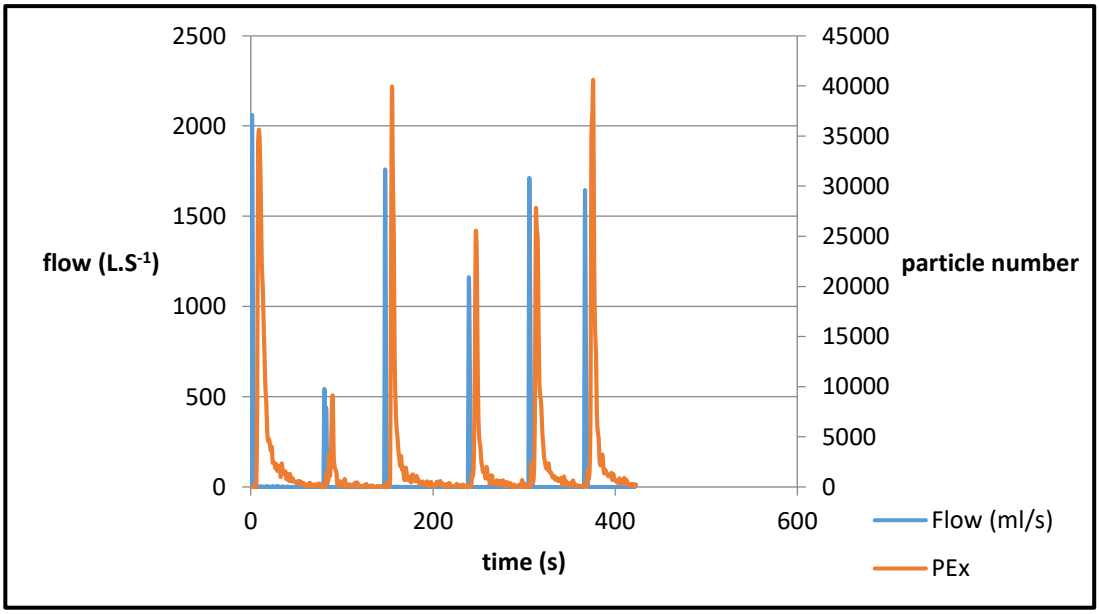

Sample storage and extraction

At the end of sampling session, the sample was transferred to a low-binding Eppendorf polypropylene vial and stored at -80°C until chemical analysis. Samples were sent from Leicester to the institute of Medicine at Sahlgrenska Academy, at the University of Gothenburg, in dry ice, where chemical analysis took place.

Proteins were extracted from each membrane by adding 140µl PEx extraction solvent, consisting of 0.01M phosphate buffered saline (PBS) (Medicago AB, Uppsala, Sweden), 0.05% TWEEN-20 (Bio-Rad, Hercules, CA, USA), and 1% bovine serum albumin (BSA). The sample vials were spun to ensure that membranes were covered by the extraction solvent and extracted by shaking at 400 rpm for 60 min at 37C in a thermomixer (Confort, Eppendorf). After locking the wafer between the vial and the lids, the vials were spun again to separate extracted samples from the wafer. The extracted material was pipetted into 3 separate vials of 40µl each: 1 each for SPA and albumin ELISA and the third for storage, as a back-up. Each of the 40µl samples for SPA and albumin assays were further diluted with dilution buffer provided in ELISA kits to 120µl. All vials were then stored at -20°C and analysed within 7 days. **Figure 2.6** shows a schematic representation of the extraction protocol for further SPA and albumin ELISA.

Chemical analysis

SPA was quantified using a human surfactant protein A ELISA (BioVendor, Heidelberg, Germany) and albumin using a high sensitivity two site ELISA (ICL, Portland, USA) according to the product datasheet, with minor modifications concerning buffer composition, calibration standards and incubation times. Calibration standards and controls were prepared in the same assay buffer as PEx samples. **Figure 2.7 and 2.8** are a schematic summary of the SPA and albumin assays, respectively, including the minor changes applied.

Figure 2.6 Schematic representation of the extraction protocol for further SPA and albumin ELISA

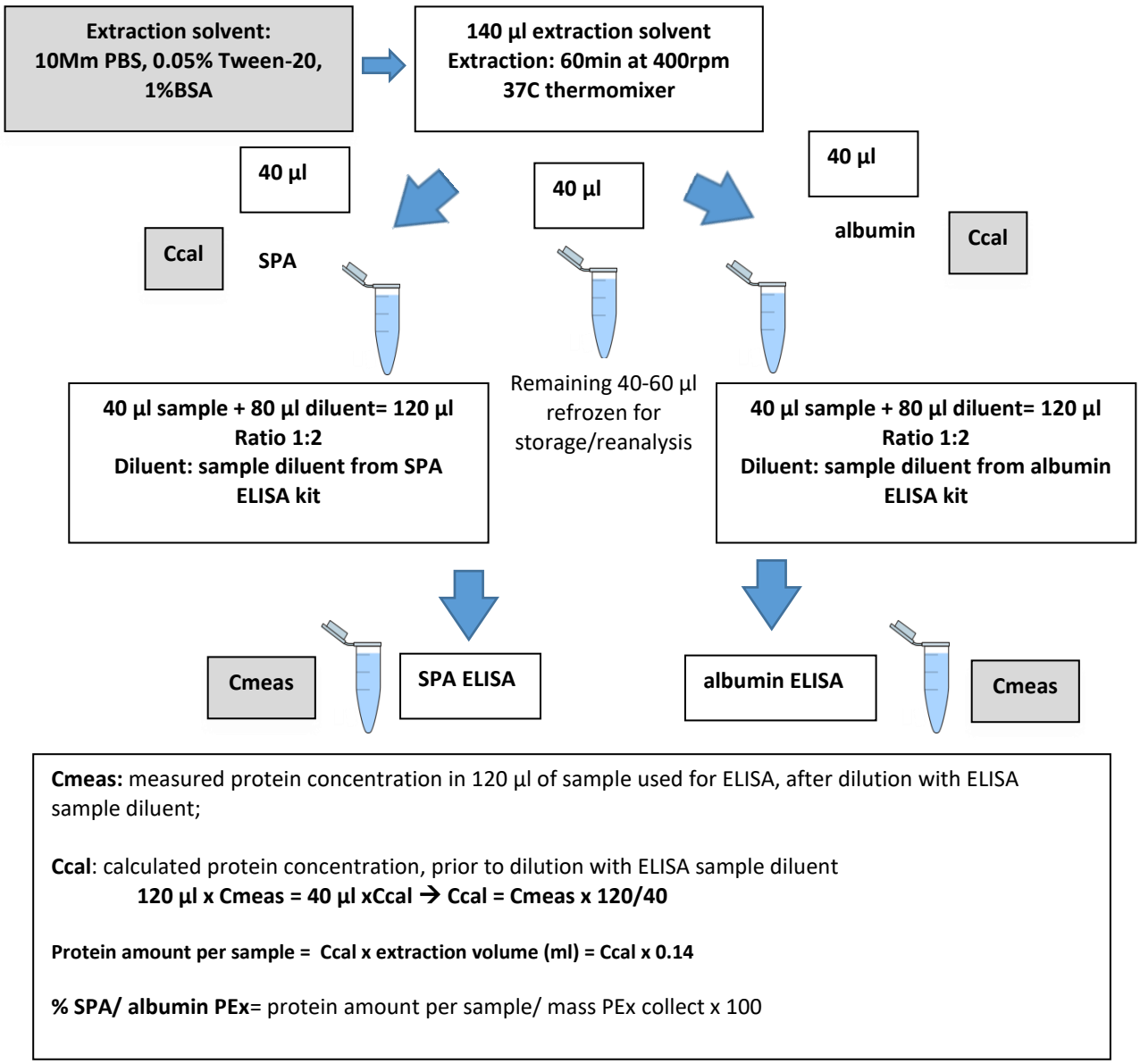

Definition of abbreviations: SPA: Surfactant protein A; PBS: phosphate buffered saline; BSA: Bovine Serum Albumin.

Figure 2.7 Summary of the SPA assay

	Concentrations (ng/ml)
Stock	100
Std 1	75
Std 2	50
Std 3	25
Std 4	10
Std 5	5
Std 6	2
Std 7	1
Std 8	0.5
Std 9	0.25

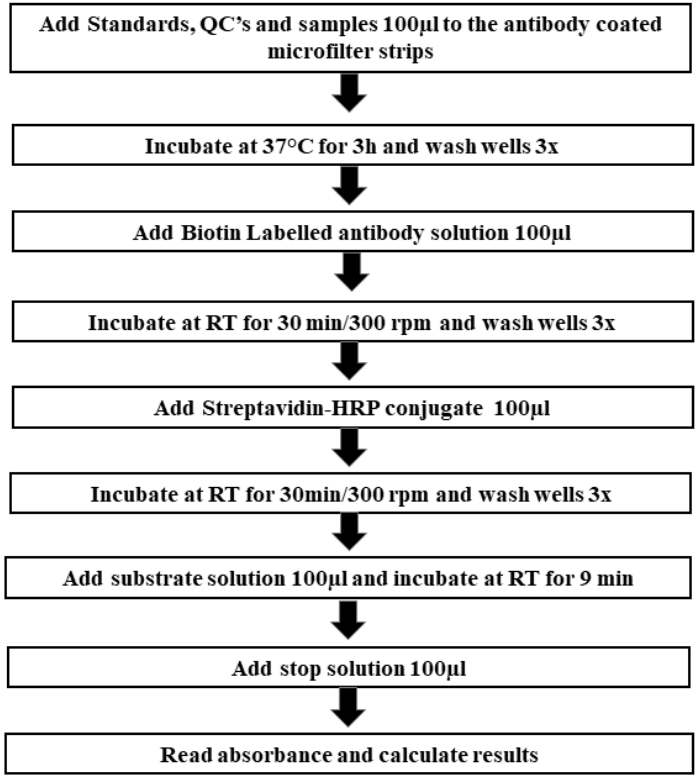

Defenition of abbreviations: QC: quality controls; Std: standard; RT: room temperature.

Figure 2.8 Summary of the albumin assay

	Concentrations (ng/ml)
A	3265
Std 1	200
Std 2	100
Std 3	50
Std 4	25
Std 5	10
Std 6	5
Std 7	2
Std 8	1
Std 9	0.5

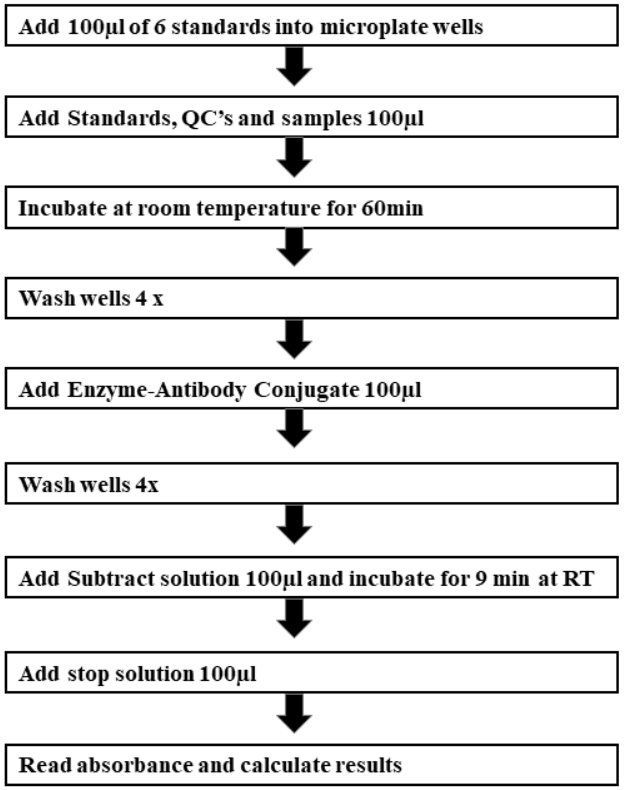

Defenition of abbreviations: QC: quality controls; Std: standard; RT: room temperature.

2.3.3 Forced oscillation techniques

Clinical measurement: impulse oscillometry and forced oscillation

Impulse oscillometry (IOS) was performed in triplicate according to standard guidelines from ERS Task Force Recommendations (119), using the Masterscreen IOS system (Erich Jaeger/ Care Fusion, Germany). A volume calibration was performed daily using a 3-L syringe supplied by the manufacturer, and the accuracy of resistance measurements was confirmed daily using a standard 0.2 $kPaL^{-1}s$ resistance mesh. Participants sat in an upright position, wore a nose clip and supported their cheeks, keeping a good seal around the mouthpiece, while an impulse waveform was delivered to their respiratory system via a loudspeaker connected to a mouthpiece, during 60 seconds of tidal breathing. A minimum of 3 consecutive measurements were performed, and each test was inspected for artefacts, discarding any portion of the test that was not suitable for analysis, leaving at least 30s of measurement. Resistance at 5 Hz (R5), resistance at 20 Hz (R20), the absolute difference between R5 and R20 (R5-R20), reactance at 5 Hz (X5) and AX were derived from pressure and flow measurements recorded. Subject variability was assessed by the coefficient of variation of R5 and R20, which had to be lower than 15%.

Forced oscillation technique

Forced oscillation technique (FOT) was performed in triplicate according to standard guidelines (119), using TremoFlo C-100 (Airwave Oscillometry System AOS™, Thorasis Montreal, Canada). Accuracy of resistance measurements was confirmed daily using a standard 0.2 $kPaL^{-1}s$ resistance mesh. Participants sat in an upright position, wore a nose clip and supported their cheeks, keeping a good seal around the mouthpiece, while an impulse waveform was delivered to their respiratory system via a loudspeaker connected to a mouthpiece, during 15 seconds of tidal breathing. A minimum of 3 consecutive measurements were performed, and each test was inspected for artefacts, discarding any portion of the test that was not suitable for analysis. Resistance at 5 Hz (R5), resistance at 19 Hz (R19), the absolute difference between R5 and R19 (R5-R19), reactance at 5 Hz (X5) and AX were derived from pressure and flow

measurements recorded. Subject variability was assessed by the coefficient of variation of R5 and R19, which had to be lower than 15%.

Physical model

A physical printed airway model was derived from an asthmatic patient, as shown on **figure 2.9**. 3D printing of the CT derived airway segmentation was performed by casting an optically clear elastomer around a CT-based, additive layer manufactured core, which was subsequently removed. The elastomer used in the model [Clear Flex(r) 50 water clear urethane rubber, Smooth-On Inc] possesses a level of elasticity similar to that of the cartilage in the trachea and left and right bronchial tubes (Young's modulus ~2.47MPa vs. averages ranging from 2.5&7.7MPa for trachea) thus allowing flow study at near-realistic compliance (277). The final printed airway represented Strahler orders 9-12 and had around seventy termini available for systematic occlusion. Systematic obstruction of the outlets of the printed model was achieved by complete occlusion with blue tack whilst clinical IOS and FOT was applied to the model for a period of 30 and 15 seconds respectively, in triplicate for each occlusion. Occlusions were applied heterogeneously and at random sequence generated by MATLAB. This process was performed twice, with and without a plastic case representing the chest wall bounded at the base by a rubber diaphragm representing the diaphragm of the lung, where the airway model was enclosed.

In order to compare the reactive component of impedance measured by the two systems, a 3L cylinder of air was used. This had no significant resistance; however, the significant mass of compressible air provided a reactance that could be measured. Forced and impulse oscillations were performed on each system as described previously.

Figure 2.9: 3D printed airway model

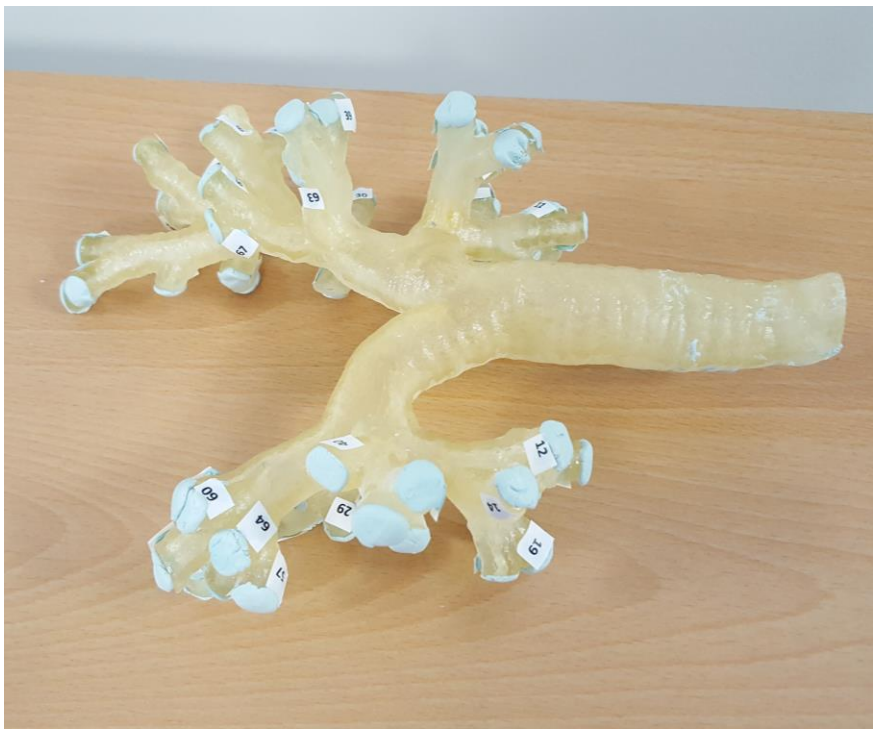

Each termini was numbered in the model; blue tack was used to obstruct each termini.

2.4 Imaging- Oxygen-enhanced MRI method

MRI scanner and gas delivery equipment

During OE-MRI acquisition O_2 is used as a contrast agent. Due to its paramagnetic nature, O_2 shortens T1 of the lung tissue, and T1-weighted images provide a dynamic investigation of O_2 wash-in and washout in the lung, during normal breathing at different fractions of the same gas. This technique was developed in the UK by Bioxydyn Limited and setup at the Radiology department in Glenfield Hospital, after appropriate verification of logistics, imaging facility and software suitability, carried by the company. The scanner used was a Siemens 1.5T Aera MRI scanner and software version MR D13.

Gas delivery circuit included gas supply, hoses, blender, tubing and masks, and were setup according to the room disposition. **Figure 2.10** shows a schematic representation of the overall OE-MRI test setup, gas delivery system and patient positioning on the MRI bed.

Image quality and scanner performance was closely monitored by phantoms image acquisition. The phantoms used were Eurospin II Test Object 05 (TO5) for T1 relaxation time assessment in each of the gel sets. A phantom image acquisition protocol was given by Bioxydyn, following the same exam card used for subjects and setup in the same manner. This test took place approximately every 6 weeks.

Appropriate protocol and OE-MRI procedures training was given to the Radiographers at Glenfield Hospital prior to any image acquisition session in a study patient. Additionally, an Imaging Manual was provided to the image acquisition site for use during the study. This included guidelines for patient positioning, gas delivery set-up, image sequence execution and data transfer methods to Bioxydyn.

Test procedure

Patients completed an MRI safety questionnaire prior to the MRI procedure. Patients were asked to take any piece of clothes or objects containing any metal, such as watches, belts, loose coins, etc. Patients then lay supine position in the scanner bed,

head first, and a disposable non-rebreathing mask was carefully fitted for the duration of the scanning session, in order to deliver medical air (21% oxygen and 79% nitrogen) and 100 % oxygen, as required for OE-MRI. Patient's position was adjusted to ensure its placement in the centre of the scanner bore, centred on the trachea carina. Patients could communicate with radiographer staff throughout the scanning session and had a hand-held buzzer with which they were able to stop the scan at any time if needed.

Gas delivery was set to medical air at the start of the scanning session, continuously at 15 L/min. Localiser scans and high-resolution image acquisitions were carried out for whole thorax coverage, followed by a coronal baseline T_1 measurement scan series. A multi-slice two dimensional coronal dynamic OE-MRI series was then performed, during which the gas supply was switched between medical air and 100% oxygen at the end of dynamic 15 and back to medical air at the end of dynamic 85, with patient breathing normally throughout the whole test. The total duration of the dynamic series was approximately 15 minutes. This sequence was performed using the same geometry, matrix, pixel dimensions and slice thickness as the 3D T1 mapping sequences. After the dynamic OE-MRI scan completion, the patient was removed from the scanner and the breathing mask removed. Each scanning session lasted no longer than 1 hour. The Radiographer completed an Image Acquisition Form (IAF) with image acquisition and subject details for each scan performed.

Data transfer and analysis

The images DICOM data and IAF were transferred to Bioxydyn electronically via the Internet Exchange Protocol (IEP) or, alternatively, via a courier if IEP was not available. Prior to DICOM image upload, all images were re-identified with a subject ID (no personal identifiable information). Time was removed and coded with "x" and "y" randomly, in order to keep the image analyst at Bioxydyn blinded to patient and double scan sequence.

An initial scan quality feedback was provided within 48h of image receipt, indicating if the scan passed or failed quality control, prior to data analysis.

Data analysis was performed using software written in MATLAB (MATLAB, The MathWorks Inc, Natrick, MA, USA) by Bioxydyn specialists. In summary, images were

corrected for respiratory motion and registered to end-expiration. T1 voxel maps were converted into dynamic maps of $\Delta PO_{2,}$ oxygen wash-in time, Tup and wash-out time Tdown, providing information about regional ventilation. A computational compartmental model developed previously (205) was used to provide information about the delivery and transport of oxygen through the model parameters Tvent (time for oxygen delivery via the conducting airways), Kox (rate of oxygen diffusion) and EoxFB (extraction of oxygen multiplied by blood flow).

The final reports provided by Bioxydyn contained a table with the summary of each parameter statistics [mean (SD), median, IQR-lower, IQR- upper] for the whole lung and an image output for each parameter.

Figure 2.10: Oxygen-enhanced MRI setup

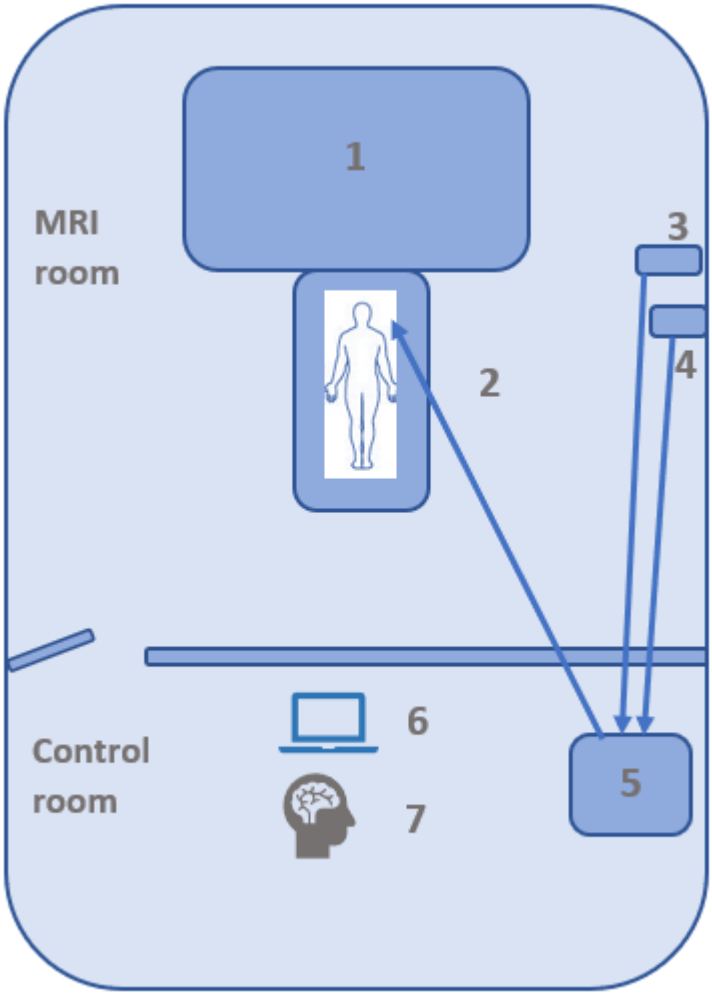

Legend: 1: MRI scanner; 2: Tubing to O_2 mask; 3: O_2 supply; 4: medical air supply; 5: O_2 blender and flowmeter; 6: scanner console; 7: radiographer.

2.5 General physiology testing considerations

In order to standardise and avoid any impact/manipulation of the small airways measurements, physiological tests on each study conducted were performed in accordance to ERS/ATS guidelines and specific task forces. Patient technique on each test was closely monitored by a qualified member of staff to ensure correct measurements. Calibration was performed daily prior to any testing, according to the specific protocol, including ambient temperature and pressure adjustment for spirometers, forced oscillation devices, lung volumes and multiple breath washout tests. The order in which each test was performed will be described in more details in each study in section 3.

2.6 Statistical analysis

Statistical analysis was performed using GraphPad prism 7 (GraphPad Software, La Jolla, CA 92037, USA), SPSS version 22 and 24 (IBM Corporation, Somers, New York, USA), SAS 9.4 (SAS Institute Inc., Cary, NC, USA.) and R (version 3.5.0, 2018.04.23, Copyright © 2018 The R foundation for statistical computing, platform: x86_64-w64-mingw32/x64). Parametric data was expressed as mean± SEM or SD (standard error of the mean, standard deviation) and non-parametric data was described as median (Q1;Q3). Parametric data were analysed by ANOVA across groups and t-test between 2 groups. Non-parametric data were analysed using Mann-Whitney and Kruskal Wallis and Wilcoxon tests. Between groups post-hoc Bonferroni/Dunn's pair wise comparison tests were used as appropriate, with a threshold for statistical significance set as $p<0.05$. Correlations between continuous variables were calculated using Pearson's correlation coefficient for parametric data and Sperman's rank test for non-parametric data. Chi-squared tests were used to compare categorical data. The method of Bland-Altman was utilised to assess the dispersions from the line of identity (95% limits of agreement).

The intraclass correlation coefficient (ICC) was calculated to compare the correlation of each repeatability visit with the baseline visit. Linear regression models were applied to Bland-Altman data to quantify bias slopes and intercepts and to analyse associations between OE-MRI parameters and clinical outcomes. Linear mixed effect modelling was

generated with R and utilised to evaluate association between fSAD and PExA biomarkers and FEV_1, FVC decline.

Sample size calculations were generated with G-power software (version 3.1.9.2).

Topological data analysis (TDA) was performed using the Ayasdi Workbench v7.1.0 software (Ayasdi, Palo Alto, California). The column set comprised Sacin, SPA % PEx, Alb % PEX and R5-R20. The metric used was the norm correlation, which is the Pearson correlation coefficient applied to the normalised variables, i.e., variables were transformed to follow a standard normal distribution. The resolution=30, gain=3, the lens applied was the neighbourhood 1 and 2 lens. Theses lenses allowed the embedding of high dimensional data into a two-dimensional space by embedding a K nearest neighbour's graph. Further details will be given on chapter 3.3.

Further detailed statistical analysis is given for each study in the next chapter.

3. Studies

3.1 Impulse oscillometry derived R5-R20 as a small airway dysfunction detection tool in adult asthma

ABSTRACT

Background: The precise contribution of small airways dysfunction in asthma has been difficult to determine due to the lack of simple, well-validated tools. Impulse oscillometry (IOS) measurements of small airways function, particularly the resistance at 5 minus 20 Hz (R5-R20) may be a measure of peripheral dysfunction but has yet to be validated from a clinical perspective. We sought to determine the clinical importance of an elevated R5-R20, whilst accounting for spirometry values and its potential to predict spirometry decline. **Methods:** 177 adults with asthma [54 (13) years of age, GINA step treatment: I-V] attended up to two visits at Glenfield hospital, Leicester, where clinical outcomes and post-bronchodilator physiological measurements from spirometry and IOS were collected. 108/177 attended a follow-up visit after a median Q1;Q3 of 2.08 (2.04:3.02) years to perform follow up post-bronchodilator spirometry. **Results:** Elevations in R5-R20 were common in patients within abnormal spirometry strata; in contrast, 12% of patients with normal spirometry had an abnormal R5-R20, indicative of early small airways disease. These patients demonstrated impaired asthma control and quality of life and a statistically significant increase in exacerbations when compared to patients with both normal spirometry and a normal R5-R20. Furthermore, it appears that R5-R20 could be a sensible marker of small airways disease status and clinical patient related outcomes change in anti-inflammatory intervention. **Discussion:** We have provided evidence using a clinical population that further supports impulse oscillometric parameter R5-R20 as an early small airways dysfunction detection tool in adult asthma.

INTRODUCTION

Asthma is a complex chronic inflammatory disease that involves both central and small airways (6,71). Multiple lines of evidence suggest that the small airways are dysfunctional (278), inflamed (279) and damaged in asthma (280). However there remains a lack of validated tools to identify disease and dysfunction in the small airways rendering standardised assessments in large clinical populations problematic.

Frequency dependence of resistance, a putative marker of small airways obstruction (resistance at 5 Hz minus 20 Hz; R5-R20) measured using the forced oscillation technique (FOT), has been shown to identify small airways dysfunction in image functional modelling studies, linking bronchoconstrictive airway models to physiological measurements and ^{3}He MRI/PET imaging of ventilation (134,135). However, in these studies FOT was evaluated at lower frequencies (< 2 Hz) which cannot be examined during spontaneous tidal breathing, making the measurements difficult to exploit in larger clinical populations.

Impulse oscillometry (IOS) is a variant form of FOT that perturbs the respiratory system with impulses containing an envelope of frequencies between 5-30 Hz, during spontaneous tidal breathing (10). IOS may therefore be a more suitable and clinically applicable tool to measure peripheral dysfunction in adults and children with asthma (136). Elevated frequency dependence of resistance measured using IOS, has been shown to predict loss of asthma control in children with well controlled asthma (281) and correlates with measures of small airway inflammation (282), exacerbations (12) and response to inhaled corticosteroids including small particle formulations in adult asthma (13,283,284) in small selected asthma populations.

Despite the potential clinical value of R5-R20 as a small airway dysfunction detection tool, to date there has been limited anatomical validation of IOS derived values linking them to the small airways. In addition, the clinical expression of elevation in R5-R20 in the presence of ‘normal’ spirometry in asthma has not been fully examined, making it difficult to evaluate the role of R5-R20 as an ‘early’/small airways dysfunction tool in asthma and its value in predicting lung function decline. This is important as spirometry derived measures of expiratory flow limitation primarily probe the central airways (94). Other putative small airway measures such as forced expiratory flow rates over selected lung volumes e.g. FEF_{25-75}, have been shown to add little to conventional spirometry

measures in large population studies (285) and suffer from poor measurement repeatability, likely to be a consequence of effort dependence (286).

We sought to provide further clinical validation of IOS derived R5-R20 as a small airway detection tool in asthma and its usefulness in early disease. We hypothesised that patients with adult asthma and an elevated R5-R20 would have poorer disease control, quality of life and more exacerbations. Furthermore, we hypothesised that R5-R20 is an early predictor of FEV_1 and FVC decline, in adult asthmatics and could be used in clinical trials settings.

METHODS

The study protocol was approved by the National Research Ethics Committee – East Midlands Leicester (approval number 08/H0406/189) and all subjects gave their written informed consent.

177 adults with asthma were recruited from Glenfield Hospital in Leicester, UK. Current smokers and patients with a smoking history of ≥ 10 pack years were excluded. Asthma was diagnosed by a physician according to the current British Thoracic Society guidelines (287) and asthma severity was defined according to the Global Initiative for Asthma (GINA) treatment intensity steps (2).

Study Protocol

All participants attended a study visit not less than six weeks following an asthma exacerbation. Physiological tests were performed 15 minutes after administration of 400g of short-acting bronchodilator via volumatic. Patients had withheld their inhaled bronchodilator for a period of at least 6h (short acting) and 12h (long acting) prior study visit.

In addition to the collection of demographic and clinical details, six-point Juniper asthma control questionnaire (ACQ-6) and standardised asthma quality of life

questionnaire (AQLQ) (269,270) were completed. IOS was performed using a Jaeger MasterScreen (Viasys Healthcare GmbH, Hoechberg, Germany) (119) and spirometry, according to ATS/ERS standards (271).

108/177 patients were followed-up, 2 years in average after baseline visit, performing a further post-bronchodilator spirometry.

Physiological Measurements

All physiological tests were performed in the seated position by individuals with appropriate training and UK accreditation.

IOS measurements were performed in triplicate according to standard guidelines (119) and as previously reported (140). Volume calibration was performed daily using a 3-L volume syringe, and the accuracy of resistance measurements was confirmed daily using a standard 0.2 $kPa.s.L^{-1}$ resistance mesh. Mean values for resistance R5, R20, R5-R20, reactance at 5 Hz (X5) and the area of reactance (AX) were derived as previously described (288).

Spirometry values were converted to standardised residuals (SR) using multi ethnic life course normative regression equations developed by the Global Lung Initiative (GLI) (272). An FEV_1 and FVC SR of < -1.64 were defined as abnormal and an FEV_1/FVC ratio below the GLI derived lower limit of normal (LLN) was considered to be abnormal.

Elevated R5-R20

IOS values are known to be associated with height, sex and age. Despite the lack of well-established reference values for IOS parameters from a large and mixed adult population, efforts have been taken place to address this need (136). We utilised normative values appropriately adjusted for age, sex and height for IOS that have been developed in a large healthy Caucasian population of a similar median age to the asthma population in this study (125).

Using the predicted values from this KORA cohort (Cooperative Health Research in the Region Augsburg), we considered that patients with R5-R20 above the 50^{th} percentile

(but below 95th percentile) were trending to an abnormally high value and potentially early peripheral disease, and established abnormally high R5-R20 when above the 95th percentile.

Statistical Analysis

Statistical analyses were performed using SAS 9.4 (SAS Institute Inc., Cary, NC, USA.) and Prism 7 for graphical plots (GraphPad Software Inc., La Jolla, CA, USA).

A *p*-value of <0.05 was taken as the threshold for statistical significance. Comparisons between or across groups were performed using Student's t-test or one-way analysis of variance for parametric data, the Mann–Whitney *U*-test or Kruskal–Wallis test for nonparametric data, and Fisher's exact test or the chi-squared test for proportions. Bonferroni/Dunn corrections for multiple comparisons were used as appropriate. Correlations between continuous variables were calculated using Pearson's correlation coefficient *(R*). Log-normally distributed variables were log-transformed as appropriate. Poisson regression models were utilised to investigate the associations between R5-R20 and retrospective exacerbation frequency. Linear mixed effect modelling was utilised to evaluate the association of R5-R20 and FEV_1 and FVC decline in a subset of the study cohort.

RESULTS

R5-R20 and Asthma Clinical Expression

Figure 3.1.1 and **Table 3.1.1** show a summary of our clinical population stratified according to Spirometry: patients in group 1 had FVC Z score < -1.64 (n=30); patients in group 2 had FVC Z score ≥ -1.64 and FEV1/FVC ≥ LLN (n=95); patients in group 3 had FVC Z score≥ -1.64 but FEV_1/FVC < LLN (n=52). We used FVC to primarily stratify our population because this parameter is more sensitive to premature airway

closure, a feature of small airways dysfunction, rather than FEV_1/FVC, which is affected by resistance anywhere in the airway tree (106).

The results show that group 1 (gas trapping, Low FVC) demonstrated statistically differences in ACQ-6, as well as more frequent exacerbations when compared to the early airways disease group (group 2).

It can be seen from **figure 3.1.1** that the prevalence of small airways dysfunction assessed with R5-R20 varied across the three spirometry strata, with groups 1 and 3 (abnormal spirometry) having the highest proportion of patients with high values of R5-R20. Additionally, the definition of dysfunction based upon 50^{th} or 95^{th} percentile significantly influenced the prevalence of small airway dysfunction (29 and 12% respectively).

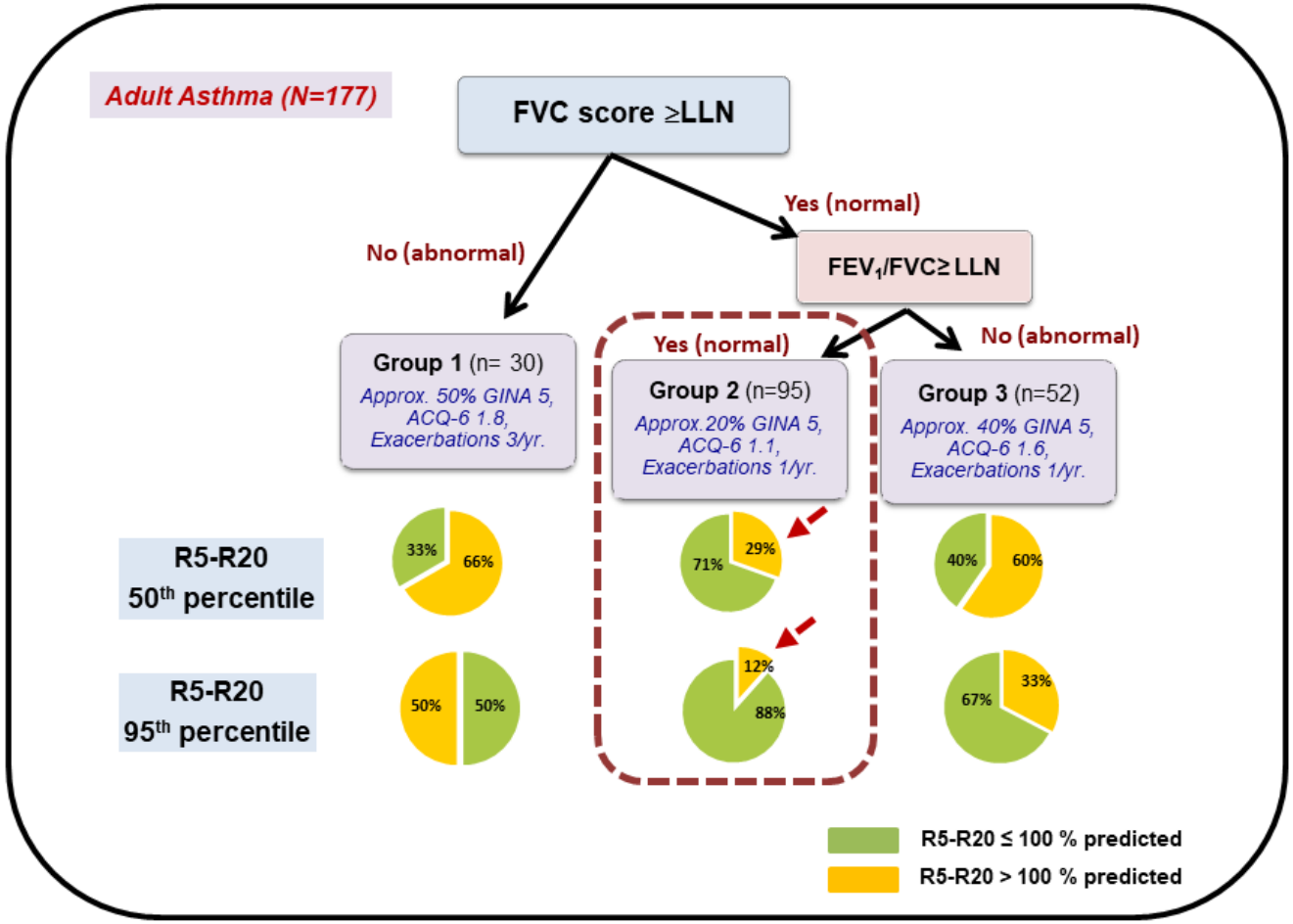

Figure 3.1.1: Stratification of the study population according to FVC Z score and FEV_1/FVC LLN. Pie charts presenting the percentage of patients in each group with R5-R20> 100% predicted, utilizing both the 50th and the 95th percentile equations, as stated.

Table 3.1.1: Clinical characteristics of the asthma population

	Group 1 (n=30) FVC Z score <-1.64	**Group 2 (n=95) FEV_1/FVC≥ LLN + FVC Z score >-1.64**	**Group 3 (n=52) FEV_1/FVC < LLN + FVC Z score >-1.64**	**Kruskal-Wallis p-value**
Age (years)	60 (45;65)	56 (45;65)	58 (47;64)	0.734
Sex [% male (n)][b]	53 (16)	40 (38)	54 (28)	0.250
BMI (kg/m^2)	28 (24;34)	28 (25;32)	27 (23;30)	0.200
Smoking pack year history	0 (0;0)¥	0 (0;2)	0 (0;4)	0.039
GINA treatment step (number per group: 1, 2-4, 5)[b]	2, 14, 14	11, 67, 17	4, 28, 20	0.007
ACQ-6	1.83 (0.77;3.07)	1.14 (0.58;1.71)Δ,µ	1.62 (0.83;2.79)	0.002
AQLQ	5.19 (3.67;5.94)	5.67 (4.78;6.31)	5.62 (3.76;6.27)	0.052
Exacerbations (year prior to visit 1)	3 (1-4)	1 (0-3)	1 (0-3)	<0.0001
GLI-FEV_1 Z score	-2.82 (-3.37; -2.27) Δ,¥	-0.43 (-1.02;0.37)µ	-1.91 (-2.46; -1.26)	<0.0001
R5 $kPa.s.L^{-1}$	0.52 (0.42;0.63) Δ	0.39 (0.31;0.47) µ	0.48 (0.33;0.58)	<0.0001
R5 %predicted (50^{th} percentile)	197 (166;289) Δ,¥	123 (106;146) µ	149 (125;191)	<0.0001
R5 %predicted (95^{th} percentile)	117 (96;162)Δ	88 (74;106)µ	105 (85;139)	<0.0001
R20 $kPa.s.L^{-1}$	0.35 (0.31;0.48)	0.33 (0.28;0.38)	0.35 (0.29;0.44)	0.061
R20 %predicted (50^{th} percentile)	167 (136;198)Δ	135 (115;156)µ	153 (128;184)	0.0002
R20 %predicted (95^{th} percentile)	108 (91;135)Δ	91 (79;106)µ	103 (88;123)	0.0017
R5-R20 $kPa.s.L^{-1}$	0.15 (0.07;0.21)Δ	0.05 (0.03;0.09)µ	0.09 (0.04;0.18)	<0.0001
R5-R20% predicted (50^{th} percentile)	195 (120;311)Δ	84 (50;132)µ	171 (67;244)	<0.0001
R5-R20 % predicted (95^{th} percentile)	100 (48;143)Δ	38 (23;66)µ	70 (25;116)	<0.0001

Definition of abbreviations: R5-R20: Resistance at 5Hz minus resistance at 20 Hz; LLN: Lower limit of normal; BMI: Body Mass Index; ACQ-6: 6-point asthma control questionnaire; AQLQ:

Asthma quality of life questionnaire; FEV_1: Forced expiratory volume in one second; FVC: Forced vital capacity; Z-FEV_1 = Global lung Initiative (GLI) Z score; R5-R20: Resistance at 5 Hz minus resistance at 20 Hz. Data expressed as median, Q1;Q3. **b**: χ^2 test p value. Δ $p<0.05$ group 1 vs group 2; µ $p<0.05$ group 2 vs group 3; ¥ $p<0.05$ group 1 vs group 3.

Next, we sought to evaluate group 2 further, (patients with normal FVC and FEV_1/FVC ratio), representative of early small airways disease. We sub-categorised group 2: 2 A- patients with normal R5-R20; 2 B- R5-R20> 100% calculated with 50^{th} percentile and R5-R20<100% calculated with 95^{th} percentile and 2 C- patients with R5-R20>100% calculated with 95^{th} percentile. In total 39 patients had an elevated R5-R20, with 11 of those above the 95^{th} percentile (12% as seen in figure 1). **Figure 3.1.2** panel A shows a dot plot of the study population where is visible a number of patients with high R5-R20 [> 50^{th} percentile and < 95^{th} percentile (orange)] and very high R5-R20 [> 95^{th} percentile (red)], despite normal spirometry. Additionally, panels B, C and D show asthma patient reported outcomes (ACQ-6, AQLQ) and exacerbations across the three groups. ACQ-6 is significantly higher in the group with R5-R20 above 95^{th} percentile, followed by patients above 50^{th} percentile (p=0.015). AQLQ and number of exacerbations show a similar but non-significant trend for worst outcomes for groups B and C.

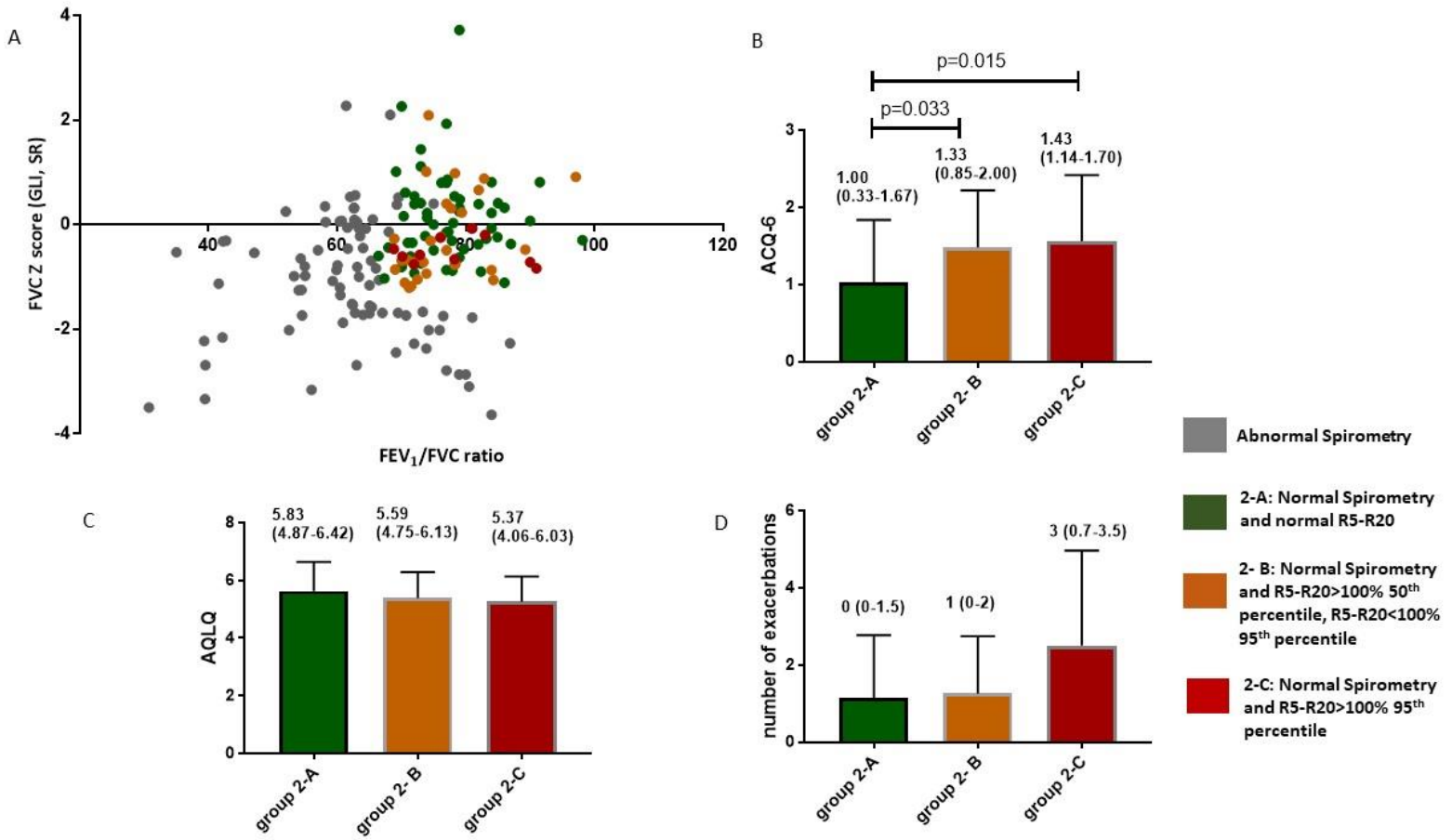

Figure 3.1.2: Population stratification and clinical outcomes. (A) Dot plot presenting study population according to spirometric outcomes (grey: FVC<LLN and/or FEV_1/FVC<LLN; green: FVC≥LLN and FEV_1/FVC≥LLN; orange: FVC≥LLN and FEV_1/FVC≥LLN and R5-R20>100% by 50th percentile and R5-R20<100% by 95th percentile; red: FVC≥LLN and FEV_1/FVC≥LLN and R5-R20>100% by 95th percentile. ACQ-6 (B), AQLQ (C) and exacerbations (D) across group 2- subgroups.

Poisson regression was utilised to examine whether R5-R20 was associated with retrospective exacerbations captured over a 1-year period prior to the first study visit, as seen on **table 3.1.2**.

Exacerbations were characterised by international consensus criteria developed by the ATS/ERS (289) and moderate to severe exacerbation were evaluated in this analysis.

The dependent variable in the regression models was the number of exacerbations experienced during one calendar year prior to the first study visit. Independent variables were age, gender, ACQ-6, IOS derived R5-R20, Global lung initiative FEV_1 Z score, GINA treatment steps were rebased to GINA I, GINA II-IV and GINA V to evaluate the effects of inhaled and oral corticosteroids separately. Covariates were Z normalised to allow scale invariance and effect size comparisons. Poisson regression models were constructed by sequentially adding variables that were significant predictors individually, and then testing the remaining variables to assess if they made a significant additional contribution, until the optimal model was reached, as assessed using the Akaike Information Criterion. The model identified that the R5-R20, GINA treatment step, age, height and ACQ-6 were all significant independent predictors of exacerbations, with R5-R20 demonstrating a similar numerical (but small) effect size to ACQ-6 for normalised transformed variables. Forced oscillation parameters have shown wide variation according to height, thus, this parameter was utilised instead of BMI. Higher resistance values exceeding the limits established adjusted for height may be indicative of peripheral airway dysfunction.

Table 3.1.2: Poisson regression models of retrospective exacerbations

Variable	Incident rate ratio	95% Wald confidence interval of incident rate ratio	p value
Model 1: AIC = 607.6, Omnibus test: likelihood ratio $\chi 2 = 89.6$, $p<0.001$			
Z-Age	0.83	0.74:-0.94	**0.003**
Z-Height	0.82	0.74:-0.94	**0.001**
Sex (1=Female, 0 = Male reference category) 1	1.01	0.80:1.21	0.91
Z-ACQ-6	1.22	1.08:1.37	**0.001**
Rebased GINA step (GINA I as reference step) GINA II-IV GINA V	 2.24 3.42	 1.13:4.43 1.68:6.96	 **0.021** **0.001**
Z-R5-R20	1.12	1.02:1.23	**0.016**
Model 2: AIC = 597.3, Omnibus test: likelihood ration $\chi 2 = 89.8$, $p<0.001$			
Z-Age	0.84	0.74:-0.94	**0.003**
Z-Height	0.83	0.73:0.94	**0.005**
Sex (1=Female, 0 = Male reference category) 1	0.99	0.78:1.25	0.92
Z-ACQ-6	1.24	1.01:1.39	**<0.0001**
Rebased GINA step (GINA I as reference step) GINA II-IV GINA V	 2.25 3.36	 1.14:4.46 1.65:6.85	 **0.02** **0.001**
Z-R5-R20	1.13	1.03:1.25	**0.013**
GLI-FEV_1 Z score	1.02	0.94:1.11	0.62

Definition of abbreviations: Z = Z normalised data to allow scale invariant comparisons for co variates. Z-FEV_1 = Global lung Initiative (GLI) Z score. Incident rate ratios are the fold-change in annual exacerbation risk for one Z score increase in age, height, R5-R20, ACQ-6, GLI FEV_1 Z score. For ordinal/nominal variables (Sex & GINA step) the rate ratios refer to the exacerbation risk above the reference category (Male Sex, GINA treatment step).

Lung function decline

Linear mixed effects modelling of FEV_1 and FVC decline over two visits (adjusting for age, sex, pack years of previous smoking exposure, height) in the decline subset (108/177 patients) identified an overall decline of -84 (-60;-108) and -0.09 (-0.06; -0.13) mls/year, for FEV_1 and FVC, respectively (**Table 3.1.3 and Table 3.1.4**). Although there was a clear association (and large effect size) between baseline absolute R5-R20 and FEV_1 -33 mls (-42:-25) mls/unit change in FEV_1 ($p<0.05$), the interaction of R5-R20 and time in the models did not identify a significant interaction effect. There was in addition a clear association between baseline R5-R20 and FVC ($p<0.0001$) but no evidence of an interaction with time in decline modelling.

Table 3.1.3: Linear Mixed Model Analysis of FEV_1 decline

Effect	Estimate	Standard Error	t Value	Pr > |t|	Lower	Upper
Intercept	-59.395	868.127	-0.068	0.946	-1727.3905	1608.5752
Time (years)	-84.369	12.202	-6.914	<0.0001	-108.2186	-60.4271
Age (years)	-16.798	3.817	-4.401	<0.0001	-24.1314	-9.46356
Sex Female						
Sex Male	-67.551	101.366	-0.666	0.507	-262.3133	127.2071
Height (cm)	20.357	4.938	4.122	<0.0001	10.8685	29.8456
Pack year	-9.983	6.090	-1.639	0.104	-21.6836	1.7169
R5-R20 (kPa.s.L^{-1})Ł	-33.4629	4.6074	-7.263	<0.0001	-42.31679	-24.60704
Time* R5-R20 (kPa.s.L^{-1})Ł	0.2051	1.2183	0.168	0.867	-2.190679	2.5825485

Definition of abbreviations: FEV_1: Forced expiratory volume in one second; R5: resistance at 5 Hz; R20: resistance at 20 Hz; Ł = mean centred absolute value of R5-R20×100

Table 3.1.4: Linear Mixed Model Analysis of FVC decline

Effect	Estimate	Standard Error	t Value	Pr > |t|	Lower	Upper
Intercept	-2.498790	1.031175	-2.423	0.0164	-4.49420	-0.5036
Time (years)	-0.093712	0.018048	-5.192	<0.0001	-0.12934	-0.0587
Age (years)	-0.023272	0.003356	-6.935	<0.0001	-0.0298	-0.0168
Sex Female						
Sex Male	-0.376845	0.122804	-3.069	0.0025	-0.61456	-0.1389
Height (cm)	0.044678	0.005701	7.836	<0.0001	0.03364	0.0557
Pack year	0.008516	0.005115	1.665	0.0978	-0.0014	0.0184
R5-R20 (kPa.s.L^{-1})Ł	-0.277793	0.049042	-5.664	<0.0001	-0.3727	-0.1829
Time* R5-R20 (kPa.s.L^{-1})Ł	0.004572	0.018065	0.253	0.8005	-0.0306	0.0403

Definition of abbreviations: R5: resistance at 5 Hz; R20: resistance at 20 Hz; Ł = mean centred absolute value of R5-R20×100

Impact of anti-inflammatory therapy on small airways disease

Having established the sensitivity of R5-R20 to small airways disease and clinical asthma patient related outcome measures, we next sought to evaluate its sensitivity to anti-inflammatory intervention. We initially conducted a power calculation to identify the population size needed in a placebo-controlled asthma intervention trial to detect a 0.03 Kpa.s.L^{-1} treatment effect which was identified consistently across a number of inhaled steroid comparator asthma trials (13,284,290,291) assuming a standard deviation of 0.05 Kpa.s.L-1 (140) at a 90% power and 5% significance level. We identified that 58 patients would be required per treatment arm to detect such as treatment effect.

We subsequently identified two three-month duration anti-inflammatory randomised double-blind placebo-controlled phase 2 trials in moderate-severe uncontrolled asthma that have been previously reported (292,293) evaluating known targets relevant to asthma pathology in the small airways (IL-13 and the CRTH2 receptor DP2). FOT was measured in both trials as an exploratory outcome measure. Neither trial alone was powered to detect our pre-identified treatment effect. However, the pooled treatment effect [95% CI] of the two anti-inflammatory therapies was [-0.04 kPa.s.L-1 (-0.08:-0.01), p=0.02], favouring anti-inflammatory therapy compared to placebo (**Table 3.1.5**).

Table 3.1.5: Pooled clinical trial data using R5-R20 as a marker

	Change from baseline to week 12		**Treatment effect**
	Tralokinumab (n = 39)	Placebo (n = 30)	
Change in R5-R20 (kPa.s.L^{-1})	-0.05 (0.11)	-0.01 (0.11)	-0.04 (0.11) p = 0.19
	Fevipiprant (n = 29)	Placebo (n = 32)	
Change in R5-R20 (kPa.s.L^{-1})	-0.03 (0.11)	0.02 (0.11)	-0.05 (0.011) p = 0.11
Pooled estimate change in R5-R20 (kPa.s.L^{-1})	-0.037 (0.11)	0.003 (0.11)	-0.044 (0.11) p = 0.02 95% CI: -0.08 to -0.01

Change and treatment effect on R5-R20 (Resistance at 5 HZ minus resistance at 20 Hz) of two three-month duration anti-inflammatory randomised double blind placebo controlled phase 2 trials in moderate-severe uncontrolled asthma, for both intervention and placebo. Pooled estimated treatment effect [95% CI] of the two anti-inflammatory therapies is shown.

DISCUSSION

In our study, we have provided evidence to support impulse oscillometry derived R5-R20 measurements, as a 'small airway dysfunction' detection tool in asthma.

Impulse oscillometry, although not widely accepted as a clinical physiological tool yet, has the advantage of being more specific to the small airways compartment, which is not fully achieved with spirometric parameters such as FEV_1, FEF_{25-75} and FEV_3/FVC, as well as being easy to perform, rapid and patient-friendly (294). Our observations open the possibility to identify small airway dysfunction in larger population studies, using IOS and other available forced oscillation approaches at conventional tidal breathing frequencies (5-20Hz). This has advantages over low frequency approaches which are problematic to measure in clinical studies due to interference of measured pressure and flow signals with higher harmonics of breathing.

We have shown in a relatively large clinical population of adult asthmatics that elevation in R5-R20 is associated with clinically significant differences in asthma control and quality of life and more frequent exacerbations, in both the presence and absence of abnormal spirometry. Moreover, in our study patients within the FVC<LLN strata representing gas trapping (106) demonstrated the poorest clinical outcomes, highest R5-R20 values and 50% of this strata demonstrated an R5-R20 > 95^{th} percentile. FVC has been regarded as a marker of peripheral airway status and gas trapping in asthma. We also demonstrated that patients with normal spirometry with an abnormal R5-R20 had poorer clinical outcomes when compared to patients with both normal spirometry and R5-R20. Finally, we have demonstrated that R5-R20 is independently associated with asthma exacerbations whilst adjusting for potential confounders.

Despite the fact that R5-R20 was independently associated with FEV_1 and FVC after adjusting for common confounders, we did not detect an effect on FEV_1 or FVC decline in a smaller subset of our asthmatic cohort. This may have been due to the relatively small sample size, short duration of follow up, as well as low spirometry-sampling frequency in our decline study. Future studies evaluating larger population samples are required to fully address the question of whether R5-R20 is a forward predictor of FEV_1 decline in asthma. Indeed, Newby *et al* have previously demonstrated that eosinophilic airway inflammation is a significant predictor of FEV_1 decline in adult asthma (FEV_1 decline of -25.7ml/year), utilizing a population of 97 patients with severe asthma, with

several study visits over a 6 year follow-up period (295). Accordingly, the main limitation in our decline study was the absence of multiple follow-up visits and the short period of time between baseline and follow-up.

Interestingly, our power calculations showed that only 58 patients per arm would be required to detect a clinically significant change in R5-R20 (0.03 $Kpa.s.L^{-1}$), in a placebo-controlled asthma intervention, following an anti-inflammatory treatment, which could be easily achieved in research settings and vital in the parameter and technique establishment.

In addition, alongside clinical findings, computational models bridging these results with anatomical validation to probe R5-R20 as a marker of small airways would provide further compelling evidence that small airway narrowing is the dominant driver of abnormal R5-R20 measurements (296).

In conclusion, easy and rapid recognition of peripheral disease in asthma, in its early stages, is crucial to appropriately manage long-term morbidities and disease progress. R5-R20 measured with forced oscillation technique is a potentially simple detection tool for population level studies to identify small airways dysfunction. Future studies are now required in larger populations at risk of FEV_1 decline to evaluate this measurement as early disease tool and its association with biological markers of small airways disease.

3.2 Comparison of forced and impulse oscillometry measurements: a clinical population and printed airway model study

ABSTRACT

Background: The use of commercialised forced oscillation (FOT) devices to assess impedance in obstructive diseases such as asthma has gained popularity. However, it has yet to be fully established whether resistance and reactance measurements are comparable across different FOT devices, particularly in disease.

Methods: We compared two commercially available FOT devices: Impulse Oscillometry (IOS) and TremoFlo FOT (Thorasys) in a) clinical adult population of healthy controls (n=14), asymptomatic smokers (n=17) and individuals with asthma (n=73) and b) a 3D printed CT-derived airway tree model resistance, as well as a 3 L standardised volume reactance. Bland-Altman plots and linear regressions were used to evaluate bias between the devices.

Results: Resistance measurements at both 5 and 20 Hz were numerically higher with IOS compared to FOT, with evidence of small and statistically significant proportional systematic bias and a positive Bland-Altman regression slope at both 5 and 20 Hz.

In contrast, the IOS device recorded reactances that were less negative at both 5 Hz and 20 Hz and significantly smaller reactance areas when compared to TremoFlo. Larger statistically significant proportional systematic biases were demonstrated with both reactance at 5 Hz and reactance area (AX) between the devices with a negative Bland-Altman regression slope.

The printed airway resistance and standardised volume reactance confirmed the observations seen in patients.

Discussion: We have demonstrated that the impulse oscillation system and TremoFlo FOT demonstrate comparative bias, particularly when comparing airway reactance in patients. Our results highlight the need for further standardisation across FOT measurement devices, specifically using variable test loads for reactance standardisation.

INTRODUCTION

The forced oscillation technique (FOT), introduced by DuBois *et al* in 1956 (118), is a method for non-invasively assessing lung mechanics by examining the relationship between pressure and flow whilst forced oscillations are delivered to the respiratory system by a loudspeaker or piston (119). The waveform delivered may be a sine wave at a single frequency, a combination of sine waves at multiple discrete frequencies, or a train of pulses which is mathematically decomposed in theory to a continuous spectrum of frequencies [a variant known as impulse oscillometry (IOS)] (10). The waveform delivered determines the frequencies at which the mechanical impedance of the respiratory system is measured.

The FOT technique is simple, non-invasive and only requires passive co-operation from the patients, rendering its usefulness in young children and the elderly (122). As a consequence, there has been an expansion of research involving FOT in recent years in a range of clinical settings.

A number of studies have evaluated the utility of FOT, most commonly IOS in both adults and children. IOS has for some time been the major commercial clinical testing device for FOT measurements in adults. IOS studies report its utility in predicting loss of asthma control, exacerbation events and response to inhaled therapies in adults and children with asthma when reviewed collectively (126,136).

International recommendations for FOT testing exist (119), however there remains significant differences in FOT values measured in healthy controls across specialised testing centres (297), highlighting the need for further methodological standardisation for patient testing and between-device comparisons.

A number of commercial FOT devices are currently available for patient testing of which the two most commonly deployed devices in clinical studies are the TremoFlo C-100 (Thorasys Medical Systems, Montreal, Canada) sinusoidal FOT device and the Jaeger Masterscope CT IOS (CareFusion, Hoechberg, Germany) device.

The purpose of this study was to evaluate and compare the impedance (resistance and reactance) between these two commercial devices using (i) a clinical population study of adults with asthma, aged matched healthy volunteers and asymptomatic smokers and

(ii) using a three-dimensional printed airway resistance phantom and standardised volume (reactance only) phantoms. We hypothesised that both devices would yield comparable resistance and reactance without evidence of systematic measurement bias between the two devices.

MATERIAL AND METHODS

Clinical Population

The study protocol was approved by the National Research Ethics Committee – East Midlands Leicester (approval number: 08/H0406/189) and all subjects gave their written informed consent. All methods described and performed in the study followed the relevant guidelines and regulations.

104 adult volunteers (73 individuals with asthma, 14 healthy volunteers and 17 asymptomatic smokers) were screened and recruited at Glenfield Hospital, Leicester, from secondary care asthma clinics, via recruitment from primary care across GP surgeries in Leicestershire and from an existing research database at the NIHR Respiratory Biomedical Research Centre, Leicester, UK.

Asthma patients had a physician diagnosis of asthma and one or more of the following objective physiological criterion: Methacholine PC20 ≤8mg/ml, bronchodilator reversibility to 400 mg of inhaled Salbutamol of FEV_1 ≥12% and 200mls or peak flow variability of ≥ 20% over two weeks.

All asthmatic patients had been free from exacerbations for at least 6 weeks prior to study entry. Asthmatic patients and healthy controls currently smoking or with a smoking pack history greater than 10 were excluded.

Study Protocol

Patients attended a single visit and the following data was collected: informed consent, medical history and current medication, Spirometry, IOS and FOT. Additionally, asthmatics were administered two questionnaires: juniper asthma control questionnaire ACQ-6, juniper asthma quality of life questionnaire AQLQ (267,270).

Physiological Measurements

All physiological tests were performed in the seated position by individuals with appropriate training and UK accreditation. Physiological tests were performed 15 minutes after administration of short-acting bronchodilator (inhaled salbutamol administered via a volumatic device: 400μg). IOS and TremoFlo were performed sequentially before spirometry, and patients were advised to avoid deep inspirations during the testing protocol. Patients were asked to maintain normal quiet breathing pattern for 30 seconds prior to IOS and TremoFlo measurements, in order to normalise their lung volume history.

IOS measurements were performed in triplicate according to standard guidelines, with a Jaeger MasterScreen IOS system (Carefusion, Germany, JLAB software version 5.22.1.50) (119). A volume calibration was performed daily using a 3-L volume syringe, and the accuracy of resistance measurements was confirmed daily using a standard 0.2 kPa.s.L^{-1} resistance mesh. Participants wore a nose clip and supported their cheeks, while impulse waveforms were delivered to their respiratory system via a loudspeaker connected to a mouthpiece, during 60 seconds of tidal breathing. Mean values for resistance at 5 Hz (R5), at 20 Hz (R20), the absolute difference between R5 and R20 (R5-R20), reactance at 5 Hz (X5) and the area of reactance (AX, the area under the reactance curve from 5 Hz to the resonant frequency) were derived as previously reported (140). Acceptability criteria for IOS measurements included coherence values of ≥ 0.6 at 5 Hz, between test coefficient of variation of Zrs of < 15% (with a minimum of three tests) and the absence of the following features within the flow tracings gauged by visual inspections: swallowing, glottis closure, leak around the mouthpiece, and improper seal with the nose clip.

FOT was performed in triplicate according to standard guidelines (119), using TremoFlo C-100 (Airwave Oscillometry System AOS^{TM}, Thorasys Montreal, Canada, software version: 1.0.34.32), utilising the default signal processing settings [multi-frequency waveform AOS 5 to 37 Hz (adults)]. Accuracy of resistance measurements was confirmed daily using a standard 0.2 kPa.s.L^{-1} resistance mesh. Participants sat in an upright position, wore a nose clip and supported their cheeks, keeping a good seal around the mouthpiece, while a sinusoidal waveform containing multiple frequencies was delivered to their respiratory system via a loudspeaker connected to a mouthpiece,

during 16 seconds of tidal breathing. A minimum of three consecutive measurements were performed, and each test was inspected for artefacts, discarding any portion of the test that was not suitable for analysis. R5, resistance at 19 Hz (R19), R5-R19, X5 and AX were derived from pressure and flow measurements recorded. Subject variability was assessed by the coefficient of variation of Zrs which had to be lower than 15% (with a minimum of three measurements).

Spirometry was performed according to international guidelines (271). Values were converted to standardised residuals (SR) using multi ethnic life course normative regression equations developed by the Global Lung Initiative (GLI) (272). A FEV_1 SR of < -1.64 was defined as abnormal and a FEV_1/FVC ratio below the GLI derived lower limit of normal (LLN) was considered to be abnormal.

Physical printed central airway model

A physical printed airway model was derived from an adult asthmatic patient (female, age=64, FEV_1/FVC=71%, FEV_1%=95%) as a model airway resistance with finite and negligible reactance. 3D printing of the CT derived airway segmentation was performed by casting an optically clear elastomer around a CT-based, additive layer manufactured core, which is subsequently removed. The elastomer used in the latter model (Clear Flex(r) 50 water clear urethane rubber, Smooth-On Inc) possesses a level of elasticity similar to that of the cartilage in the trachea and left and right bronchial tubes (Young's modulus ~2.47MPa vs. averages ranging from 2.5&7.7MPa for trachea) thus allowing flow study at near-realistic compliance.

The final printed airway represents the larger airways and had approximately 70 termini available for systematic occlusion, as shown in the methods section (**figure 2.9**). Each termini was then numbered randomly from 1-70, and identified with a small labelling sticker. Systematic obstruction of the outlets of the printed model was achieved by complete occlusion with blue tack whilst clinical IOS and TremoFlo was applied to the model for a period of 15-30 seconds in triplicate for each occlusion. Occlusions were applied heterogeneously and at random sequence generated by MATLAB 2014A [MathWorks©, USA)] using the 'randi.m' function with the argument '70' to randomly draw an integer from 1,2,…to 70.

Additionally, a 3L volume calibration cylinder of air (CareFusion Calibration Pump, Germany) was utilised as standard reactance with finite and small resistance. The significant mass of compressible air provided a reactance that could be measured. The precise resonant frequency and reactance of the 3L volume was not possible to determine, however we would expect the resonant frequency to be high (≥ 70 Hz) because there is no mass associated with the airways and the effective spring constant is high for a small volume such as 3 litres. Nonetheless, the 3L volume provides a reliable reactance standard for between-device comparison.

Forced and impulse oscillations were performed on each system as described previously.

Statistical Analysis

Statistical analyses were performed using Prism 7 (GraphPad Software Inc., La Jolla, CA, USA) and SAS 9.4 (SAS Institute Inc., Cary, NC, USA.). A *p*-value of <0.05 was taken as the threshold for statistical significance. Comparisons between or across groups were performed using Student's t-test or the Wilcoxon rank test for non-parametric data, and one-way analysis of variance/ Kruskal Wallis test for parametric/non-parametric data. Tukey's and Dunn's corrections were applied for multiple comparisons between clinical groups. The method of Bland-Altman analysis was utilised to visualise systematic bias between the two measurement devices (298). Linear regression models were applied to the Bland-Altman data to quantify bias slopes and intercepts between TremoFlo and IOS measurements.

RESULTS

Clinical population

Table 3.2.1 shows a summary of the clinical characteristics of the study population. Age differed numerically across groups (p=0.018, one-way ANOVA), however statistically significant differences were not seen between groups (asthmatic vs. asymptomatic smokers: p=0.067, asthmatic vs. healthy controls: p=0.079, Tukey's post-

test). The asthmatic individuals were primarily Global Initiative for Asthma [GINA (2)] treatment steps II to IV, with sub optimal control of symptoms, Asthma Control Questionnaire [ACQ-6 (mean, SD): 1.07, 1.05)].

As expected, both FEV_1 (L) and FEV_1 standardised residual (SR) were significantly different across the three groups, with significantly more expiratory flow limitation in the asthmatic group when compared with healthy controls. Similar results were found for Forced Vital Capacity (FVC) and FEV_1/FVC.

Table 3.2.1: Clinical characteristics

	Healthy controls (n=14)	**Asymptomatic smokers (n=17)**	**Asthma (n=73)**	**p-value**
Age (years)	50 (18)	50 (14)	59 (14)	0.018
Sex [% male (n)][b]	57 (8)	29 (5)	53 (39)	0.276
BMI (kg/m^2)	26.2 (4.3)	29.6 (5.9)	30.0 (6.0)	0.089
Smoking pack year history	6 (0)	27.6 (14)	8.5 (8)*	0.0003
GINA treatment step (number per group: 1, 2-4, 5)[b]	-	-	4, 58, 11	-
ACQ-6	-	-	1.04 (1.05)	-
AQLQ	-	-	5.66 (1.33)	-
FEV_1 (L)	3.47 (0.86)	2.95 (0.80)	2.54 (0.85) φ	0.0007
FEV_1 GLI score	0.89 (1.21)	-0.02 (0.7)	-0.93 (1.27) φ,*	<0.0001
FVC (L)	4.39 (0.87)	3.65 (1.01)	3.46 (0.87) φ	0.003
FVC GLI score	0.99 (1.40)	-0.09 (0.87)	-0.37 (1.05) ¥, φ	0.0002
FEV_1/FVC	0.78 (0.05)	0.81 (0.06)	0.71 (0.11) φ,*	0.0003

Definition of abbreviations: BMI: Body Mass Index; GINA: Global Initiative for Asthma; ACQ-6: 6-point asthma control questionnaire; AQLQ: Asthma quality of life questionnaire; FEV_1: Forced Expiratory Volume in the first second; GLI: Global Lung Function Initiative; FVC: Forced Vital Capacity. Data presented as mean (SD), b: number per group, c: χ^2 test p value; One Way ANOVA test followed by Tukey multiple comparison test; ¥ $p<0.05$ healthy vs. smokers. φ $p<0.05$ healthy vs. asthma; * $p<0.05$ smokers vs. asthma.

Impedance measurements from impulse oscillometry and TremoFlo are summarised in **Table 3.2.2**. Asthmatic subject demonstrated significantly greater resistance values and reactances that were more negative when compared to healthy subjects across a range of frequencies. In contrast, asymptomatic smokers demonstrated significantly higher resistances at both 5 Hz (IOS) and 20 (19) Hz (IOS/FOT) when compared to healthy volunteers ($p<0.05$). Additionally, at 20 (19) Hz asymptomatic smoker demonstrated numerically more positive reactance values when compared to asthmatic subjects ($p <0.05$).

Table 3.2.2: Forced oscillation physiological parameters

	Healthy controls (n=14)	**Asymptomatic smokers (n=17)**	**Asthma (n=73)**	**Kruskal Wallis p-value**
R5 (IOS) (Kpa.s.L^{-1})	0.29 (0.06)¥	0.38 (0.10)	0.41 (0.14) φ	0.002
R5 (FOT) (Kpa.s.L^{-1})	0.25 (0.06)	0.33 (0.08)	0.37 (0.13) φ	0.0007
R20 (IOS) (Kpa.s.L^{-1})	0.27 (0.05)¥	0.34 (0.07)	0.32 (0.08) φ	0.018
R19 (FOT) (Kpa.s.L^{-1})	0.24 (0.04)¥	0.30 (0.06)	0.30 (0.08) φ	0.013
R5-R20 (IOS) (Kpa.s.L^{-1})	0.03 (0.03)	0.04 (0.06)	0.09 (0.08) φ,*	0.0005
R5-R19 (FOT) (Kpa.s.L^{-1})	0.02 (0.04)	0.03 (0.06)	0.08 (0.08) φ,*	0.002
AX (IOS) (Kpa.L^{-1})	0.25 (0.14)	0.48 (0.55)	0.87 (0.85) φ	0.00
AX (FOT) (Kpa.L^{-1})	0.39 (0.23)	0.81 (0.82)	1.91 (1.93) φ	0.0007
X5 (IOS) (Kpa.s.L^{-1})	-0.09 (0.03)	-0.12 (0.04)	-0.15 (0.08) φ	0.007
X5 (FOT) (Kpa.s.L^{-1})	-0.08 (0.03)	-0.12 (0.06)	-0.18 (0.12) φ	0.001
X20 (IOS) (Kpa.s.L^{-1})	0.08 (0.03)	0.08 (0.06)	0.04 (0.05) φ,*	0.001
X19 (FOT) (Kpa.s.L^{-1})	0.03 (0.03)	0.02 (0.05)	-0.03 (0.07) φ,*	0.002

Definition of abbreviations: R5: Resistance at 5 Hz; R20: Resistance at 20 Hz; R5-R20: Resistance at 5 Hz minus 20 Hz; R19: Resistance at 19 Hz; R5-R19: Resistance at 5 Hz minus 19 Hz; AX: Area of Reactance; X5: Reactance at 5 Hz; X20: Reactance at 20 Hz. Data presented as mean (SD). Kruskal Wallis test followed by Dunn's multiple comparison post-test ¥ $p<0.05$ healthy vs. smokers. φ $p<0.05$ healthy vs. asthma; * $p<0.05$ smokers vs. asthma.

Clinical population- between-devices comparison

Table 3.2.3 and 3.2.4 show the mean difference between IOS and TremoFlo, standard deviation, 95% confidence interval of the mean difference and p values derived from Wilcoxon rank tests by disease group (**Table 3.2.3**) and overall population (**Table 3.2.4**), respectively. Additionally, **Figure 3.2.1** demonstrates comparative dot plots of numerical values for Resistance at 5 Hz (R5), Resistance at 20 (19) Hz [R20 (19)], Resistance at 5 Hz minus 20 (19) Hz [R5-R20 (19)], Reactance area (AX), Reactance at 5 Hz (X5) and Reactance at 20 (19) Hz [X20 (19)] across the different population groups, for both IOS (dots) and TremoFlo (stars).

Data demonstrate that IOS consistently measured higher resistance values when compared to TremoFlo at both 5 Hz and 20 Hz ($p<0.05$). These observations were consistent across all disease groups (**Table 3.2.3**) and in the pooled study population (**Table 3.2.4**). In contrast, reactance values were consistently more positive at both 5 and 20 Hz when comparing IOS to TremoFlo. Consequently, the low frequency reactance area between 5 Hz and resonant frequency was consistently and significantly larger when measured with TremoFlo compared to IOS ($p <0.05$).

Table 3.2.3: Mean differences and SD of differences between IOS and TremoFlo across the different groups

	Healthy Controls				Asymptomatic Smokers				Asthma			
	Mean Difference (IOS-TremoFlo)	Standard Deviation of the mean difference	p-value	95% CI	Mean Difference (IOS-TremoFlo)	Standard Deviation of the mean difference	p-value	95% CI	Mean Difference (IOS-TremoFlo)	Standard Deviation of the mean difference	p-value	95% CI
R5 ($Kpa.s.L^{-1}$)	0.03	0.03	0.0031	(0.0123; 0.0514)	0.06	0.05	0.0008	(0.0310; 0.0784)	0.04	0.07	<0.0001	(0.0288; 0.0515)
R20(19) ($Kpa.s.L^{-1}$)	0.02	0.03	0.0085	(0.0094; 0.0401)	0.04	0.03	0.0003	(0.0170; 0.0522)	0.03	0.03	<0.0001	(0.0191; 0.0340)
R5-R20(19) ($Kpa.s.L^{-1}$)	0.01	0.03	0.3258	(-0.0131; 0.0237)	0.02	0.04	0.0395	(0.0014; 0.0376)	0.01	0.06	0.0231	(0.0017; 0.0198)
AX ($Kpa.L^{-1}$)	-0.16	0.15	0.0012	(-0.2425; -0.0742)	-0.33	0.45	<0.0001	(-0.3807; -0.1324)	-1.08	1.36	<0.0001	(-1.144; -0.498)
X5 ($Kpa.s.L^{-1}$)	-0.01	0.02	0.2958	(-0.0153; 0.0056)	0.00	0.03	0.956	(-0.0136; 0.0161)	0.02	0.07	0.0332	(0.0011; 0.024)
X20(19) ($Kpa.s.L^{-1}$)	0.05	0.02	0.0001	(0.0367; 0.0558)	0.06	0.04	<0.0001	(0.0363; 0.0796)	0.06	0.03	<0.0001	(0.0497; 0.0631)

Definition of abbreviations: R5: Resistance at 5 Hz; R20(19): Resistance at 20/19 Hz; R5-R20(19): Resistance at 5 minus 20(19) Hz; AX: Area of Reactance; X5: Reactance at 5 Hz; X20(19): Reactance at 20(19) Hz. p-values obtained from Wilcoxon signed rank test (paired test), 95% confidence intervals are for the median of the difference.

Table 3.2.4: Mean differences and SD of differences between IOS and TremoFlo in the overall population

	Overall Population			
	Mean Difference (IOS-TremoFlo)	**Standard Deviation of the mean difference**	**p-value**	**95% CI**
R5 (Kpa.s.L^{-1})	0.04	0.06	<0.0001	(0.0320; 0.0496)
R20(19) (Kpa.s.L^{-1})	0.03	0.03	<0.0001	(0.0211; 0.0333)
R5-R20(19) (Kpa.s.L^{-1})	0.01	0.05	0.0019	(0.0050; 0.0192)
AX (Kpa.L^{-1})	-0.81	1.20	<0.0001	(-0.7696; 0.3283)
X5 (Kpa.s.L^{-1})	0.02	0.06	0.1224	(-0.0012; 0.0137)
X20(19) (Kpa.s.L^{-1})	0.06	0.03	<0.0001	(0.0484; 0.0599)

Definition of abbreviations: R5: Resistance at 5 Hz; R20(19): Resistance at 20/19 Hz; R5-R20(19): Resistance at 5 minus 20(19) Hz; AX: Area of Reactance; X5: Reactance at 5 Hz; X20(19): Reactance at 20(19) Hz. p-values obtained from Wilcoxon signed rank test (paired test), 95% confidence intervals are for the median of the difference.

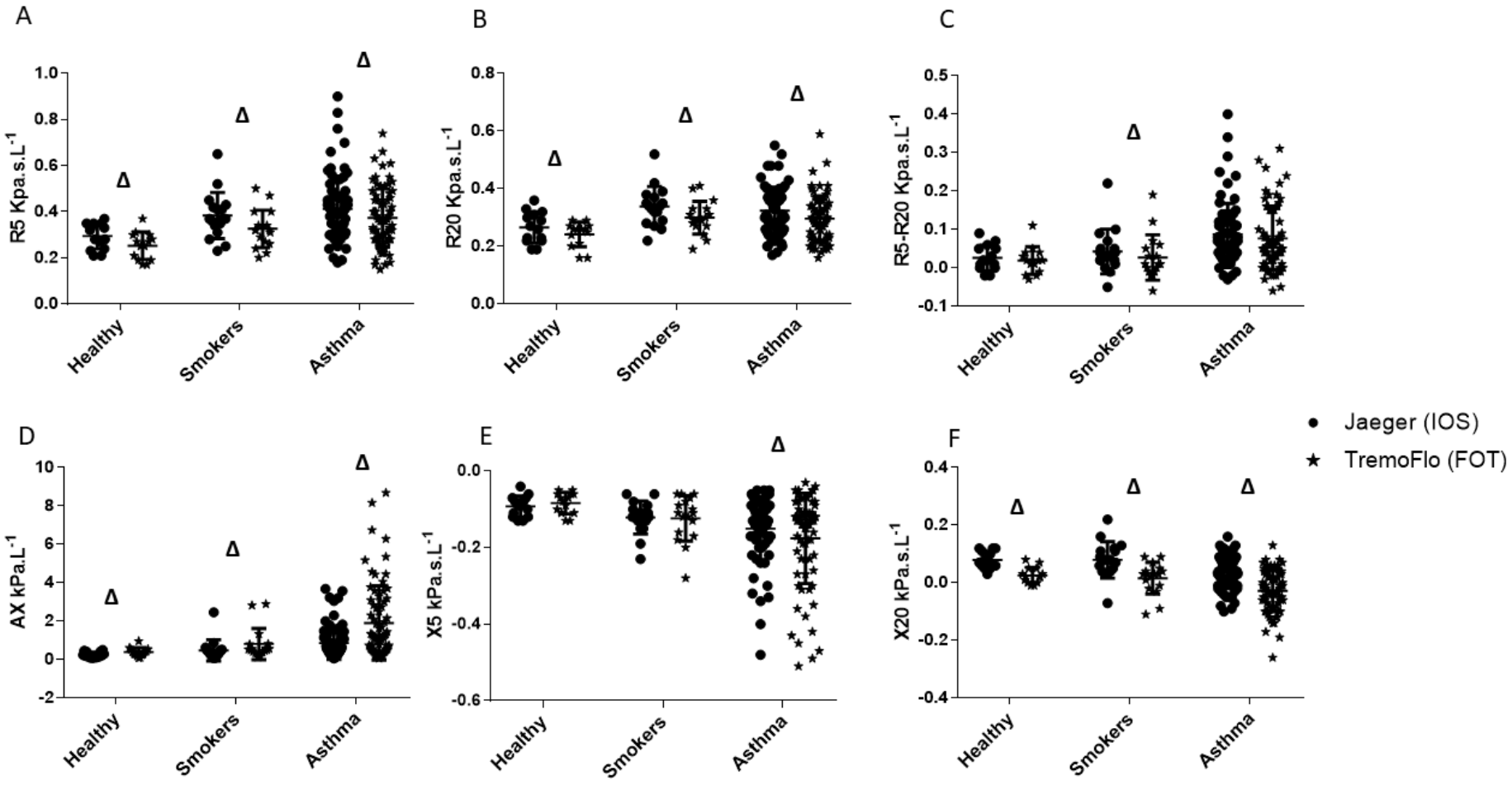

Figure 3.2.1: Dot plots of Resistance (A, B, C) and Reactance (D, E, F) for Jaeger (IOS) (dots) and TremoFlo (stars) devices in the three clinical populations. Δ $p < 0.05$ for within group comparison of IOS and TremoFlo values.

An exemplar set of comparative figures reporting frequency as a function of resistance and reactance is provided in **Figure 3.2.2** in three patients per clinical group, healthy controls, patients with asthma and asymptomatic smokers, respectively, measured with Impulse Oscillometry (IOS) (closed symbols) and TremoFlo (open symbols). Resistance values were higher across all frequency spectrum when measured with IOS, in all three different groups. Reactance presents more negative values measured with TremoFlo when compared to IOS, again, for all three different populations.

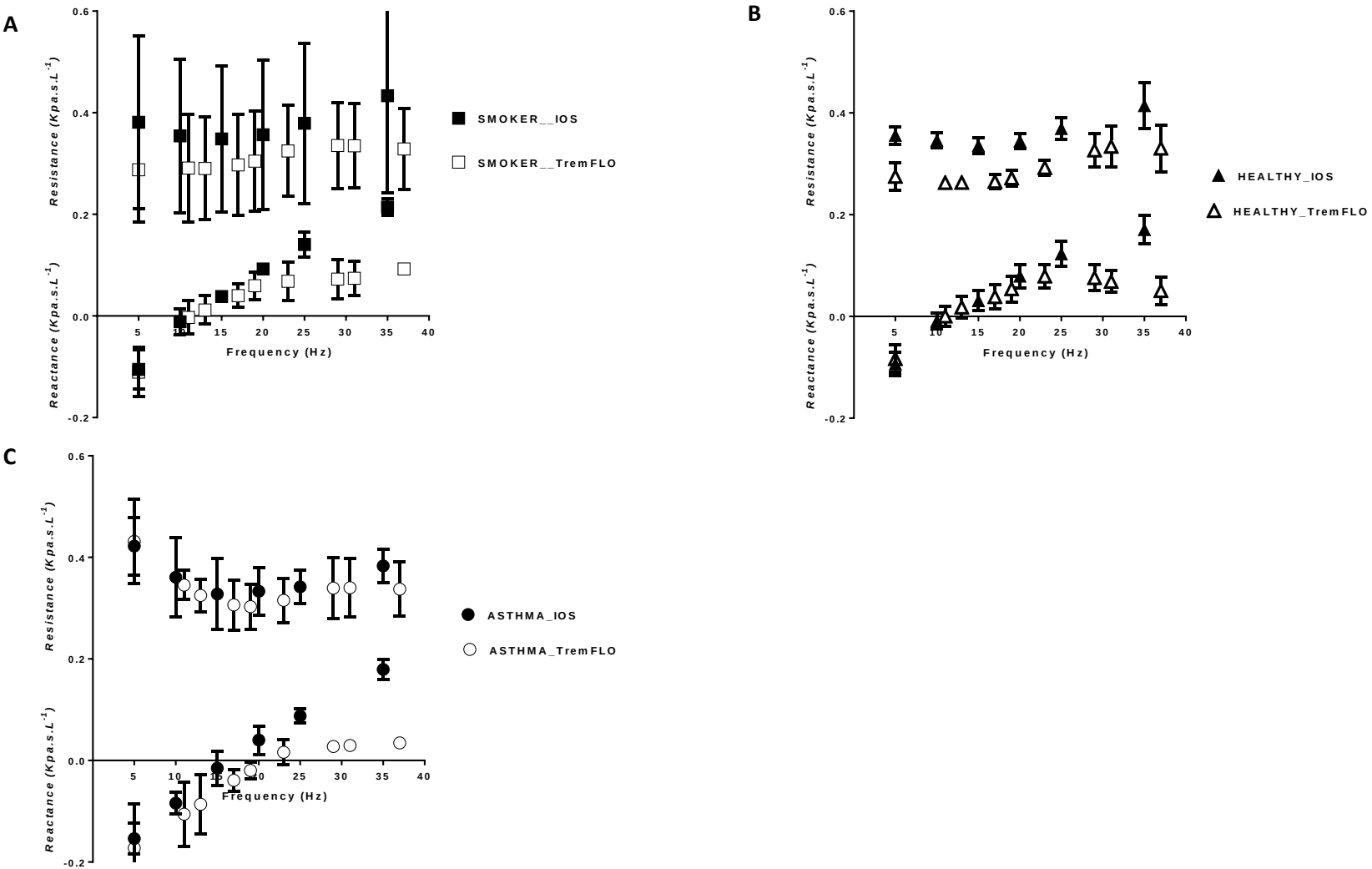

Figure 3.2.2: **Frequency as a f unction of resistance and reactance in three patients per clinical group**: asymptomatic smokers (A), healthy controls (B) and patients with asthma (C).

Having established that there were numerical differences between IOS and TremoFlo in our clinical populations, we next sought to establish whether the differences demonstrated a systematic bias using Bland-Altman plots of Rrs (resistance) and Xrs (reactance) values comparing the differences between IOS and TremoFlo devices (y-axis) and the mean measurement value (x-axis). **Figure 3.2.3 and Figure 3.2.4** demonstrate Bland-Altman plots for resistance and reactance respectively. Additionally, **Table 3.2.5** presents the linear regression slope, intercept, regression R^2 and model p-values by applying linear regression to the Bland-Altman plots.

The data demonstrate that there were small, numerically positive and statistically significant ($p<0.05$) regression slopes for both R5, R20 (mean Bland-Altman bias, R5 = 0.04 Kpa.s.L^{-1} and R20 (19) = 0.032 Kpa.s.L^{-1}) suggesting that the IOS device consistently measures slightly larger resistances for any given frequency across the comparative frequency range when compared to TremoFlo. However, R^2 for the models was very small suggesting that the proportional bias, although statistically significant, accounted for a small proportion of the variance of the data.

In contrast larger proportional systematic biases were demonstrated when comparing reactance values between the two devices. Regression slopes applied to Bland-Altman plots were consistently negative for all reactance parameters (X20 and AX; $p <0.05$ all slopes), with the largest proportional systematic bias and regression R^2 values being demonstrated for AX.

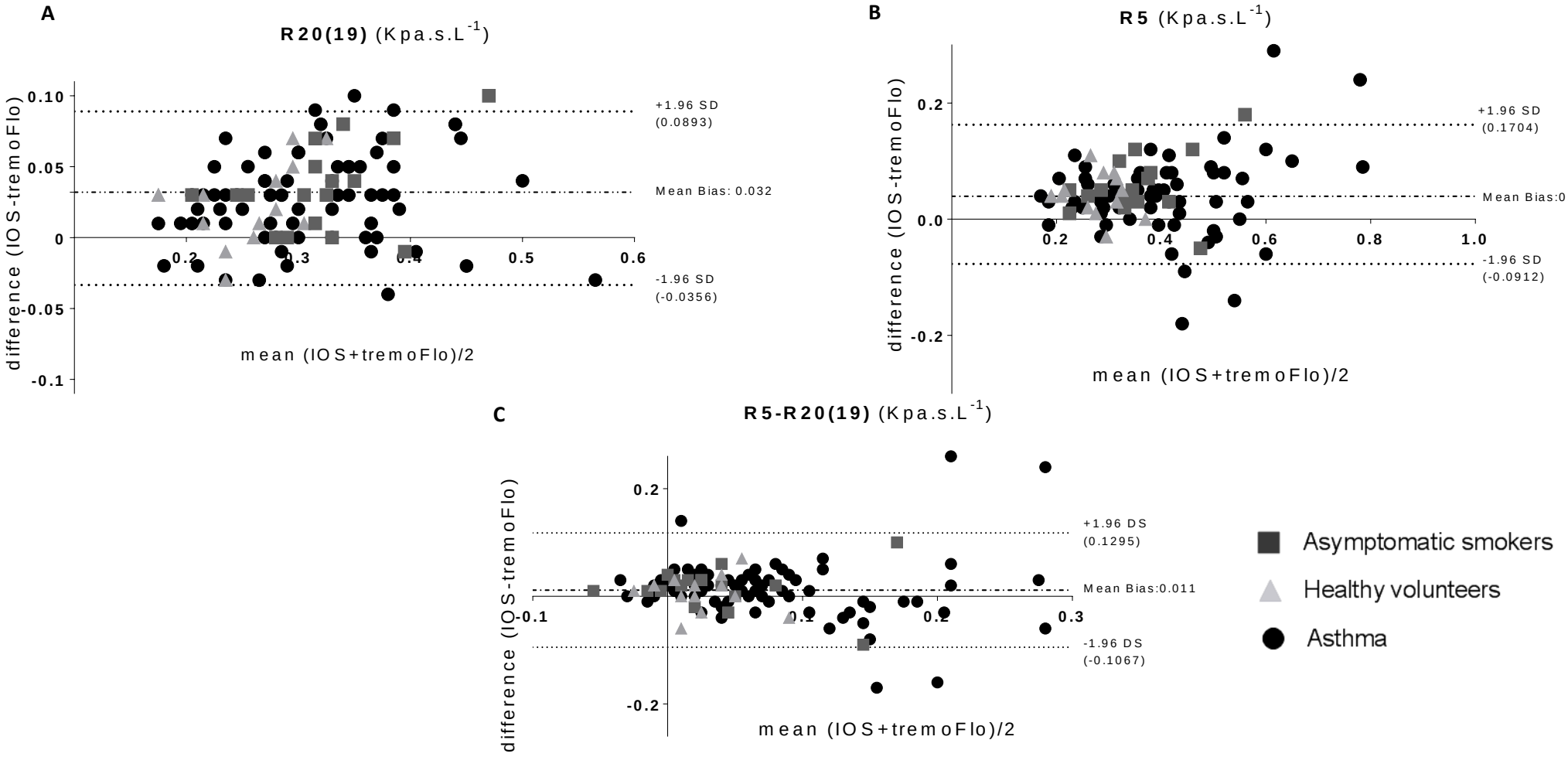

Figure 3.2.3: Bland-Altman plots of resistance. (A) Mean Resistance (IOS+TremoFlo)/2) at 20(19) Hz and the difference between IOS and FOT resistance at 20(19) Hz; (B) Mean Resistance (IOS+TremoFlo)/2) at 5 Hz and the difference between IOS and FOT resistance at 5 Hz; (C) Mean Resistance (IOS+TremoFlo)/2) at 5 minus 20(19) Hz and the difference between IOS and FOT resistance at 5 minus 20(19) Hz.

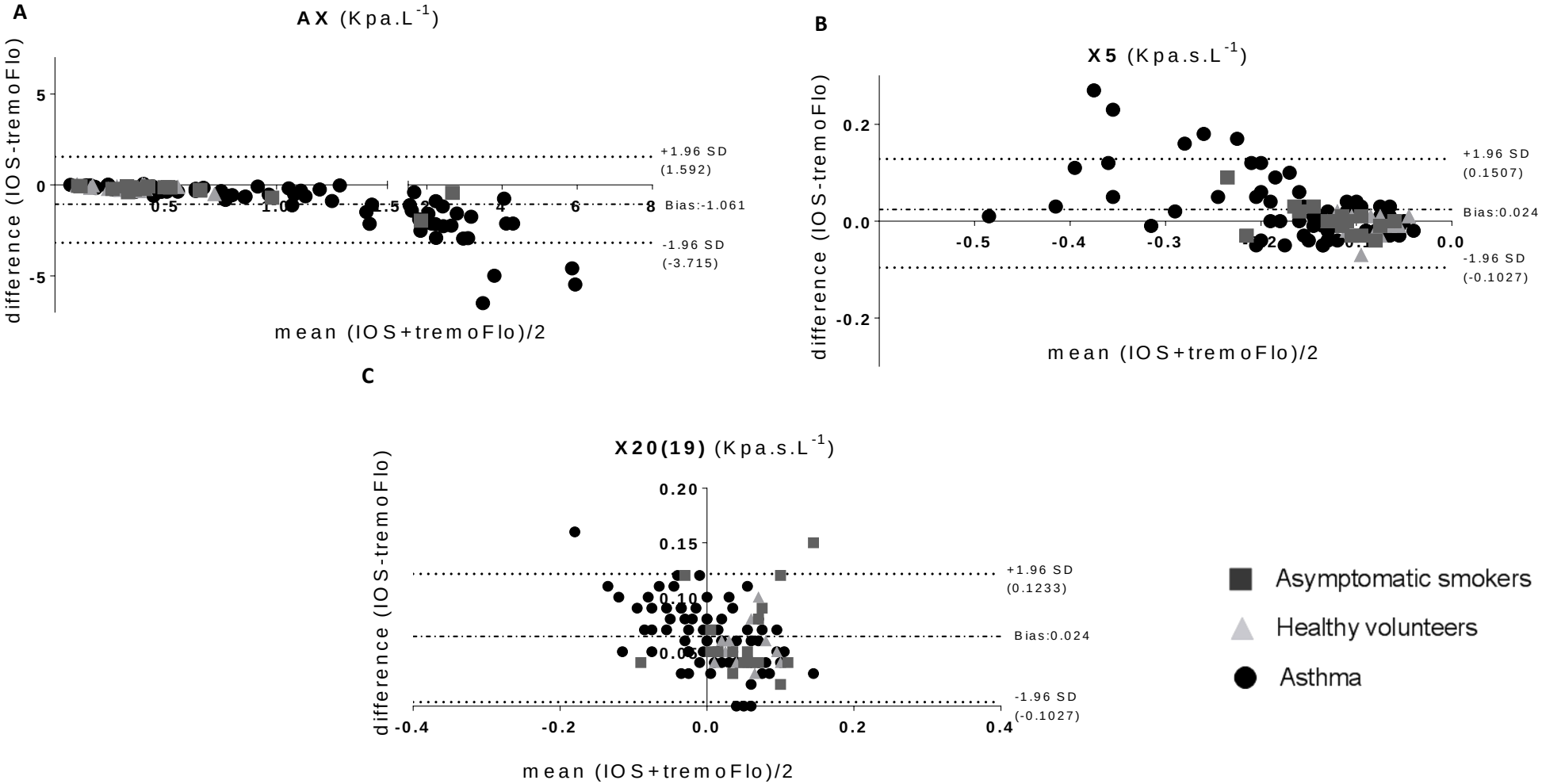

Figure 3.2.4: Bland-Altman plots of reactance. (A) Mean Area of Reactance (AX) (IOS+TremoFlo)/2) and the difference between IOS and FOT AX; (B) Mean Reactance (FOT+TremoFlo)/2) at 5 Hz and the difference between IOS and FOT reactance at 5 Hz; (C) Mean Reactance (FOT+TremoFlo)/2) at 20(19) Hz and the difference between IOS and FOT resistance at 20(19) Hz.

Table 3.2.5: Bland Altman derived linear regression models for the overall study population bias (IOS minus TremoFlo)

	Estimate	Std. Error	Model p-value	Model R^2
Intercept	0.0037	0.019	**0.039**	**0.0319**
Mean R5 slope	**0.101**	0.0484		
Intercept	-0.00015	0.0125	**0.023**	**0.0402**
Mean R20 (19) slope	**0.0922989**	0.0400204		
Intercept	0.014	0.0072	0.634	-0.0076
Mean R5-R20(19) slope	-0.035	0.073		
Intercept	0.122	0.087	**<0.0001**	**0.711**
Mean AX slope	**-0.833**	0.0526		
Intercept	-0.0364	0.0091	**<0.0001**	**0.303**
Mean X5 slope	**-0.360915**	0.053655		
Intercept	0.0596	0.0028	0.00013	**0.126**
Mean X20(19) slope	**-0.176**	0.0443		

Definition of abbreviations: R5: Resistance at 5 Hz; R20(19): Resistance at 20/19 Hz; R5-R20(19): Resistance at 5 minus 20(19) Hz; AX: Area of Reactance; X5: Reactance at 5 Hz; X20(19): Reactance at 20(19) Hz. P-values obtained from linear regression models.

3D printed airway resistance and volume reactance phantoms

In agreement with the results in patients, sequential heterogeneous occlusion of the end termini of a 3D printed physical airway model (**Figure 3.2.5**) produced an exponential increase in both R5 and R20 (19) using both devices, higher with the IOS device. In contrast, for R5-R20 (19) sequential occlusion of end termini in the airway model alone had no effect across a range of outlet occlusions and both devices generated near identical numerical values in **Figure 3.2.5 D**. We identified a consistently negative sign for R5-R20 (19) in the printed airway, explained by the lack of an effective elastance in the printed model at the end termini of airways.

Similarly to the clinical outcomes, the 3L volume reactance demonstrated that for frequencies typically below resonant frequency in patients, TremoFlo Xrs values were consistently more negative than IOS values with the greatest deviation from the line of unity occurring between 5-10 Hz (**Figure 3.2.6).** Additionally, we fitted a theoretical model to the reactance spectrums for both devices measuring the cylinder (**figure 3.2.7**). We then plotted the fitted reactance curves against each other to highlight the difference between the devices at additional frequencies beyond those measured. This plot shows a clear deviation from the line y=x across all frequencies, especially at the lower end of the scale. The line y=x was calculated based on the following augmented RIC model equation (299):

$$Z = \frac{A(RA + R_p)}{\left[A(1 - \omega^2 IC_e) + \omega^2 {R_p}^2 C_p C_e\right]^2 + \left[\omega C_e (RA + R_p)\right]^2}$$

$$+ \frac{\omega(IA - {R_p}^2 C_p)\left[A(1 - \omega^2 IC_e) + \omega^2 {R_p}^2 C_p C_e\right] - \omega C_e (RA + R_p)^2}{\left[A(1 - \omega^2 IC_e) + \omega^2 {R_p}^2 C_p C_e\right]^2 + \left[\omega C_e (RA + R_p)\right]^2} i,$$

$$\text{where } A = 1 + (\omega R_p C_p)^2.$$

Z=impedance; C*p*=peripheral airway compliance; C*e*= extra thoracic compliance R= large airway resistance; R*p*= peripheral resistance; ω=radian frequency; I= inertance.

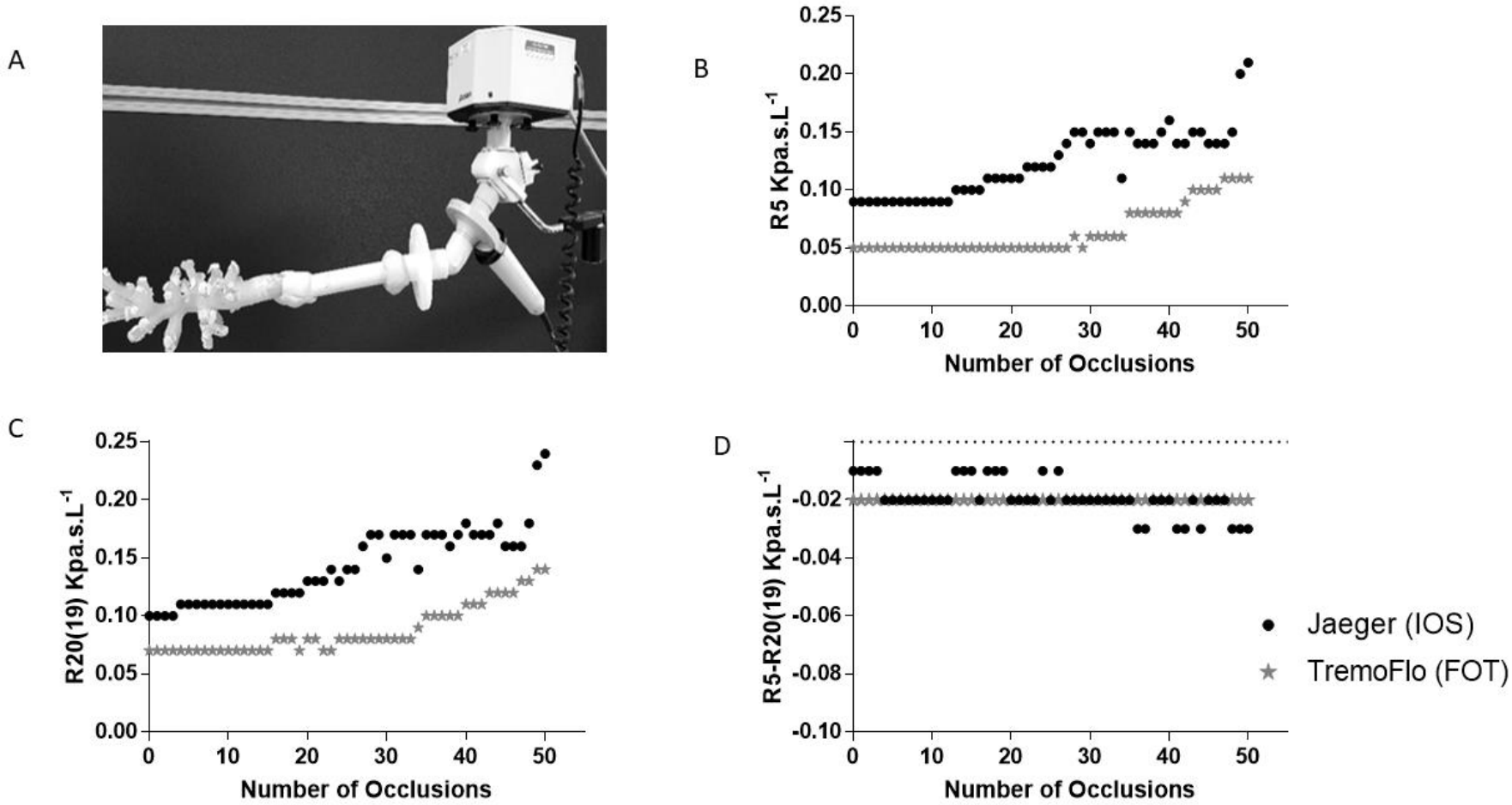

Figure 3.2.5: Sequential random occlusion of the 3D printed airway model. Figure illustrating sequential random occlusion of the end termini of a 3D printed CT scan derived physical airway model, with occluded end termini number on the x-axis and (A) and resultant resistance at 5Hz (B), 20(19) Hz (C) and resistance at 5 minus 20(19) Hz [R5-R20(19)] (D), measured with TremoFlo (black dots) and Jaeger (grey stars) devices.

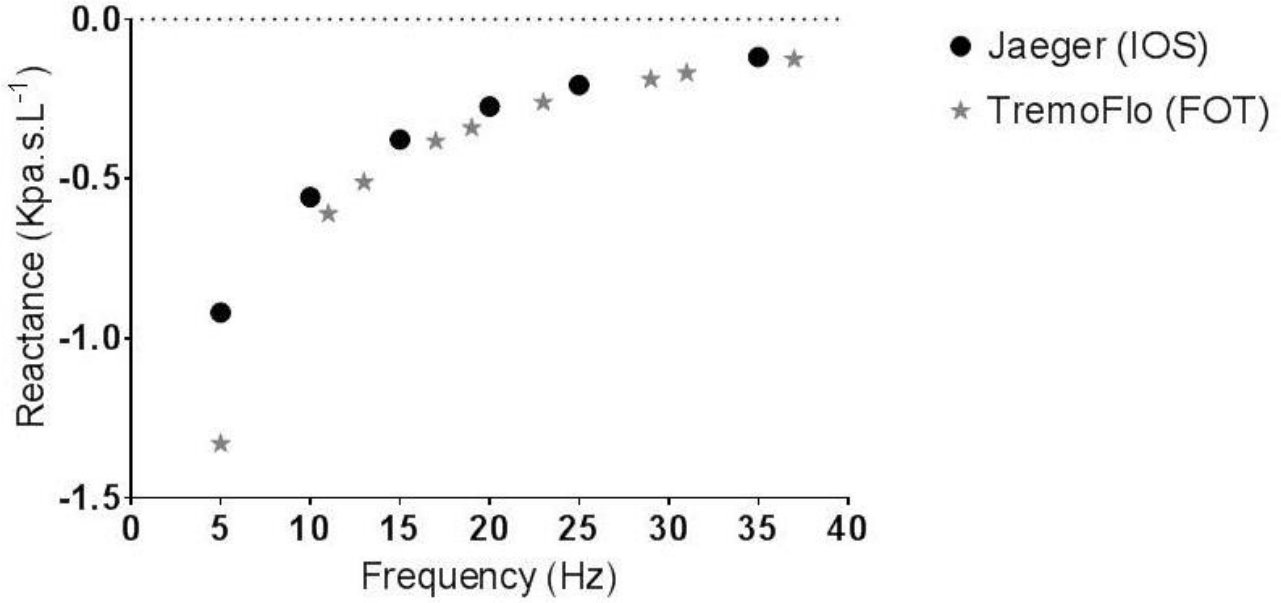

Figure 3.2.6: Reactance measured with a 3L cylinder with the (FOT) and Jaeger (IOS) devices, at different frequencies and direct comparison of reactance values between (FOT) (grey stars) and Jaeger (IOS) (black dots), at different frequencies.

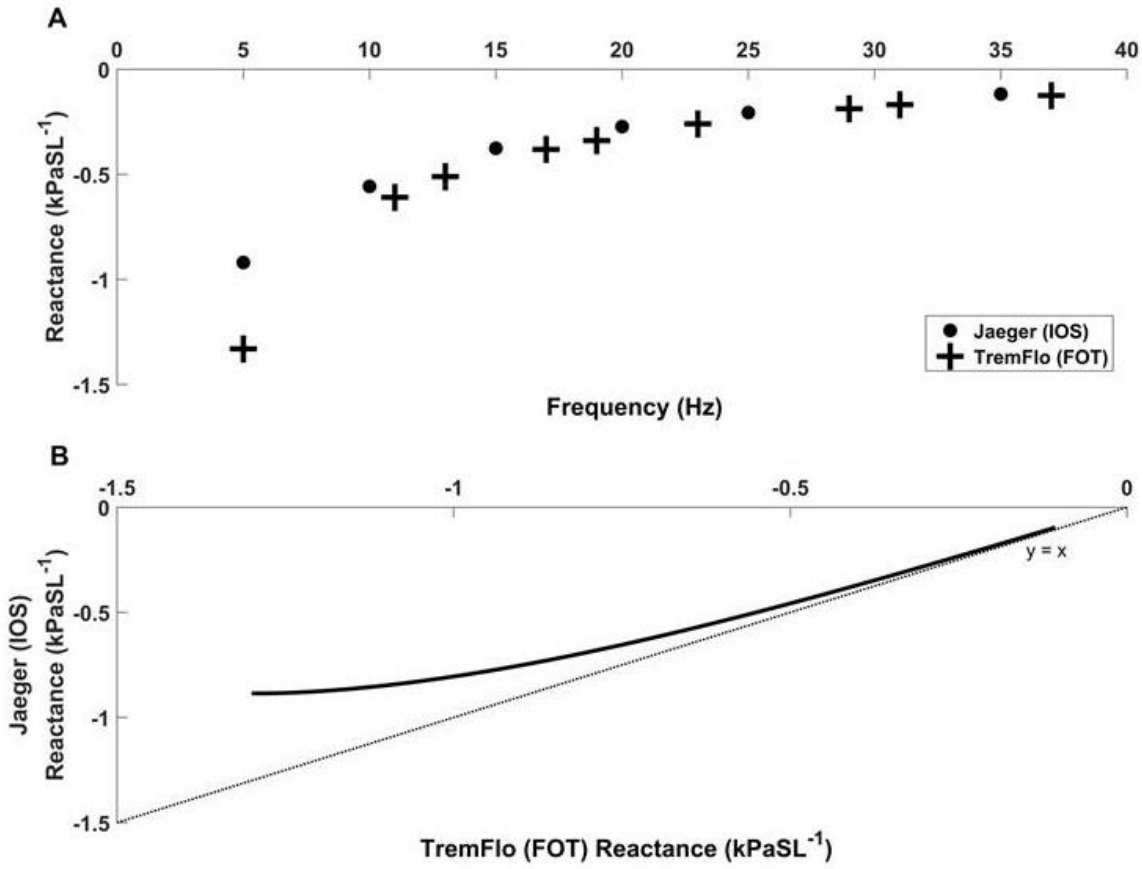

Figure 3.2.7: A) Reactance measured with a 3L cylinder with FOT (crosses) and IOS (dots). B) Fitted theoretical model (x=y) to the reactance spectrums and measured reactance curves for both devices, across different frequencies.

DISCUSSION

Measurement of lung mechanics with forced oscillation techniques with either TremoFlo or IOS may have potential advantages over traditional spirometry: rapid, minimal cooperation needed, less time consuming and offering potentially greater sensitivity in detecting peripheral airway obstruction. Moreover, FOT and IOS are becoming increasingly available due to the proliferation of commercial devices and while the outcomes seem comparable and similar, the different design of testing devices, hardware and oscillation signal properties and post processing including filtering, makes it extremely important to understand between-device measurement comparisons, to facilitate clinical studies in the future and FOT further standardisation efforts.

Here, we report the first study to compare forced oscillation outcomes measured by impulse oscillometry and TremoFlo, the two devices most commonly used and commercially available. Our device comparisons resulted from a clinical population (asthmatics, aged matched asymptomatic smokers and healthy volunteers) and a phantom study evaluating resistance and reactance.

Our results demonstrated a systematic and proportionate bias in Rrs and Xrs measurements when comparing TremoFlo and IOS, such that resistance values measured with IOS appear to be higher (with an overall small numerical difference and small positive bias slope) and reactance values less negative (with larger numerical differences and a large negative bias slope) when compared to TremoFlo measured values. These observations were replicated in a 3D printed airway phantom (resistance) and volume phantom (reactance).

We speculate that the systematic overestimation of Rrs by IOS occurs due to a number of potential differences in the oscillation signal including differences in the amplitude content of the IOS pulse train and subsequent impact upon signal:noise across the range of frequencies. Specifically, the periodic pulse train of the IOS generates an impedance spectrum at the fundamental frequency (5 Hz) and its harmonics (multiples of 5 Hz). The temporal resolution in the IOS is a function of the period interval between pulses (also inversely related to the fundamental frequency). The signal:noise ratio is more related to the fact that the amplitude of the signal is concentrated at the fundamental frequency (5Hz), and at the same time the fundamental frequency runs the risk of being

distorted by the subsequent harmonics and may explain any numerical differences in resistance between the two devices particularly at 5 Hz.

On the other hand, the IOS system allows the measurements of 5 impedance spectra per second that may better capture the within-breath variability of Xrs, which is not available with pseudo-random noise systems like TremoFlo, using the default settings of the TremoFlo device. Consequently, IOS may provide more accurate values of Xrs.

Additionally, IOS calculates reactance area by extrapolation (if the AX is greater than the highest harmonic 35 Hz) in contrast to TremoFlo which assigns the highest harmonic value (37 Hz) if a resonant frequency is not reached, in patients. These differences in signal properties and processing however are unlikely to be relevant as we observed larger AX values using the TremoFlo system compared to IOS.

Three previous published studies have compared resistance and reactance measurements using various FOT devices applied to phantoms and in some cases small patient cohorts (147,148,300). Zimmermann *et al*, compared a custom built FOT device with the commercial TremoFlo, Resmon and IOS devices in 12 healthy adult volunteers and *in vitro*, with two test standards with known impedance. In agreement with our results they demonstrated differences in measured resistance values between TremoFlo and IOS *in vivo*, attributing these differences to how the two systems process breathing patterns differently. However, their *in vitro* model failed to demonstrate the same pattern, due to the use of simple resistance mesh and lack of consideration for branching of the airway tree. Thus, our *in vitro* models have considered the branching of the airway tree, and results were in line with the clinical population results, a numerically higher resistance measured with IOS (300). A weakness in our *in vitro* model is the lack of small airways, which could perhaps be addressed with a computational model simulation, based on the same CT scan patient data. However, our aim here was to compare the overall resistance changes when airways were occluded, between devices. Minimal differences were seen in Xrs examined at a single frequency of 5 Hz between TremoFlo and IOS in Zimmermann study, both in the *in vitro* and in vivo experiments, whereas in our study, TremoFlo demonstrated a more negative reactance in both cases. The discordancy with our results is likely to be due to the fact that we evaluated asthmatic and asymptomatic smokers with invariable flow and parenchymal heterogeneity. This suggests that the branched structure of the airway tree and presence

of breathing may account for some of the differences seen between devices and further *in vitro* studies should consider models with varying loads to address the proportional bias in reactance and resistance found in our study.

A similar comparative study performed by Hellinckx *et al* compared IOS with FOT (non-commercial device) and body plethysmography in 49 subjects with a variety of airway disease and pulmonary fibrosis (148). Rrs IOS was slightly higher than Rrs FOT, especially at lower frequencies. In contrast, IOS generated a slightly higher resonant frequency when compared to FOT but the two devices were generally comparable. However, for both Rrs and Xrs, a systematic measurement bias was not observed. The results of this study are difficult to interpret due to the clinical heterogeneity of the population studied.

Finally, Tanimura *et al* performed a comparison between IOS and the commercial MostGraph (MG) device utilising phantom models and a small healthy population (147). The study has also shown an increase of approximately 10% in the resistance measured with IOS when compared with FOT, which was attributed to apparatus characteristics, differences in the two oscillation signals and data post processing.

Potential limitations of our study include (i) the absence of a cohort with severe airflow obstruction e.g. COPD which may have allowed us to determine between-device bias across a wider range of resistance and elastance/reactance area. (ii) The use of post bronchodilator measurement may render our observations more pertinent to clinical scenarios where post bronchodilator values may be of most utility such as in population level detection and evaluation of anti-inflammatory therapy response. In contrast, pre-bronchodilator values may be of utility for evaluating bronchodilator response, airways hyper responsiveness and airway smooth muscle targeted therapies such as bronchial thermoplasty. Moreover, the use of bronchodilator might have underestimated the differences encountered between devices in asthma and asymptomatic smokers. (iii) Finally, differences in the acquisition time between the IOS and TremoFlo may have introduced bias. However, a previous study by Watz *et al*, concluded that FOT data were minimally impacted by acquisition duration in asthmatic subjects and healthy volunteers (301).

In conclusion, we demonstrate in a large asthma population study that resistance measured with IOS is slightly overestimated when compared to TremoFlo with an

overall systematic and proportional bias and that reactance values measured using TremoFlo FOT are substantially more negative when compared to IOS with a larger systematic and proportional bias. Our observations were reproduced in a phantom three-dimensional printed airway resistance model and a standard volume reactance.

Further between-device standardisation will be required before IOS and FOT systems are suitable for deployment in larger clinical population studies. In this regard, a standard test load with known reactance would be of benefit to the FOT community.

3.3 Particles in exhaled air (PExA): non-invasive phenotyping of small airways disease in adult asthma

ABSTRACT

Rationale: Asthma is often characterised by inflammation, damage and dysfunction of the small airways, but no standardised biomarkers are available.

Objectives: Using a novel approach -Particles in Exhaled Air (PExA)- we sought to a) sample and analyse abundant protein biomarkers: surfactant protein A (SPA) and albumin in adult asthmatic and healthy patients and b) relate protein concentrations with physiological markers using phenotyping.

Methods: 83 adult asthmatics and 21 healthy volunteers were recruited from a discovery cohort in Leicester, UK, and 32 adult asthmatics as replication cohort from Sweden. Markers of airways closure/small airways dysfunction were evaluated using forced vital capacity (FVC), impulse oscillometry (IOS) and multiple breath washout. SPA/albumin from PEx (PExA sample) were analysed using ELISA and corrected for acquired particle mass. Topological data analysis (TDA) was applied to small airway physiology and PExA protein data to identify phenotypes. **Results:** PExA manoeuvres were feasible, including severe asthmatic subjects. TDA identified a clinically important phenotype of asthmatic patients with multiple physiological markers of peripheral airway dysfunction, and significantly lower levels of both SPA and albumin.

Conclusion: We report that the PExA method is feasible across the spectrum of asthma severity and could be used to identify small airway disease phenotypes.

INTRODUCTION

Asthma is a disease associated with inflammation, remodelling and dysfunction (2,302) that extends to the smaller airways (71). However, a standardised definition of small airways disease has remained problematic due to a lack of validated non-invasive physiological and pathological tools to measure dysfunction and disease within this compartment. The existing approaches are either invasive (not suitable for population

studies e.g. trans bronchial and surgical lung biopsy) (303) or both invasive and difficult to standardise, such as broncho-alveolar lavage sampling (304).

In the past few years a novel non-invasive technique sampling endogenous aerosol particles, carrying non-volatile material from the small airways (PExA) has been developed, first reported by Almstrand *et al* (14). The approach has potential advantages, including the ability to sample small airway surface liquid non-invasively and the ability to normalise biomarker concentrations to particle mass. To date, promising but exploratory studies have been conducted using the PExA technique, applying proteomics (16,17,244,259) and lipid analysis of phosphatidylcholines (15,245) that support a small airway organ for PEx particles. Specifically, exhaled particle numbers have been shown to be correlated with physiological measures of airways closure (242) and are most enriched during repeated airways closure and reopening breathing manoeuvres in contrast to tidal breathing (240). This manoeuvre is therefore likely to promote sampling from the terminal bronchioles, and alveoli. Furthermore, Larsson *et al* have reported that different breathing manoeuvres generate distinct phospholipid profiles and that the airway closure manoeuvre was the most likely manoeuvre associated with the peripheral compartment (264). Additionally, a pilot study in a population with asthma showed that increased airway inflammation due to birch pollen exposure was associated with less exhaled particles and therefore, suggestive of a reduced number of small airways available for the closure and re-opening and particle generation (259). Finally, a recent study has identified ingested methadone in PExA particles, further suggesting a communicative link between PExA particle and the systemic circulation/small airways (305).

These observations would suggest that PEx (PExA sample) may be an appropriate matrix to study asthmatic small airways biology if further validated.

Immunoglobulins, albumin, as well as lung specific proteins such as surfactant proteins have been detected in PEx and are amongst the most abundant proteins (244). Both albumin and surfactant protein A (SPA) can be measured in PEx at low limits of detection using immunoassays (16,17). SPA is a key immunomodulatory protein involved in innate immune recognition and regulation of surface tension (254). For example, SPA can inhibit allergen-specific IgE binding to mite allergens (306), increases phagocytosis of bacteria and viruses by macrophages, monocytes and

neutrophils (250). Previous studies in chronic bronchitis have suggested that surfactant dysfunction may be responsible for airflow obstruction and potentially reversible (307).

Albumin is a plasma protein and its presence in PEx, although not fully understood, may reflect breakdown of the alveolar basement membrane and/or increased airway vascular permeability (210).

In the present study, we hypothesised that: a) PExA method is both feasible across the spectrum of asthma severity and reliable with respect to quantification of both SPA and albumin and b) candidate biomarkers SPA and albumin derived from PEx, are associated with both airways closure and small airway dysfunction phenotypes in adult asthmatics.

We sought to test these hypotheses in a discovery and replication cohort.

METHODS

Discovery Cohort

The discovery study protocol was approved by the National Research Ethics Committee – East Midlands Leicester (approval number: 08/H0406/189) and all subjects gave their written informed consent.

104 volunteers were screened and recruited at Glenfield Hospital, Leicester, from secondary care asthma clinics, and from an existing research database at the NIHR Respiratory Biomedical Research Centre, Leicester, UK.

83 asthma patients, of which 74 could produce PEx samples with enough material to analyse [Global Initiative for Asthma (GINA) (2), treatment steps: I=9, II-III=25 and IV-V=40] and 21 healthy aged matched volunteers, were identified and met the entry criteria of the study outlined below (**Figure 3.3.1** and **Table 3.3.1**).

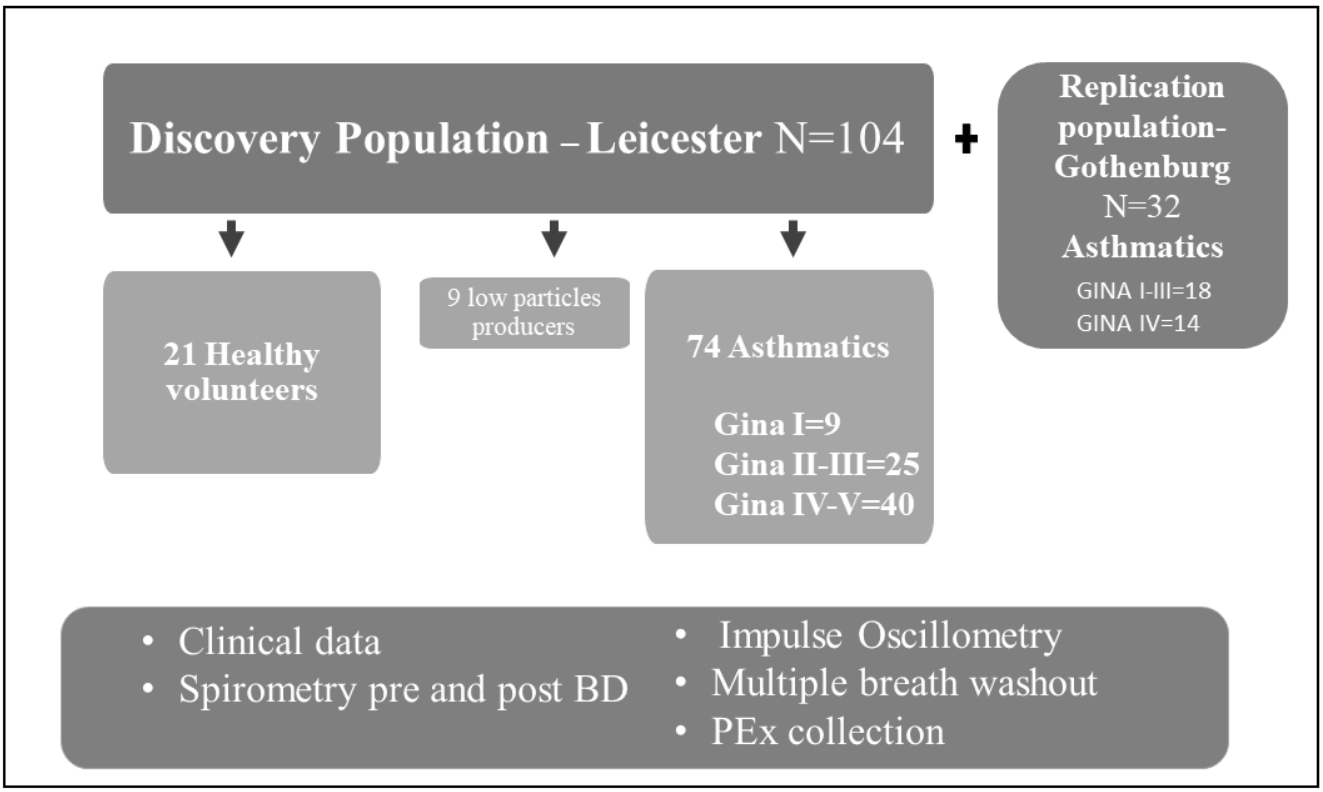

Figure 3.3.1: Study design and assessments. *Definition of abbreviations*: GINA: Global initiative for asthma; BD: bronchodilator.

Table 3.3.1: Number of patients undergoing each breathing test from the discovery population

Test	**Healthy Controls N=21**	**Asthma N=83**
PEx collection	21	74
Spirometry	16	69
Impulse Oscillometry	17	66
Multiple breath SF6 washout	19	68
Induced Sputum	7	33

Asthma patients had a physician diagnosis of asthma and one or more of the following physiological criterion: Methacholine PC20 ≤8mg/ml, bronchodilator reversibility to 400 mcg of inhaled salbutamol of FEV_1 ≥12% and 200mls or peak flow variability of ≥ 20% over two weeks. Patients had been free from exacerbations for at least six weeks prior to study entry. Asthma patients currently smoking or with a smoking pack history greater than or equal to ten were excluded.

Replication Cohort

An additional Swedish cohort of n= 32 asthmatic patients (GINA I-III=18, GINA IV= 14) was evaluated as a replication population (**Table 3.3.2**). Patients were between 27 and 60 years of age, 15 subjects were male, and all had persistent asthma symptoms and were either never or ex-smokers [mean (range) pack year exposure of 7.5 (1.25-16.13)]. Patients were recruited from primary care centres across Skaraborg Country in West Sweden, with approval by the regional ethics committee at the University of Gothenburg, Sweden. All patients met the inclusion criteria, as previously reported (308).

Table 3.3.2: Demographic and clinical data according to GINA step treatment in the Replication population

Clinical Characteristics	GINA I-III (n=18)	GINA IV (n=14)	Mann-Whitney p value
Sex (% male)¥	44	50	0.1
Age (years)	42 (30;48)	50 (42;55)	0.033
BMI (kg/m^2)	24.1 (21.6;28.9)	27.9 (24;30.3)	0.342
FEV_1/FVC	73 (68.7;79.9)	71.9 (62.4;74.8)	0.419
FVC % predicted	95.4 (85.9;103.2)	91.7 (81.7;100.8)	0.536
FVC Z score	-0.44 (-1.34;0.31)	-0.81 (-1.66;0.06)	0.536
FEV1 % predicted	91.6 (77.3;100.5)	86.2 (66.3;97.3)	0.338
FEV1 Z score	-0.74 (-1.89;0.04)	-1.33 (-2.88; -0.26)	0.333
R5-R20 ($KPa.s.L^{-1}$)	0.04 (0.03;0.07)	0.12 (0.06;0.18)	0.006

Definition of abbreviations: BMI: body mass index; FEV_1= forced expiratory volume in one second; FVC: forced vital capacity; R5: resistance at 5Hz; R20: resistance at 20Hz.
Data expressed as median, Q1;Q3; **¥** P value based on chi-square test.

Study design

Patients attended for up to two visits within a week. Data obtained during visit 1 were: medical history and current medication, skin prick testing, six-point asthma control questionnaire [ACQ-6] (270) and asthma quality of life questionnaire [AQLQ] (267) for the asthma cohort, and spirometry plus reversibility. At the second visit, lung physiology measurements were performed 15 minutes following the administration of 400 mcg of salbutamol via a spacer: impulse oscillometry (IOS), multiple breath washout (MBW), spirometry and PExA.

Induced sputum was performed after PExA, using a previously published standard operating procedure (309). Samples were sent for differential cell count. Only 42% of patients were able to produce a viable sputum sample, therefore, not included in the main results (see **appendix 1** for results).

Physiological measurements

Spirometry was performed according to ATS/ERS recommendations (271) using a Vitalograph Alpha AL 21523 device (Vitalograph, Maids Moreton, Buckingham, MK18 1SW) in the discovery cohort and a Jaeger Masterscreen (Care Fusion, Germany) device in the replication cohort.

IOS measurements and quality control were performed in line with ERS Task Force recommendations (119) using the Masterscreen IOS (Erich Jaeger/Care Fusion, Germany), in both cohorts. The device was calibrated daily using a standardised resistance and measurements were performed in triplicate, as described previously and in detail in the methods section (140).

MBW testing was performed in the discovery population, using a modified photoacoustic INNOCOR (Innovision, Odense, Denmark) SF-6 gas analyser. Measurements were performed 2-3 times within visit to ensure that at least two FRC values were within 10% of each other. Several parameters were derived from the raw MBW data using a custom MATLAB software [MATLAB 2015a, Natick, Massachusetts: The MathWorks Inc., 2015], including lung clearance index (LCI) and phase three slope derived measures of conductive (Scond) and acinar (Sacin) ventilation heterogeneity as previously described (154,190).

PEx was collected using identical instruments in both cohorts and patients followed the standard breathing manoeuvre (259): full exhalation till residual volume (RV), followed by breath hold for about 5 seconds and rapid inspiration till total lung capacity, finishing with a steady exhalation back to RV, at a peak flow of about 1500 ml/s **(Figures 2.4 and 2.5, methods section)**.

PEx was extracted using PBS/ 0.05% Tween and particles SPA/albumin evaluated using the human surfactant protein A ELISA (BioVendor, Heidelberg, Germany), with monclonal anti-human SPA and a high sensitivity ELISA for Albumin (ICL, Portland, USA) (for further details see **methods section 2.3.2.**). Protein concentrations were derived from four parameter fitted standard curves and were normalised to acquired PEx mass (ng) to yield a % of SPA and albumin. Intra and inter assay coefficient of variation were < 10% for both SPA and albumin (see **appendix 2**).

Statistical analysis

Statistical analyses were performed using SPSS 22 and SPSS 24 (IBM Corporation, Somers, NY, USA) and Prism 7 for graphical plots (GraphPad Software Inc., La Jolla, CA, USA). A *p*-value of <0.05 was taken as the threshold for statistical significance. Comparisons between or across groups were performed using either ANOVA/Kruskal–Wallis test for parametric/non-parametric data and the fisher's exact test for proportions. Bonferroni/Dunn corrections for multiple comparisons were used as appropriate. Correlations between continuous variables were calculated using Spearman's correlation coefficient *(Rs*).

Topological Data Analysis (TDA) was utilised to evaluate putative small airway phenotypes. The central idea in TDA is that the shape of the data has meaning; by understanding the underlying shape of a data set it is possible to discover interesting features such as clusters or subgroups (310–312). TDA generates two dimensional networks of nodes connected by lines and edges to neighbouring nodes based upon patient similarity. Nodes in the network represent clusters of patients and edges connect nodes that contain patients that share phenotypic similarity. Nodes are subsequently coloured by the average value of their respective patients. TDA offers the advantage of being sensitive to large and small scale patterns, which are often not detected with other

methods, such as principal components analysis and cluster analysis. Furthermore, simple cluster analysis requires pre-specification of the number of clusters to be generated and doesn't allow within cluster analysis of clinical heterogeneity; on the other hand, TDA allows for analysis of heterogeneity within a network.

TDA was performed using the Ayasdi software platform (ayasdi.com, Ayasdi Inc., Menlo Park CA). The construction of networks is based in different input variables, which then allow the identification of networks and sub-groups of interest. In our analysis, the column set comprised Sacin, SPA % PEx, Alb % PEx and R5-R20. The TDA input parameters were chosen with a view to identifying composite phenotypes of both small airways dysfunction and PExA protein associated disease (GINA step treatment, R5-R20, % SPA, % albumin).

Two types of parameters are defined to generate a TDA network: measurement/ notion of similarity, called a metric, which measures the distance between two points in space, and lenses, which are real valued functions on the data points.

Lenses are used to create overlapping bins in the data set, where the bins are preimages under the lens of an interval. Overlapping families of intervals are used to create overlapping bins in the data. Metrics are used with lenses to construct the Ayasdi output. Here, the bins were preimages of rectangles or higher dimensional analogues. Bins were defined by resolution, which determined the number of bins and *gain*, which determines the degree of overlap of the intervals. Once the bins were constructed, we performed a clustering step on each bin, using single linkage clustering with a fixed heuristic for the choice of the scale parameter (313). Two nodes were connected if the corresponding clusters contained data points in common. We used two types of lenses, the neighbourhood 1 and 2 lens. Theses lenses allowed the embedding of high dimensional data into a two-dimensional space by embedding a K nearest neighbours graph. Similarly to operating a camera, different lens, focus and other setting will generate different shapes and outcomes. The lens function is based on the notion of distance between points in the dataset. In making a TDA graph, the points in the data set are clustered within bins, defined by setting the resolution of the analysis. The metric used was the norm correlation, which is the Pearson correlation coefficient applied to the normalised variables, the resolution and gain where 30 and 3 respectively. To determine how groups of points defined in a TDA graph differ, a non-parametric

statistical test (Kruskal-Wallis) or the Chi-Squared test was used to identify parameters that had $p<0.05$ for either one of the tests, see **Tables 3.3.8 and 3.3.9**.

Results

Feasibility Study

PExA repeated airway closure manoeuvres was feasible across the spectrum of asthma severity (**Tables 3.3.3 and 3.3.4**), after simple explanation and demonstration.

The median time to collect 50-100 ng of PEx material was approximately 9 minutes (range 5; 14) and equated to approximately 4 (2; 7) airway closure manoeuvres (**Figure 3.3.2 A and B**). Seven out of 47 patients with severe asthma (GINA IV-V), generated low amounts of particles for biomarkers analysis compared to 2/36 GINA I-III asthmatics (chi squared p value =0.157).

A significant relationship was found between mean number of particles generated per exhalation manoeuvre and airflow obstruction measured with spirometry (FEV_1/FVC) - **Figure 3.3.2 C**- but not with the protein concentration normalised to ng of acquired PEx mass and (**Figure 3.3.2 D**). These results suggest that the normalisation to ng of mass removed any sampling bias due to airflow obstruction and the number of subtended airways available in the lung for particle generation.

Table 3.3.3: PEx sampling feasibility according to GINA step treatment

	Healthy controls	**GINA I**	**GINA II-III**	**GINA IV-V**
Patients performing PExA	21	10	26	47
Sample collected	21	9	26	40
Sample time (min)	7 (5)	10 (6)	10 (5)	12 (9)
Mean particles per breath	77294 (61230)	40609 (26015)	48281 (30914)	43144 (42828)
Mass PEx acquired (ng)	104.1 (19.72)	98.64 (17.35)	96.73 (22.52)	94.17 (25.86)
Low number of particles (sample not collected)¥	0	1	1	7
Mean particles per breath in the low producers‡	-	11882	10325	6322

Definition of abbreviations: GINA: Global Initiative for Asthma. Data expressed as mean, SD; ¥ Chi-square test: 0.157; ‡: not enough sample acquired for protein analysis.

Table 3.3.4: PEx sampling feasibility according to presence or absence of airflow obstruction

	Healthy controls	**$FEV_1/FVC \geq$ LLN**	**$FEV_1/FVC <$ LLN**
Patients performing PEx	21	44	30
Sample collected	21	44	26
Sample time		8 (4)	15 (9)
Mean particles per breath	77294 (61230)	53370 (32731)	40000 (43703)
Mass PEx acquired (ng)	104.1 (19.72)	98.5 (20.32)	90.66 (28.25)
Low number of particles (sample not collected)	0	0	4
Mean particles per breath in the low producers‡	-	-	7010 (2857)

Definition of abbreviations: FEV_1: Forced expiratory volume in the first second; FVC: forced vital capacity; LLN: lower limit of normal. Data expressed as mean, SD; ‡: not enough sample acquired for protein analysis.

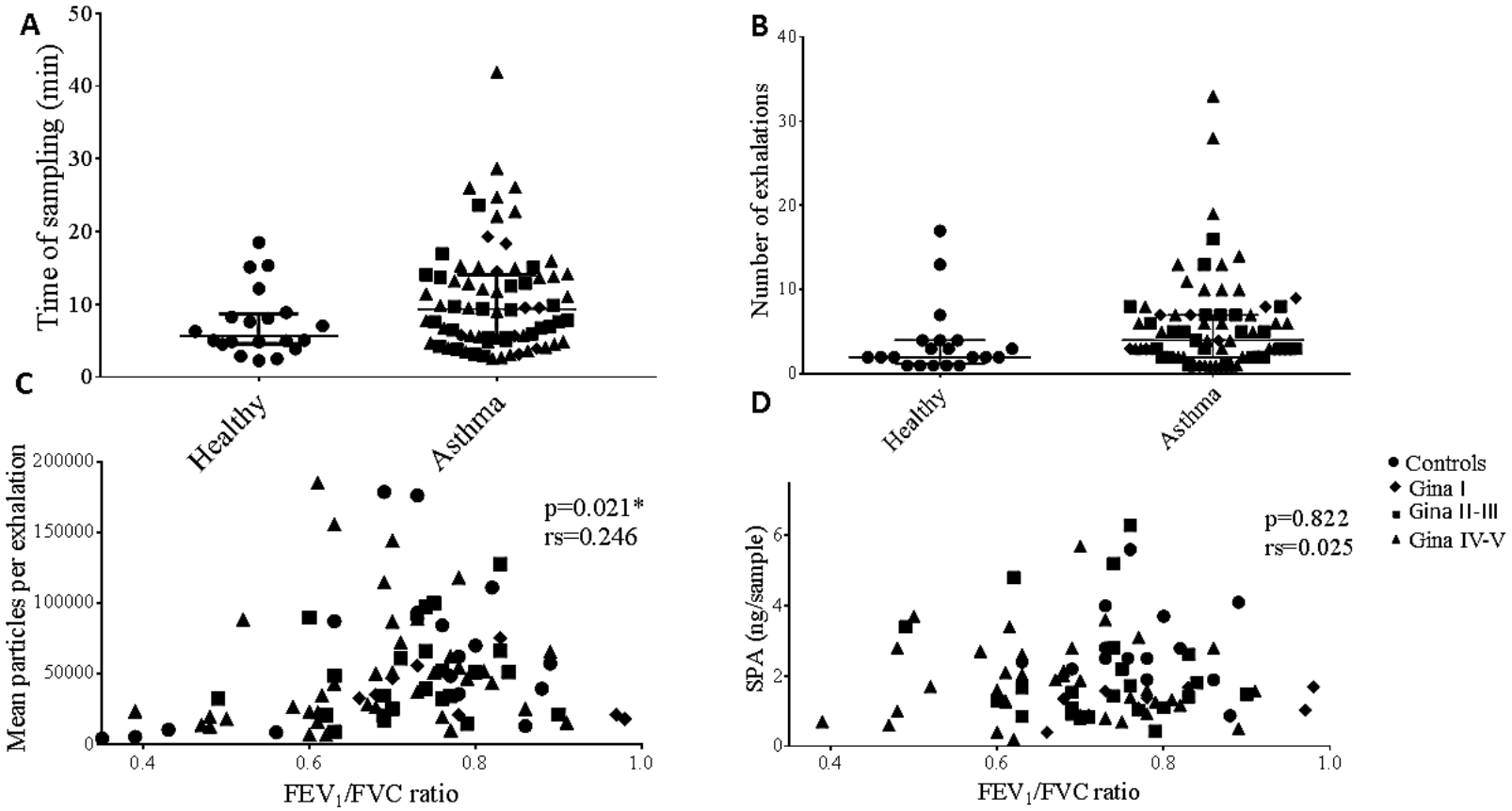

Figure 3.3.2 A, B, C, D: PExA sampling outcomes. (A) Number of exhalations in the controls group [5 (3-9)] and asthmatics [8 (5-12)]. (B) Time required to sample >30ng PEx in the controls group [6 (5-9)] and asthmatics [9 (5-14)]; (C) Relationship between mean number of particles per exhalation and FEV_1/FVC.(D) Relationship between total number of ng of SP-A per sample and FEV_1/FVC. Dots represent healthy controls, diamonds asthma GINA step treatment I, squares asthma GINA step treatment II and III and triangles asthma GINA step treatment IV and V.

Clinical Demographics of the Asthma Discovery Cohort

Basic demographic and clinical characteristics are summarised in **Table 3.3.5**. GINA asthma severity groups were well matched for age, sex and asthma age of onset. In contrast, GINA IV-V asthmatics had significantly poorer spirometric lung function, a greater proportion of patients had a FEV_1/FVC< lower limit of normal (LLN) and displayed multiple physiological features of small airways dysfunction (abnormal R5-R20, AX, Sacin and LCI, **Table 3.3.6**) when compared to healthy volunteers.

Table 3.3.5: Demographic and clinical data according to GINA step treatment in the discovery population

Clinical Characteristics	**Healthy controls (n=20)**	**GINA I (n=9)**	**GINA II-III (n26)**	**GINA IV-V (n=40)**	**Kruskal-Wallis p value**
Age (years)	53 (45;68)	45 (28;63)	61 (49;65)	62 (53;68)	0.139
Sex (male/female)[¥]	10/10	2/7	13/13	24/16	0.224
Age of asthma diagnosis		22 (13;48)	21 (6;49)	36 (18;49)	0.523
BMI (kg/m^2)	27 (25;30)	25 (22;28)	26 (23;32)	30 (27;33)	0.049
Pack year history	15 (2;32)	0	6 (1;7)	8 (2;12)	0.403
ACQ -6	-	0.3 (0.0;1.3)[e]	0.8 (0.8;1.9)	1.6 (0.8;2.2)	0.013
AQLQ	-	6.5 (5.7;6.9)[e]	6.2 (4.4;6.4)	5.3 (4.5;6.2)	0.036
Post BD FVC (L)	4.2 (3.2;4.7)	3.6 (3.0;4.4)	3.5 (2.9;4.5)	3.8 (3.0;4.3)	0.362
Post BD FEV_1 (L)	3.4 (2.5;3.6)	3.0 (2.1;3.4)	2.5 (2.1;3.0)	2.4 (2.1;2.9)[c]	0.007
FEV_1/FVC	0.77 (0.73;0.81)	0.73 (0.67;0.90)	0.74 (0.64;0.78)	0.68 (0.61;0.77)	0.015
FEV_1/FVC post BD LLN (≥/<)	15/1	6/3	17/6	21/17	0.043

Definition of abbreviations: BMI: body mass index; ACQ-6: 6-point asthma control questionnaire; AQLQ: asthma quality of life questionnaire; FEV_1: forced expiratory volume in one second; FVC: forced vital capacity; BD: Bronchodilator.

Data expressed as median, Q1;Q3; **¥:** p value based on chi-square test; Kruskal Wallis test followed by Dunn's multiple comparisons tests significant difference ($p<0.05$) between: c-healthy and GINA IV-V; e- GINA I and GINA IV-V.

Table 3.3.6: Small airways physiology and biomarkers data according to GINA step treatment in the discovery population

Physiology	**Healthy controls (n=20)**	**GINA I (n=9)**	**GINA II-III (n26)**	**GINA IV-V (n=40)**	**Kruskal-Wallis p value**
% PEx SPA	2.6 (2.1;4.0)	2.7 (1.8;2.8)	2.6 (1.9;3.2)	2.6 (1.6;3.2)	0.483
% PEx albumin	5.1 (5.1;6.8)	6.1 (4.9;7.6)	6.7 (3.9;8.1)	4.8 (3.7;6.7)	0.388
R5 ($KPa.s.L^{-1}$)	0.30 (0.26;0.36)[c]	0.32 (0.25;0.38)	0.37 (0.29;0.52)	0.41 (0.34;0.51)	0.032
R20 ($KPa.s.L^{-1}$)	0.28 (0.22;0.32)	0.30 (0.26;0.34)	0.31 (0.24;0.35)	0.32 (0.280.37)	0.190
R5-R20 ($KPa.s.L^{-1}$)	0.03 (0.03;0.06)	0.02 (0.01;0.05)	0.07 (0.01;0.15)	0.08 (0.02;0.16)	0.044
R5-R20 % predicted	30 (0;82)	23 (14;54)	92 (24;151)	75 (17;154)	0.036
AX ($Hz\ kPa.L^{-1}$)	0.20 (0.13;0.40)[c]	0.37 (0.15;0.56)	0.44 (0.20;2.00)	0.76 (0.20;1.69)	0.040
LCI	7.16 (6.65;7.95)[c]	7.02 (6.06;7.63)	7.81 (7.20;8.80)	8.28 (7.14;9.15)	0.008
Scond	0.026 (0.008;0.048)	0.023 (0.011;0.072)	0.039 (0.022;0.077)	0.03 (0.018;0.047)	0.200
Sacin	0.194 (0.115;0.322)[c]	0.345 (0.142;0.525)	0.304 (0.176;0.524)	0.316 (0.241;0.487)	0.033

Definition of abbreviations: R5: resistance at 5Hz; R20: resistance at 20Hz; AX: Area of reactance; LCI: Lung clearance index; Scond: conductive ventilation heterogeneity; Sacin: acinar ventilation heterogeneity.

Data expressed as median, Q1;Q3; Kruskal Wallis test followed by Dunn's multiple comparisons tests, significant difference ($p<0.05$) between: c- healthy and GINA IV-V; e- GINA I and GINA IV-V.

% SPA and Albumin and asthma treatment intensity

% SPA and % albumin were not associated with GINA treatment intensity (**Table 3.3.5, Figure 3.3.3 A**) and did not differ between asthmatics and healthy volunteers. Neither protein biomarker correlated with standardised measures of asthma control or quality of life (ACQ-6 or AQLQ).

%SPA, Albumin and Small Airways Dysfunction Phenotypes

We evaluated the correlations between % SPA and % albumin and different demographics and small airway physiological measurements, in the overall population (**Table 3.3.7**). Modest but significant correlations were found for % SPA with oscillometry parameters of small airways dysfunction (R5-R20 and AX): R5-R20 [both absolute value ($r=-0.256$, $p<0.05$) and % predicted ($r=-0.257$), $p<0.05$] and AX (-0.313, $p<0.05$). The spirometry measure of gas trapping – Forced Vital Capacity -FVC (L) also demonstrated modest but significant correlations with % SPA ($r=0.287$; $p<0.05$). In contrast, % albumin demonstrated a significant correlation with FVC and GINA treatment intensity ($r=-0.285$, $p<0.05$) only. No correlations were observed between PExA protein concentrations and with multiple breath washout derived markers of small airways dysfunction (Scond or Sacin).

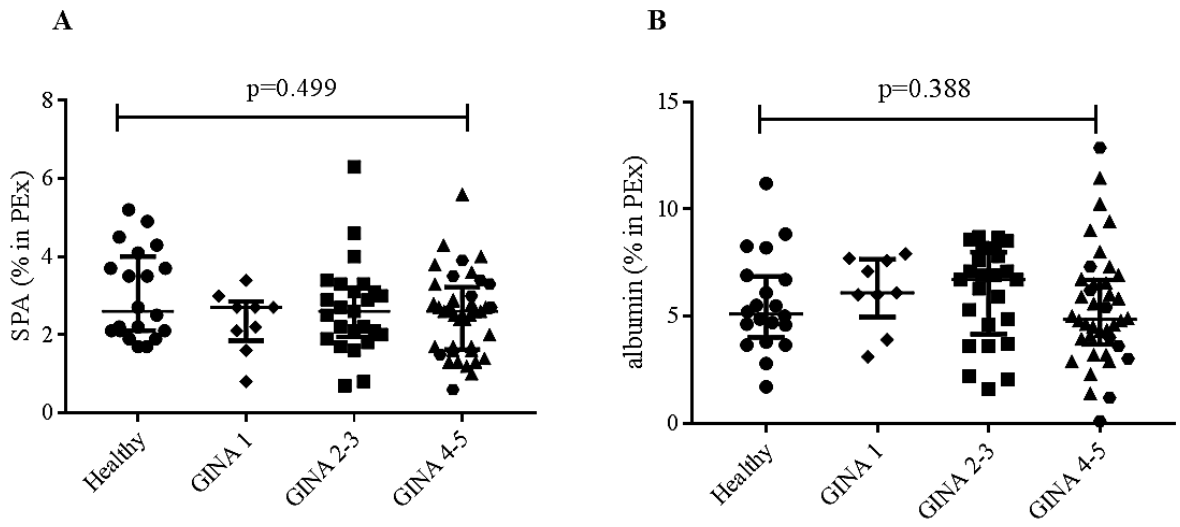

Figure 3.3.3 A, B: SPA and albumin across GINA step treatments. % of SPA (A) and albumin (B) and across GINA groups. Dots (black) represent healthy controls, diamonds asthma GINA step treatment I, squares asthma GINA step treatment II and III, triangles asthma GINA step treatment IV and grey hexagons for V. Kruskal-Wallis p value across groups is shown.

Table 3.3.7: % SPA and albumin and physiological parameters

Variable	**% SPA**	**% albumin**
Age	-0.127	0.110
Height	0.171	0.091
BMI	-0.033	-0.044
ACQ-6	0.111	0.022
AQLQ	0.024	0.090
GINA	-0.006	**-0.285***
Sputum eosinophils$^{\Delta}$	0.012	0.018
Sputum epithelial cells$^{\Delta}$	-0.161	-0.152
R20	-0.097	-0.099
R5-R20	**-0.256***	-0.124
R5-R20 % predicted	**-0.257***	-0.101
AX	**-0.313****	-0.160
LCI	-0.159	0.076
Scond	-0.067	-0.045
Sacin	0.006	0.090
FVC Z score post BD	0.163	**0.246***
FVC post BD	**0.287***	**0.251***
FEV_1 Z score post BD	0.075	0.138
FEV_1 post BD	**0.308****	0.207

Definition of abbreviations: BMI: body mass index; ACQ-6: 6-point asthma control questionnaire; GINA: global lung initiative for asthma; AQLQ: asthma quality of life questionnaire; R5: resistance at 5Hz; R20: resistance at 20Hz; AX: Area of reactance; LCI: Lung clearance index; Scond: conductive ventilation heterogeneity; Sacin: acinar ventilation heterogeneity; FVC: forced vital capacity; FEV_1: Forced expiratory volume in one second;
Data expressed as Spearman r value. *p<0.05; ** p<0.01; ***p<0.001. Δ: data based on 40 patients (42% population).

Tables 3.3.8, 3.3.9 and Figure 3.3.4 present summaries of the PExA protein and small airway physiology derived phenotypes using topological data analysis (TDA) applied to the overall discovery population. This analysis excluded four patients which did not fit in any of the three TDA categories generated. **Figure 3.3.4** demonstrates de TDA 2-dimentional networks of patients generated according to GINA step treatment (0-healthy volunteers), R5-R20 value, % SPA and % albumin. The round circles represent a network of patients with similar physiological outcomes. The lines connect network of patients (nodes) with similar outcomes.

TDA group 3 had the highest proportion and majority (n=13/47) of healthy volunteer cases when compared to the TDA group 1 and 2. % SPA and % albumin levels were well preserved within group 3, which demonstrated normal oscillometry and MBW small airway indices as well as preserved spirometry, despite 17/47 patients being classified clinically as having severe asthma (GINA IV-V) based upon treatment requirements.

In contrast, TDA group 1 was comprised of very few healthy cases (n=2/29), with most patients at GINA treatment steps III-V. Moreover, group 1 had significantly lower PExA % albumin and % SPA and concurrent evidence of abnormal post bronchodilator spirometry (FEV_1 and FVC) and small airway physiology (R5-R20, AX, Sacin) when compare to group 3 ($p<0.05$ for all comparisons). Group 1 also demonstrated the poorest asthma control and quality of life with statistically significant and clinically important ($\geq$ 0.5 units) differences in standardised asthma control and quality of life marker (ACQ-6 and AQLQ) when compared to group 3.

Finally, group 2 represented an intermediate population with reference to groups 1 and 3, again primarily comprised of asthmatic subjects (n=13/15). Additionally, group 2 had the lowest numerical % SPA ($p<0.05$ vs group 1) but in contrast to group 1, a preserved % albumin, and had evidence of small airways dysfunction compared to group 1 (R5-R20, AX, and LCI, $p<0.05$) but demonstrated preserved post bronchodilator spirometry and comparable asthma control and quality of life (ACQ-6, AQLQ) to TDA group 1.

Table 3.3.8 – demographic and clinical data according to TDA groups in the discovery population

Clinical Characteristics	**TDA group 1**	**TDA group 2**	**TDA group 3**	***P* value**
N per group (controls, GINA I, GINA II-III, GINA IV, GINA V)¥	29 (2, 2, 10, 11, 4)	15 (2, 1, 5, 7, 0)	47 (13, 6, 11, 12, 5)	0.287
% Healthy controls¥	6.9	13.3	27.6	0.066
Age (years)	62 (51;68)	65 (56;70)	59 (45;65)	0.0783
Sex (percent male)¥	55.17%	42.86%	51.06	0.7508
BMI (kg/m^2)	30 (26;34)	31 (23;34)	28 (24;30)	0.0911
Pack year smoking history	7.4 (5.0;11.0)	18.5 (3.0;34.0)	6.0 (1.0;9.0)	0.5991
GINA treatment step#	4 (3;4)	4 (3;4)	3.5 (2;4)	0.645
ACQ-6#	1.63 (0.67;2.16)	0.67 (0.28;2.67)	1.00 (0.66;1.67)	0.2727
AQLQ#	4.91 (4.12;6.03)	6.25 (5.70;6.69)	6.11 (5.21;.47)	0.0059 1 vs. 2*,1 vs. 3*
Post BD FVC (L)	2.97 (2.49;3.57)	3.40 (2.77;3.99)	3.83 (3.46;4.45)	0.0007 1 vs. 3*
Post BD FEV_1 (L)	2.19 (1.91;2.44)	2.40 (1.89;3.05)	3.08 (2.65;3.90)	<.0001 1 vs. 3*
Post BD FEV1 Z score	-1.44 (-2.59; -0.03)	-0.64 (-1.29; 0.49)	-0.49 (-1.25; 0.69)	<0.0001 1 vs. 3*
Post BD FVC Z score	-0.64 (-1.46; -0.03)	-0.27 (-0.83;0.39)	0.06 (-0.25;0.83)	0.002 1 vs. 3*
FEV_1/FVC	0.69 (0.60;0.77)	0.72 (0.69;0.77)	0.73 (0.67;0.78)	0.2056
FEV_1/FVC post BD LLN (% above)	57%	78%	70%	0.3733

Definition of abbreviations: BMI: body mass index; ACQ-6: six-point asthma control questionnaire; AQLQ: asthma quality of life questionnaire; FEV_1: forced expiratory volume in one second; FVC: forced vital capacity; BD: Bronchodilator. Data expressed as median, Q1;Q3. All tests are Kruskal-Wallis unless stated otherwise. ¥ = Fisher's exact test (controls vs asthma); # only asthma population.

Table 3.3.9 – Small airways physiology and biomarkers data according to TDA groups in the discovery population

	TDA group 1 (n=29)	**TDA group 2 (n=15)**	**TDA group 3 (n=47)**	**Kruskal-Wallis *P* value**
% SPA	2.1 (1.4;2.7)	1.7 (1.6;2.4)	3.1 (2.6;3.8)	<.0001 1 vs. 3*,2 vs. 3*
% Albumin	3.9 (2.6;4.8)	5.6 (5.0;8.0)	6.7 (4.9;7.9)	<.0001 1 vs. 2*,1 vs. 3*
R5 (KPa.s.L^{-1})	0.51 (0.44;0.64)	0.39 (0.29;0.51)	0.32 (0.25;0.39)	<.0001 1* vs. 3*
R20 (KPa.s.L^{-1})	0.34 (0.32;0.38)	0.31 (0.28;0.37)	0.30 (0.23;0.35)	0.0654
R5-R20 (KPa.s.L^{-1})	0.15 (0.12;0.20)	0.07 (0.02;0.17)	0.02 (0.01;0.05)	<.0001 All Groups*
AX (Hz kPa.L^{-1})	1.69 (1.11;3.04)	0.64 (0.26;2.12)	0.20 (0.12;0.42)	<.0001 All Groups*
LCI	8.62 (7.54;9.63)	8.77 (7.26;9.07)	7.30 (7.01;7.99)	0.0019 1 vs. 3*,**2 vs. 3***
Scond	0.036 (0.018;0.069)	0.044 (0.018;0.073)	0.029 (0.014;0.044)	0.2688
Sacin	0.412 (0.231;0.529)	0.302 (0.094;0.486)	0.269 (0.169;0.355)	0.0184 1 vs. 3*

Definition of abbreviations: R5: resistance at 5Hz; R20: resistance at 20Hz; AX: Area of reactance; LCI: Lung clearance index; Scond: conductive ventilation heterogeneity; Sacin: acinar ventilation heterogeneity. Data expressed as median, Q1;Q3. All tests are Kruskal-Wallis unless stated otherwise. ¥ = Chi-Squared test.

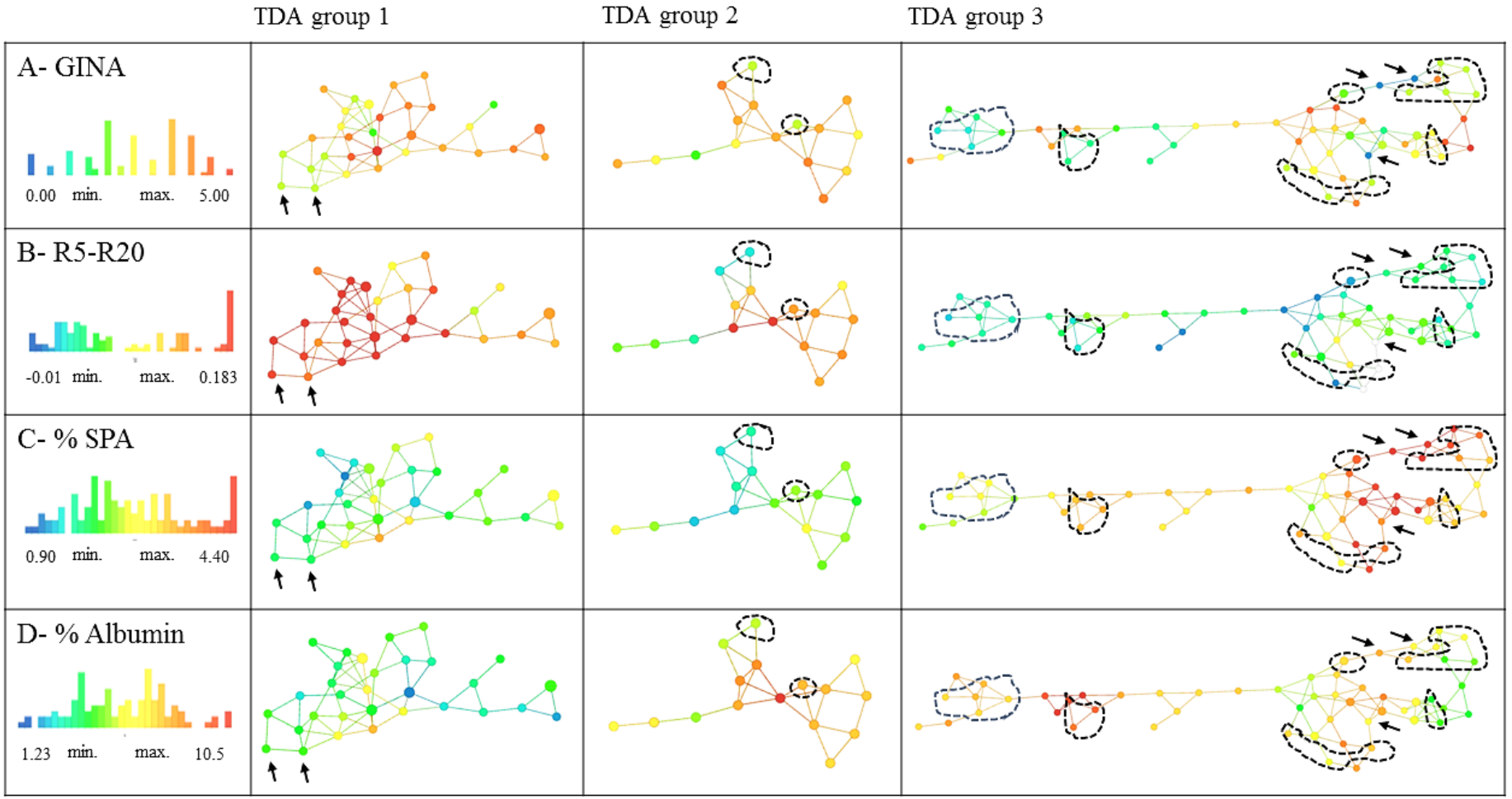

Figure 3.3.4: TDA analysis. *(Legend in the next page)*

Figure 3: TDA analysis. Image derived from TDA analysis, showing that three different groups were generated. Healthy controls and asthma patients were clustered and annotated by the following parameters: A) GINA treatment step treatment (red- only asthma patients, 0- healthy controls only); B) R5-R20 (red-very high frequency dependence of resistance) C) %SPA (red- higher levels of SPA) and D) %albumin (red- higher levels of albumin). There was a further group of four patients not fitting in any category and therefore not included in the analysis. TDA group 1 is mainly small airways disease predominant, with low % of SPA and albumin (2 healthy controls, 27 asthmatics); TDA group 2 is an intermediate group, with low % SPA but preserved albumin (2 healthy controls, 13 asthmatics); TDA group 3 demonstrate overall normal small airway lung function and higher SPA and albumin % (13 healthy controls, 34 asthmatics). Arrows and bounded shapes represent nodes with only healthy controls and nodes with high number of healthy controls, respectively**.** It can be seen that the majority of heathy patients are located within group 3, with occasional and scarce cases within group 1 and 2.

Replication Cohort

An additional Swedish cohort of n= 32 asthmatic patients (GINA I-III=18, GINA IV= 14) was evaluated as a replication population. Patients performed spirometry, IOS and PExA in a similar manner to our discovery population, therefore, it was used as a comparison cohort.

In the replication and discovery populations (**Figure 3.3.5 A and C**), % SPA correlated with absolute FVC (rs= 0.378, p=0.001 discovery and rs=0.543; p=0.001 replication), in the asthma population.

For % albumin (**figure 3.3.5 B and D**), only the discovery cohort demonstrated correlations with absolute FVC (rs=0.261, p=0.032). The replication cohort demonstrated a non-statistical, but visual trend for association between FVC and % albumin (**Figure 3.3.5 B and D**).

In contrast to the discovery cohort, we did not identify significant correlations between R5-R20 and either % SPA or % albumin in PEx, however, the trend was similar, higher values of R5-R20 associated with lower % SPA (data not presented).

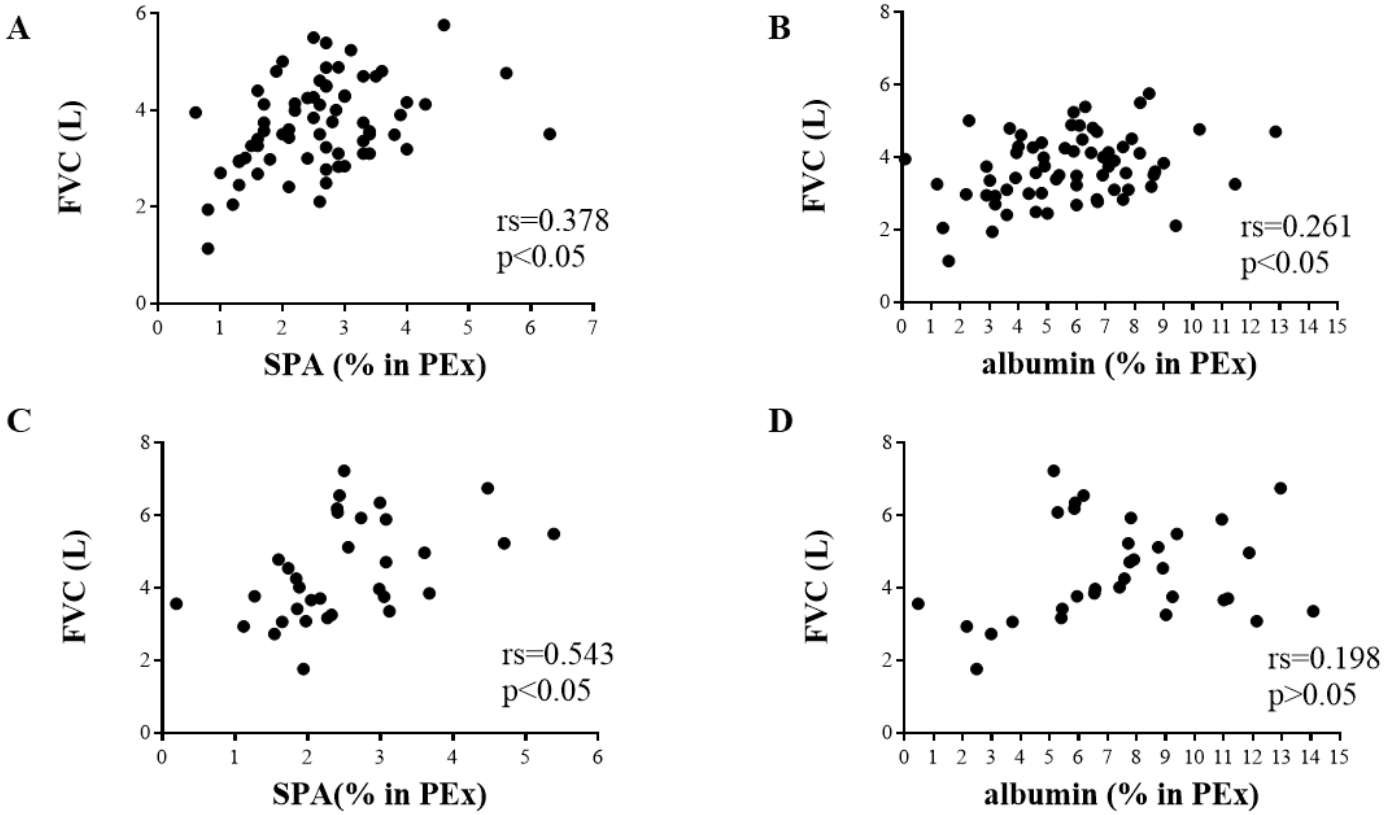

Figure 3.3.5 A, B, C, D: PEx and FVC in the replication cohort. Correlation between absolute FVC (Forced Vital Capacity) and % SPA and % of albumin, in the discovery population (4 A, 4 B) and replication population (4C, 4D).

DISCUSSION

We have shown for the first time that PExA sampling method is feasible across different asthma severity and that sufficient quantities of PEx can be sampled to allow protein biomarker analysis.

Furthermore, we have demonstrated using unbiased statistical phenotyping with TDA analysis that there appear to be phenotypes of patients with low % SPA and/or % albumin values, comprising primarily asthmatic subjects with concurrently abnormal small airway physiological indices captured by IOS and MBW. One of the small airway disease phenotypes had clinically important disease (assessed by validated patient reported outcome measures) when compared to the phenotype of patients without small airway abnormalities. A further phenotype appeared to have well-controlled asthma and spirometry with isolated physiological abnormalities in the small airways. Lower % SPA values were a reconciling feature of both small airway phenotypes, suggesting that the deficiency in SPA may possibly be causal to airways closure in the small airways.

Finally, we have identified that the % SPA is associated with FVC, a marker of airways closure and gas trapping (106) in both a discovery and an independent replication population.

The ability to measure protein biomarkers from the smaller airways offers a window of opportunity to study the pathobiology of small airways disease. Furthermore, low SPA levels in PEx, corrected for acquired particle mass and potential bias due to sampling in the context of airflow obstruction, was not only associated with small airways dysfunction/airway closure captured by IOS, MBW and FVC measurements, but also identified two phenotypes of patients with multiple physiological markers of small airways dysfunction and impaired asthma control/quality of life. These findings not only add credence to the notion that PEx samples originate from the smaller airways but also for a potential causal association between SPA deficiency and small airways dysfunction/ airways closure. The small airway phenotype extended across the spectrum of asthma severity and was not associated with eosinophilic airways inflammation suggesting that it may require alternative approaches of treatment that extend beyond inhaled corticosteroids and drugs that modify type 2 inflammation in asthma.

Previous studies have evaluated pooled PEx samples for SPA and albumin % in both mild asthma and obstructive lung diseases (COPD and bronchiolitis obliterans

syndrome-BOS) (240,245,260). These studies suggest that SPA is associated with obstructive lung disease COPD and BOS, providing a sound justification to study the role of SPA and albumin in asthma and their association with airways dysfunction.

There is compelling evidence from animal models and observational studies, linking SPA to asthmatic airway dysfunction and inflammation. Genetic variation of SPA has been shown to alter host immunological response to bacterial infection with mycoplasma in asthma (314), which may in turn be regulated by mast cells TNF receptor expression. These observations are further supported by animal models of SPA knockout that suggest that SPA deficiency amplifies allergic CD4 T cell driven airway inflammation (315). Ledford *et al* have recently reported in a systematic review that SPA/D are dysregulated in eosinophil-dominated inflammatory diseases, suggesting a therapeutic potential role of SPA/D, yet to be tested in humans (316). Broncho alveolar lavage studies in asthma and healthy report conflicting data on the role and concentration of SPA (253,317), highlighting the potential limitations of BAL in measuring protein biomarkers in asthma.

Our findings and previous literature on PExA, would suggest that PEx % SPA in asthma reflect protein concentrations in the small airways lining fluid and that deficiency of this protein may then directly promote airway closure and ventilation heterogeneity. There is some evidence of beneficial outcomes derived from inhaled synthetic surfactant in allergic asthma (318), and PEx SPA quantification may provide an opportunity to stratify patients for SPA targeted intervention trials in the future.

We utilised a combination of IOS, MBW and FVC to measure small airways dysfunction and airways closure, respectively. It is well recognised that small airways dysfunction associates with both asthma symptoms and key asthma traits e.g. hyper responsiveness (279). A recent systematic review has highlighted the evidence supporting R5-R20 as a small airway detection tool in asthma (136). Reduction in FVC has been associated with bronchoconstriction occurring due to airway closure and increased levels of airway hyperresponsiveness (106,319). Therefore, our findings that FVC was proportional to the % of SPA and albumin found in PEx, provides evidence that small airway closure may be due to an alteration in protein composition in the airway surface liquid in asthma.

Previous studies have demonstrated that treatment with both inhaled and oral steroids in asthma attenuates plasma protein and albumin in sputum supernatants in asthma (320). In support of this, TDA group 3 demonstrated lower numerical median GINA treatment and preserved % albumin compared to TDA group 1 who had both a low % albumin and % SPA. However, both hypothesis that albumin in the RTLF could be increased or decreased due to airway inflammation should be considered. Higher levels of albumin may equate to increased vascular permeability or transudation of albumin due to increased hydrostatic pressure, but the exact mechanist requires further research.

Limitations of our study include the relatively small sample size – nonetheless, this study represents the largest study to apply the PExA technique to a well characterised cohort of adult asthmatics to date. Moreover, further studies are required to identify the relationship between protein marker of type 2 inflammation in PExA and SPA% in asthma. Studies that directly compare SPA concentration in sputum supernatant and PEx would further add to the validation of PEx as a small airway specific matrix. Of note however, in a separate adult asthma population of 42 individuals across different severities (GINA I-V), % SPA and absolute SPA in PEx did not correlate with serum SPA ($p=0.265$, $p=0.579$ respectively, data not shown).

Furthermore, additional validation of SPA and albumin in PEx are required with respect to measurement repeatability and healthy population normative ranges.

We conclude that the PExA method has the potential to non-invasively sample the small airways derived proteins in asthma (including severe asthmatics with high unmet need) and that two exemplar PExA proteins (SPA and albumin) are associated with small airway dysfunction phenotypes in asthma. Further studies are now required to reproduce our findings and further develop PEx as a novel matrix to study small airway biology non-invasively.

3.4 Short-term repeatabillity and longitudinal change of particle in exhalaed air derived SPA and albumin in adult asthma

ABSTRACT

Background: The Particles in Exhaled Air (PExA) method allows sampling of protein biomarkers from the small airways. However, for PExA to be suitable for clinical trials further information is required on within patient repeatability of putative biomarkers over time. Furthermore, the relationship between PExA biomarkers and longitudinal outcomes in asthma has not been reported.

Methods: We sought to evaluate the intra and inter-individual variation of two candidate small airways dysfunction biomarkers: Surfactant protein A (SPA) and albumin derived from PExA, and their relationship with longitudinal FEV_1 decline and changes in small airway physiology (impulse oscillometry derived R5-R20 and AX). We conducted a repeatability study with 18 patients [13 patients with stable asthma (GINA III-IV) and 5 healthy controls] to establish the within visit, 2 week and three-month repeatability of SPA and albumin. Furthermore, we utilised the information from the repeatability study to establish the relationship between abnormal increase/decrease in SPA, albumin and small airways physiology/spirometry in a longitudinal cohort (52 asthmatics and 9 healthy volunteers), followed up on average at 28 (26:35) [median (Q1;Q3)] months, with repeated measures.

Results: Short-term repeatability for both % SPA and % albumin was excellent (intra class correlation > 0.9 for both proteins within visit and at 2 weeks) and good at three months (intra class correlation > 0.75 for both proteins). In the longitudinal study we did not identify that baseline % SPA or % albumin influenced FEV_1 decline using linear mixed models. However, we identified that patients that had a reduction in either % SPA or % albumin, such that their longitudinal follow up value was lower than predicted based upon the lower limit of the 95% confidence interval (derived from the 2- week repeatability data), demonstrated worsening of small airway markers R5-R20 and AX.

Conclusions: We demonstrate that % SPA and % albumin from PEx are highly repeatable over three months and thus suitable as biomarkers for small airway directed trials. Whilst we did not identify an association with FEV_1

decline, our cohort was relatively small and further research is required in larger asthma populations to understand how PEx proteins influence lung function trajectories.

INTRODUCTION

Particles in exhaled air (PExA) is a novel method to sample non-volatile particle material, which is believed to originate from the small airways of the lungs (14,244). A few pilot studies have been conducted to explore the PExA behaviour, in both healthy individuals and asthma (242,321). Exhaled particles seem to vary greatly between individuals and although a possible mechanism for this observation might be the breathing manoeuvre, it is not fully understood, as the variation remains high even after following a standardised PEx (PExA material) collection breathing sequence (240). Bake *et al* have recently shown in a healthy population that specific variables such as age, weight and spirometry account for less than 30% of the inter-individual variability of mean particles exhaled (262).

The PEx matrix has been shown to be rich in phospholipids and proteins, and research has been conducted to further explore the link between potential biomarkers originated from the respiratory tract lining fluid (RTLF) and airway disease such as asthma (15,16,259), chronic obstructive pulmonary disease (COPD) (17) and bronchiolitis obliterans syndrome (BOS) (260). The study of protein content from PEx has numerous advantages when compared to other methods, such as bronchioalveolar lavage (BAL), sputum induction and exhaled breath condensate (EBC): rapid, non-invasive and possible standardisation of samples for acquired exhaled particle mass.

Surfactant protein A (SPA), an important immunomodulatory protein with innate immune response and regulatory functions, and albumin, a plasma protein (210,254) present in PEx, are amongst the most abundant proteins in PEx and potentially important in the study of small airways dysfunction in asthma. Earlier studies have demonstrated a possible association between lower levels of SPA and albumin in PEx and increased airway obstruction and inflammation (15–17,259), however, little is known about the variation of SPA and albumin in the RTLF over time and the consequences of variation on lung (including small airway) function.

In order to extend the PExA method further and use of its candidate protein biomarkers in clinical trials, it is crucial to understand the repeatability and stability of these biomarkers over time.

We therefore aimed to determine the intra-individual variability of PEx particle number, SPA and albumin over time (within visit, 2 weeks and three months). Repeatability data was used to generate sample size calculations to estimate the number of individuals necessary to include in future clinical trials using SPA as outcome measure. Moreover, we sought to evaluate the relationship between baseline protein levels and their relationship with physiological (spirometry and small airways dysfunction measurements) change over a period of 2 to 3 years, in an adult population of healthy controls and patients with asthma.

METHODS

Study Population

The study protocol was approved by the National Research Ethics Committee – East Midlands Leicester (approval number: 08/H0406/189) and all subjects gave their written informed consent.

18 individuals (13 patients with asthma, 5 healthy controls) attended 3 study visits over a 3-month period – for the short-term repeatability study. An additional cohort of 53 patients with adult asthma and 9 healthy controls attended 2 study visits, separated by 28 (26:35) [median (Q1;Q3)] months, in a longitudinal outcome study.

Asthma patients had a physician diagnosis of asthma and one or more of the following physiological criterion: Methacholine PC20 ≤8mg/ml, bronchodilator reversibility to 400 mcg of inhaled salbutamol of FEV_1 ≥12% and 200mls or peak flow variability of ≥ 20% over two weeks. Patients had been free from exacerbations for at least six weeks

prior to study entry. Asthmatics and healthy controls currently smoking or with a smoking pack history greater than or equal to ten were excluded.

Study Design

Figure 3.4.1 A shows an overview of study design, both short-term repeatability and longitudinal. In sum, in the short-term repeatability study, patients performed PExA at every visit [2 sessions during visit 1 (3 for patients that performed additional pre-bronchodilator measurements), 1 session during visit 2 and 3]. Additional demographics and lung function measurements were collected: demographics including spirometry, impulse oscillometry (IOS), fractional exhaled nitric oxide at a flow rate of 50mls.s (FeNO) and peripheral blood eosinophil measurements during visit 1. Additional FeNO measurement were performed at visits 2 and 3.

Patients in the longitudinal cohort performed post bronchodilator PExA, spirometry, asthma questionnaires and IOS at both visits.

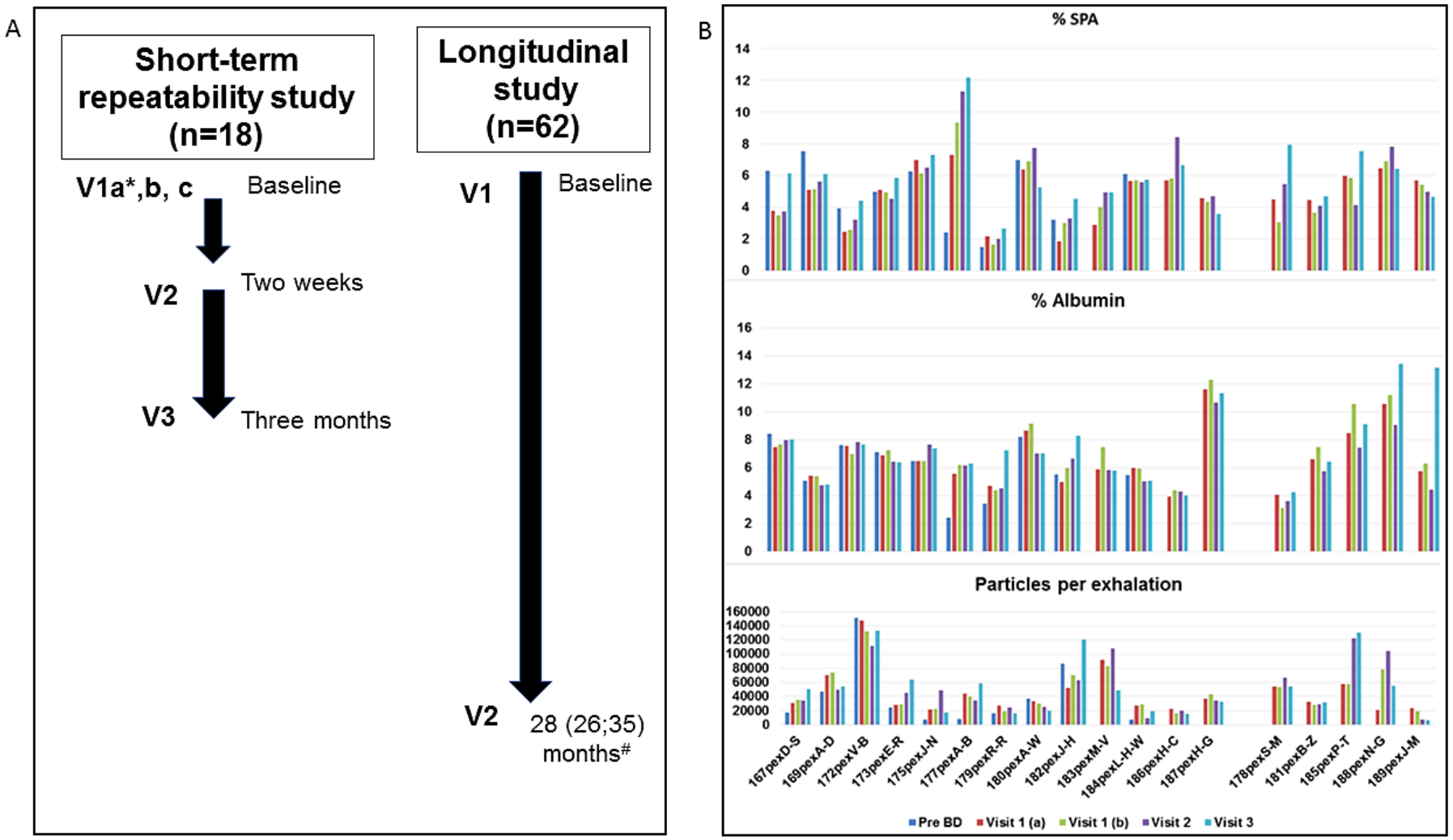

Figure 3.4.1 A and B: (**A**) **Summary of studies conducted** [* pre-bronchodilator; # median (Q1;Q3)]; (**B**) **% Albumin, % SPA and number of particles per exhalation for each individual and visit, in the short-term repeatability cohort** (last 5 patients: healthy controls).

Physiological measurements

Spirometry was performed within the ATS/ERS recommendations (271) using a Vitalograph Alpha AL 21523 device (Vitalograph, Maids Moreton, Buckingham, MK18 1SW).

IOS measurements and quality control were performed according to the ERS Task Force recommendations (119) using the Masterscreen IOS (Erich Jaeger/Care Fusion, Germany). The device was calibrated daily using a standardised resistance and measurements were performed in triplicate, as described previously (140).

FeNO was measured following the recently published guidelines on standardised techniques for measuring exhaled Nitric Oxide by ATS and ERS (217).

PEx was collected with PExA 1.0 instrument as previously described (16), following a standard breathing manoeuvre (17): full exhalation till residual volume (RV), followed by breath hold for about 5 seconds and rapid inspiration till total lung capacity, finishing with a steady exhalation back to RV, at a peak flow of about 1500 ml/s (see methods section for further details).

PEx was extracted using PBS/ 0.05% Tween and particles SPA/Albumin evaluated using ELISA. Protein concentrations were derived from 4 parameter standard curves and were normalised to acquired PEx mass (ng) to yield a % of SPA and albumin. Intra and inter assay coefficient of variation were typically < 10% for both SPA and Albumin in all assays (see **appendix 3 and 4**).

Statistical analysis

Statistical analyses were performed using SPSS 24 (IBM Corporation, Somers, NY, USA) and Prism 7 for graphical plots (GraphPad Software Inc., La Jolla, CA, USA). A *p*-value of <0.05 was taken as the threshold for statistical significance. Comparisons between visits were performed using student paired t test for parametric data and the Wilcoxon rank test for non-parametric data. Between group-comparison were

performed using ANOVA and Kruskal-Wallis tests for parametric and non-parametric data, respectively. The intraclass correlation coefficient (ICC) was calculated to compare the correlation of each repeatability visit with the baseline visit. Bland-Altman plots were used to evaluate systematic bias between repeatability visits. Linear Mixed models were generated with R to evaluate the relationship between baseline PExA % SPA and % albumin measurement and FEV_1, FVC decline. Sample size calculations were generated with G-power software (version 3.1.9.2).

RESULTS

Short-term repeatability

Table 3.4.1 shows the clinical characteristics of the short-term repeatability cohort. Healthy controls were mainly male individuals, in contrast to the asthmatic group, with more female patients, however, the two groups were well match for age. Patients with asthma were mainly GINA step treatment IV, with well controlled disease, as seen by the 6-point asthma control questionnaire (ACQ-6) (267) and asthma quality of life questionnaire (AQLQ) (269) [mean, SD: 0.83 (0.72), 6.0 (0.85), respectively]. Spirometric and lung volumes did not differ significantly between groups. On the other hand, IOS parameters were significantly higher in the asthmatic group [example, Resistance at 5 minus resistance at 20 Hz (R5-R20), p=0.008].

Table 3.4.1: Clinical characteristics- Baseline short-term repeatability

	Healthy controls (n=5)	**Asthma (n=13)**	**Mann Whitney test p value**
Gender (male/female)¥	4/1	4/9	0.060
Age (years)	44 (17)	52 (16)	0.330
BMI (Kg/m^2)	23.2 (3.3)	30.7 (4.9)	**0.005**
Smoking pack year history	0 (0)	0.8 (2.8)	>0.999
GINA treatment step	-	4 (0.5)	-
FeNO (50 mls/s)	14 (4)	25 (13)	0.090
ACQ-6	-	0.83 (0.72)	-
AQLQ	-	6.0 (0.85)	-
FEV_1 Z score	-0.23 (0.99)	-0.49 (0.80)	0.687
FVC Z score	-0.38 (1.05)	-0.11 (0.91)	0.500
FEV_1/FVC	0.82 (0.05)	0.76 (0.07)	0.091
R5 ($kPa.s.L^{-1}$)	0.28 (0.06)	0.41 (0.07)	**0.005**
R20 ($kPa.s.L^{-1}$)	0.27 (0.07)	0.34 (0.05)	**0.046**
R5-R20 ($kPa.s.L^{-1}$)	0.01 (0.02)	0.07 (0.04)	**0.008**
AX ($kPa.L^{-1}$)	0.14 (0.06)	0.66 (0.37)	**0.0003**
RV (L)	1.89 (0.40)	2.01 (0.61)	0.833
RV/TLC (%)	29.2 (4.2)	33.6 (11.8)	0.143
TLC (L)	6.45 (0.95)	5.62 (1.16)	0.167
FRC (L)	3.33 (0.83)	2.81 (0.67)	0.173
Blood eosinophils (10^9/L)	0.17 (0.15)	0.20 (0.12)	0.648
Blood neutrophils (10^9/L)	4.44 (3.21)	3.69 (0.72)	0.443

Data expressed as mean (SD). *Definition of abbreviations:* BMI: body mass index; GINA: global initiative for asthma; FeNO: fraction of exhaled nitric oxide; ACQ-6: six-point asthma control questionnaire; AQLQ: asthma quality of life questionnaire; FEV_1: forced expiratory volume in one second; FVC: forced vital capacity; R5: resistance at 5 Hz; R20: resistance at 20 Hz; R5-R20: resistance at 5 Hz minus 20 Hz; AX: area of reactance; RV: residual volume; TLC: total lung capacity; FRC: functional residual capacity. ¥: chi square test.

PEx biomarkers variability

Figure 3.4.1 B shows a visual representation of % albumin, % SPA and mean particle number per exhalation on each visit, for each patient, where the first 13 individuals are patients with asthma and the last 5 healthy controls. Correspondingly, **Figure 3.4.2** presents Bland-Altman plots (298) for % SPA variation between visit 1 and 2 (**A**) and visit 1 and 3 (**B**), and for % albumin, between visit 1 and 2 (**C**) and visit 1 and 3 (**D**). Additionally, **figure 3.4.2 A** and **B** shows the variation of % SPA and % albumin before and after bronchodilator (400 mcg of inhaled salbutamol) respectively, during visit 1 for 10 patients with asthma. Again, good agreement is shown between samples for most patients. The mean, standard deviation and 95% confidence intervals of intra and between visits are shown in **table 3.4.2**, showing overall a very good agreement between samples, with majority of Intraclass-correlation (ICC) values greater than 0.8, indicating good overall agreement, which can be also seen with the Bland-Altman plots.

Furthermore, it can be seen from **figure 3.4.1B** that bronchodilator administration within a visit although significantly affecting the total number of exhaled particle, did not influence the % SPA and % albumin as the latter are corrected for acquired particle mass. This observation demonstrates that the % values of PEx biomarkers are likely to be independent of the potential bias of exhaled particle mass.

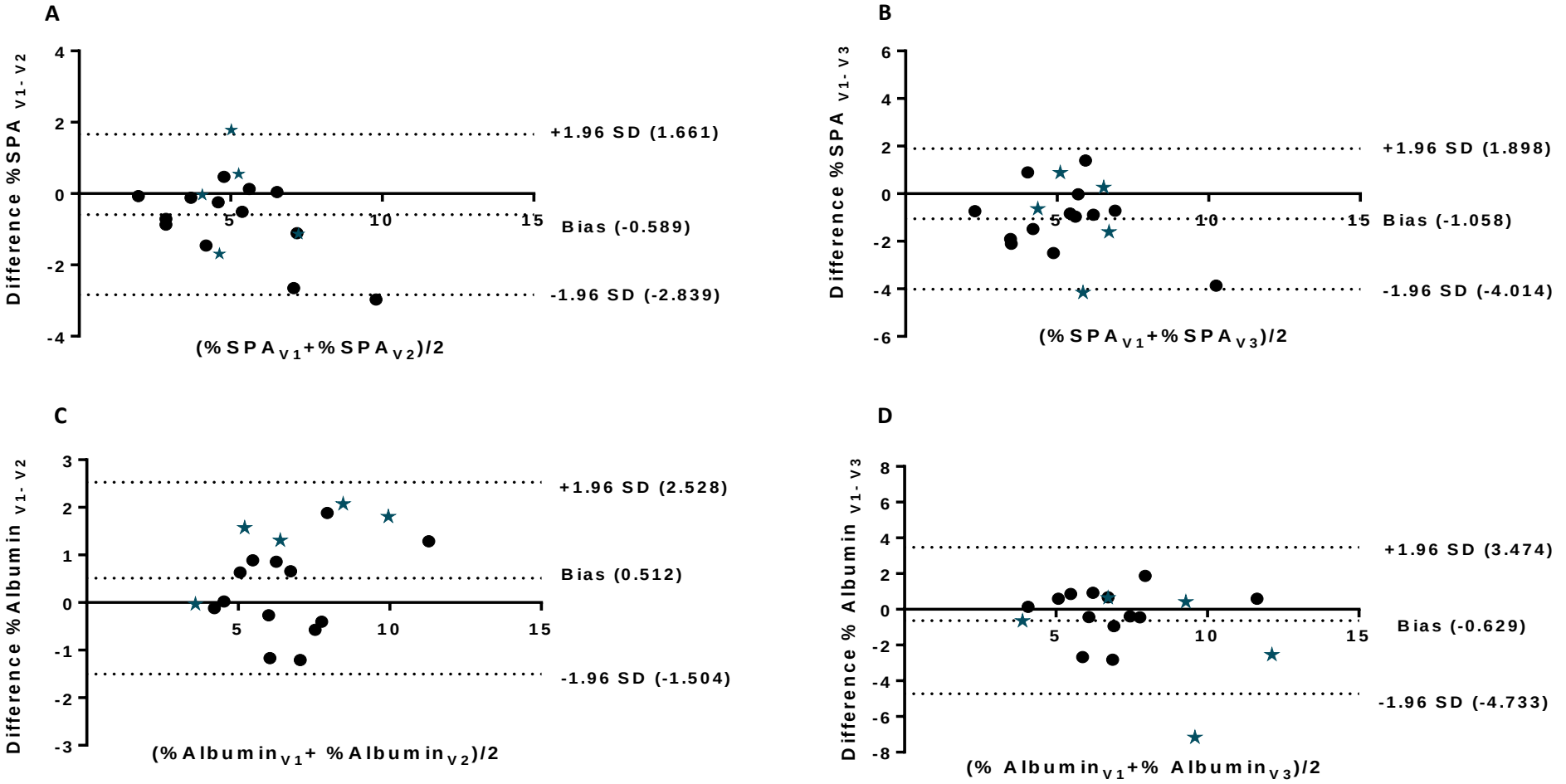

Figure 3.4.2: Bland-Altman plots of SPA and albumin between visits. (A) mean % SPA and the difference between % SPA at visit 1 minus visit 2; (B) mean % SPA and the difference between % SPA at visit 1 minus visit 3; (C) mean % albumin and the difference between % albumin at visit 1 minus visit 2; (D) mean % albumin and the difference between % albumin at visit 1 minus visit 3. Black dots: asthmatic patients; blue stars: healthy controls.

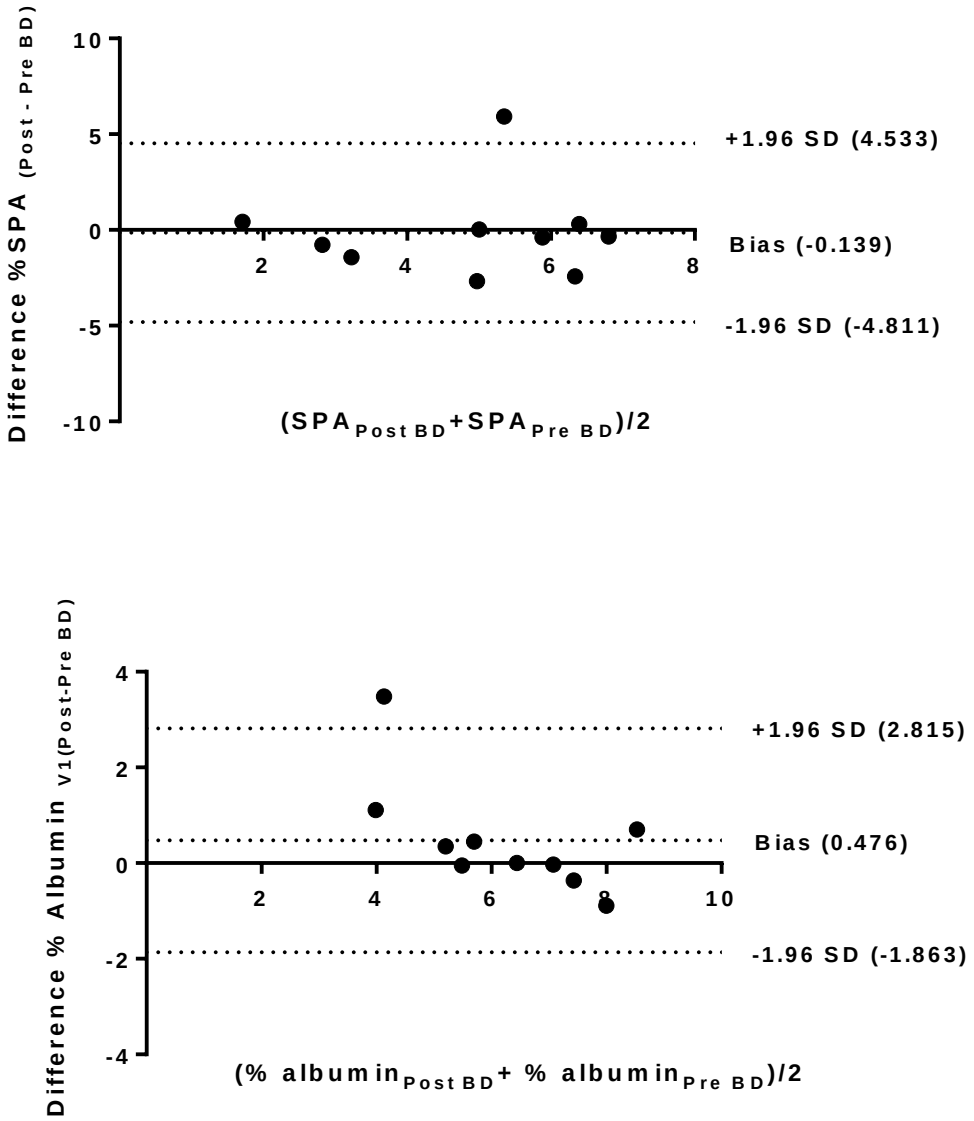

Figure 3.4.3: Bland-Altman plots of SPA and albumin between pre and post bronchodilator. (A) mean % SPA and the difference between % SPA at visit 1 post-bronchodilator minus visit 1 pre-bronchodilator; (B) mean % albumin and the difference between % albumin at visit 1 post-bronchodilator minus visit 1 pre-bronchodilator.

Table 3.4.2: Intra and between-visit variability of PEx variables

	Baseline Values		**Variability at 2 weeks**		**Variability at 3 months**	
	Mean (SD)	ICC£	Mean (SD) change from baseline (95% CI)	ICC$	Mean (SD) change from baseline (95% CI)	ICC$
SPA %PEx	5.20 (1.99)	0.920	0.28 (0.51), (0.03;0.54)	0.982	0.75 (1.43), (0.04;1.46)	0.834
Albumin %PEx	6.89 (2.22)	0.966	-0.51 (1.03), (-1.02;0.00)	0.920	0.63 (2.09), (-0.41;1.67)	0.782
Mean particles per exhalation	46921 (29904)	0.934	5454 (24438), (-6699;17607)	0.845	4969 (27219), (-8567;18505)	0.825

Definition of Abbreviations: ICC: Intraclass correlation coefficient; £: of duplicate samples collected at baseline; $: of samples collected at baseline vs follow-up visits.

Sample size calculation

A samples size calculation can be based on an estimate of the expected spread of values, i.e., standard deviation (SD). To date, there is no data available on the normal tendency of % SPA in PExA over time or accepted minimal clinically important difference (MCID). Thus, the data from our population presented in **table 3.4.2** regarding the mean, SD and 95% confidence intervals of % SPA inter-visit repeatability in stable asthma were used to estimate the MCID of this biomarker and the necessary sample size required in future interventional clinical trials in asthma. Therefore, using the calculated standard deviations, MCID in % SPA was considered ±0.51% and ± 1.43% over a 2-week and 3-month period, respectively.

Table 3.4.3 shows the sample size required to observe a significant change in % SPA over a 2-week and three-month period in each group, intervention and placebo. Calculations were performed using G-power software (version 3.1.9.2), given a parallel group study design, using a parametric paired t-test, two-tailed significance level of 5% and power of 80% and 95%, following the standard formula below (322). A drop-out of 15% was considered and accounted for in the sample size calculations.

Sample size= $\frac{2\sigma^2(u+v)^2}{d^2}$

σ = standard deviation of between-visit changes

u = one-sided percentage point of the normal distribution corresponding to 100% - power (eg. if power = 80%, u = 0.84)

v = percentage point of the normal distribution corresponding to the (two-tailed) significance level (eg. if significance level = 5%, v = 1.96)

d = difference in between-visit changes to be detected

Table 3.4.3: Sample size calculations for %SPA

	At two weeks treatment		At three months treatment	
Power (%)	**80**	**95**	**80**	**95**
SPA %PEx	22	33	23	36

Power calculation with respect to 2-week and 3-months treatment and change in PExA biomarker given a 2-group dependent paired t-test, at 80 and 95% power and 5% two-tailed significance.

Longitudinal cohort

Clinical characteristics and lung function of the longitudinal cohort are summarised in **Table 3.4.4 and 3.4.5** respectively, for both visits. There was a mean (SD) of 30 (4) and 33 (5) months between baseline and follow-up for the asthmatic group and healthy controls, respectively.

Between groups comparison

There were significant differences in FeNO and spirometric parameters in the follow-up visit between groups, with worst outcomes for patients with asthma. However, no statistically significant differences were encountered with IOS and PExA parameters. The % SPA and mean particle per exhalation, although higher on average for healthy controls, showed no significant difference (p=0.406, p=0.120, respectively).

Baseline and follow-up comparison

Overall, healthy controls demonstrate improved lung function, particularly FVC % predicted and Z score (p=0.016 for both). Patients with asthma show improved asthma

symptoms and quality of life (p=0.023) in the follow-up visit. However, spirometric parameters show a decline in lung function (example, FVC p=0.010). In contrast, IOS parameters show a non-significant trend for improvement.

Table 3.4.4: Clinical characteristics- Longitudinal study

	Healthy controls (n=9)			**Asthma** (n=53)			
	Baseline	Follow-up	**Paired Wilcoxon test**	Baseline	Follow-up	**Paired Wilcoxon test**	**Healthy vs Asthma follow-up Mann Whitney test**
Follow-up duration months	-	33 (5)	-	-	30 (4)	-	0.04
Age (years)	50 (19)	53 (19)		58 (12)	60 (12)		0.220
Sex (male/female)¥		4/5			29/24		0.529
BMI (Kg/m^2)	26.8 (4.2)	28.4 (6.3)	0.734	29.6 (6.1)	29.7 (6.3)	0.588	0.543
GINA treatment step	-	-	-	3.3 (1.3)	3.4 (1.2)	0.152	
ACQ-6	-	-	-	1.23 (0.92)	1.02 (1.01)	0.156	
AQLQ	-	-	-	5.54 (1.2)	5.71 (1.4)	0.023	
FeNO	-	16 (7)		-	33 (23)		0.027

Data expressed as mean (SD). *Definition of abbreviations:* BMI: body mass index; GINA: global initiative for asthma; FeNO: fraction of exhaled nitric oxide; ACQ-6: 6-point asthma control questionnaire; AQLQ: asthma quality of life questionnaire; SPA: surfactant protein A. ¥ chi-square test.

Table 3.4.5: Lung physiology & Biology- Longitudinal study

	Healthy controls n-9			Asthma			
	Baseline	Follow-up	**Paired Wilcoxon test**	Baseline	Follow-up	**Paired Wilcoxon test**	**Healthy vs Asthma follow-up Mann Whitney test**
Follow-up duration (months)	-	33 (5)	-	-	30 (4)	-	0.04
FEV_1 (L)	3.13 (0.48)	3.30 (0.96)	0.078	2.55 (0.68)	2.49 (0.72)	0.092	0.008
FEV_1 % predicted	105 (17)	117 (16)	**0.047**	86 (20)	87 (20)	0.540	<0.0001
FEV_1 Z score	0.28 (1.20)	1.38 (0.94)	**0.031**	-0.96 (1.39)	-0.81 (1.29)	0.252	<0.0001
FVC	4.01 (0.69)	4.27 (1.00)	0.469	3.68 (0.86)	3.53 (0.85)	**0.010**	0.045
FVC % predicted	107 (18)	125 (17)	**0.016**	96 (16)	97 (14)	0.770	<0.0001
FVC Z score	0.37 (1.22)	1.60 (1.04)	**0.016**	-0.31 (1.20)	-0.23 (0.92)	0.645	<0.0001
FEV_1/FVC	0.78 (0.06)	0.77 (0.05)	0.312	0.70 (0.12)	0.70 (0.12)	0.832	0.099
R5-R20 ($kPa.s.L^{-1}$)	0.03 (0.03)	0.04 (0.03)	0.719	0.09 (0.09)	0.09 (0.09)	0.766	0.075
AX ($kPa.L^{-1}$)	0.28 (0.20)	0.31 (0.14)	0.812	1.06 (1.14)	0.86 (0.94)	0.259	0.153
X5 ($kPa.s.L^{-1}$)	-0.09 (0.03)	-0.10 (0.03)	0.656	-0.16 (0.09)	-0.15 (0.09)	0.318	0.210
SPA %	2.94 (1.26)	3.66 (1.16)	0.383	2.57 (1.08)	3.26 (0.93)	**0.0002**	0.406
Mean particles per exhalation	$8.4x10^4$	$6.6x10^4$	0.910	$3.5x10^4$	$4.0x10^4$	0.887	0.120

Data expressed as mean (SD). *Definition of abbreviations:* FEV_1: forced expiratory volume in one second; FVC: forced vital capacity; R5: resistance at 5 Hz; R20: resistance at 20 Hz; R5-R20: resistance at 5 Hz minus 20 Hz; AX: area of reactance; SPA: surfactant protein A.

Interestingly, both healthy controls and asthmatic patients present in average a higher % SPA in the follow-up visit, statistically significant in asthma (p=0.0002), despite no changes in the mean particles exhaled. However, this was not the case for all patients. Next, we utilised the 95% confidence intervals calculated from our repeatability cohort at 3 months to define what would represent a clinically significant change in % SPA both improvement ($\%SPA_{FU}$-$\%SPA_{baseline}$>1.46%), or deterioration ($\%SPA_{FU}$-

$\%SPA_{baseline}$<0.04%) in our asthma population. Thus, our population was separated in three groups: group with clinically significant increase; group with clinically significant decrease and group within limits established ($\%SPA_{FU}$-$\%SPA_{baseline}$<1.46 and >0.04%) (**table 3.4.6, figure 3.4.4**), and clinical and physiological parameters were compared. No significant differences were encountered; however, there was a trend for worst clinical outcomes for the patients with significant decrease [example, ACQ-6 baseline: 1.59 (0.95)- decline vs 1.41 (1.09)-improvement] and greater lung function decline [example, FEV_1 change: -0.40 (294) mls - decline vs 0 (284) - improvement]. Interestingly, patients with a decrease in % SPA at follow-up showed a slight worsening of R5-R20 [0.007 (0.03)] and virtually no change in AX [-0.01 (0.19)], compared to % SPA improvers [-0.003 (0.073), -0.77 (1.63), R5-R20, AX, respectively], and patients with preserved % SPA [-0.001 (0.073), -0.06 (0.41), R5-R20, AX, respectively].

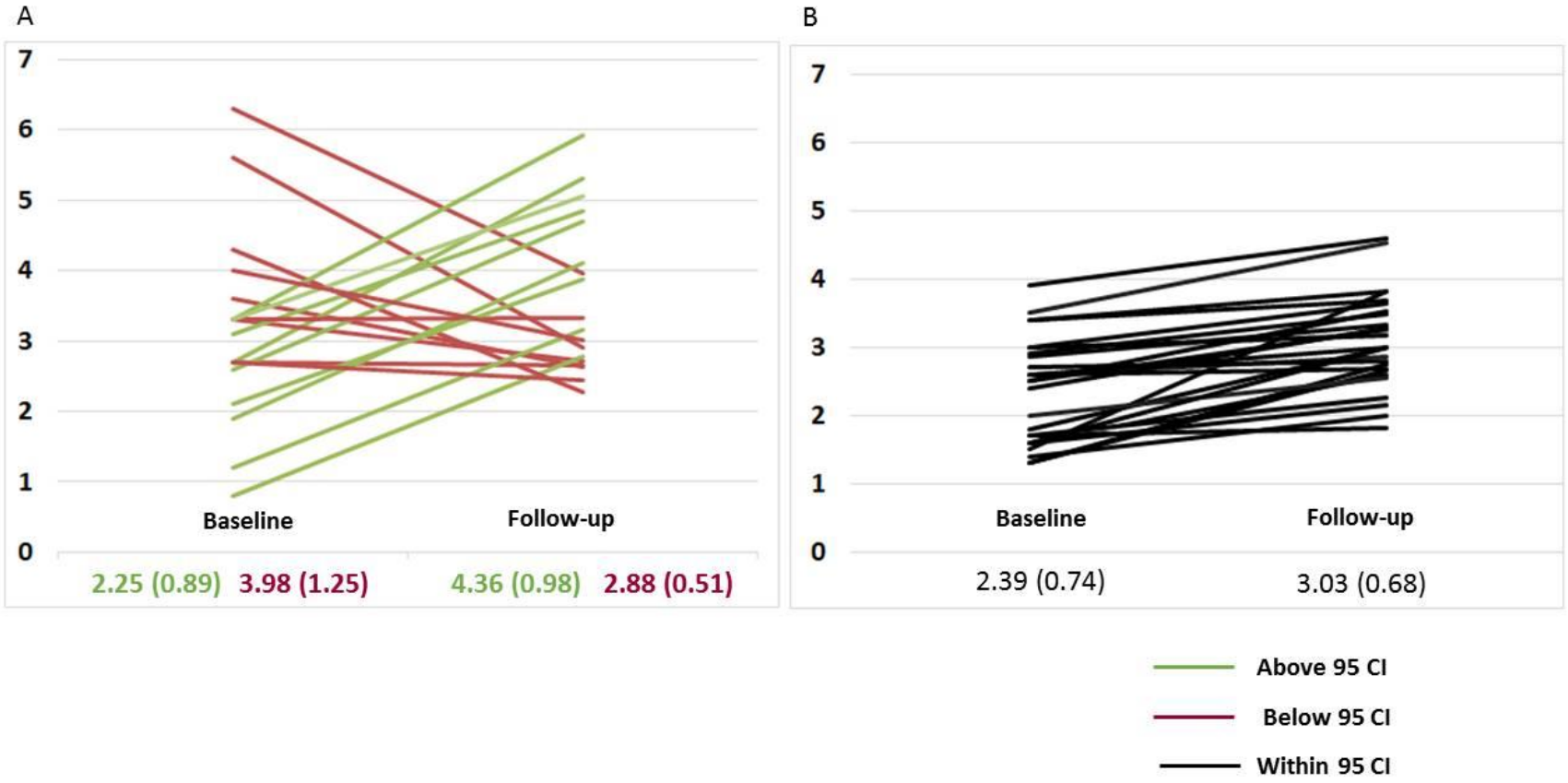

Figure 3.4.4: % SPA at baseline and follow-up (2.5 years) visits. (A) patients with clinically significant reduction (red lines) and improvement (green lines). (B) patients with stable levels. Mean and SD presented.

Table 3.4.6: Lung physiology & Biology- Longitudinal study

	Group with clinically significant SPA decrease (n=9) ($\%SPA_{FU}$-$\%SPA_{baseline}$<0.04%)	**Group with clinically significant SPA increase** (n=10) ($\%SPA_{FU}$-$\%SPA_{baseline}$>1.46%)	**Group within 95% confidence** (n=27) ($\%SPA_{FU}$-$\%SPA_{baseline}$<1.46 and >0.04%)	**p value**
Sex (% male)	5 (55)	4 (40)	17 (63)	0.456
Age (years)	62 (7)	57 (14)	63 (13)	0.189
GINA (I, II-III, IV-V)	0, 4, 5	1, 2, 7	2, 6, 19	0.645
Weight difference (follow-up-baseline)	0.4 (2.2)	-0.61 (5.2)	-3.0 (15)	0.322
Exacerbations (between visits)	1 (1.66)	1 (1.12)	1 (1.65)	0.377
ACQ-6 (baseline)	1.59 (0.95)	1.41 (1.09)	1.12 (0.87)	0.393
ACQ-6 (follow-up)	0.69 (0.68)	1.10 (0.95)	1.15 (1.15)	0.504
ACQ-6 (difference)	-0.91 (1.21)	-0.31 (1.14)	0.07 (0.96)	0.069
AQLQ (baseline)	5.20 (1.28)	5.55 (0.87)	5.65 (1.15)	0.585
AQLQ (follow-up)	5.53 (2.00)	6.22 (0.82)	5.66 (1.32)	0.523
AQLQ (difference)	0.33 (1.86)	0.85 (0.71)	0.01 (0.68)	0.158
FeNO (follow-up)	34 (20)	32 (18)	33 (25)	0.981
FEV1 (difference mls)	-40 (294)	0 (282)	-107 (242)	0.539
FVC (difference mls)	-121 (439)	67 (274)	-144 (326)	0.862
R5-R20 (difference)	0.007 (0.03)	-0.033 (0.073)	0.01 (0.043)	0.070
AX (difference)	-0.01 (0.19)	-0.77 (1.63)	-0.06 (0.41)	0.075

Data expressed as mean (SD). *Definition of abbreviations:* GINA: global initiative for asthma; FeNO: fraction of exhaled nitric oxide; ACQ-6: six-point asthma control questionnaire; AQLQ: asthma quality of life questionnaire; FEV_1: forced expiratory volume in one second; FVC: forced vital capacity; R5: resistance at 5 Hz; R20: resistance at 20 Hz; R5-R20: resistance at 5 Hz minus 20 Hz; AX: area of reactance; p value based on A-NOVA comparison test.

Relationship between lung function change, exacerbation frequency and PEx proteins

Generalised linear mixed models were applied to the longitudinal PExA cohort, with R5-R20, AX, FEV_1, FEV_1/FVC and FVC as dependent variables (in separate models). The independent variables were age, gender, height, GINA treatment intensity, time (in years), mean % SPA or mean % albumin (**table 3.4.7**). Age, height and % SPA were found to be statistically significant predictors of both FEV_1 and FVC, with higher % SPA associated with (higher) FEV_1. Moreover, FVC was found to decrease over time. No association was found between FEV_1 or FEV_1/FVC and % albumin, however, higher % albumin was associated with a higher FVC. Gender, height and % SPA were statistically significant predictors of the small airway measurement R5-R20, such that a lower % SPA was associated with a higher R5-R20 in the follow-up visit; similar results were found with AX (data not shown). Likewise, age, gender, height and % albumin were found to be statistically significant predictors of R5-R20 and AX (lower % albumin was associated with a higher R5-R20).

No significant interactions between time and % SPA or % albumin were found however, indicating that the protein concentration at baseline was not associated with decline in lung function over time.

Exacerbations were modelled using a negative binomial generalised linear model. The independent variables were age, gender, height, GINA treatment intensity, time (years), % SPA (model 1) and % albumin (model 2) (data not shown). No statistically significant results were found.

Table 3.4.7: Linear mixed effect models: % SPA and % albumin

%SPA model					
Model 1: FEV_1 (dependant variable)					
	Estimate	**Std. Error**	**Df**	**t value**	**p value**
Age (years)	-0.027668	0.006720	42.99	-4.117	0.0001 ***
Male	-0.054214	0.192392	42.98	-0.282	0.779
Height (m)	0.027648	0.010085	42.84	2.741	0.009**
%SPA	0.189986	0.077297	46.90	2.458	0.018 *
Time (years)	-0.021288	0.015154	46.73	-1.405	0.167
%SPA * Time	-0.002968	0.012838	46.36	-0.231	0.818
Model 2: FVC (dependant variable)					
Age	-0.020024	0.006505	43.29	-3.078	0.004 **
Male	0.151556	0.186214	43.26	0.814	0.420
Height (m)	0.053396	0.009755	43.02	5.474	>0.0001 ***
SPA	0.159254	0.076228	50.58	2.089	0.042 *
Time (years)	-0.050768	0.020006	47.61	-2.538	0.015 *
%SPA * Time	-0.004628	0.016978	46.97	-0.273	0.786
Albumin					
Model 1: FEV_1 (dependant variable)					
Age (years)	-0.031664	0.007179	42.88	-4.411	<0.0001***
Male	-0.105230	0.205366	42.80	-0.512	0.611
Height (m)	0.032515	0.010129	42.65	3.210	0.002
Albumin	0.063706	0.033565	47.82	1.898	0.064

Time (years)	-0.020363	0.015210	46.54	-1.339	0.187
% albumin * Time	-0.003349	0.005523	46.40	-0.606	0.547
Model 2: FVC (dependant variable)					
Age (years)	-0.0250906	0.0066019	42.97	-3.801	0.0004**
Male	0.0553237	0.1887672	42.80	0.293	0.771
Height (m)	0.0572031	0.0093016	42.53	6.150	<0.0001***
Albumin	0.0761970	0.0317565	52.92	2.399	0.020*
Time (years)	-0.0516125	0.0201458	47.27	-2.562	0.014*
% albumin* Time	0.0006517	0.0073206	47.02	0.089	0.929

Generalised linear mixed models fitted to the following dependent variables:FEV_1 and FVC. Independent variables are: age, gender, height, GINA, time mean SPA or mean albumin. A random intercept was included in the model. *Definition of abbreviations:* FEV_1: forced expiratory volume in one second; FVC: forced vital capacity; SPA: surfactant protein A.

DISCUSSION

We present the first PExA study evaluating the intra and inter-individual change of two PExA protein biomarkers- surfactant protein A (SPA) and albumin, and exhaled particles over time, both short and long-term variability, in health and individuals with asthma. Moreover, we evaluate the interaction between these protein biomarkers and lung function over time.

To date, little is known about the variation of the proteins studied across different time points, which is a crucial information in the establishment of novel and valuable disease status biomarkers. Literature shows that exhaled particulate variation amongst different subjects is high (16,259,262), however, our results show for the very first time the behaviour of these particles longitudinally, over a series of different collection points. Similarly, our study showed that exhaled particles were significantly different amongst individuals, as well as % SPA and % albumin, in both controls and patients with asthma.

Our results show that intra-individual variation is low in short-term, with very good agreement between visits within two weeks and three months, for SPA, albumin and also number of exhaled particles. This was true for both healthy controls, and patients with controlled asthma. Moreover, patients with asthma showed similar SPA and albumin results pre and post 400mcg of inhaled salbutamol. Thus, SPA and albumin seem to be potentially reliable biomarkers of disease status in asthma. Our sample size simulation showed that about 36 patients per group (intervention, placebo) would be required to see a meaningful change in % SPA in interventional clinical trials settings, at three-months treatment. Larson *et al* have shown in a small population that exhaled particles were lower during pollen season, in patients with allergic asthma, perhaps due to the fact that inflammation reduced the diameter and number of small airways involved in the particle formation process (259). However, no differences were seen between levels of SPA and albumin, as well as spirometric parameters, between pollen and non-pollen season, maybe due to the low number of individuals included.

Our observational longitudinal study demonstrated an overall improvement in the % of SPA and albumin between baseline and follow-up visit at 28 months in average. However, this was not the case for all the patients and we aimed to understand if the

baseline clinical features, baseline lung function and lung function change was different for patients with asthma that had clinically significant reduction or improvement in % SPA. Moreover, we sought to understand if levels of % SPA and % albumin predicted lung function decline. Interestingly, although not statistically significant, there were important differences between patients with a clinically significant improvement or decline in % SPA. Patients with decline in % SPA showed a trend for weight gain, higher frequency of exacerbations, worst asthma control and quality of life at baseline, greater lung function decline and no change/worsening of impulse oscillometric parameters linked to the small airway status. Furthermore, although we didn't detect a robust decline effect or interaction with time, mixed effect models applied in our study showed that impulse oscillometry indices of small airways dysfunction status, both area of reactance (AX) and frequency dependence of resistance (R5-R20) seemed to be affected by the baseline % of SPA and albumin, with individuals with higher levels of these proteins at visit 1 presenting improvement in both indices at follow-up visit. Likewise, FVC and FEV_1 appeared to decline at follow-up for individuals with lower baseline levels of SPA and both albumin and SPA are potentially good predictors of FVC decline.

Our results are important due to the novelty of the findings and possible applications in further studies and potentially in clinical settings. However, further studies, with larger and different cohorts, as well as further biomarker's exploitation from PExA are imperative for its establishment.

A major restriction to our study was the limited number of visits possible to conduct in the long-term repeatability, which would have benefit from extra time-points to assess lung function, thus leading to more robust results in the mixed effects models. Therefore, we were not powered to detect lung function decline with our population size. Nevertheless, no longitudinal data on PExA and lung function is available in the literature thus far, making our study unique and a starting point for further research.

In conclusion, we demonstrate that % SPA, % albumin and particles exhaled from PEx are variable amongst individuals, but stable over two weeks and three months within an individual, in both health and asthma, and could be predictor biomarkers of lung function decline, as well as targeted outcomes in interventional clinical trials. Further research would be beneficial to solidly establish the minimal clinically important

differences of PExA protein biomarkers in asthma and its role in small airways disease progression.

3.5 Evaluation of bronchodilator responses to inhaled fluticasone/formoterol in moderate to severe asthma using dynamic oxygen enhanced MRI

ABSTRACT

Background: The precise impact of bronchodilator on lung physiology and function is poorly understood. Here we sought to evaluate the impact of an inhaled aerosol with a high fine particle fraction using dynamic time resolved oxygen enhanced MRI (OE-MRI) biomarkers and airway physiological indices.

Methods: Sixteen adult asthmatics [GINA III-IV] with mild airflow limitation were recruited from Glenfield Hospital, Leicester, UK. On two separate visits, patients performed spirometry, multiple breath SF6 washout (MBW) and OE-MRI before and 30 minutes after two inhalations of flutiform [fluticasone/formoterol (250/10 µg)] via a spacer. OE-MRI image analysis was performed on 1.5 Tesla MRI scanner blind to inhaler sequence by Bioxydyn (Manchester, UK) with voxel-based quantification of a variety of imaging biomarkers. The study was powered to detect a significant change in ventilation heterogeneity markers of effective oxygen mixing time (Tvent), washout dynamics of ΔPO_2 (Tdown) and oxygen extraction into the blood phase (EoxFb).

Results: We identified a significant reduction in ΔPO_2 and ventilation/perfusion (V/Q) ratio ($p<0.05$) after flutiform administration. When patients were stratified according to MBW changes in conductive ventilation heterogeneity (Scond), patients with changes in Scond above the median improvement post flutiform demonstrated significant OE-MRI improvements in all ventilation heterogeneity imaging markers [wash-in dynamics of ΔPO_2 (Tup), Tdown and Tvent]. A number of OE-MRI imaging biomarkers were significantly associated with sputum eosinophilia, exacerbations and asthma symptoms.

Conclusion: OE-MRI biomarkers are sensitive to high fine particle fraction bronchodilators in asthma and associated with physiological measurements of ventilation heterogeneity and eosinophilic airway inflammation, warranting further evaluation as imaging biomarkers in asthma trials.

INTRODUCTION

Ventilation heterogeneity (VH) can be measured non-invasively using the single or Multiple breath gas washout (MBW) (190). Studies have demonstrated that small airway VH is associated with asthma control, exacerbations and response to inhaled therapy (163). However, the information obtained from functional physiological measurements is associated with limitations including lack of regional information in the lung on ventilation and lack of sensitivity to early VH.

Oxygen-enhanced magnetic resonance (OE-MR) imaging was originally proposed in 1996 as a technique for evaluation of regional ventilation using molecular oxygen as the contrast agent (192). When oxygen is exchanged between air in the alveoli and parenchymal tissue water and blood in the capillary beds, the oxygen does not only couple to haemoglobin but also dissolves as molecular oxygen in the blood plasma and tissue water (18). Since oxygen is paramagnetic, the dissolved molecular oxygen then shortens the T1 relaxation time, leading to a detectable signal change.

Some investigators have asserted the potential for clinical application of dynamic oxygen-enhanced MR imaging for evaluation of regional ventilation and oxygen, and demonstrated the significance of oxygen enhancement in normal volunteers and patients with obstructive small airway diseases such as asthma and COPD (204,206). In addition, McGrath *et al* have recently developed a novel physiological model of gas mixing and ventilation heterogeneity derived from dynamic OE-MRI data in asthma patients (205). The model describes a number of parameters associated with gas delivery and conduction in the large airways and associated diffusion and gas transfer across the alveolar capillary membrane in the small airways. It is therefore possible that OE-MRI could be used to study the response of the airways to bronchodilators with a broader penetration depth than conventional bronchodilators by assessing the ventilation heterogeneity as well as gas transport and perfusion using physiological models.

Fluticasone propionate/formoterol is an inhaled corticosteroids (ICS) and long-acting β-agonist (LABA) combination therapy (Flutiform®) used for asthma treatment, with reported symptoms and lung function benefits (323). Flutiform has a high fine particle fraction (FPF) formulation, meaning that a significant proportion of the drug particles are fine (<5μm) and more prone to deposit in the peripheral airway regions of the lung (324).

Here we sought to (i) evaluate the sensitivity of dynamic OE-MRI in assessing bronchodilator responses to flutiform, (ii) compare standard physiological bronchodilator responsiveness to OE-MRI bronchodilator responses and (iii) evaluate whether OE-MRI biomarkers are associated with patient outcomes in moderate to severe asthmatic patients.

METHODS

Study design

This study protocol was approved by the National Research Ethics Committee- East Midlands Leicester (approval number: UNOLE0491).

Figure 3.5.1 shows an outline of the three core study visits. At visit 1, after informed consent had been obtained, patients underwent clinical characterisation, blood sampling and a sputum induction.

At visits 2 & 3 patients had withheld all bronchodilator therapy for an appropriate duration (e.g., 4 hours for SABA, 12 hours for LABA). Pre-bronchodilator fractional exhaled nitric oxide testing, spirometry, MBW (visit 2) and OE-MRI (visit 3) was performed.

Immediately following the baseline lung function and OE-MRI imaging, patients were administered two inhalations of fluticasone/formoterol [250/10 μg] via a volumatic device, followed by the second (post-bronchodilator) lung function (spirometry and MBW) and OE-MRI scan (30 minutes post flutiform).

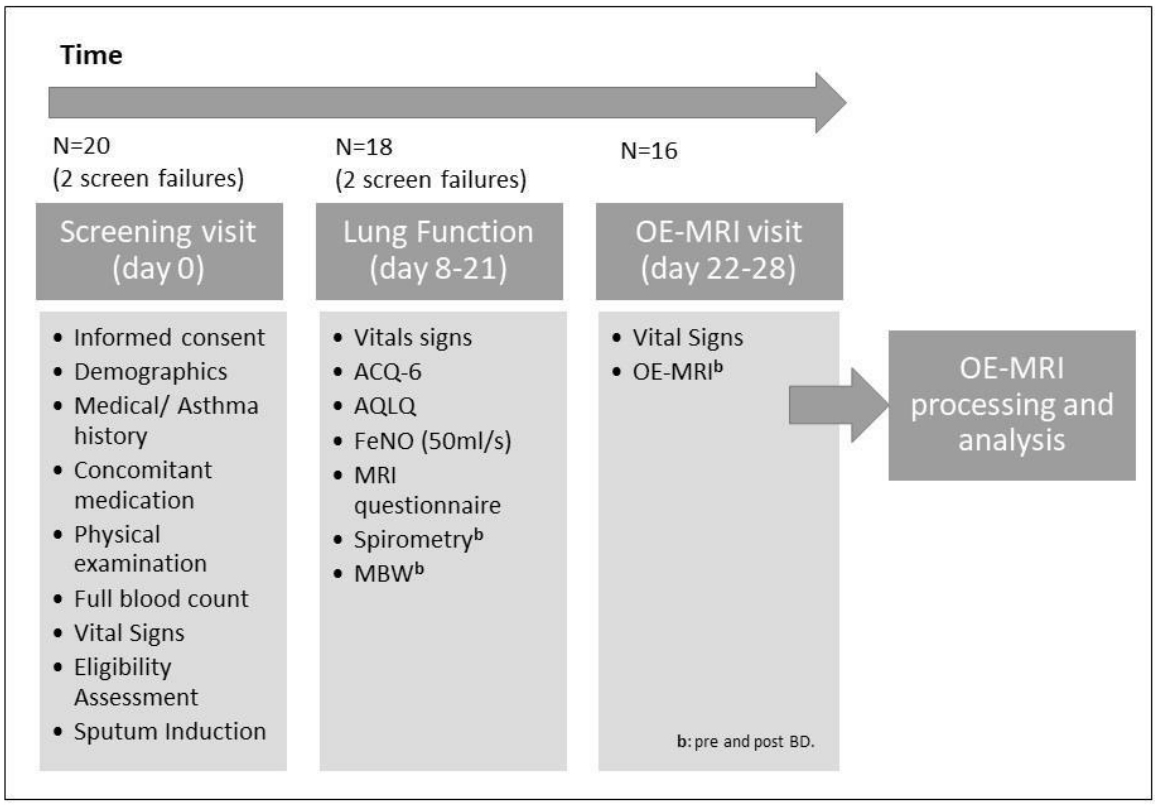

Figure 3.5.1: Diagram of the study design and visits. *Definition of Abbreviations*: FeNO: fraction of nitric oxide; ACQ-6: 6-point asthma control questionnaire; AQLQ: Asthma quality of life questionnaire; MBW: multiple breath washout test.

Study population

The study population included adult male and female patients with moderate-to-severe asthma (GINA III-IV), identified from a respiratory research database and the severe asthma clinic at Glenfield Hospital, Leicester, UK.

Inclusion criteria included a physician diagnosis of asthma and one or more of the following (i) $PC_{20} \leq 8$ mg/ml, (ii) bronchodilator reversibility $FEV_1 > 12\%/200$mls, (iii) Peak flow variability of $\geq 20\%$ over 2 weeks; documented spirometry showing post-bronchodilator FEV_1% predicted of $\geq 60\%$ and a FEV_1/FVC ratio of $< 70\%$.

Exclusion criteria included patients who had an exacerbation within the previous 6 weeks requiring oral steroids or antibiotics, taking concurrent leukotriene receptor antagonist therapy or Omalizumab in the previous 6 months, history of thermoplasty therapy, presence of non-reversible active lung disease, currently smokers or a pack year smoking history >10 pack years. Additionally, patients that did not fulfil the MRI safety questionnaire requirements were excluded.

Study investigations

Sputum was induced and assessed for differential cellular count (absolute numbers and percentages) and performed according to ATS/ERS criterion and as previously reported (309).

Spirometry was performed within the ATS/ERS recommendations (271) in the sitting position using a Vitalograph Alpha AL 21523 (Vitalograph, Maids Moreton, Buckingham, MK18 1SW). The spirometer was calibrated daily using a 3-L volume syringe.

MBW test was performed as described previously (140,154), using a modified photoacoustic INNOCOR (Innovision, Odense, Denmark) SF-6 gas analyser. Measurement were performed 2-3 times within visit to ensure that at least two functional residual volume (FRC) values were within 10% of each other (151). Several parameters were derived from the raw MBW data using custom MATLAB software [MATLAB 2015a, Natick, Massachusetts: The MathWorks Inc., 2015], including lung clearance index (LCI) and phase three slope derived measures of conductive (Scond) and acinar (Sacin) ventilation heterogeneity as previously reported (190).

FeNO was measured at flow rate of 50 mls/s following published guidelines on standardsed techniques for measuring exhaled nitric oxide by ATS and ERS (325).

Oxygen-enhanced MRI

Patients completed an MRI safety questionnaire at visit 2 as a pre-requisite to taking part in the OE-MRI. Detailed information on scanning procedures was provided in an imaging manual, which was followed by trained radiographers at Glenfield Hospital, Leicester, UK. On attendance for scanning, patients were supine on the MRI scanner bed and a disposable non-rebreathing mask was fitted for the duration of the scanning

session, in order to deliver medical air and 100 % oxygen, as required for OE-MRI. Patients were in continuous communication with radiographer staff throughout the scanning session and had a hand-held buzzer with which they were able to stop the scan at any time if needed.

Figure 3.5.2 shows the OE-MRI imaging acquisition processing and analysis pipeline. In summary, gas delivery was set to medical air at the start of the scanning session. Localiser scans and high-resolution image acquisitions were carried out, followed by a baseline T_1 measurement scan series. This was then followed by the dynamic OE-MRI series, during which the gas supply was switched between medical air (21% oxygen) and 100% oxygen. The total duration of the delivery of 100 % oxygen lasted no more than 15 minutes. After dynamic OE-MRI scan completion, the patient was removed from the scanner and the breathing mask removed. Each scanning session lasted no longer than 1 hour (combined pre and post flutiform imaging). **Figure 3.5.3** shows exemplar maps of pre and post flutiform images of a representative patient (A16) for three of the parameters analysed (delta PO_2, Tup, Tdown). The example shows a clear change in the regional heterogeneity and higher O_2 enhancement after bronchodilator.

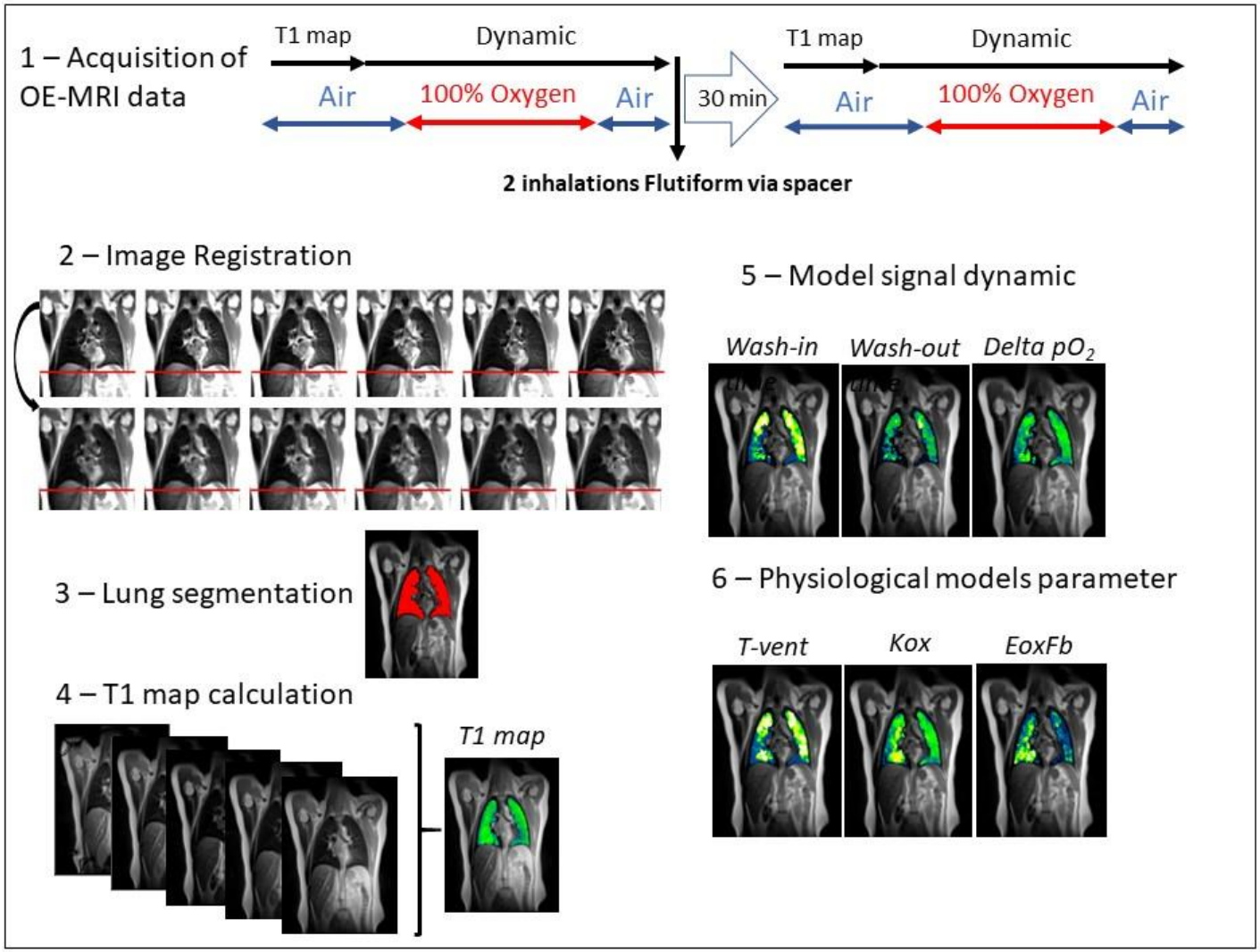

Figure 3.5.2: OE-MRI acquisition and processing pipeline.

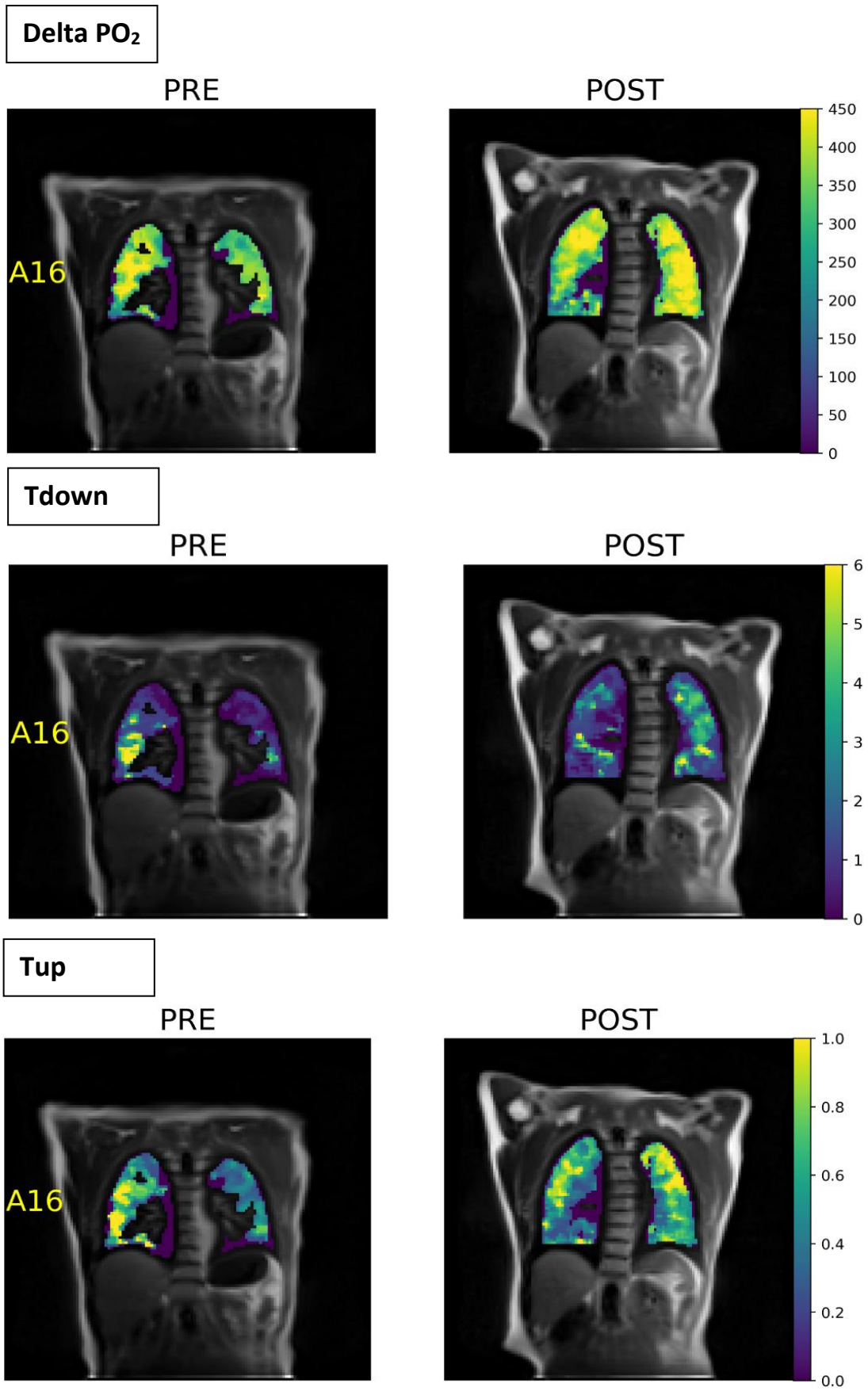

Figure 3.5.3: OE-MRI parameter maps for a representative patient (A16) pre and post flutiform.

OE-MRI processing and parameters

The images DICOM data and IAF were transferred to Bioxydyn electronically via the Internet Exchange Protocol (IEP) or, alternatively, via a courier if IEP was not available. Prior to DICOM image upload, all images were re-identified with a subject ID (no personal identifiable information). Time was removed and coded with "x" and "y", to keep the image analyst at Bioxydyn blinded to patient and scan sequence.

After an initial QC, data analysis was performed using software written in MATLAB (MATLAB, The MathWorks Inc, Natrick, MA, USA) by Bioxydyn specialists. In summary, images were corrected for respiratory motion and registered to end-expiration. T1 voxel maps were converted into dynamic maps of ΔPO_2, oxygen wash-in time (Tup) and wash-out time (Tdown), providing information about regional ventilation. A computational compartmental model developed previously (205) was used to provide information about the delivery and transport of oxygen through the model parameters Tvent (time for oxygen delivery via the conducting airways), Kox (rate of oxygen diffusion) and EoxFB (extraction of oxygen multiplied by blood flow).

The final reports provided by Bioxydyn contained a table with the summary of each parameter statistics [mean (SD), median, IQR-lower, IQR- upper) for the whole lung and an image output for each parameter.

Statistical Methods

The study was designed to achieve 80% power to detect a minimal clinically important difference at a two-tailed 5% significance level for the parameters Tvent, Tdown and EoxFb. Statistical analysis including linear regressions and negative binominal analysis was performed using Prism 7 (GraphPad Software Inc., La Jolla, CA, USA), SPSS 24 (IBM Corporation, Somers, New York, USA) and SAS 9.4 (SAS Institute Inc., Cary, NC, USA.). Comparisons between pre and post flutiform were performed using paired parametric t-test for parametric data and Wilcoxon test for non-parametric data. A p-value of <0.05 was taken as the threshold for statistical significance.

Results

Table 3.5.1 and **figure 3.5.1** show a summary of the population clinical characteristics and study procedures. A total of 20 patients were screened but only 16 were included in the study (2 patients screen failed because they were unable to perform MBW, 1 patient was on oral steroids and a further patient had no objective physiological evidence of asthma).

Our population (8 male/8 female) were mainly on GINA step IV treatment (medium to high dose ICS, including severe asthmatics). The majority were never smokers. The population demonstrated a mean ACQ-6 >1 unit indicative of suboptimal asthma control and mean (SD) bronchodilator reversibility of 258 (225) mls and 12 (11) %.

Table 3.5.1: Demographic and Clinical Characteristics

Study ID	**Age**	**Sex**	**Smoking**	**Atopy (yes=1,no=0)**	**GINA step**	**Prescribed ICS dose µg/day (BDP equivalent)**	**Exacerbations (in the previous year)**	**FEV_1 % pred[a]**	**FEV_1/FVC[a]**	**FEV_1/FVC > LLN[a] (Y/N)**	**Reversibility (FEV_1 diff mls, %)**	**Sputum eosinophils (%)**	**ACQ-6**	**AQLQ**
A07	62	M	N,0	1	IV	800	0	80	0.69	Y	650, 25	5.5	1.30	4.87
A08	51	M	N, 0	0	IV	800	0	63	0.57	N	190, 11	0.5	1.00	5.91
A09	69	M	N, 0	1	IV	800	1	63	0.55	N	280, 18	4.5	1.30	6.33
A11	59	M	X, 6	1	IV	800	0	92	0.71	Y	500, 17	2.25	0.67	6.54
A12	64	M	N, 0	1	IV	800	0	88	0.70	Y	180, 7	0	0.83	6.41
A13	67	F	N, 0	1	IV	800	1	67	0.71	Y	0, 0	5.25	0.33	6.56
A14	55	F	N, 0	1	IV	800	1	95	0.75	Y	0, 0	0	1.17	4.04
A15	63	M	N, 0	1	III	400	0	81	0.60	N	330, 15	0	0.17	6.89
A16	40	F	N, 0	1	IV	800	2	86	0.65	N	260, 13	0	4.00	2.37
A17	65	F	N, 0	1	IV	800	0	96	0.66	Y	240, 13	2	2.67	5.31
A19	43	F	N, 0	1	IV	800	1	89	0.72	Y	240, 9	5	1.33	4.69
A20	46	M	X, 5	0	IV	800	0	69	0.62	N	940, 44	29.25	1.33	6.48
A23	65	F	N,0	0	IV	1000	0	61	0.61	N	160, 11	-	0.67	5.30
A24	61	F	X,1	0	IV	1600	0	81	0.64	N	20, 3	5.75	1.17	6.22
A25	64	M	N, 0	1	III	400	0	81	0.68	N	140, 5	-	1.17	6.67
A26	62	F	N,0	0	IV	1600	4	49	0.51	N	0, 0	2.5	1.83	6.02
Mean (SD)	58 (9)	-	-	-	-	862 (324)	0.62 (1.05)	78 (1.4)	0.65 (0.07)	-	258 (255), 12 (11)	2.37 (0;5.3)[#]	1.31 (0.92)	5.66 (1.20)

Definition of Abbreviations: GINA: Global initiative for asthma; ICS: inhaled corticosteroid; FeNO: fraction of nitric oxide; FEV_1: Forced expiratory volume in one second; FVC: Forced vital capacity; LLN: Lower limit of normal; ACQ-6: 6-point asthma control questionnaire; AQLQ: Asthma quality of life questionnaire. a: post bronchodilator, based on Global Lung Initiative (GLI) equations. #median (Q1;Q3).

Change in physiological and OE-MRI parameters post flutiform are shown in figure **3.5.4** and **Table 3.5.2**, respectively. FEV_1 showed a significant improvement after flutiform, even for patients with partial reversibility. There was a non-significant trend for improvement in Scond (p=0.133) and Sacin (p=0.106) parameters (not shown). ΔPO_2 demonstrated a significant reduction post flutiform (p=0.006, -11% change), as well as V/Q ratio (p=0.014, -16% change). Tup, Tdown and Tvent and Kox also demonstrated non-significant trends for reduction. No significant changes were found in the compartmental model parameter EoxFB.

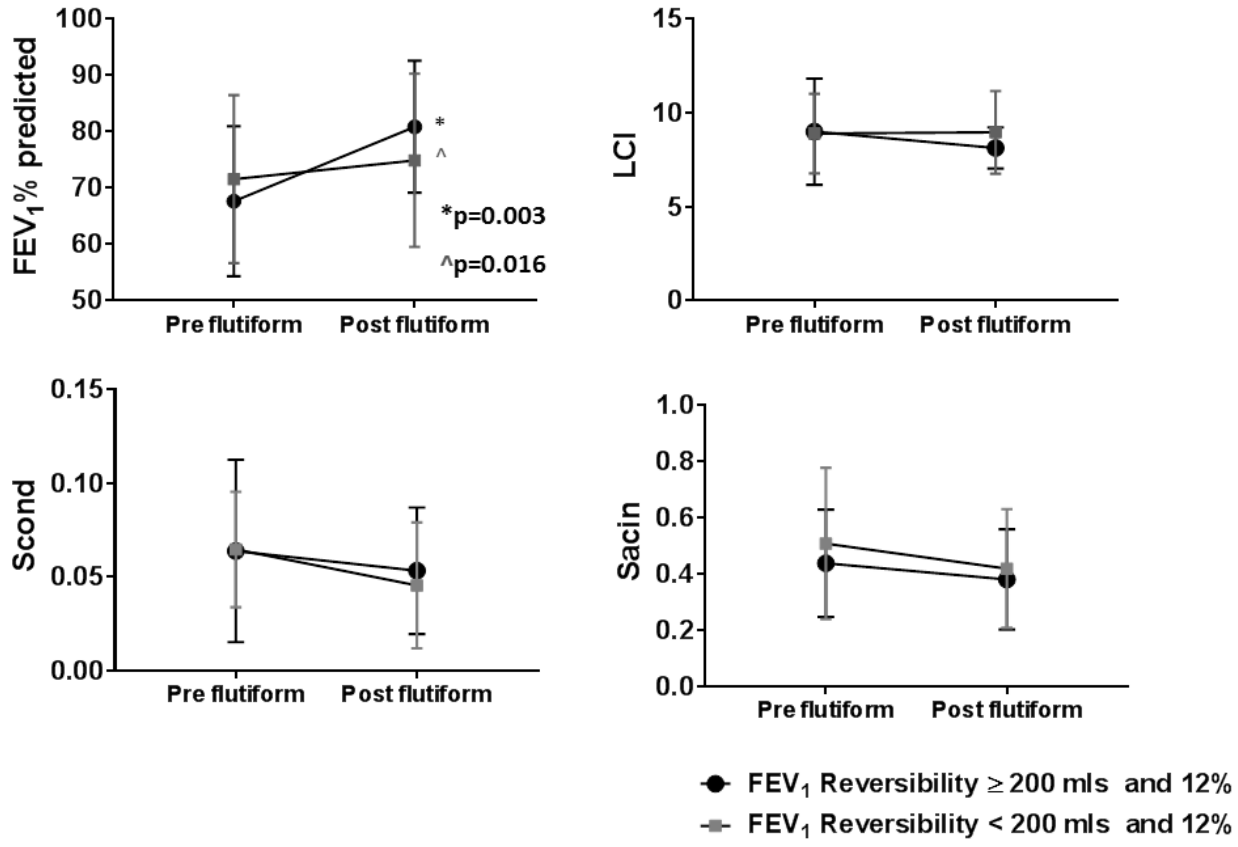

Figure 3.5.4: Physiological parameters pre and post flutiform administration. Paired t-test p-values are showed for FEV_1 (* bronchodilator responders, ^ partial bronchodilator responders). *Definition of abbreviations*: FEV_1: Forced expiratory volume in one second; LCI: Lung clearance index; Scond (conductive ventilation heterogeneity); Sacin (acinar ventilation heterogeneity).

Table 3.5.2: Oxygen-Enhanced MRI outcomes pre and post flutiform

	Pre flutiform	**Post flutiform**	**Change (Post-Pre)**	**p value**
ΔPO_2 (mmHg)	375 (325; 398)	323 (244; 382)	-35.94 (-74.92; 4.96)	**0.006**
Tup (min)	0.76 (0.62; 1.25)	0.76 (0.56; 0.88)	-0.18 (-0.44; 0.07)	0.058
Tdown (min)	1.29 (1.17; 1.69)	1.27 (1.08; 1.43)	-0.16 (-0.77; 0.18)	0.171
Tvent[a] (s)	53.3 (47.6; 60.2)	50.0 (37.2; 55.9)	-2.76 (-7.94; 0.31)	0.051
Kox[a] (ml O_2/s/ml lung)	0.67 (0.52; 0.73)	0.56 (0.41; 0.68)	-0.02 (-0.20; 0.02)	0.065
EoxFB[a] (ml blood/s/ml lung)	22.5 (18.5; 29.7)	19.7 (18.1; 22.7)	-2.32 (-8.06; 1.52)	0.231
V/Q (ratio)	0.10 (0.09; 0.12)	0.09 (0.07; 0.11)	-0.02 (-0.02; 0.00)	**0.014**
Max delta change (%)	18.5 (13.5; 21.0)	16.9 (11.0; 18.5)	-1.04 (-5.19; 1.49)	0.117
Ventilation (ml O_2/min/ml lung)	0.65 (0.47; 0.78)	0.61 (0.49; 0.75)	-0.02 (-0.21; 0.14)	0.342
Perfusion (ml blood/min/ml lung)	5.63 (3.69; 6.99)	5.89 (4.67; 6.73)	0.62 (-0.63; 2.13)	0.211

Values expressed as median (Q1; Q3). p value derived from Wilcoxon paired rank test. **a:** parameters derived from McGrath model. *Definition of abbreviations*: ΔPO_2: changes in O_2 partial pressure; Tup: O_2 wash-in time; Tdown: O_2 wash-out time; Tvent: time for O_2 delivery via the conducting airways; Kox: rate of O_2 diffusion; EoxFB: extraction of O_2 multiplied by blood flow; V/Q: ventilation-perfusion ratio.

Figures 3.5.5 and 3.5.6 present OE-MRI ventilation heterogeneity biomarkers (Tup, Tdown and Tvent) pre and post flutiform in two exemplar patients (A11 and A23). The first patient (A11) showed a concordant improvement in both FEV_1 (500mls, 17 %) and the ventilation heterogeneity marker Scond (-0.016 units, -70 %). It can be seen that for all three OE-MRI ventilation heterogeneity biomarkers there is an improvement post flutiform with a leftward shift for the individual voxel-based histograms for each of the three biomarkers indicative of reduce heterogeneity.

In contrast (as seen in **Figure 3.5.6**), patient A23 demonstrated a bronchodilator response that is lower than the ATS/ERS criterions (180 mls and 11%) and a concurrent worsening of Scond (+ 0.057 units, +90 %). It can be seen from the OE-MRI images and voxel-based histograms that the administration of flutiform lead to a deterioration in all three ventilation heterogeneity markers and rightward shift and widening of the histograms for all three markers indicative of increased ventilation heterogeneity.

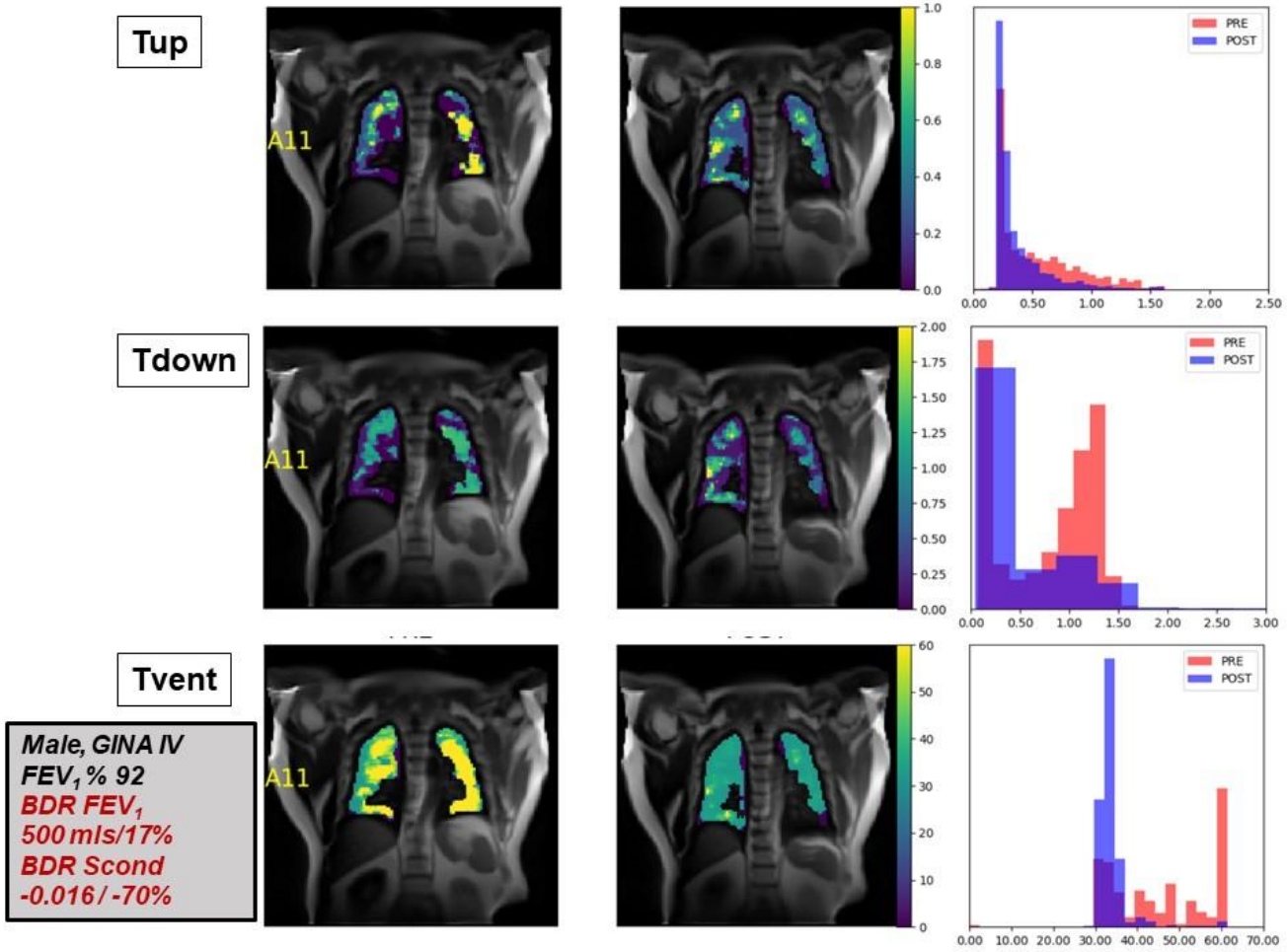

Figure 3.5.5: **Tup (wash-in), Tdown (washout) and T vent (time for O_2 delivery through the conducting airways) OE-MRI parameters for an exemplar patient (A11, male, 59) with a large FEV_1 and concurrent Scond (conductive ventilation heterogeneity) improvement post flutiform.**

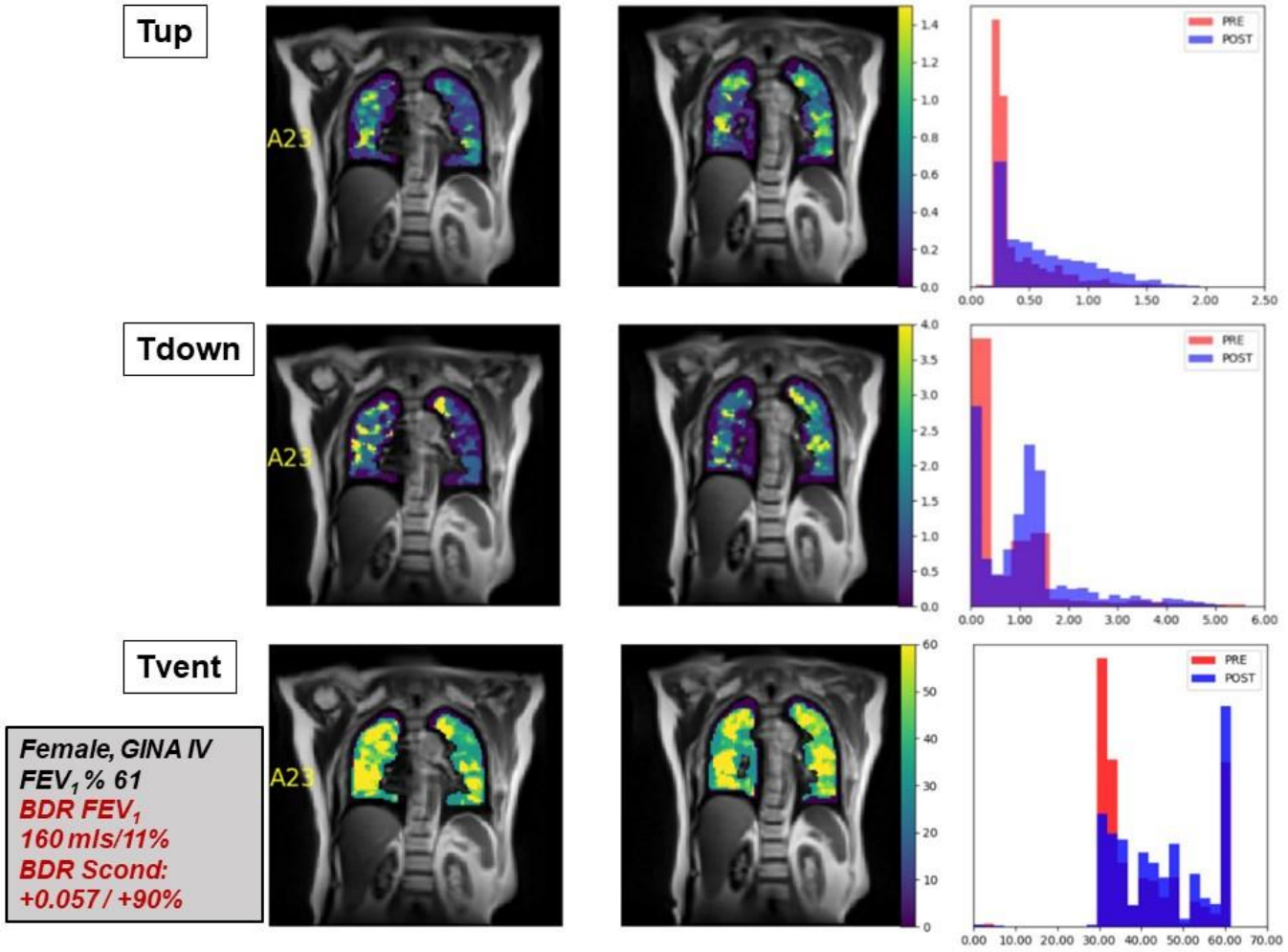

Figure 3.5.6: Tup , Tdown and Tvent (time for O_2 delivery through the conducting airways) OE-MRI parameters for an exemplar patient (A23, Female, 65) with post flutiform FEV_1 change that is less than the minimal clinically important improvement and a deterioration in Scond (conductive ventilation heterogeneity) post flutiform.

In view of the dichotomisation of OE-MRI responses when stratified by Scond bronchodilator response in the two patients exemplified in **Figures 3.5.5 and 3.5.56** we sought to explore whether patients with an Scond change post flutiform ≥ median change (-0.022) demonstrated different OE-MRI imaging responses to patients with an Scond change post flutiform less than the median (**Table 3.5.3)**.

There was clear evidence in patients with a change (improvement) in Scond above median after flutiform and of statistically significant changes in, Tvent, Tdown, Tup, V/Q ($p < 0.05$) and a non-statistically significant trend for ΔPO_2. No significant changes were found in the OE-MRI parameters in patients with Scond changes below the median (worsening). Additionally, dichotomisation of bronchodilator responses based upon acinar ventilation heterogeneity (Sacin) and global ventilation heterogeneity (LCI) did not yield a similar dichotomisation of OE-MRI indices of ventilation heterogeneity or V/Q (**table 3.5.4 and 3.5.5**).

Table 3.5.3: Change in median OE-MRI parameters and change in Scond

	Scond change above median (n=8) **(p value)**	**Scond change below median (n=8)** **(p value)**
Scond change	-0.032 (-0.57; 0.029) (0.002)	-0.002 (-0.049; 0.013) (0.469)
FEV_1 change (ml, %)	215 (117; 372), 7 (4; 11) (0.016)	250 (40;457), 10 (1.5;13) (0.031)
Change ΔPO_2 (mmHg)	-40.4 (-115.5; 4.96) (0.055)	-35.9 (-64.7; 17.8) (0.078)
Change Tvent (s)[a]	-6.28 (-10.84;-1.01) (**0.023**)	-1.19 (-6.69; 5.53) (0.844)
Change Tdown (min)	-0.52 (-1.18; -0.16) (**0.016**)	0.14 (-0.29; 0.53) (0.641)
Change Tup (min)	-0.18 (-0.39; -0.04) (**0.039**)	-0.18 (-0.44; 0.29) (0.461)
Change EoxFB (ml blood/s/ml lung)[a]	-2.08 (-10.89; 1.52) (0.383)	-2.32 (-8.06; 3.32) (0.641)
Change Kox (ml O_2/s/ml lung)[a]	-0.10 (-0.26; 0.03) (0.148)	0 (-0.16; 0.01) (0.406)
Change V/Q (ratio)	-0.01 (-0.03; 0.00) (0.094)	-0.02 (-0.02; 0.01) (0.187)

Values expressed as median change (Q1;Q3) Post-Pre flutiform. p values derived from Wilcoxon paired rank test. **a:** parameters derived from McGrath model. *Definition of abbreviations*: Scond: Conductive ventilation heterogeneity; ΔPO_2: changes in O_2 partial pressure; Tup: O_2 wash-in time; Tdown: O_2 wash-out time; Tvent: time for O_2 delivery via the conducting airways; Kox: rate of O_2 diffusion; EoxFB: extraction of O_2 multiplied by blood flow; V/Q: ventilation-perfusion ratio.

Table 3.5.4: Change in median OE-MRI parameters and change in Sacin

	Sacin change above median (n=8) **(p value)**	**Sacin change below median (n=8)** **(p value)**
Sacin change	0.116 (0.037; 0.363) (0.008)	0 (-0.077; 0.007) (0.641)
FEV_1 change (ml, %)[#]	150 (0; 275), 5 (0; 10) (0.062)	240 (182-457); 9 (6-13) (0.008)
Change ΔPO_2 (mmHg)	-48.9 (-112.4; 27.3) (0.109)	-30.99 (-72.64; -15.99) (**0.023**)
Change Tvent (s)	-1.43 (-7.94; 3.34) (0.461)	-4.93 (-10.77; -0.48) (0.055)
Change Tdown (min)	0.02 (-0.06; 0.53) (0.812)	-0.34 (-1.16; -0.01) (**0.039**)
Change Tup (min)	-0.05 (-0.34; 0.08) (0.461)	-0.31 (-0.46; 0.03) (0.078)
Change EoxFB (ml blood/s/ml lung)[a]	0.02 (-8.99; 1.20) (0.641)	-4.42 (-6.91; 4.32) (0.461)
Change Kox (ml O_2/s/ml lung)[a]	-0.07 (-0.20; 0.02) (0.297)	-0.02 (-0.25; 0.01) (0.219)
Change V/Q (ratio)	-0.02 (-0.02; 0) (0.187)	-0.01 (-0.03; 0) (0.094)

Values expressed as median change (Q1;Q3) Post-Pre flutiform. p values derived from Wilcoxon paired rank test. **a:** parameters derived from McGrath model. *Definition of abbreviations*: Sacin: acinar ventilation heterogeneity; ΔPO_2: changes in O_2 partial pressure; Tup: O_2 wash-in time; Tdown: O_2 wash-out time; Tvent: time for O_2 delivery via the conducting airways; Kox: rate of O_2 diffusion; EoxFB: extraction of O_2 multiplied by blood flow; V/Q: ventilation-perfusion ratio.

Table 3.5.5: Change in median OE-MRI parameters and change in LCI

	LCI change above median (p value) (n=8)	**LCI change below median (p value) (n=8)**
LCI change	-0.55 (-2.22; -0.21) (0.008)	0.37 (0.16; 0.87) (0.008)
FEV_1 change (ml, %)[#]	235 (145;570), 8 (5;15) (0.016)	210 (12;255), 6 (0.6;11) (0.031)
Change ΔPO_2 (mmHg)	-25.42 (-64.7; 4.96) (0.109)	-46.62 (-115.40; 5.05) (**0.039**)
Change Tvent (s)	-2.76 (-7.77; 0.05) (0.195)	-3.78 (-10.84; 3.16) (0.148)
Change Tdown (min)	-0.25 (-1.04; 0.13) (>0.195)	-0.07 (-0.61; 0.22) (0.641)
Change Tup (min)	-0.21 (-0.39; 0) (0.195)	-0.09 (-0.49; 0.10) (0.312)
Change EoxFB (ml blood/s/ml lung)[a]	-2.35 (-8.99; 1.52) (0.312)	-2.08 (-6.91; 3.32) (0.547)
Change Kox (ml O_2/s/ml lung)[a]	0.01 (-0.16; 0.03) (0.578)	-0.10 (-0.26; 0) (0.109)
Change V/Q (ratio)	-0.01 (-0.02; 0) (0.375)	-0.02 (-0.03; 0) (**0.031**)

Values expressed as median change (Q1;Q3) Post-Pore flutiform. p values derived from Wilcoxon paired rank test. **a:** parameters derived from McGrath model. *Definition of abbreviations*: LCI: lung clearance index; ΔPO_2: changes in O_2 partial pressure; Tup: O_2 wash-in time; Tdown: O_2 wash-out time; Tvent: time for O_2 delivery via the conducting airways; Kox: rate of O_2 diffusion; EoxFB: extraction of O_2 multiplied by blood flow; V/Q: ventilation-perfusion ratio.

Table 3.5.6 shows the change in the OE-MRI parameters according to the airway inflammation status: high sputum eosinophils (>1.9%) and normal sputum eosinophils (<1.9%) (326). There was a significant change in ΔPO_2, Tvent, EoxFb and V/Q in the high eosinophils group following the administration of flutiform, with smaller improvements in Tvent and larger improvements in Kox, V/Q and ΔPO_2 in comparison to patients without a significant sputum eosinophilia. Moreover, patients with high sputum eosinophil counts had higher Scond values [0.047 (0.040; 0.063) vs 0.075 (0.022-0.102), pre BD, respectively].

Furthermore, two negative binomial models were generated, both with exacerbations in the previous year as dependent variable, and independent variables as sputum eosinophils and ΔPO_2 (model 1) and sputum eosinophils and V/Q (model 2) (**see table 3.5.7**). Increased ΔPO_2 (pre-bronchodilator) was significantly associated with an increased risk of exacerbations and increased V/Q (pre-bronchodilator) was also significantly associated with increased risk of exacerbations (for an increase of 0.01 in V/Q, number of exacerbations increased by approximately 2 per year). In addition, a linear regression model with ACQ-6 as dependent variable (**table 3.5.8)** and pre-bronchodilator FEV_1, ΔPO2 and V/Q as independent variables (spearman correlations: $p<0.1$) was generated. This model revealed that the independent parameters pre-bronchodilator ΔPO_2 and V/Q were also strongly associated with asthma control. These results lead us to speculate that OE-MRI parameters are not only related with exacerbation frequency but also clinical outcomes.

Table 3.5.6: Change in median OE-MRI parameters according to sputum Eosinophils

	Eosinophils <1.9% (n=5)	**Eosinophils >1.9% (n=9)**
FEV_1 change (ml, %)	190 (90; 295), 6 (3; 10) (0.125)	240 (25; 575), 10 (1; 15) (0.016)
Scond change	0.031 (0.004; 0.03) (0.125)	0.016 (-0.018; 0.056) (0.261)
Change ΔPO_2 (mmHg)	-26.7 (-92.3; 10.2) (0.312)	-61.3 (-103.6; -29.7) (**0.008**)
Change Tvent (s)[a]	-6.10 (-6.61; 1.51) (0.187)	-3.76 (-13.62; -0.66) (**0.039**)
Change Tdown (min)	-0.16 (-1.84; 0.66) (0.437)	-0.34 (-0.75; 0.17) (0.250)
Change Tup (min)	-0.40 (-0.65; 0.03) (0.187)	-0.21 (-0.42; 0.05) (0.129)
Change EoxFB (ml blood/s/ml lung)[a]	0.42 (-10.97; 2.91) (>0.999)	-6.21 (-8.78; 2.85) (0.250)
Change Kox (ml O_2/s/ml lung)[a]	0.00 (-0.25; 0.06) (0.625)	-0.15 (-0.25; 0.01) (**0.039**)
Change V/Q (ratio)	0.00 (-0.03; 0.01) (0.500)	-0.02 (-0.02; -0.01) (**0.012**)

Values expressed as median change (Q1;Q3) Post-Pre flutiform. p values derived from Wilcoxon paired rank test. * median (Q1;Q3), pre and post flutiform. Patients A23 and A25 excluded (no sputum obtained). **a:** parameters derived from McGrath model. *Definition of abbreviations*: FEV1: Forced expiratory volume in the first second; Scond: Conductive ventilation heterogeneity; ΔPO_2: changes in O_2 partial pressure; Tup: O_2 wash-in time; Tdown: O_2 wash-out time; Tvent: time for O_2 delivery via the conducting airways; Kox: rate of O_2 diffusion; EoxFB: extraction of O_2 multiplied by blood flow; V/Q: ventilation-perfusion ratio.

Table 3.5.7: Negative binomial models of exacerbations and OE-MRI parameters

	Estimate	Standard error	Z value	Pr (>|z|)
Model 1- ΔPO_2				
Intercept	-8.603	4.293	-2.004	**0.045**
$\Delta PO_{2\ (pre\ BD)}$	0.023	0.011	2.032	**0.042**
Sputum eosinophils	-0.264	0.220	-1.196	0.232
Model 2- V/Q				
Intercept	-7.123	3.094	-2.303	**0.021**
$V/Q_{\ (pre\ BD)}$	0.660	0.271	2.432	**0.015**
Sputum eosinophils	-0.150	0.146	-1.032	0.302

Model 1: dependent variable: number of exacerbations; independent variables: sputum eosinophils and ΔPO_2; Model 2: dependent variable: number of exacerbations; independent variables: sputum eosinophils and V/Q. *Definition of abbreviations:* Estimate: regression coefficient; ΔPO_2: changes in O_2 partial pressure; V/Q: ventilation-perfusion ratio; BD: bronchodilator.

Table 3.5.8: Multiple linear regression analysis using ACQ-6 as dependent variable

Independent variables	Estimate	p value	Lower 95% CI	Upper 95% CI
$FEV_1/FVC_{(pre\ BD)}$	-2.940	0.360	-9.711	3.831
$\Delta PO_{2\ (pre\ BD)}$	-0.270	0.037	-0.052	-0.002
exacerbations	-0.960	0.695	-0.623	0.430
$V/Q_{(pre\ BD)}$	123.42	0.019	24.51	222.33

Dependent variable: ACQ-6; level of significance at $p<0.05$; Constant term: 0.568. R^2: 0.534. *Definition of abbreviations*: Estimate: regression coefficient; CI: confidence interval; FEV_1: Forced expiratory volume in the first second; FVC: Forced vital capacity; ΔPO_2: changes in O_2 partial pressure; V/Q: ventilation-perfusion ratio.

DISCUSSION

We have performed the larger study to date evaluating dynamic OE-MRI in moderate to severe asthma patients and furthermore have used flutiform, an inhaled aerosol with a high fine particle fraction, to explore the impact of bronchodilators on ventilation heterogeneity and ventilation perfusion relationships in the lung.

Significant preliminary observations from our study include a consistent drop in ΔPO_2 following flutiform administration, suggesting an increased extraction of oxygen from the lungs that was superior than the additional ventilation triggered by the bronchodilator. Secondly, the multiple breath washout marker of conductive airway ventilation heterogeneity Scond appears to better stratify OE-MRI imaging response of ventilation heterogeneity than spirometry defined reversibility. Finally, we demonstrated that a number of OE-MRI parameters appear to be associated with the presence of eosinophilic airway inflammation, asthma exacerbations and clinical outcomes.

Our study is therefore important as it demonstrates that OE-MRI may have the potential to be utilised as imaging biomarkers in clinical trials of bronchodilators and potentially anti-inflammatory compounds in moderate to severe asthma. The smaller sample sizes required for OE-MRI endpoints when compared to clinical endpoints such as exacerbations events render the imaging biomarkers as potential tools in early phase clinical trials.

The OE-MRI technique also has clear advantages when compared to HRCT scanning or $^{3}He/\ ^{129}Xe$ hyper polarised gas MRI: no use of ionising radiation or expensive gas, gas polarisers/deployable in most standard NHS clinical sites. OE-MRI can also be easily setup, requiring only 100% oxygen, which is available in any radiology department. We therefore speculate that OE-MRI has the potential, if further validated, to become a valuable imaging biomarker in asthma clinical trials.

Zhang and colleagues have recently conduct a pilot study with 10 patients with asthma performing OE-MRI on two occasions, one month apart (191). They found that OE-MRI imaging is feasible and reproducible in asthma. Moreover, enhancing fraction (an analogue of ΔPO_2) was smaller in asthmatics. The same group reported prolonged wash-in and washout of 100% oxygen in the lung (Tup and Tdown), reflective of ventilation

heterogeneity in asthma. In our study, we observed an important trend for Tup and Tdown reduction after bronchodilator, specifically for patients with significant improvements in the flow-dependent ventilation heterogeneity (Scond), but not for patients with improved Sacin and LCI. The results would suggest that formoterol improves ventilation heterogeneity – an effect that may have been achieved as a consequence of the high fine particle fraction of the drug within flutiform. However, this assertion would require direct comparison on inhaled bronchodilators with and without a high fine particle fraction to fully elucidate.

Verbanck *et al* have also reported partial improvement of conductive airways ventilation heterogeneity with inhaled salbutamol in asthma (162), suggesting that small conducting airways are only partially sensitive to salbutamol. Our observations with OE-MRI biomarkers of ventilation washout (Tdown, Tup and Tvent) would suggest that Scond reversibility is a useful physiological marker of patients that will achieve an improvement in ventilation heterogeneity measured with OE-MRI imaging. As such, our study is a form of validation of Scond as a simple biomarker of spatial heterogeneity in the small airways and the subsequent response to a bronchodilator.

Two additional observations of interest in our study were the overall decrease in ΔPO_2 and V/Q following the administration of flutiform. Morgan *et al* demonstrated a similar pattern in COPD patients, in response to budesonide/formoterol (20). Our study replicates these observations in asthma. Furthermore, the observation that V/Q is reduced in eosinophilic asthma patients post flutiform, coupled with the fact that there was a trend for V/Q reduction in patients with a high Scond in our study provides the intriguing hypothesis that eosinophilic inflammation within the small airways may reduce lung ventilation disproportionately to perfusion following the administration of a bronchodilator. Interestingly, the Scond parameter was overall higher in the group of patients with higher eosinophils, which again supports this hypothesis. The hypothesis is supported further by the observed significant reduction in Kox (oxygen diffusion in the small airways) post flutiform in eosinophilic patients. This may explain the lack of physiological response to bronchodilators in some patients with acute asthma exacerbations and requires further study with OE-MRI imaging and parallel biopsy studies in asthma to fully confirm however.

We failed to observe any significant overall change in the alveolar diffusion and oxygen extraction parameters from the McGrath model Kox and EoxFB. However, unlike COPD patients that have compromised O_2 extraction across the alveolar-capillary membrane, patients with asthma have preserved pulmonary perfusion as evidence by typically supranormal carbon monoxide diffusion coefficients KCO (140), which might explain the lack of signal.

There are a number of limitations to our study. Firstly, our population was limited to 16 individuals due to the exploratory nature of our study, and therefore, larger trials are now needed using OE-MRI biomarkers. Nonetheless despite the small sample sizes significant changes in a number of OE-MRI imaging biomarkers were seen when stratified by Scond change.

Secondly, our intervention was not placebo controlled or blinded and the study was open label. As a consequence, the observation reported although intriguing should be confirmed in placebo controlled blinded intervention studies.

Thirdly, we did not explore the impact of the anti-inflammatory component of flutiform (fluticasone), as this would have required further imaging after a longer time period (e.g. three months). Further studies are therefore required to explore the impact of inhaled steroids on the OE-MRI biomarkers that appear to change significantly post bronchodilator in patients with a significant sputum eosinophilia. Moreover, our analysis was only focused on whole lung parameters and perhaps detailed regional investigations (e.g. upper, lower, left, right regions) would bring further clarifications.

In conclusion, our study demonstrated for the first time that OE-MRI can be utilised to assess bronchodilator responses to ventilation heterogeneity in moderate to severe asthma and that OE-MRI imaging biomarker bronchodilator responses appear to be associated with both eosinophilic inflammation and the conductive airway ventilation heterogeneity marker Scond. Larger studies are now required to assess the impact of anti-inflammatory asthma therapies and bronchodilators in asthma using OE-MRI.

4. Conclusions

4.1 Summary of Findings

Having established the importance of assessing the small airways compartment in obstructive diseases such as asthma, the purpose of this thesis was to further investigate the physiology of the small airways disease and dysfunction in adult asthma, which is believed to cause disease persistency and exacerbations. This overall aim was approached by further exploring and validating novel and non-invasive tools targeting the peripheral airways, in order to progress the state of art in the field.

Despite its increasing popularity in the last few years, forced oscillation techniques (FOT) are still a research reality rather than clinical, lacking validation and robust reference values. FOT yields a large amount of data, however, our research focus was to study abnormally increased resistance at 5 Hz minus Resistance at 20 Hz (R5-R20), a feature that has been shown to relate with small airways dysfunction in asthma. Therefore, our first study aimed to evaluate its clinical importance. We were able to derive important results: our clinical population study identified clinical important sub-groups of patients with elevated R5-R20 values in asthma, with abnormal but also preserved spirometry, with higher number of exacerbations and poorer asthma control and quality of life. Consequently, our results revealed an important disease phenotype, supporting IOS as a small airways dysfunction detection tool in asthma. Furthermore, we investigated lung function decline and its relationship to R5-R20 parameter in a sub-study cohort of patients. Although not powered to detect changes and interaction with time, we identified an association between baseline R5-R20 and FEV_1 decline, but further research is needed to address this interesting finding further.

Next, our aim was to compare two commercialised devices to measure lung impedance: impulse oscillometry system (IOS) and TremoFlo FOT (Thorasys), using a large clinical population and two models, one for resistance and one for reactance. Our results showed that resistance measurements are dissimilar between devices, and a significant bias was demonstrated with the reactance measurements: the TremoFlo device recorded more negative reactance values when compared to IOS. The two models, printed airway resistance and standardised volume reactance confirmed the observations in patients. These findings highlight the need for further standardisation across FOT measurement devices, in order to effectively apply this useful measurement in larger clinical

population studies, across different sites. Moreover, further standardisation studies with populations should explore and account for the bronchodilator response and models should account for the branching structure of the airways, as well as presence of air.

In our next study we utilised a novel method to sample protein particles from the airway surfactant in exhaled breath, the PExA method, with a standardised breathing manoeuvre. These particles are believed to arise from the peripheral airways and we sought to explore the possibility of applying this method in severe asthma and PEx (PExA derived material) proteins, as well as explore associations with clinical outcomes and lung physiology measurements. We have shown for the first time that PExA sampling method is feasible in severe asthma and that enough quantities of PEx can be sampled to allow protein biomarker analysis. We have demonstrated that lower % of surfactant protein A (SPA) and albumin values from PEx are associated with small airways abnormalities and poorer asthma control and quality of life outcomes, by means of physiological indices captured by impulse oscillometry, multiple breath washout and spirometry and statistical phenotyping with topological data analysis (TDA).

The variation of PExA material, both overall particle numbers and protein contents, between individuals, intra-individuals and over different periods of time has not been explored to date. Therefore, our next novel study dealt with intra and between visit, short and long-term repeatability of protein biomarkers. We found that SPA and albumin exhibited good within and short-term between-visit agreement. Our long-term PExA follow-up study suggests that baseline levels of protein and albumin influence lung function change over time. As an example, higher levels of SPA led to lower changes in R5-R20 and improvement in FVC, despite the lack of significant interactions between time and % SPA and % albumin. These findings not only suggest that PExA biomarkers are stable and could be used in longitudinal settings but could also be used as biomarkers in investigating drug effects and over-time lung function change.

Lastly, our final investigation focused on imaging, targeting a known feature of small airways dysfunction: ventilation heterogeneity. We utilised a combination of oxygen enhanced magnetic resonance imaging (OE-MRI) and lung function, in a small asthmatic population, to assess proximal and peripheral biomarkers response to an inhaled fine particle fraction inhaler- flutiform (fluticasone/formoterol [250/10μg]).

Here, we identified a reduction in several imaging parameters, such as ΔPO_2, Tdown and Tvent, as well as physiological parameters after flutiform administration. There was a trend for overall improvement in Scond and Sacin derived from multiple breath washout (MBW). Additionally, significant improvement in Scond in a set of patients was associated with significant change in Tdown, Tvent and Tup, which leads us to speculate that the fine particle fraction inhaler formulation is indeed reaching and improving ventilation distribution in the peripheral conducting airways. Moreover, changes in Scond seemed to better match the imaging responses to bronchodilators than spirometric reversibility. Interestingly, our data showed that Scond parameter was overall higher and less bronchodilator-responsive in the group of patients with higher eosinophils, which might show a close link between inflammation and maldistribution of ventilation in the conducting airways. In addition, pre-bronchodilator OE-MRI parameters showed a relationship not only with eosinophilic inflammation but also number of exacerbations and asthma control. No significant changes were found in the compartmental models, which could indicate that no significant changes occur in diffusion and perfusion in asthma. In sum, flutiform administration improved both proximal and peripheral conducting airway function at 30 minutes in patients with asthma.

An important limitation to our findings is that our population was not placebo controlled or blinded and the study was open label. Therefore, our observations should be confirmed in placebo controlled blinded intervention studies.

Moreover, variables reported from the MBW test were not calculated by the investigator but derived from a customised MATLAB software by our collaborators, which might limit the verification of results in certain individuals. However, no globally accepted platform is available to derive Scond, Sacin and LCI parameters, which is certainly a limitation and an area that needs imperative action. Our study should be regarded as exploratory and an incentive for further research utilising this exciting technique, in larger populations, intervention studies, with extra detailed regional ventilation analysis.

4.2 Future Work

Our results with the forced oscillation techniques and the PExA method disclosed further validation of its applicability on probing the small airways and their relationship

with important clinical outcomes of asthma control and lung function decline. Our population from study 3.1 and 3.3 could potentially be explored further in future studies and further research follow-up visits. Other markers of peripheral airways were not studied for the present thesis, for example AX, X5, ΔXrs and ΔRrs as the main focus was frequency dependence of resistance, but these parameters could certainly add valuable information in future research. Additionally, interpreting the expiratory flow limitation given by ΔXrs and ΔRrs could lead to important insights such as their relationship to patient outcomes and exacerbations. Furthermore, our findings prove the irrefutable need for a general consensus amongst the different FOT and IOS devices, in order to further develop solid normative ranges for each resistance and reactance parameter, applicable to the general population and across different sites, aiming to further apply this promising technique in clinical settings.

The small sized nature of our study populations constituted an unavoidable limitation, especially in the lung function decline studies. Certainly, the PExA study in asthma and repeatability investigations were only exploratory, which led to a lack of more robust and conclusive findings. Nonetheless, it is the largest and only report to date to address such important questions, and future work should focus on larger heterogeneous populations and further biomarkers, such as phospholipids and different proteins involved in the inflammatory process in asthma. Moreover, future work investigating PExA biomarkers in response to asthma therapy, and perhaps surfactant therapy would most certainly lead to important findings, furthering this promising technique development. The PExA method is still limited to very specialised research groups, and Leicester Biomedical Research was the very first centre to adopt this promising technique in the United Kingdom. However, more interest is arising and future research addressing the points raised will surely derive from it.

Imaging biomarkers from the oxygen enhanced MR technique represents a unique platform to visualise spatial and temporal resolution of ventilation defects associated with asthma and COPD. Our pilot study showed that ventilation heterogeneity is present and can be assed with the OE-MRI platform in asthma, and that VH improve with fine particle fraction inhalation therapy. Additionally, Scond has the potential to be a non-invasive tool to understand peripheral airway inflammation, but further studies are needed to strengthen this hypothesis. In sum, future trials involving larger populations and interventional therapy over different time-points with fine particle fraction therapy

would consolidate our findings. Furthermore, our study shows the potential of OE-MRI to be utilised as imaging biomarkers in clinical trials of potentially anti-inflammatory compounds in moderate to severe asthma.

The overall aim of this thesis was to explore and further validate candidate biomarkers from underexplored non-invasive physiological techniques. Our studies showed novel insights and findings, which will hopefully trigger more research in the future. Taking the work as a whole, a major limitation to our studies was the fact that different cohorts were used, rather than a large single population, where forced oscillations, PExA and OE-MRI were applied in all patients. Thus, a single cohort could have perhaps led to more robust findings. Nonetheless, it is clear that our research indicates that the small airways, which account for the majority of total airways, are a very important site of dysfunction in asthma, and could be better explored with these simple, non-invasive tools, leading to their applicability and establishment in clinical settings and therapy decisions.

5. Appendices

Appendix 1: Sputum data according to GINA step treatment in the discovery population (study 3.1)

Clinical Characteristics	**Healthy (n=7)**	**GINA I (n=4)**	**GINA II-III (n=13)**	**GINA IV-V (n=16)**	**Kruskal-Wallis *P* value**
Total cell count (x10^6/ml)	4.13 (1.67-7.60)	4.77 (2.65-25.70)	7.74 (.346-19.78)	3.16 (1.39-7.13)	0.513
Viability (%)	82 (68-90)	81 (78-88)	75 (63-93)	74 (63-91)	0.937
Squamous cells (%)	0.28 (0.00-3.45)	0.20 (0.00-0.68)	0.40 (0.00-1.78)	2.45 (0.00-4.58)	0.534
Eosinophils (%)	1.00 (0.00-3.25)	2.87 (1.81-9.56)	2.40 (1.50-7.70)	2.12 (0.56-5.87)	0.190
Neutrophils (%)	85.80 (80.50-88.00)	89.78 (74.20-96.69)	72.50 (61.55-91.65)	65.75 (50.33-83.58)	0.095
Macrophages (%)	12.00 (9.80-14.00)	7.75 (1.25-14.63)	12.50 (4.75-30.95)	22.50 (11.20-34.13)	0.147
Lymphocytes (%)	0.50 (0.00-0.50)	1.37 (0.25-1.94)	0.25 (0.00-0.87)	0.67 (0.31-1.00)	0.103
Epithelial Cells (%)	0.50 (0.40-1.75)	0.25 (0.06-0.62)	1.50 (0.25-3.12)	1.87 (0.06-3.12)	0.103

Data expressed as median (Q1;Q3). GINA: Global Initiative for Asthma.

Appendix 2: Intra/inter-assay coefficient of variance for SPA and albumin assays in the discovery cohort (study 3.1)

		Assay 1 (t=0)		Assay 2 (t=0+10 months)		Assay 3(t=0+19 months)		Inter-assay CV (%)
		CV (%)	Mean concentration (mg/ml)	CV (%)	Mean concentration (mg/ml)	CV (%)	Mean concentration (mg/ml)	
Albumin	**QC1**	2.50	78.41	1.47	81.59	1.76	69.09	8.51
	QC2	0.23	15.10	15.26	14.60	2.99	12.41	10.19
	QC3	-		8.63	2.89	7.51	2.76	-
	Serum	7.76	75.59	2.14	76.31	2.46	76.27	0.54
	PEx1	5.76	7.54	0.97	19.20	16.56	5.98	-
	PEx2	0.68	5.54	7.08	8.02	-	-	-
SPA	**QC1**	1.24	6.29	0.61	6.77	6.48	3.80	-
	QC2	4.20	1.66	11.28	1.53	3.09	1.86	-
	QC3	-	-	10.09	0.39	4.89	0.66	-
	Serum	2.88	2.39	4.25	2.60	0.76	3.09	13.40
	PEx1	2.62	7.44	8.66	5.19	11.12	3.5	-
	PEx2	2.83	3.29	1.82	4.05	-	-	-

Definition of abbreviations: QC1: high quality control; QC2: Low quality control; QC3: very low-quality control; CV%: coefficient of variation. Values expressed as CV% between 2 values.

Appendix 3: intra coefficient of variance for SPA and albumin assays- longitudinal visit (study 3.4)

		Assay	
		CV (%)	Mean concentration (mg/ml)
SPA	**QC1**	0.83	3.27
	QC2	3.33	2.07
	QC3	6.34	0.81
	Serum	3.45	2.86
	PEx1	2.88	2.46
	PEx2	3.56	2.98
	PEx3	3.71	4.75
	PEx4	5.09	6.24

Definition of abbreviations: QC1: high quality control; QC2: Low quality control; QC3: very low-quality control; CV%: coefficient of variation. Values expressed as CV% between 2 values.

Appendix 4: intra/inter-assay coefficient of variance for SPA and albumin assays- short term repeatability (study 3.4)

		Assay 1		**Assay 2**		**Inter-assay CV (%)**
		CV (%)	Mean concentration (mg/ml)	CV (%)	Mean concentration (mg/ml)	
Albumin	**QC1**	3.82	52.51	12.46	68.42	18.61
	QC2	2.41	9.98	5.47	11.38	9.27
	QC3	5.13	2.54	3.55	3.25	-
	Serum 1	4.62	73.62	4.22	90.16	-
	Serum 2	4.40	63.13	5.07	94.86	-
SPA	**QC1**	4.17	3.25	1.05	3.58	-
	QC2	0.83	2.01	2.81	1.96	-
	QC3	2.05	0.78	10.17	0.89	-
	Serum 1	3.69	2.99	2.39	3.04	1.17
	Serum 2		2.90	0	2.95	1.21

Definition of abbreviations: QC1: high quality control; QC2: Low quality control; QC3: very low quality control; CV%: coefficient of variation. Values expressed as CV% between 2 values.

6. References

1. Perez T. Is it really time to look at distal airways to improve asthma phenotyping and treatment? Eur Respir J. 2011;38:1252–4.

2. Global Initiative For Asthma (GINA). Global Strategy For Asthma Management and Prevention [Internet]. Global Initiative for Asthma. 2017. Available from: www.ginasthma.org

3. Finkas LK, Martin R. Role of Small Airways in Asthma. Immunol Allergy Clin North Am. 2016;36(3):473–82.

4. Contoli M, Santus P, Papi A. Small airway disease in asthma: pathophysiological and diagnostic considerations. Curr Opin Pulm Med [Internet]. 2015;21(1):68–73. Available from: http://ovidsp.ovid.com/ovidweb.cgi?T=JS&PAGE=reference&D=medl&NEWS=N&AN=25415403

5. Bjermer L. Targeting small airways, a step further in asthma management. Clin Respir J. 2011;5(3):131–5.

6. Contoli M, Kraft M, Hamid Q, Bousquet J, Rabe KF, Fabbri LM, et al. Do small airway abnormalities characterize asthma phenotypes? In search of proof. Clin Exp Allergy. 2012;42(8):1150–60.

7. Enright PL, Lebowitz MD, Cockroft DW, Wise RA. Physiologic measures: Pulmonary function tests. Asthma outcome. Am J Respir Crit Care Med. 1994;149(2 II).

8. Ruppel GL, Enright PL. Pulmonary Function Testing. Respir Care. 2012;57(1):165–75.

9. Pellegrino R, Viegi G, Brusasco V, Crapo RO, Burgos F, Casaburi R, et al. Interpretative strategies for lung function tests. Eur Respir J. 2005;26(5):948–68.

10. Smith HJ, Reinhold P, Goldman MD. Forced oscillation technique and impulse oscillometry. Eur Respir Mon [Internet]. 2005;31:72. Available from: http://erspublications.com/lookup/doi/10.1183/1025448x.00031005

11. Yanai M, Sekizawa K, Ohrui T, Sasaki H, Takishima T. Site of airway

obstruction in pulmonary disease: direct measurement of intrabronchial pressure. J Appl Physiol [Internet]. 1992;72(3):1016–23. Available from: http://www.ncbi.nlm.nih.gov/pubmed/1568955

12. Gonem S, Umar I, Burke D, Desai D, Corkill S, Owers-Bradley J, et al. Airway impedance entropy and exacerbations in severe asthma. Eur Respir J. 2012;40(5):1156–63.

13. Hozawa S, Terada M, Hozawa M. Comparison of budesonide/formoterol Turbuhaler with fluticasone/salmeterol Diskus for treatment effects on small airway impairment and airway inflammation in patients with asthma. Pulm Pharmacol Ther. 2011;24(5):571–6.

14. Almstrand A-C, Ljungström E, Lausmaa J, Bake B, Sjövall P, Olin A-C. Airway monitoring by collection and mass spectrometric analysis of exhaled particles. Anal Chem. 2009;81(2):662–8.

15. Almstrand A-C, Josefson M, Bredberg A, Lausmaa J, Sjövall P, Larsson P, et al. TOF-SIMS analysis of exhaled particles from patients with asthma and healthy controls. Eur Respir J. 2012;39(1):59–66.

16. Larsson P, Mirgorodskaya E, Samuelsson L, Bake B, Almstrand A-C, Bredberg A, et al. Surfactant protein A and albumin in particles in exhaled air. Respir Med. 2012;106(2):197–204.

17. Lärstad M, Almstrand A-C, Larsson P, Bake B, Larsson S, Ljungström E, et al. Surfactant protein a in exhaled endogenous particles is decreased in chronic obstructive pulmonary disease (COPD) Patients: A Pilot Study. PLoS One. 2015;10(12):e0144463.

18. Ohno Y, Hatabu H. Basics concepts and clinical applications of oxygen-enhanced MR imaging. Eur J Radiol. 2007;64(3):320–8.

19. Kauczor HU, Kreitner KF. Contrast-enhanced MRI of the lung. Eur J Radiol. 2000;34(3):196–207.

20. Morgan AR, Parker GJM, Roberts C, Buonaccorsi GA, Maguire NC, Hubbard Cristinacce PL, et al. Feasibility assessment of using oxygen-enhanced magnetic resonance imaging for evaluating the effect of pharmacological treatment in

COPD. Eur J Radiol [Internet]. 2014;83(11):2093–101. Available from: http://dx.doi.org/10.1016/j.ejrad.2014.08.004

21. Risau W. Mechanisms of angiogenesis. Nature [Internet]. 1997 Apr 17;386:671. Available from: http://dx.doi.org/10.1038/386671a0

22. Weibel ER. What makes a good lung? Swiss Med Wkly [Internet]. 2009;139(27–28):375–86. Available from: http://europepmc.org/abstract/MED/19629765%5Cnhttp://dx.doi.org/smw-12270%5Cnhttp://www.ncbi.nlm.nih.gov/pubmed/19629765

23. Varner VD, Nelson CM. Computational models of airway branching morphogenesis. Seminars in Cell and Developmental Biology. 2016;

24. McNulty W, Usmani OS. Techniques of assessing small airways dysfunction. Eur Clin Respir J [Internet]. 2014;1(1):25898. Available from: https://www.tandfonline.com/doi/full/10.3402/ecrj.v1.25898

25. Weibel ER, Gomez DM. Architecture of the human lung. Science (80-). 1962;137(3530).

26. Horsfield K, Cumming G. Morphology of the bronchial tree in man. Respir Physiol. 1968;26(2):173–82.

27. Bordas R, Lefevre C, Veeckmans B, Pitt-Francis J, Fetita C, Brightling CE, Kay D, Siddiqui S BK. Development and Analysis of Patient-Based Complete Conducting Airways Models. PLoS One. 2015;10(12):e0144105.

28. Konstantinos Katsoulis K, Kostikas K, Kontakiotis T. Techniques for assessing small airways function: Possible applications in asthma and COPD. Respir Med. 2016;119:e2–9.

29. Usmani OS, Barnes PJ. Assessing and treating small airways disease in asthma and chronic obstructive pulmonary disease. Ann Med [Internet]. 2012;44(2):146–56. Available from: http://www.ncbi.nlm.nih.gov/pubmed/21679101

30. Lapperre TS, Willems LNA, Timens W, Rabe KF, Hiemstra PS, Postma DS, et al. Small airways dysfunction and neutrophilic inflammation in bronchial biopsies and BAL in COPD. Chest. 2007;131(1):53–9.

31. Hogg JC, McDonough JE, Suzuki M. Small airway obstruction in COPD: New insights based on micro-CT imaging and MRI imaging. Chest. 2013;143(5):1436–43.

32. Burgel PR. The role of small airways in obstructive airway diseases. Eur Respir Rev. 2011;20(119):23–33.

33. Macklem P. The Physiology of Small Airways. Am J Respir Crit Care Med [Internet]. 1998 May 1;157(5):S181–3. Available from: https://doi.org/10.1164/ajrccm.157.5.rsaa-2

34. Mead J, Takishima T, Leith D. Stress distribution in lungs: a model of pulmonary elasticity. J Appl Physiol. 1970;28(5):596–608.

35. West JB. Pulmonary Pathophysiology: The Essentials. Lippincott Williams & Wilkins, 8th edition. 2013.

36. Macklem PT, Mead J. Resistance of central and peripheral airways measured by a retrograde catheter. J Appl Physiol [Internet]. 1967 Mar 1;22(3):395 LP-401. Available from: http://jap.physiology.org/content/22/3/395.abstract

37. Contoli M, Bousquet J, Fabbri LM, Magnussen H, Rabe KF, Siafakas NM, et al. The small airways and distal lung compartment in asthma and COPD: A time for reappraisal. Vol. 65, Allergy: European Journal of Allergy and Clinical Immunology. 2010. p. 141–51.

38. Brown R, Woolcock AJ, Vincent NJ, Macklem PT. Physiological effects of experimental airway obstruction with beads. J Appl Physiol [Internet]. 1969 Sep 1;27(3):328 LP-335. Available from: http://jap.physiology.org/content/27/3/328.abstract

39. Hubner RH, Herzog D. COPD treatment: About collateral channels and collapsing airways. European Respiratory Journal. 2016.

40. Kaminsky DA, Bates JHT, Irvin CG. Effects of Cool, Dry Air Stimulation on Peripheral Lung Mechanics in Asthma. Am J Respir Crit Care Med [Internet]. 2000 Jul 1;162(1):179–86. Available from: https://doi.org/10.1164/ajrccm.162.1.9806079

41. Kraft M, Pak J, Martin RJJ, Kaminsky D, Irvin CGG. Distal Lung Dysfunction at

Night in Nocturnal Asthma. Am J Respir Crit Care Med [Internet]. 2001 Jun 1;163(7):1551–6. Available from: https://doi.org/10.1164/ajrccm.163.7.2008013

42. Yanai M, Sekizawa K, Ohrui T, Sasaki H, Takishima T. Site of airway obstruction in pulmonary disease: direct measurement of intrabronchial pressure. J Appl Physiol [Internet]. 1992 Mar 1;72(3):1016 LP-1023. Available from: http://jap.physiology.org/content/72/3/1016.abstract

43. Underwood JCE, Cross SS, (Firm) ES. General and systematic pathology [Internet]. Edinburgh: Churchill Livingstone; 2009. Available from: http://www.clinicalkey.com/dura/browse/bookChapter/3-s2.0-B9780443068881X00016

44. Weibel ER, Gil J. Electron microscopic demonstration of an extracellular duplex lining layer of alveoli. Respir Physiol [Internet]. 1968;4(1):42–57. Available from: http://www.ncbi.nlm.nih.gov/pubmed/4867416

45. Hohlfeld JM. The role of surfactant in asthma. Respir Res [Internet]. 2002;3:4. Available from: http://www.pubmedcentral.nih.gov/articlerender.fcgi?artid=64815&tool=pmcentrez&rendertype=abstract

46. Saxena S. Lung surfactant. Resonance [Internet]. 2005 Aug;10(8):91–6. Available from: https://doi.org/10.1007/BF02866749

47. Hamid Q, Tulic MK, Hamid Q. New insights into the pathophysiology of the small airways in asthma. Ann Thorac Med [Internet]. 2006;27(1):28–33. Available from: http://www.pubmedcentral.nih.gov/articlerender.fcgi?artid=2732069&tool=pmcentrez&rendertype=abstract

48. Shaw RJ, Djukanovic R, Tashkin DP, Millar a. B, Du Bois RM, Corris P a. The role of small airways in lung disease. Respir Med [Internet]. 2002;96(2):67–80. Available from: http://linkinghub.elsevier.com/retrieve/pii/S0954611101912168

49. McDonough JE, Yuan R, Suzuki M, Seyednejad N, Elliott WM, Sanchez PG, et al. Small-Airway Obstruction and Emphysema in Chronic Obstructive Pulmonary Disease. N Engl J Med. 2011;365(17):1567–75.

50. Hogg JC, Chu F, Utokaparch S, Woods R, Elliott WM, Buzatu L, et al. The Nature of Small-Airway Obstruction in Chronic Obstructive Pulmonary Disease. N Engl J Med [Internet]. 2004 Jun 24;350(26):2645–53. Available from: https://doi.org/10.1056/NEJMoa032158

51. Cottini M, Lombardi C, Micheletto C. Small airway dysfunction and bronchial asthma control : the state of the art. Asthma Res Pract. 2015;1:1–11.

52. Hogg JC, Macklem PT, Thurlbeck WM. Site and nature of airway obstruction in chronic obstructive lung disease. N Engl J Med [Internet]. 1968;278(25):1355–60. Available from: http://www.ncbi.nlm.nih.gov/pubmed/5650164

53. Ryu JH, Colby T V, Hartman TE. Idiopathic Pulmonary Fibrosis: Current Concepts. Mayo Clin Proc [Internet]. 1998;73(11):1085–101. Available from: http://www.sciencedirect.com/science/article/pii/S0025619611638202

54. Coares EO CJ. Pulmonary function in sarcoidosis. J Clin Invest. 1951;30(8):848–52.

55. Allen TC. Pathology of small airways disease. Arch Pathol Lab Med. 2010;134(5):702–18.

56. Hogg JC. Pathophysiology of airflow limitation in chronic obstructive pulmonary disease. Lancet. 2004;364(9435):709–21.

57. Myers JL, Colby T V. Pathologic manifestations of bronchiolitis, constrictive bronchiolitis, cryptogenic organizing pneumonia, and diffuse panbronchiolitis. Clin Chest Med [Internet]. 1993;14(4):611–22. Available from: http://www.ncbi.nlm.nih.gov/pubmed/8313666

58. Nasser S. An imperfect ``PAST'' Lessons learned from the National Review of Asthma Deaths (NRAD) UK. Respir Res [Internet]. 2016;17(1):87. Available from: http://dx.doi.org/10.1186/s12931-016-0393-9

59. Lang DM. Severe asthma: Epidemiology, burden of illness, and heterogeneity. Allergy Asthma Proc. 2015;36(6):418–24.

60. Martinez FD, Holt PG. Role of microbial burden in aetiology of allergy and asthma. Lancet. 1999;354 Suppl:SII12-I15.

61. Bousquet J, Mantzouranis E, Cruz AA, Aït-Khaled N, Baena-Cagnani CE, Bleecker ER, et al. Uniform definition of asthma severity, control, and exacerbations: document presented for the World Health Organization Consultation on Severe Asthma. J Allergy Clin Immunol [Internet]. 2010 Nov [cited 2017 Apr 23];126(5):926–38. Available from: http://www.ncbi.nlm.nih.gov/pubmed/20926125

62. Vanfleteren LEGW, Kocks JWH, Stone IS, Breyer-Kohansal R, Greulich T, Lacedonia D, et al. Moving from the Oslerian paradigm to the post-genomic era: are asthma and COPD outdated terms? Thorax [Internet]. 2014 Jan 1;69(1):72 LP-79. Available from: http://thorax.bmj.com/content/69/1/72.abstract

63. Lötvall J, Akdis CA, Bacharier LB, Bjermer L, Casale TB, Custovic A, et al. Asthma endotypes: A new approach to classification of disease entities within the asthma syndrome. J Allergy Clin Immunol. 2011;127(2):355–60.

64. Wenzel SE. Asthma phenotypes: the evolution from clinical to molecular approaches. Nat Med [Internet]. 2012;18(5):716–25. Available from: http://www.nature.com/doifinder/10.1038/nm.2678

65. Lipworth B. Targeting the small airways asthma phenotype: If we can reach it, should we treat it? Ann Allergy, Asthma Immunol. 2013;110(4):233–9.

66. Kraft M, Djukanovic R, Wilson S, Holgate ST, Martin RJ. Alveolar tissue inflammation in asthma. Am J Respir Crit Care Med [Internet]. 1996;154(5):1505–10. Available from: http://www.atsjournals.org/doi/abs/10.1164/ajrccm.154.5.8912772

67. Kraft M, Pak J, Martin RJ, Kaminsky D, Irvin CG. Distal lung dysfunction at night in nocturnal asthma. Am J Respir Crit Care Med. 2001;163(7):1551–6.

68. Anderson SD. How does exercise cause asthma attacks? Curr Opin Allergy Clin Immunol. 2006;6(1):37–42.

69. Kaminsky DA, Irvin CG, Gurka DA, Feldsien DC, Wagner EM, Liu MC, et al. Peripheral airways responsiveness to cool, dry air in normal and asthmatic individuals. Am J Respir Crit Care Med [Internet]. 1995;152(6 I):1784–90. Available from: https://doi.org/10.1164/ajrccm.152.6.8520737

70. Zeidler MR, Goldin JG, Kleerup EC, Kim HJ, Truong DA, Gjertson DW, et al. Small airways response to naturalistic cat allergen exposure in subjects with asthma. J Allergy Clin Immunol. 2006;118(5):1075–81.

71. Lipworth B, Manoharan A, Anderson W. Unlocking the quiet zone: The small airway asthma phenotype. Lancet Respir Med. 2014;2(6):497–506.

72. Vrijlandt EJLE, Gerritsen J, Boezen HM, Grevink RG, Duiverman EJ. Lung Function and Exercise Capacity in Young Adults Born Prematurely. Am J Respir Crit Care Med. 2006;173(8):890–6.

73. Van Den Berge M, Ten Hacken NHT, Cohen J, Douma WR, Postma DS. Small airway disease in asthma and COPD: Clinical implications. Chest. 2011;139(2):412–23.

74. Carroll N, Elliot J, Morton A, James A. The structure of large and small airways in nonfatal and fatal asthma. Am Rev Respir Dis [Internet]. 1993;147(2):405–10. Available from: http://www.atsjournals.org/doi/abs/10.1164/ajrccm/147.2.405

75. Carroll N, Cooke C, James A. The distribution of eosinophils and lymphocytes in the large and small airways of asthmatics. Eur Respir J. 1997;10(2):292–300.

76. Perez T, Chanez P, Dusser D, Devillier P. Small airway impairment in moderate to severe asthmatics without significant proximal airway obstruction. Respir Med. 2013;107(11):1667–74.

77. Melchor R, Biddiscombe MF, Mak VH, Short MD, Spiro SG. Lung deposition patterns of directly labelled salbutamol in normal subjects and in patients with reversible airflow obstruction. Thorax [Internet]. 1993;48(5):506–11. Available from: http://www.pubmedcentral.nih.gov/articlerender.fcgi?artid=464503&tool=pmcentrez&rendertype=abstract

78. Usmani OS. Small-airway disease in asthma: pharmacological considerations. Curr Opin Pulm Med [Internet]. 2015;21(1):55–67. Available from: http://www.ncbi.nlm.nih.gov/pubmed/25415404

79. Sullivan S, D Rasouliyan L, Russo P A, Kamath T, Chipps B E. Extent, patterns, and burden of uncontrolled disease in severe or difficult-to-treat asthma. Allergy

[Internet]. 2007;62(2):126–33. Available from: https://doi.org/10.1111/j.1398-9995.2006.01254.x

80. Schatz M, Hsu J-WY, Zeiger RS, Chen W, Dorenbaum A, Chipps BE, et al. Phenotypes determined by cluster analysis in severe or difficult-to-treat asthma. J Allergy Clin Immunol [Internet]. 2014;133(6):1549–56. Available from: http://www.sciencedirect.com/science/article/pii/S0091674913015546

81. Murphy AC, Proeschal A, Brightling CE, Wardlaw AJ, Pavord I, Bradding P, et al. The relationship between clinical outcomes and medication adherence in difficult-to-control asthma. Thorax [Internet]. 2012;67(8):751–3. Available from: http://www.ncbi.nlm.nih.gov/pubmed/22436168%5Cnhttp://thorax.bmj.com/content/67/8/751.full.pdf

82. Melani AS, Bonavia M, Cilenti V, Cinti C, Lodi M, Martucci P, et al. Inhaler mishandling remains common in real life and is associated with reduced disease control. Respir Med. 2011;105(6):930–8.

83. Adcock IM, Ford PA, Bhavsar P, Ahmad T, Chung KF. Steroid resistance in asthma: Mechanisms and treatment options. Curr Allergy Asthma Rep. 2008;8(2):171–8.

84. Schiphof-Godart L, van der Wiel E, Ten Hacken NHT, van den Berge M, Postma DS, van der Molen T. Development of a tool to recognize small airways dysfunction in asthma (SADT). Health Qual Life Outcomes [Internet]. 2014;12:155. Available from: http://www.pubmedcentral.nih.gov/articlerender.fcgi?artid=4253607&tool=pmcentrez&rendertype=abstract

85. Decramer M, Demedts M van de WK. Isocapnic hyperventilation with cold air in healthy non-smokers, smokers and asthmatic subjects. Bull Eur Physiopathol Respir. 1984;(20(3)):237–43.

86. Sue-Chu M. Winter sports athletes: Long-term effects of cold air exposure. Br J Sports Med. 2012;46(6):397–401.

87. Denlinger LC, Phillips BR, Ramratnam S, Ross K, Bhakta NR, Cardet JC, et al. Inflammatory and comorbid features of patients with severe asthma and frequent exacerbations. Am J Respir Crit Care Med. 2017;195(3):302–13.

88. Carr TF, Altisheh R, Zitt M. Small airways disease and severe asthma. World Allergy Organ J [Internet]. 2017 Jun 21;10(1):20. Available from: http://www.ncbi.nlm.nih.gov/pmc/articles/PMC5479008/

89. in 't Veen JC, Beekman AJ, Bel EH. Recurrent exacerbations in severe asthma are associated with enhanced airway closure during stable episodes. Am J Respir Crit Care Med [Internet]. 2000;161. Available from: https://doi.org/10.1164/ajrccm.161.6.9906075

90. Bourdin A, Paganin F, Préfaut C, Kieseler D, Godard P, Chanez P. Nitrogen washout slope in poorly controlled asthma. Allergy Eur J Allergy Clin Immunol. 2006;61(1):85–9.

91. Postma DS, Brightling C, Fabbri L, Van Molen TD, Nicolini G, Papi A, et al. Unmet needs for the assessment of small airways dysfunction in asthma: Introduction to the ATLANTIS study. Eur Respir J. 2015;45(6):1534–8.

92. Thien F. Measuring and imaging small airways dysfunction in asthma. Asia Pac Allergy [Internet]. 2013;3(4):224–30. Available from: http://apallergy.org/DOIx.php?id=10.5415/apallergy.2013.3.4.224

93. Hayes D, Kraman SS. The physiologic basis of spirometry. Respir Care. 2009;54(12):1717–26.

94. Polak AG. A model-based method for flow limitation analysis in the heterogeneous human lung. Comput Methods Programs Biomed. 2008;89(2):123–31.

95. McFadden ER, Linden DA. A reduction in maximum mid-expiratory flow rate. A spirographic manifestation of small airway disease. Am J Med. 1972;52(6):725–37.

96. Hansen JE, Sun XG, Wasserman K. Discriminating measures and normal values for expiratory obstruction. Chest. 2006;129(2):369–77.

97. Gelb AF, Williams AJ, Zamel N. Spirometry. Chest [Internet]. 1983 Nov 10;84(4):473–4. Available from: http://dx.doi.org/10.1378/chest.84.4.473

98. Crapo R, Morris A, Gardner R. Reference spirometric values using techniques and equipment that meet ATS recommendations. Am Rev Respir Dis.

1981;123(6):659–64.

99. Miller M, M Grove D, C Pincock A. Time domain spirogram indices. Their variability and reference values in nonsmokers. Am Rev Respir Dis. 1985 Dec 1;132:1041–8.

100. Morris ZQ, Coz A, Starosta D. An Isolated Reduction of the FEV_3/FVC Ratio Is an Indicator of Mild Lung Injury. Chest [Internet]. 2017 Nov 2;144(4):1117–23. Available from: http://dx.doi.org/10.1378/chest.12-2816

101. Börekçi S, Demir T, Görek Dilektaşlı A, Uygun M, Yıldırım N. A Simple Measure to Assess Hyperinflation and Air Trapping: 1-Forced Expiratory Volume in Three Second / Forced Vital Capacity. Balkan Med J [Internet]. 2017 Mar 28;34(2):113–8. Available from: http://www.ncbi.nlm.nih.gov/pmc/articles/PMC5394291/

102. Cohen J, Postma DS, Vink-Klooster K, Van Der Bij W, Verschuuren E, Ten Hacken NHT, et al. FVC to slow inspiratory vital capacity ratio: A potential marker for small airways obstruction. Chest. 2007;132(4):1198–203.

103. Barros ARG de, Pires MB, Raposo NMF. Importance of slow vital capacity in the detection of airway obstruction. J Bras Pneumol. 2013;39(3):317–22.

104. Miller MR, Pincock AC. Repeatability of the moments of the truncated forced expiratory spirogram. Thorax [Internet]. 1982 Mar 1;37(3):205 LP-211. Available from: http://thorax.bmj.com/content/37/3/205.abstract

105. Chinn DJ, Cotes JE. Transit time indices derived from forced expiratory spirograms: Repeatability and criteria for curve selection and truncation. Eur Respir J. 1994;7(2):402–8.

106. Sorkness RL, Bleecker ER, Busse WW, Calhoun WJ, Castro M, Chung KF, et al. Lung function in adults with stable but severe asthma: air trapping and incomplete reversal of obstruction with bronchodilation. J Appl Physiol. 2007;104(2):394–403.

107. Yoo Y, Ji TC, Yu J, Do KK, Sun HC, Young YK. Comparison of percentage fall in FVC at the provocative concentration of methacholine causing a 20% fall in FEV1between patients with asymptomatic bronchial hyperresponsiveness and

mild asthma. Chest. 2007;132(1):106–11.

108. Gibbons WJ, Sharma A, Lougheed D, Macklem PT. Detection of excessive bronchoconstriction in asthma. Am J Respir Crit Care Med. 1996;153(2):582–9.

109. Milanese M, Crimi E, Scordamaglia a, Riccio a, Pellegrino R, Canonica GW, et al. On the functional consequences of bronchial basement membrane thickening. J Appl Physiol. 2001;91(3):1035–40.

110. Papi A, Paggiaro P, Nicolini G, Vignola AM, Fabbri LM. Beclomethasone/formoterol vs fluticasone/salmeterol inhaled combination in moderate to severe asthma. Allergy Eur J Allergy Clin Immunol. 2007;62(10):1182–8.

111. Lundblad LKA, Thompson-Figueroa J, Allen GB, Rinaldi L, Norton RJ, Irvin CG, et al. Airway hyperresponsiveness in allergically inflamed mice: The role of airway closure. Am J Respir Crit Care Med. 2007;175(8):768–74.

112. Criée CP, Sorichter S, Smith HJ, Kardos P, Merget R, Heise D, et al. Body plethysmography - Its principles and clinical use. Respir Med. 2011;105(7):959–71.

113. Jain V V, Abejie B, Bashir MH, Tyner T, Vempilly J. Lung volume abnormalities and its correlation to spirometric and demographic variables in adult asthma. J Asthma [Internet]. 2013;50(6):600–5. Available from: http://www.ncbi.nlm.nih.gov/pubmed/23521185

114. Kraft M, Cairns CB, Ellison MC, Pak J, Irvin C, Wenzel S. Improvements in Distal Lung Function Correlate With Asthma Symptoms After Treatment With Oral Montelukast. Chest [Internet]. 2006;130(6):1726–32. Available from: http://linkinghub.elsevier.com/retrieve/pii/S0012369215508945

115. Hughes JMB, Pride NB. Examination of the carbon monoxide diffusing capacity (DL CO) in relation to its KCO and VA components. Am J Respir Crit Care Med. 2012;186(2):132–9.

116. Y.-C. Huang LGQ. Clinical Significance Of Isolated Decrease In Single Breath Lung Volume-Total Lung Capacity Ratio (va/tlc). Am J Respir Crit Care Med. 2016;196:A6351.

117. Borrill ZL, Houghton CM, Woodcock AA, Vestbo J, Singh D. Measuring bronchodilation in COPD clinical trials. Br J Clin Pharmacol. 2005;59(4):379–84.

118. DuBois AB, Brody AW, Lewis DH, Burgess BF. Oscillation Mechanics of Lungs and Chest in Man. J Appl Physiol [Internet]. 1956 May 1;8(6):587 LP-594. Available from: http://jap.physiology.org/content/8/6/587.abstract

119. Oostveen E, MacLeod D, Lorino H, Farré R, Hantos Z, Desager K, et al. The forced oscillation technique in clinical practice: methodology, recommendations and future developments. Eur Respir J Off J Eur Soc Clin Respir Physiol. 2003;22:1026–41.

120. Naji N, Keung E, Kane J, Watson RM, Killian KJ, Gauvreau GM. Comparison of changes in lung function measured by plethymography and IOS after bronchoprovocation. Respir Med. 2013;107(4):503–10.

121. Turkeshi E, Zelenukha D, Vaes B, Andreeva E, Frolova E, Degryse JM. Predictors of poor-quality spirometry in two cohorts of older adults in Russia and Belgium: A cross-sectional study. npj Prim Care Respir Med. 2015;25:15048.

122. Goldman MD. Clinical application of forced oscillation. Pulm Pharmacol Ther. 2001;14:341–50.

123. Michaelson ED, Grassman ED, Peters WR. Pulmonary mechanics by spectral analysis of forced random noise. J Clin Invest. 1975;56(5):1210–30.

124. Smith H, Reinhold P. Forced oscillation technique and impulse oscillometry Peculiarities of aperiodic waveforms. Eur Respir Mon [Internet]. 2005;31:72–105. Available from: http://www.carefusion.co.uk/documents/international/articles/respiratory-care/mechanical-ventilation/RC_Forced-oscillation-technique-IOS_JA_EN.pdf

125. Schulz H, Flexeder C, Behr J, Heier M, Holle R, Huber RM, et al. Reference Values of Impulse Oscillometric Lung Function Indices in Adults of Advanced Age. PLoS One. 2013;8(5):e63366.

126. Bickel S, Popler J, Lesnick B, Eid N. Impulse oscillometry: Interpretation and practical applications. Chest. 2014;146(3):841–7.

127. Otis AB, Mckerrow CB, Bartlett RA, Mead J, Mcilroy MB, Selver-Stone NJ, et al. Mechanical factors in distribution of pulmonary ventilation. J Appl Physiol [Internet]. 1956;8(4):427–43. Available from: http://jap.physiology.org/content/jap/8/4/427.full.pdf

128. Navajas D, Maksym GN, Bates JH. Dynamic viscoelastic nonlinearity of lung parenchymal tissue. J Appl Physiol [Internet]. 1995;79(1):348–56. Available from: http://www.ncbi.nlm.nih.gov/pubmed/7559242

129. Lutchen KR, Gillis H. Relationship between heterogeneous changes in airway morphometry and lung resistance and elastance. J Appl Physiol. 1997;83(4):1192–201.

130. Hantos Z, Daroczy B, Suki B, Galgoczy G, Csendes T. Forced oscillatory impedance of the respiratory system at low frequencies. J Appl Physiol [Internet]. 1986;60(1):123–32. Available from: http://www.ncbi.nlm.nih.gov/pubmed/2935519

131. Brashier B, Salvi S. Measuring lung function using sound waves: Role of the forced oscillation technique and impulse oscillometry system. Breathe. 2015;11(1):57–65.

132. Leary D, Bhatawadekar SA, Parraga G, Maksym GN. Modeling stochastic and spatial heterogeneity in a human airway tree to determine variation in respiratory system resistance. J Appl Physiol [Internet]. 2012;112(1):167–75. Available from: http://jap.physiology.org/cgi/doi/10.1152/japplphysiol.00633.2011

133. Hantos, Z; Daroczy, B; Suki, B; Daróczy, B; Suki, B; Nagy, S; Fredberg, JJ; Daroczy B. Input impedance and peripheral inhomogeneity of dog lungs. J Appl Physiol [Internet]. 1992;72(1):168–78. Available from: http://jap.physiology.org/content/jap/72/1/168.full.pdf%5Cnhttp://www.ncbi.nlm.nih.gov/pubmed/1537711

134. Tgavalekos NT. Identifying airways responsible for heterogeneous ventilation and mechanical dysfunction in asthma: an image functional modeling approach. J Appl Physiol [Internet]. 2005;99(6):2388–97. Available from: http://jap.physiology.org/cgi/doi/10.1152/japplphysiol.00391.2005

135. Campana L, Kenyon J, Zhalehdoust-Sani S, Tzeng Y-S, Sun Y, Albert M, et al.

Probing airway conditions governing ventilation defects in asthma via hyperpolarized MRI image functional modeling. J Appl Physiol [Internet]. 2009;106(4):1293–300. Available from: http://jap.physiology.org/cgi/doi/10.1152/japplphysiol.91428.2008

136. Galant SP, Komarow HD, Shin H-WW, Siddiqui S, Lipworth BJ. The case for impulse oscillometry in the management of asthma in children and adults. Ann Allergy Asthma Immunol [Internet]. 2017 Mar 9;118(6):664–71. Available from: http://dx.doi.org/10.1016/j.anai.2017.04.009

137. Manoharan A, Anderson WJ, Lipworth J, Lipworth BJ. Assessment of Spirometry and Impulse Oscillometry in Relation to Asthma Control. Lung. 2015;193(1):47–51.

138. Park JW, Lee YW, Jung YH, Park SE, Hong CS. Impulse oscillometry for estimation of airway obstruction and bronchodilation in adults with mild obstructive asthma. Ann Allergy, Asthma Immunol. 2007;98(6):546–52.

139. Houghton CM, Woodcock AA, Singh D. A comparison of lung function methods for assessing dose-response effects of salbutamol. Br J Clin Pharmacol [Internet]. 2004;58(2):134–41. Available from: http://www.pubmedcentral.nih.gov/articlerender.fcgi?artid=1884595&tool=pmcentrez&rendertype=abstract

140. Gonem S, Natarajan S, Desai D, Corkill S, Singapuri A, Bradding P, et al. Clinical significance of small airway obstruction markers in patients with asthma. Clin Exp Allergy. 2014;44(4):499–507.

141. Cavalcanti J V., Lopes AJ, Jansen JM, Melo PL. Detection of changes in respiratory mechanics due to increasing degrees of airway obstruction in asthma by the forced oscillation technique. Respir Med. 2006;100(12):2207–19.

142. Bikov A, Pride NB, Goldman MD, Hull JH, Horvath I, Barnes PJ, et al. Glottal aperture and buccal airflow leaks critically affect forced oscillometry measurements. Chest. 2015;148(3):731–8.

143. Anderson WJ, Zajda E, Lipworth BJ. Are we overlooking persistent small airways dysfunction in community-managed asthma? Ann Allergy, Asthma Immunol. 2012;109(3):185–9.

144. Saadeh C, Cross B, Gaylor M, Griffith M. Advantage of impulse oscillometry over spirometry to diagnose chronic obstructive pulmonary disease and monitor pulmonary responses to bronchodilators: An observational study. SAGE Open Med [Internet]. 2015;3:2050312115578957. Available from: http://ovidsp.ovid.com/ovidweb.cgi?T=JS&CSC=Y&NEWS=N&PAGE=fulltext&D=emed13&AN=2015002535%5Cnhttp://sfx.ucl.ac.uk/sfx_local?sid=OVID:embase&id=pmid:&id=doi:10.1177/2050312115578957&issn=2050-3121&isbn=&volume=3&issue=&spage=&pages=&date=2015&title=SAGE+Op

145. Hamakawa H, Sakai H, Takahashi A, Zhang J, Fujinaga T, Shoji T, et al. Forced oscillation technique as a non-invasive assessment for lung transplant recipients. Adv Exp Med Biol. 2010;662:293–8.

146. Paredi P, Goldman M, Alamen A, Ausin P, Usmani OS, Pride NB, et al. Comparison of inspiratory and expiratory resistance and reactance in patients with asthma and chronic obstructive pulmonary disease. Thorax. 2010;65(3):263–7.

147. Tanimura K, Hirai T, Sato S, Hasegawa K, Muro S, Kurosawa H, et al. Comparison of two devices for respiratory impedance measurement using a forced oscillation technique: Basic study using phantom models. J Physiol Sci. 2014;64(5):377–82.

148. Hellinckx J, Cauberghs M, De Boeck K, Demedts M. Evaluation of impulse oscillation system: Comparison with forced oscillation technique and body plethysmography. Eur Respir J. 2001;18(3):564–70.

149. Teague WG, Tustison NJ, Altes TA. Ventilation heterogeneity in asthma. J Asthma [Internet]. 2014;51(7):677–84. Available from: http://www.tandfonline.com/doi/full/10.3109/02770903.2014.914535

150. Robertson JS, Siri WE, Jones HB. Lung ventilation patterns determined by analysis of nitrogen elimination rates; use of mass spectrometer as a continuous gas analyzer. J Clin Invest. 1950;29(5):577–90.

151. Robinson PD, Latzin P, Verbanck S, Hall GL, Horsley A, Gappa M, et al. Consensus statement for inert gas washout measurement using multiple- and single- breath tests. Eur Respir J Off J Eur Soc Clin Respir Physiol [Internet].

2013;41(3):507–22. Available from: http://www.ncbi.nlm.nih.gov/pubmed/23397305

152. Verbanck S, Schuermans D, Van Muylem a, Paiva M, Noppen M, Vincken W. Ventilation distribution during histamine provocation. J Appl Physiol [Internet]. 1997;83(6):1907–16. Available from: http://www.ncbi.nlm.nih.gov/pubmed/9390962

153. Crawford A, Makowska M. Convection-and diffusion-dependent ventilation maldistribution in normal subjects. J Appl Physiol [Internet]. 1985;59(3):838–46. Available from: http://jap.physiology.org/content/jap/59/3/838.full.pdf

154. Gonem S, Singer F, Corkill S, Singapuri A, Siddiqui S, Gustafsson P. Validation of a photoacoustic gas analyser for the measurement of functional residual capacity using multiple-breath inert gas washout. Respiration. 2014;87(6):462–8.

155. Gonem S, Scadding A, Soares M, Singapuri A, Gustafsson P, Ohri C, et al. Lung clearance index in adults with non-cystic fibrosis bronchiectasis. Respir Res [Internet]. 2014;15(1):59. Available from: http://respiratory-research.com/content/15/1/59

156. Horsley AR, Gustafsson PM, Macleod KA, Saunders C, Greening AP, Porteous DJ, et al. Lung clearance index is a sensitive, repeatable and practical measure of airways disease in adults with cystic fibrosis. Thorax [Internet]. 2007;63(2):135–40. Available from: http://thorax.bmj.com/cgi/doi/10.1136/thx.2007.082628

157. Schibler A, Schneider M, Frey U, Kraemer R. Moment ratio analysis of multiple breath nitrogen washout in infants with lung disease. Eur Respir J. 2000;15(6):1094–101.

158. Fuchs SI, Buess C, Lum S, Kozlowska W, Stocks J, Gappa M. Multiple breath washout with a sidestream ultrasonic flow sensor and mass spectrometry: A comparative study. Pediatr Pulmonol. 2006;41(12):1218–25.

159. Verbanck S, Schuermans D, Noppen M, Van Muylem A, Paiva M, Vincken W. Evidence of acinar airway involvement in asthma. Am J Respir Crit Care Med. 1999;159(5 I):1545–50.

160. Macleod KA, Horsley AR, Bell NJ, Greening AP, Innes JA, Cunningham S.

Ventilation heterogeneity in children with well controlled asthma with normal spirometry indicates residual airways disease. Thorax [Internet]. 2008;64(1):33–7. Available from: http://thorax.bmj.com/cgi/doi/10.1136/thx.2007.095018

161. Gustafsson PM. Peripheral airway involvement in CF and asthma compared by inert gas washout. Pediatr Pulmonol. 2007;42(2):168–76.

162. Verbanck S, Schuermans D, Paiva M, Vincken W. Nonreversible conductive airway ventilation heterogeneity in mild asthma. J Appl Physiol [Internet]. 2003;94(4):1380–6. Available from: http://www.ncbi.nlm.nih.gov/pubmed/12471044

163. Farah CS, King GG, Brown NJ, Downie SR, Kermode JA, Hardaker KM, et al. The role of the small airways in the clinical expression of asthma in adults. J Allergy Clin Immunol. 2012;129(2):381–7.

164. Farah CS, King GG, Brown NJ, Peters MJ, Berend N, Salome CM. Ventilation heterogeneity predicts asthma control in adults following inhaled corticosteroid dose titration. J Allergy Clin Immunol. 2012;130(1):61–8.

165. Thompson BR, Douglass JA, Ellis MJ, Kelly VJ, O'Hehir RE, King GG, et al. Peripheral lung function in patients with stable and unstable asthma. J Allergy Clin Immunol. 2013;131(5):1322–8.

166. Verbanck S, Schuermans D, Vincken W. Inflammation and airway function in the lung periphery of patients with stable asthma. J Allergy Clin Immunol. 2010;125(3):611–6.

167. King GG, Downie SR, Verbanck S, Thorpe CW, Berend N, Salome CM, et al. Effects of methacholine on small airway function measured by forced oscillation technique and multiple breath nitrogen washout in normal subjects. Respir Physiol Neurobiol. 2005;148(1–2 SPEC. ISS.):165–77.

168. Van Muylem A, Verbanck S, Estenne M. Monitoring the lung periphery of transplanted lungs. Respir Physiol Neurobiol. 2005;148(1–2 SPEC. ISS.):141–51.

169. Verbanck S, Schuermans D, Vincken W. Small airways ventilation heterogeneity and hyperinflation in COPD: Response to tiotropium bromide. Int J COPD.

2007;2(4):625–34.

170. Verbanck S, Schuermans D, Meysman M, Paiva M, Vincken W. Noninvasive assessment of airway alterations in smokers: The small airways revisited. Am J Respir Crit Care Med. 2004;170(4):414–9.

171. Wenzel SE, Fahy J V., Irvin C, Peters SP, Spector S, Szefler SJ, et al. Proceedings of the ATS workshop on refractory asthma: Current understanding, recommendations, and unanswered questions. Am J Respir Crit Care Med. 2000;162(6):2341–51.

172. Wenzel S. Severe asthma in adults. Am J Respir Crit Care Med. 2005;172(2):149–60.

173. Parker H, Horsfield K CG. Morphology of distal airways in the human lung. J Appl Physiol. 1971;31(3):286–91.

174. Weibel ER, Gomez DM. Architecture of the human lung. Use of quantitative methods establishes fundamental relations between size and number of lung structures. Science [Internet]. 1962;137(3530):577–85. Available from: http://www.ncbi.nlm.nih.gov/pubmed/14005590

175. Litzlbauer HD, Korbel K, Kline TL, Jorgensen SM, Eaker DR, Bohle RM, et al. Synchrotron-based micro-CT imaging of the human lung acinus. Anat Rec. 2010;293(9):1607–14.

176. Busacker A, Newell JD, Keefe T, Hoffman EA, Granroth JC, Castro M, et al. A multivariate analysis of risk factors for the air-trapping asthmatic phenotype as measured by quantitative CT analysis. Chest. 2009;135(1):48–56.

177. Gupta S, Siddiqui S, Haldar P, Entwisle JJ, Mawby D, Wardlaw AJ, et al. Quantitative analysis of high-resolution computed tomography scans in severe asthma subphenotypes. Thorax. 2010;65(9):775–81.

178. Hackx M, Bankier AA, Gevenois PA. Chronic obstructive pulmonary disease: CT quantification of airways disease. Radiology [Internet]. 2012;265(1):34–48. Available from: http://www.ncbi.nlm.nih.gov/pubmed/22993219

179. Zhang J, Hasegawa I, Hatabu H, Feller-Kopman D, Boiselle PM. Frequency and Severity of Air Trapping at Dynamic Expiratory CT in Patients with

Tracheobronchomalacia. Am J Roentgenol. 2004;182(1):81–5.

180. Ueda T, Niimi A, Matsumoto H, Takemura M, Hirai T, Yamaguchi M, et al. Role of small airways in asthma: investigation using high-resolution computed tomography. J Allergy Clin Immunol. 2006;118(5):1019–25.

181. Gono H, Fujimoto K, Kawakami S, Kubo K. Evaluation of airway wall thickness and air trapping by HRCT in asymptomatic asthma. Eur Respir J. 2003;22(6):965–71.

182. Newman KB, Lynch DA, Newman LS, Ellegood D, Newell JD. Quantitative computed tomography detects air trapping due to asthma. Chest. 1994;106(1):105–9.

183. Mitsunobu F, Ashida K, Hosaki Y, Tsugeno H, Okamoto M, Nishida N, et al. Decreased computed tomographic lung density during exacerbation of asthma. Eur Respir J. 2003;22(1):106–12.

184. Tunon-de-Lara JM, Laurent F, Giraud V, Perez T, Aguilaniu B, Meziane H, et al. Air trapping in mild and moderate asthma: effect of inhaled corticosteroids. J Allergy Clin Immunol [Internet]. 2007;119:583–90. Available from: http://www.ncbi.nlm.nih.gov/pubmed/17204317

185. Goldin JG, Tashkin DP, Kleerup EC, Greaser LE, Haywood UM, Sayre JW, et al. Comparative effects of hydrofluoroalkane and chlorofluorocarbon beclomethasone dipropionate inhalation on small airways: Assessment with functional helical thin-section computed tomography. J Allergy Clin Immunol [Internet]. 1999;104(6):s258–67. Available from: http://linkinghub.elsevier.com/retrieve/pii/S0091674999700436

186. Hartley RA, Barker BL, Newby C, Pakkal M, Baldi S, Kajekar R, et al. Relationship between lung function and quantitative computed tomographic parameters of airway remodeling, air trapping, and emphysema in patients with asthma and chronic obstructive pulmonary disease: A single-center study. J Allergy Clin Immunol. 2016;137(5).

187. Galbán CJ, Han MK, Boes JL, Chughtai KA, Meyer CR, Johnson TD, et al. Computed tomography–based biomarker provides unique signature for diagnosis of COPD phenotypes and disease progression. Nat Med [Internet].

2012;18(11):1711–5. Available from: http://www.nature.com/doifinder/10.1038/nm.2971

188. Wijesuriya S, Chandratreya L, Medford AR. Chronic pulmonary emboli and radiologic mimics on CT pulmonary angiography: A diagnostic challenge. Chest. 2013;143(5):1460–71.

189. Burrowes KS, Doel T, Brightling C. Computational modeling of the obstructive lung diseases asthma and COPD. J Transl Med [Internet]. 2014;28(12):Suppl 2: S5. Available from: http://www.pubmedcentral.nih.gov/articlerender.fcgi?artid=4255909&tool=pmcentrez&rendertype=abstract

190. Gonem S, Hardy S, Buhl N, Hartley R, Soares M, Kay R, et al. Characterization of acinar airspace involvement in asthmatic patients by using inert gas washout and hyperpolarized 3helium magnetic resonance. J Allergy Clin Immunol [Internet]. 2016 Feb [cited 2017 Jun 25];137(2):417–25. Available from: http://linkinghub.elsevier.com/retrieve/pii/S0091674915008805

191. Zhang WJ, Niven RM, Young SS, Liu YZ, Parker GJM, Naish JH. Dynamic oxygen-enhanced magnetic resonance imaging of the lung in asthma - Initial experience. Eur J Radiol. 2015;84(2):318–26.

192. Edelman RR, Hatabu H, Tadamura E, Li W, Prasad P V. Noninvasive assessment of regional ventilation in the human lung using oxygen-enhanced magnetic resonance imaging. Nat Med. 1996;2(11):1236–9.

193. Löffler R, Müller CJ, Peller M, Penzkofer H, Deimling M, Schwaiblmair M, et al. Optimization and evaluation of the signal intensity change in multisection oxygen-enhanced MR lung imaging. Magn Reson Med [Internet]. 2000;43(6):860–6. Available from: http://www.ncbi.nlm.nih.gov/pubmed/10861881

194. Nakagawa T, Sakuma H, Murashima S, Ishida N, Matsumura K, Takeda K. Pulmonary ventilation-perfusion MR imaging in clinical patients. J Magn Reson Imaging. 2001;14(4):419–24.

195. Dietrich O. Proton MRI Based Ventilation Imaging: Oxygen-Enhanced Lung MRI and Alternative Approaches. In Berlin, Heidelberg: Springer Berlin

Heidelberg; p. 1–26. Available from: https://doi.org/10.1007/174_2016_80

196. Hatabu H, Tadamura E, Chen Q, Stock KW, Li W, Prasad P V., et al. Pulmonary ventilation: Dynamic MRI with inhalation of molecular oxygen. Eur J Radiol. 2001;37(3):172–8.

197. Ohno Y, Hatabu H, Takenaka D, Adachi S, Van Cauteren M, Sugimura K. Oxygen-enhanced MR ventilation imaging of the lung: Preliminary clinical experience in 25 subjects. Am J Roentgenol. 2001;177(1):185–94.

198. Müller CJ, Schwaiblmair M, Scheidler J, Deimling M, Weber J, Löffler RB, et al. Pulmonary diffusing capacity: assessment with oxygen-enhanced lung MR imaging preliminary findings. Radiology. 2002;222(2):499–506.

199. Ohno Y, Hatabu H, Takenaka D, Van Cauteren M, Fujii M, Sugimura K. Dynamic oxygen-enhanced MRI reflects diffusing capacity of the lung. Magn Reson Med. 2002;47(6):1139–44.

200. Ohno Y, Hatabu H, Higashino T, Nogami M, Takenaka D, Watanabe H, et al. Oxygen-enhanced MR imaging: correlation with postsurgical lung function in patients with lung cancer. Radiology [Internet]. 2005;236(2):704–11. Available from: http://www.ncbi.nlm.nih.gov/pubmed/15972343

201. Jakob PM, Wang T, Schultz G, Hebestreit H, Hebestreit A, Hahn D. Assessment of human pulmonary function using oxygen-enhanced T(1) imaging in patients with cystic fibrosis. Magn Reson Med. 2004;51(5):1009–16.

202. Kershaw LE, Naish JH, McGrath DM, Waterton JC, Parker GJM. Measurement of arterial plasma oxygenation in dynamic oxygen-enhanced MRI. Magn Reson Med. 2010;64(6):1838–42.

203. Ohno Y, Koyama H, Matsumoto K, Onishi Y, Nogami M, Takenaka D, et al. Oxygen-enhanced MRI vs. quantitatively assessed thin-section CT: Pulmonary functional loss assessment and clinical stage classification of asthmatics. Eur J Radiol. 2011;77(1):85–91.

204. Ohno Y, Iwasawa T, Seo JB, Koyama H, Takahashi H, Oh Y-M, et al. Oxygen-enhanced magnetic resonance imaging versus computed tomography: multicenter study for clinical stage classification of smoking-related chronic obstructive

pulmonary disease. Am J Respir Crit Care Med. 2008;177(10):1095–102.

205. McGrath D, Naish J, Young S, Olsson L, Hutchinson C, Vestbo J, et al. Compartmental Model Analysis of Oxygen-Enhanced MRI and DCE-MRI Detects Pre-morbid Lung Damage in Smokers. In: Proceedings 17th Scientific Meeting, International Society for Magnetic Resonance in Medicine [Internet]. 2009. p. 2016. Available from: /MyPathway2009/2016

206. Ohno Y, Chen Q, Hatabu H. Oxygen-enhanced magnetic resonance ventilation imaging of lung. Eur J Radiol. 2001;37(3):164–71.

207. Doberer D, Trejo Bittar HE, Wenzel SE. Should lung biopsies be performed in patients with severe asthma? Eur Respir Rev. 2015;24(137):525–39.

208. van Veen IH, ten Brinke A, Gauw SA, Sterk PJ, Rabe KF, Bel EH. Consistency of sputum eosinophilia in difficult-to-treat asthma: A 5-year follow-up study. J Allergy Clin Immunol. 2009;124(3).

209. Hermans C, Dong P, Robin M, Jadoul M, Bernard A, Bersten AD, et al. Determinants of serum levels of surfactant proteins A and B and Clara cell protein CC16. Biomarkers. 2003;8(6):461–71.

210. Khor YH, Teoh AKY, Lam SM, Mo DCQ, Weston S, Reid DW, et al. Increased vascular permeability precedes cellular inflammation as asthma control deteriorates. Clin Exp Allergy. 2009;39(11):1659–67.

211. Tsoumakidou M, Tzanakis N, Siafakas NM. Induced sputum in the investigation of airway inflammation of COPD. Respir Med. 2003;97(8):863–71.

212. Gershman NH, Liu H, Wong HH, Liu JT, Fahy J V. Fractional analysis of sequential induced sputum samples during sputum induction: Evidence that different lung compartments are sampled at different time points. J Allergy Clin Immunol. 1999;104(2 I):322–8.

213. Jayaram L, Pizzichini MM, Cook RJ, Boulet LP, Lemière C, Pizzichini E, et al. Determining asthma treatment by monitoring sputum cell counts: Effect on exacerbations. Eur Respir J. 2006;27(3):483–94.

214. Bonini M, Usmani OS. The role of the small airways in the pathophysiology of asthma and chronic obstructive pulmonary disease. Ther Adv Respir Dis

[Internet]. 2015;9(6):281–93. Available from: http://journals.sagepub.com/doi/10.1177/1753465815588064

215. Haslam P, Baughman RP. Report of ERS Task Force: Guidelines for measurement of acellular components and standardization of BAL. Eur Respir J. 1999;14(2):245–8.

216. Karamanou M, Androutsos G. Antoine-Laurent de Lavoisier (1743–1794) and the birth of respiratory physiology. Thorax [Internet]. 2013;68(10):978–9. Available from: http://thorax.bmj.com/lookup/doi/10.1136/thoraxjnl-2013-203840

217. Dweik RA, Boggs PB, Erzurum SC, Irvin CG, Leigh MW, Lundberg JO, et al. An official ATS clinical practice guideline: Interpretation of exhaled nitric oxide levels (FENO) for clinical applications. Am J Respir Crit Care Med. 2011;184(5):602–15.

218. Holmgren H, Ljungström E, Almstrand ACA-C, Bake B, Olin A-CAC. Size distribution of exhaled particles in the range from 0.01 to 2.0μm. J Aerosol Sci. 2010;41(5):439–46.

219. Strimbu K, Tavel J a. What are Biomarkers? Curr Opin HIV AIDS. 2011;5(6):463–6.

220. Wheelock CE, Goss VM, Balgoma D, Nicholas B, Brandsma J, Skipp PJ, et al. Application of 'omics technologies to biomarker discovery in inflammatory lung diseases. Eur Respir J. 2013;42(3):802–25.

221. Lawal O, Ahmed WM, Nijsen TME, Goodacre R, Fowler SJ. Exhaled breath analysis: a review of 'breath-taking' methods for off-line analysis. Metabolomics. 2017;13(10):110.

222. Dragonieri S, Schot R, Mertens BJA, Le Cessie S, Gauw SA, Spanevello A, et al. An electronic nose in the discrimination of patients with asthma and controls. J Allergy Clin Immunol. 2007;120(4):856–62.

223. Fens N, Zwinderman AH, van der Schee MP. Exhaled breath profiling enables discrimination of chronic obstructive pulmonary disease and asthma. Am J Respir Crit Care Med. 2009;180(11):1076–82.

224. Smolinska A, Klaassen EMM, Dallinga JW, Van De Kant KDG, Jobsis Q, Moonen EJC, et al. Profiling of volatile organic compounds in exhaled breath as a strategy to find early predictive signatures of asthma in children. PLoS One. 2014;9(4).

225. Ibrahim B, Basanta M, Cadden P, Singh D, Douce D, Woodcock A, et al. Non-invasive phenotyping using exhaled volatile organic compounds in asthma. Thorax [Internet]. 2011;66(9):804–9. Available from: http://thorax.bmj.com/cgi/doi/10.1136/thx.2010.156695

226. Asthma: diagnosis, monitoring and chronic asthma management (NICE guidelines) [Internet]. 2017 [cited 2018 Jul 15]. Available from: https://www.nice.org.uk/guidance/ng80

227. Montuschi P, Santonico M, Mondino C, Pennazza G, Maritini G, Martinelli E, et al. Diagnostic performance of an electronic nose, fractional exhaled nitric oxide, and lung function testing in asthma. Chest. 2010;137(4):790–6.

228. Bel EH. Measuring adherence to inhaled corticosteroids in asthma: Getting closer! Am J Respir Crit Care Med. 2012;186(11):1067–8.

229. van Veen IH, Sterk PJ, Schot R, Gauw SA, Rabe KF, Bel EH, et al. Alveolar nitric oxide versus measures of peripheral airway dysfunction in severe asthma. Eur Respir J. 2006;27(5):951–6.

230. Kurik MV, Rolik LV, Parkhomenko NV, Tarakhan LI SN. Physical properties of a condensate of exhaled air in chronic bronchitis patients. Vrach Delo. 1987;7:37–9.

231. Horváth I, Hunt J, Barnes PJ, Alving K, Antczak A, Baraldi E, et al. Exhaled breath condensate: Methodological recommendations and unresolved questions. Eur Respir J. 2005;26(3):523–48.

232. Robroeks CMHHT, Rijkers GT, Jöbsis Q, Hendriks HJE, Damoiseaux JGMC, Zimmermann LJI, et al. Increased cytokines, chemokines and soluble adhesion molecules in exhaled breath condensate of asthmatic children. Clin Exp Allergy. 2010;40:77–84.

233. Effros RM, Dunning MB, Biller J, Shaker R. The promise and perils of exhaled

breath condensates. Am J Physiol Lung Cell Mol Physiol [Internet]. 2004;287(6):L1073-80. Available from: http://www.ncbi.nlm.nih.gov/pubmed/15531756

234. Li W, Pi X, Qiao P, Liu H. Collecting protein biomarkers in breath using electret filters: A preliminary method on new technical model and human study. PLoS One. 2016;11(3):e0150481.

235. Olin A-C. Particles in Exhaled Air A Novel Method of Sampling Non-Volatiles in Exhaled Air. Volatile Biomarkers. 2013.

236. Hinds WC. Aerosol technology: Properties, Behavior, and Measurement of Airborne Particles. Wiley-Interscience Publication. 1999. 233-259 p.

237. Macklem PT, Proctor DF, Hogg JC. The stability of peripheral airways. Respir Physiol. 1970;8(2):191–203.

238. Dawson S V, Elliott E a. Wave-speed limitation on expiratory flow-a unifying concept. J Appl Physiol [Internet]. 1977;43(3):498–515. Available from: http://www.ncbi.nlm.nih.gov/pubmed/914721

239. Naureckas ET, Dawson C a, Gerber BS, Gaver DP, Gerber HL, Linehan JH, et al. Airway reopening pressure in isolated rat lungs. J Appl Physiol. 1994;76(3):1372–7.

240. Holmgren H, Gerth E, Ljungström E, Larsson P, Almstrand A-C, Bake B, et al. Effects of breath holding at low and high lung volumes on amount of exhaled particles. Respir Physiol Neurobiol. 2013;185(2):228–34.

241. Almstrand A-C, Bake B, Ljungström E, Larsson P, Bredberg A, Mirgorodskaya E, et al. Effect of airway opening on production of exhaled particles. J Appl Physiol. 2010;108(3):584–8.

242. Holmgern H, Ljungström E, Almstrand AC, Bake B OA. Size distribution of exhaled particles in the range from 0.01 to 2.0 mm. J Aerosol Sci. 2010;41:439–46.

243. Haslbeck K, Schwarz K, Hohlfeld JM, Seume JR, Koch W. Submicron droplet formation in the human lung. J Aerosol Sci. 2010;41(5):429–38.

244. Bredberg A, Gobom J, Almstrand A-C, Larsson P, Blennow K, Olin A-C, et al. Exhaled endogenous particles contain lung proteins. Clin Chem. 2012;58(2):431–40.

245. Bredberg A, Josefson M, Almstrand A-C, Lausmaa J, Sjövall P, Levinsson A, et al. Comparison of exhaled endogenous particles from smokers and non-smokers using multivariate analysis. Respiration. 2013;86(2):135–42.

246. Liu MY, Wang LM, Li E, Enhorning G. Pulmonary surfactant will secure free airflow through a narrow tube. J Appl Physiol [Internet]. 1991;71(2):742–8. Available from: http://www.ncbi.nlm.nih.gov/pubmed/1938748

247. Wright JR. Immunoregulatory functions of surfactant proteins. Nat Rev Immunol [Internet]. 2005;5(1):58–68. Available from: http://www.nature.com/doifinder/10.1038/nri1528

248. Devendra G, Spragg RG. Lung surfactant in subacute pulmonary disease. Respir Res [Internet]. 2002;3:11. Available from: http://respiratory-research.biomedcentral.com/articles/10.1186/rr168

249. Kuroki Y, Takahashi M, Nishitani C. Pulmonary collectins in innate immunity of the lung. Cell Microbiol. 2007;9(8):1871–9.

250. Hohlfeld JM, Erpenbeck VJ, Krug N. Surfactant proteins SP-A and SP-D as modulators of the allergic inflammation in asthma. Pathobiology. 2002;70(5):287–92.

251. Karinch AM, Floros J. 5’ splicing and allelic variants of the human pulmonary surfactant protein A genes. Am J Respir Cell Mol Biol [Internet]. 1995;12(1):77–88. Available from: http://www.ncbi.nlm.nih.gov/entrez/query.fcgi?cmd=Retrieve&db=PubMed&dopt=Citation&list_uids=7811473

252. Ali M, Umstead TM, Haque R, Mikerov AN, Freeman WM, Floros J, et al. Differences in the BAL proteome after Klebsiella pneumoniae infection in wild type and SP-A-/- mice. Proteome Sci [Internet]. 2010 Jun;8(1):34. Available from: https://doi.org/10.1186/1477-5956-8-34

253. Van De Graaf EA, Jansen HM, Lutter R, Alberts C, Kobesen J, de Vries IJ, et al.

Surfactant protein A in bronchoalveolar lavage fluid. J Lab Clin Med [Internet]. 1992 Nov 16;120(2):252–63. Available from: http://www.translationalres.com/article/0022-2143(92)90133-6/abstract

254. Wang Y, Voelker DR, Lugogo NL, Wang G, Floros J, Ingram JL, et al. Surfactant protein A is defective in abrogating inflammation in asthma. Am J Physiol Lung Cell Mol Physiol [Internet]. 2011;301(4):L598-606. Available from: http://www.pubmedcentral.nih.gov/articlerender.fcgi?artid=3191759&tool=pmcentrez&rendertype=abstract

255. Pastva AM, Mukherjee S, Giamberardino C, Hsia B, Lo B, Sempowski GD, et al. Lung Effector Memory and Activated CD4+ T Cells Display Enhanced Proliferation in Surfactant Protein A-Deficient Mice during Allergen-Mediated Inflammation. J Immunol [Internet]. 2011;186(5):2842–9. Available from: http://www.jimmunol.org/cgi/doi/10.4049/jimmunol.0904190

256. Fanali G, Di Masi A, Trezza V, Marino M, Fasano M, Ascenzi P. Human serum albumin: From bench to bedside. Mol Aspects Med. 2012;33(3):209–90.

257. Nicholson JP, Wolmarans MR, Park GR. The role of albumin in critical illness. Br J Anaesth. 2000;85(4):599–610.

258. Hohlfeld JM, Ahlf K, Enhorning C, Balke K, Erpenbeck VJ, Petschallies J, et al. Dysfunction of pulmonary surfactant in asthmatics after segmental allergen challenge. Am J Respir Crit Care Med. 1999;159(6):1803–9.

259. Larsson P, Lärstad M, Bake B, Hammar O, Bredberg A, Almstrand AC, et al. Exhaled particles as markers of small airway inflammation in subjects with asthma. Clin Physiol Funct Imaging. 2015;37(5):489–97.

260. Petrea A. Ericson, Ekaterina Mirgorodskaya, Oscar S. Hammar, Emilia A. Viklund, Ann-Charlotte R. Almstrand, Per J-W. Larsson, Gerdt C. Riise A-CO. Low Levels of Exhaled Surfactant Protein A Associated With BOS After Lung Transplantation. Transpl Direct. 2016;2(9):e103.

261. Holmgren H, Ljungström E. Influence of Film Dimensions on Film Droplet Formation. J Aerosol Med Pulm Drug Deliv [Internet]. 2012;25(1):47–53. Available from: http://online.liebertpub.com/doi/abs/10.1089/jamp.2011.0892

262. Bake B, Ljungström E, Claesson A, Carlsen HK, Holm M, Olin A-C, et al. Exhaled Particles After a Standardized Breathing Maneuver. J Aerosol Med Pulm Drug Deliv [Internet]. 2017 Mar 9;30(4):267–73. Available from: https://doi.org/10.1089/jamp.2016.1330

263. Wright SM, Hockey PM, Enhorning G, Strong P, Reid KB, Holgate ST, et al. Altered airway surfactant phospholipid composition and reduced lung function in asthma. J Appl Physiol. 2000;89(4):1283–92.

264. Larsson P, Bake B, Wallin A, Hammar O, Almstrand AC, Lärstad M, et al. The effect of exhalation flow on endogenous particle emission and phospholipid composition. Respir Physiol Neurobiol. 2017;243:39–46.

265. Usmani OS. Small airways dysfunction in asthma: Evaluation and management to improve asthma control. Allergy, Asthma Immunol Res. 2014;6(5):376–88.

266. Reddel HK, Taylor DR, Bateman ED, Boulet LP, Boushey HA, Busse WW, et al. An official American Thoracic Society/European Respiratory Society statement: Asthma control and exacerbations - Standardizing endpoints for clinical asthma trials and clinical practice. Am J Respir Crit Care Med. 2009;180(1):59–99.

267. Juniper EF, Byrne PM, Guyatt GH, Ferrie PJ, King DR. Development and validation of a questionnaire to measure asthma control. Eur Respir J [Internet]. 1999 Oct 1;14(4):902 LP-907. Available from: http://erj.ersjournals.com/content/14/4/902.abstract

268. Juniper EF, Guyatt GH, Epstein RS, Ferrie PJ, Jaeschke R, Hiller TK. Evaluation of impairment of health related quality of life in asthma: development of a questionnaire for use in clinical trials. Thorax [Internet]. 1992 Feb 1;47(2):76 LP-83. Available from: http://thorax.bmj.com/content/47/2/76.abstract

269. Juniper EF, Buist AS, Cox FM, Ferrie PJ, King DR. Validation of a Standardized Version of the Asthma Quality of Life Questionnaire. Chest [Internet]. 1999 Feb 21;115(5):1265–70. Available from: http://dx.doi.org/10.1378/chest.115.5.1265

270. Juniper EF, Svensson K, Mörk A-C, Ståhl E. Measurement properties and interpretation of three shortened versions of the asthma control questionnaire. Respir Med [Internet]. 2005 Jun 19;99(5):553–8. Available from: http://dx.doi.org/10.1016/j.rmed.2004.10.008

271. Miller MR, Hankinson J, Brusasco V, Burgos F, Casaburi R, Coates A, et al. Standardisation of spirometry. Eur Respir J [Internet]. 2005 Aug 1;26(2):319 LP-338. Available from: http://erj.ersjournals.com/content/26/2/319.abstract

272. Quanjer PH, Stanojevic S, Cole TJ, Baur X, Hall GL, Culver BH, et al. Multi-ethnic reference values for spirometry for the 3–95-yr age range: the global lung function 2012 equations. Eur Respir J [Internet]. 2012 Nov 30;40(6):1324 LP-1343. Available from: http://erj.ersjournals.com/content/40/6/1324.abstract

273. Crapo RO, Casaburi R, Coates AL, Enright PL, Hankinson JL, Irvin CG, et al. Guidelines for Methacholine and Exercise Challenge Testing - 1999. Am J Respir Crit Care Med. 2000;161(1):309–29.

274. Pavord ID, Pizzichini MMM, Pizzichini E, Hargreave FE. The use of induced sputum to investigate airway inflammation. Thorax. 1997;52:498–501.

275. Wanger J, Clausen JL, Coates A, Pedersen OF, Brusasco V, Burgos F, et al. Standardisation of the measurement of lung volumes. Eur Respir J. 2005;26(3):511–22.

276. Verbanck S, Schuermans D, Van Muylem A, Melot C, Noppen M, Vincken W, et al. Conductive and acinar lung-zone contributions to ventilation inhomogeneity in COPD. Am J Respir Crit Care Med. 1998;157(5 I):1573–7.

277. Tawhai MH, Hunter P, Tschirren J, Reinhardt J, McLennan G, Hoffman E a. CT-based geometry analysis and finite element models of the human and ovine bronchial tree. J Appl Physiol. 2004;97(6):2310–21.

278. Usmani OS, Singh D, Spinola M, Bizzi A, Barnes PJ, Usmani OS, Singh D, Spinola M, Bizzi A BP. The prevalence of small airways disease in adult asthma: A systematic literature review. Respir Med. 2016;116:19–27.

279. Hamid Q, Song Y, Kotsimbos TC, Minshall E, Bai TR, Hegele RG, et al. Inflammation of small airways in asthma. J Allergy Clin Immunol. 1997;100(1):44–51.

280. Hyde DM, Hamid Q, Irvin CG. Anatomy, pathology, and physiology of the tracheobronchial tree: Emphasis on the distal airways. J Allergy Clin Immunol [Internet]. 2018 Feb 21;124(6):S72–7. Available from:

http://dx.doi.org/10.1016/j.jaci.2009.08.048

281. Shi Y, Aledia AS, Galant SP, George SC. Peripheral airway impairment measured by oscillometry predicts loss of asthma control in children. J Allergy Clin Immunol [Internet]. 2018 Feb 21;131(3):718–23. Available from: http://dx.doi.org/10.1016/j.jaci.2012.09.022

282. Williamson PA, Clearie K, Menzies D, Vaidyanathan S LB, Williamson PA, Clearie K, Menzies D, Vaidyanathan S, Lipworth BJ. Assessment of Small-Airways Disease Using Alveolar Nitric Oxide and Impulse Oscillometry in Asthma and COPD. Lung. 2011;189(2):121–9.

283. Yamaguchi M, Niimi A, Ueda T, Takemura M, Matsuoka H, Jinnai M, Otsuka K, Oguma T, Takeda T, Ito I MH, Yamaguchi M, Niimi A, Ueda T, Takemura M, Matsuoka H, et al. Effect of inhaled corticosteroids on small airways in asthma: Investigation using impulse oscillometry. Pulm Pharmacol Ther. 2009;22(4):326–32.

284. Hoshino M. Comparison of Effectiveness in Ciclesonide and Fluticasone Propionate on Small Airway Function in Mild Asthma. Allergol Int. 2010;9(1):59–66.

285. Quanjer PH, Weiner DJ, Pretto JJ, Brazzale DJ, Boros PW. Measurement of FEF25-75% and FEF75% does not contribute to clinical decision making. Eur Respir J [Internet]. 2014 Apr 1;43(4):1051 LP-1058. Available from: http://erj.ersjournals.com/content/43/4/1051.abstract

286. Pellegrino R, Brusasco V, Miller MR. Question everything. Eur Respir J [Internet]. 2014 Apr 1;43(4):947 LP-948. Available from: http://erj.ersjournals.com/content/43/4/947.abstract

287. BTS/SIGN. BTS/SIGN British Guideline on the Management of Asthma. British Thoracic Society/Scottish Intercollegiate Guidelines Network 2016. Thorax [Internet]. 2016;69(Suppl 1):i1 LP-i192. Available from: http://thorax.bmj.com/content/69/Suppl_1/i1.abstract

288. Gonem S, Corkill S, Singapuri A, Gustafsson P, Costanza R, Brightling CE, et al. Between-visit variability of small airway obstruction markers in patients with asthma. Eur Respir J. 2014;44(1).

289. Chung KF, Wenzel SE, Brozek JL, Bush A, Castro M, Sterk PJ, et al. International ERS/ATS guidelines on definition, evaluation and treatment of severe asthma. Eur Respir J [Internet]. 2014 Jan 1;43(2):343–73. Available from: http://erj.ersjournals.com/content/early/2013/11/27/09031936.00202013.abstract

290. Hozawa S, Terada M, Hozawa M. Comparison of the effects of budesonide/formoterol maintenance and reliever therapy with fluticasone/salmeterol fixed-dose treatment on airway inflammation and small airway impairment in patients who need to step-up from inhaled corticosteroid monotherapy. Pulm Pharmacol Ther. 2014;27(2):190–6.

291. Hozawa S, Terada M, Haruta Y, Hozawa M. Comparison of early effects of budesonide/formoterol maintenance and reliever therapy with fluticasone furoate/vilanterol for asthma patients requiring step-up from inhaled corticosteroid monotherapy. Pulm Pharmacol Ther [Internet]. 2016;37:15–23. Available from: http://www.sciencedirect.com/science/article/pii/S1094553916300050

292. Russell RJ, Chachi L, FitzGerald JM, Backer V, Olivenstein R, Titlestad IL, et al. Effect of tralokinumab, an interleukin-13 neutralising monoclonal antibody, on eosinophilic airway inflammation in uncontrolled moderate-to-severe asthma (MESOS): a multicentre, double-blind, randomised, placebo-controlled phase 2 trial. Lancet Respir Med [Internet]. 2018;6(7):499–510. Available from: http://www.sciencedirect.com/science/article/pii/S2213260018302017

293. Gonem S, Berair R, Singapuri A, Hartley R, Laurencin MFM, Bacher G, et al. Fevipiprant, a prostaglandin D2receptor 2 antagonist, in patients with persistent eosinophilic asthma: a single-centre, randomised, double-blind, parallel-group, placebo-controlled trial. Lancet Respir Med. 2016;4(9):699–707.

294. Deepak D, Prasad A, Atwal SS, Agarwal K. Recognition of small airways obstruction in asthma and COPD - The road less travelled. J Clin Diagnostic Res. 2017;11(3):TE01-TE05.

295. Newby C, Agbetile J, Hargadon B, Monteiro W, Green R, Pavord I, et al. Lung function decline and variable airway inflammatory pattern: Longitudinal analysis of severe asthma. J Allergy Clin Immunol. 2014;134(2):287–94.

296. Foy B, Bell A, Siddiqui SH KD. Low frequency lung resistance is a global bronchoconstriction detection measure, but is still sensitive to small airways disease. In: American Thoracic Society. 2018. p. A3928–A3928.

297. Oostveen E, Boda K, van der Grinten CPM, James AL, Young S, Nieland H, et al. Respiratory impedance in healthy subjects: baseline values and bronchodilator response. Eur Respir J [Internet]. 2013 Dec 1;42(6):1513 LP-1523. Available from: http://erj.ersjournals.com/content/42/6/1513.abstract

298. Martin Bland J, Altman D. Statistical methods for assessing agreement between two methods of clinical measurement. Lancet [Internet]. 2018 Feb 22;327(8476):307–10. Available from: http://dx.doi.org/10.1016/S0140-6736(86)90837-8

299. Diong B, Rajagiri A, Goldman M, Nazeran H. The augmented RIC model of the human respiratory system. Med Biol Eng Comput. 2009;51(6):395–404.

300. Zimmermann SC, Watts JC, Bertolin A, Jetmalani K, King GG TC. Discrepancy between in vivo and in vitro comparisons of forced oscillation devices. J Clin Monit Comput. 2017;1–4.

301. Watts JC, Farah CS, Seccombe LM, Handley BM, Schoeffel RE, Bertolin A, et al. Measurement duration impacts variability but not impedance measured by the forced oscillation technique in healthy, asthma and COPD subjects. ERJ Open Res. 2016;2(2).

302. Benayoun L, Druilhe A, Dombret M-C, Aubier M, Pretolani M. Airway Structural Alterations Selectively Associated with Severe Asthma. Am J Respir Crit Care Med [Internet]. 2003 May 15;167(10):1360–8. Available from: https://doi.org/10.1164/rccm.200209-1030OC

303. Wahidi MM, Rocha AT, Hollingsworth JW, Govert JA, Feller-Kopman D, Ernst A. Contraindications and Safety of Transbronchial Lung Biopsy via Flexible Bronchoscopy. Respiration [Internet]. 2005;72(3):285–95. Available from: https://www.karger.com/DOI/10.1159/000085370

304. HY R. Bronchoalveolar lavage and other methods to define the human respiratory tract milieu in health and disease. Lung. 2011;189(2):87–99.

305. Ljungkvist G, Ullah S, Tinglev Å, Stein K, Bake B, Larsson P, Almstrand AC, Viklund E, Hammar O, Sandqvist S, Beck O OA. Two techniques to sample non-volatiles in breath—exemplified by methadone. J Breath Res. 2017;12(1):016011.

306. Wang JY, Kishore U, Lim B. L, Strong P, Reid KBM. Interaction of human lung surfactant proteins A and D with mite (Dermatophagoides pteronyssinus) allergens. Clin Exp Immunol. 1996;106:367–73.

307. Anzueto A, Jubran A, Ohar JA, Piquette CA, Rennard SI, Colice G, et al. Effects of aerosolized surfactant in patients with stable chronic bronchitis: a prospective randomized controlled trial. JAMA. 1997;278:1426–31.

308. Kjellberg S, Houltz BK, Zetterström O, Robinson PD, Gustafsson PM. Clinical characteristics of adult asthma associated with small airway dysfunction. Respir Med [Internet]. 2016 Feb 21;117:92–102. Available from: http://dx.doi.org/10.1016/j.rmed.2016.05.028

309. Brightling CE, Ward R, Woltmann G, Bradding P, Sheller JR, Dworski R, et al. Induced sputum inflammatory mediator concentrations in eosinophilic bronchitis and asthma. Am J Respir Crit Care Med. 2000;162(3 I):878–82.

310. Siddiqui S, Shikotra A, Richardson M, Doran E, Choy D, Bell A, et al. Airway pathological heterogeneity in asthma: Visualization of disease microclusters using topological data analysis. J Allergy Clin Immunol. 2018;7:pii: S0091-6749(18)30039-3.

311. Carlsson G. Topology and data. Bull Am Math Soc. 2009;46:255–308.

312. P. Y. Lum, G. Singh, A. Lehman, T. Ishkanov, M. Vejdemo-Johansson, M. Alagappan JC& GC. Extracting insights from the shape of complex data using topology. Sci Rep. 2013;3:1236.

313. Singh G, Mémoli F, Carlsson GE. Topological Methods for the Analysis of High Dimensional Data Sets and 3D Object Recognition. Eurographics Symp Point-Based Graph. 2007;91–100.

314. Ledford JG, Voelker DR, Addison KJ, Wang Y, Nikam VS, Degan S, et al. Genetic variation in SP-A2 leads to differential binding to Mycoplasma

pneumoniae membranes and regulation of host responses. J Immunol [Internet]. 2015 Jun 15;194(12):6123 LP-6132. Available from: http://www.jimmunol.org/content/194/12/6123.abstract

315. Scanlon ST, Milovanova T, Kierstein S, Cao Y, Atochina EN, Tomer Y, et al. Surfactant Protein-A inhibits Aspergillus fumigatus-induced allergic T-cell responses. Respir Res [Internet]. 2005;6(1):97. Available from: https://doi.org/10.1186/1465-9921-6-97

316. Ledford JG, Addison KJ, Foster MW, Que LG. Eosinophil-Associated Lung Diseases. A Cry for Surfactant Proteins A and D Help? Am J Respir Cell Mol Biol [Internet]. 2014 Jun 24;51(5):604–14. Available from: https://doi.org/10.1165/rcmb.2014-0095TR

317. Cheng G, Ueda T, Numao T, Kuroki Y, Nakajima H, Fukushima Y, et al. Increased levels of surfactant protein A and D in bronchoalveolar lavage fluids in patients with bronchial asthma. Eur Respir J [Internet]. 2000 Nov 1;16(5):831 LP-835. Available from: http://erj.ersjournals.com/content/16/5/831.abstract

318. Babu KS, Woodcock DA, Smith SE, Staniforth JN, Holgate ST, Conway JH. Inhaled synthetic surfactant abolishes the early allergen-induced response in asthma. Eur Respir J [Internet]. 2003 Jun 1;21(6):1046 LP-1049. Available from: http://erj.ersjournals.com/content/21/6/1046.abstract

319. Chapman DG, Berend N, King GG, Salome CM. Increased airway closure is a determinant of airway hyperresponsiveness. Eur Respir J [Internet]. 2008 Dec 1;32(6):1563 LP-1569. Available from: http://erj.ersjournals.com/content/32/6/1563.abstract

320. Belda J, Margarit G, Martínez C, Bellido-Casado J, Casan P, Torrejón M, et al. Anti-inflammatory effects of high-dose inhaled fluticasone versus oral prednisone in asthma exacerbations. Eur Respir J [Internet]. 2007 Dec 1;30(6):1143–9. Available from: http://erj.ersjournals.com/content/30/6/1143.abstract

321. Holmgren H, Bake B, Olin A-C, Ljungström E. Relation between humidity and size of exhaled particles. J Aerosol Med Pulm Drug Deliv. 2011;24(5):253–60.

322. Kirkwood BB, Sterne J. Essential medical statistics. Malden, MA: Blackwell

Science. 2003.

323. Tan RA, Corren J. Clinical utility and development of the fluticasone/formoterol combination formulation (Flutiform((R)) for the treatment of asthma. Drug Des Devel Ther. 2014;8:1555–61.

324. Johal B, Howald M, Fischer M, Marshall J, Venthoye G. Fine Particle Profile of Fluticasone Propionate/Formoterol Fumarate Versus Other Combination Products: the DIFFUSE Study. Comb Prod Ther [Internet]. 2013 Dec;3(1):39–51. Available from: https://doi.org/10.1007/s13556-013-0003-9

325. ATS/ERS Recommendations for Standardized Procedures for the Online and Offline Measurement of Exhaled Lower Respiratory Nitric Oxide and Nasal Nitric Oxide, 2005. Am J Respir Crit Care Med [Internet]. 2005 Apr 15;171(8):912–30. Available from: https://doi.org/10.1164/rccm.200406-710ST

326. Green RH, Brightling CE, Woltmann G, Parker D, Wardlaw AJ, Pavord ID. Analysis of induced sputum in adults with asthma: Identification of subgroup with isolated sputum neutrophilia and poor response to inhaled corticosteroids. Thorax. 2002;57(10):875–9.